TU Delft

Simulation-Based Evaluation of Port Resilience Strategies

A Case Study of the Port of Rotterdam

F.J.W. de Waal

Student Number: 4709594 • Date of Defense: August 29th, 2025

Delft University of Technology
Faculty of Technology, Policy and Management

Simulation-Based Evaluation of Port Resilience Strategies:
A Case Study of the Port of Rotterdam

Management of Technology - Master Thesis

Name: F.J.W. de Waal
Student Number: 4709594
Date: August 16, 2025

1st Supervisor: Dr. S. Balakrishnan
Section: Transport and Logistics

2nd Supervisor: Dr. M. Yang

Section: Safety and Security Science

Thesis Committee:
Dr. J.A. Annema
Section: Transport and Logistics
Dr. M. Yang
Section: Safety and Security Science

Delft University of Technology
Faculty of Technology, Policy and Management

Contents

Table 1: List of Abbreviations

Abbreviation	**Full Term**
ABM	Agent-Based Model
AIS	Automatic Identification System
CPT	Cumulative Prospect Theory
DES	Discrete-Event Simulation
DSS	Decision Support System(s)
GCSN	Global Container Shipping Network
GIS	Geographic Information System
IQR	Interquartile Range
MCDA	Multi-Criteria Decision Analysis
MCDM	Multi-Criteria Decision-Making
PLE	Personal Learning Edition (AnyLogic)
PoR	Port of Rotterdam
PRF	Performance Response Function(s)
ROI	Return on Investment
SRITS	Sea–Rail Intermodal Transportation System
TEN-T	Trans-European Transport Network
TEU	Twenty-foot Equivalent Unit
TTR	Time-to-Recovery
VTS	Vessel Traffic System(s)

Preface

This thesis was written as the final part of fulfilling the requirements for the Master of Science degree in Management of Technology, at Delft University of Technology. It concludes my studies at the Faculty of Technology, Policy and Management.

I would like to express my gratitude to my first supervisor, Dr. S. Balakrishnan, for his guidance, constructive feedback, and encouragement throughout the research process. I am also very grateful to my second supervisor, Dr. M. Yang, whose advice on resilience and systemic risk perspectives provided valuable insights that greatly supported this work. I would further like to thank Dr. J.A. Annema for serving on my thesis committee and for his thoughtful feedback, which has helped improve both the quality and scope of this work.

On a more personal note, I would like to thank my family and friends for their patience, encouragement, and understanding during this period. I also want to thank Daan for the support during the late hours and sparring with me on various occasions.

A special thanks goes to my girlfriend, Iris, for her continuous support, motivation, and belief in me throughout this journey.

Finally, I hope that this thesis will contribute in some way to the ongoing conversation on how ports and logistics networks can prepare for and recover from disruptions, and that it may inspire further research in the field of maritime resilience.

Felix de Waal
Mareson, August 2025

Abstract

The increasing frequency and severity of disruptions in global supply chains have underscored the need for resilient port operations. Ports represent critical nodes in the maritime–hinterland interface. Systemic risks arising from disruptive events like droughts, labor strikes, or demand fluctuations can propagate rapidly across interconnected transport networks. Existing research on port resilience largely focuses on isolated components of port operations or infrastructure, offering limited insights into systemic risks that span the entire system. As a result, the interplay between strategies, the adaptive role of stakeholders, and their systemic impacts on the whole supply chain remain insufficiently understood. This study addresses this gap by asking: How can systemic risks in port operations be minimized through resilience-based strategies, identified via a simulation of port disruptions and recovery?

To answer this question, a hybrid simulation approach is adopted, combining discrete event simulation (DES) and agent-based modeling (ABM) in the AnyLogic platform. DES captures port and terminal operations, including queuing dynamics, capacity constraints and resource allocation. ABM represents the adaptive decision-making of inland transport actors such as barge, truck, and rail operators. This integration allows for the simultaneous assessment of process-level efficiency and actor-level adaptability. The Port of Rotterdam serves as the case study, given its status as Europe's largest multimodal hub and its relevance for resilience planning at the sea–port–land interface. Three disruption scenarios, namely a labor strike, drought affecting inland barge transport, and sea-side vessel demand fluctuations were modeled. Along with these distinct systemic risks, five resilience strategies were evaluated. These include autonomous facilities, dynamic rerouting, inland transshipment hub activation, capacity buffer expansion, and a collaborative strategy combining automation with rerouting. Performance was assessed using container throughput, delay costs, transport costs, delivery rate distributions, facility utilization and recovery time.

The results demonstrate that no single strategy is universally effective across all disruption types. Autonomous facilities enhanced throughput and reduced delays under capacity-limited disruptions such as labor strikes, but offered diminishing returns in the demand fluctuation scenario where a single transport mode becomes loaded too heavily. Dynamic rerouting and hub activation proved most effective minimizing delays in external disruptions such as drought and demand fluctuation, by enabling flows to bypass bottlenecks and stabilizing recovery times. Buffer expansion provided cost-effective shock absorption for short, localized events but lacked adaptability in more persistent disruptions. The collaborative strategy consistently outperformed individual measures, producing the lowest peak delays, fastest recovery times, and stable delivery distributions. However, it also pushed the system closer to full utilization, implying increased operational intensity and potential vulnerability under compounded shocks. These findings align with resilience literature distinguishing between absorptive capacity (buffers) and adaptive capacity (rerouting), while extending the discussion by showing that joint application of measures can generate synergistic resilience effects.

From a practical perspective, the analysis suggests that port authorities should prioritize au-

tomation to enhance internal robustness, while logistics providers and carriers benefit more from flexible routing options. The collaborative strategy demonstrates the value of coordinated investment across stakeholders, yet also highlights the importance of governance mechanisms to manage the risks of high-intensity operations. Cost reflections indicate that while automation requires large upfront investments, rerouting-heavy strategies may impose higher variable transport costs, making trade-offs between capital expenditure and operational flexibility central to decision-making.

This study contributes to resilience research by conducting systemic risk analysis through a hybrid ABM–DES model and by integrating both absorptive and adaptive strategies within a comparative framework. While results are calibrated to the Port of Rotterdam, the methodological approach and conceptual insights are generalizable to other large multimodal ports, albeit with performance outcomes contingent on local infrastructural and regulatory conditions. Limitations include simplified operational processes, underrepresentation of customs and scheduling constraints, and the absence of a full cost–benefit model. Future research should extend the simulation with predictive routing algorithms, incorporate detailed economic evaluation, and integrate stakeholder-driven scenario weighting.

Overall, the findings show that resilience in port–hinterland systems is multi-faceted: infrastructure-oriented measures provide robustness, routing measures deliver adaptability, and buffering offers low-cost stability. The combination of strategies, particularly automation and rerouting, can yield superior resilience outcomes but at the cost of higher operational intensity. These insights provide both theoretical advancement and practical guidance for designing resilience strategies that balance performance, cost-effectiveness, and systemic robustness in complex port networks.

Table 2: List of Abbreviations

Abbreviation	**Full Term**
ABM	Agent-Based Model
AIS	Automatic Identification System
CPT	Cumulative Prospect Theory
DES	Discrete-Event Simulation
DSS	Decision Support System(s)
GCSN	Global Container Shipping Network
GIS	Geographic Information System
IQR	Interquartile Range
MCDA	Multi-Criteria Decision Analysis
MCDM	Multi-Criteria Decision-Making
PLE	Personal Learning Edition (AnyLogic)
PoR	Port of Rotterdam
PRF	Performance Response Function(s)
ROI	Return on Investment
SRITS	Sea–Rail Intermodal Transportation System
TEN-T	Trans-European Transport Network
TEU	Twenty-foot Equivalent Unit
TTR	Time-to-Recovery
VTS	Vessel Traffic System(s)

Chapter 1

Introduction

When a single container ship ran aground in the Suez Canal in 2021, it froze 12% of global trade and cost the European economy an estimated USD 73billion [1]. It was a vivid reminder that in a world where over 90% of trade by volume moves by sea [2], a disruption at one chokepoint can send shockwaves through supply chains worldwide. At the heart of Europe's maritime network lies the Port of Rotterdam; the continent's largest seaport. The port handles more than 14 million TEUs and over 440 million tonnes of cargo annually. Its strategic location and extensive hinterland connections via inland waterways, rail, and road make it a critical gateway for goods entering and leaving Europe. Beyond its operational scale, the port is an economic powerhouse for the Dutch economony, generating around 3.2% of the Netherlands' GDP each year [3].

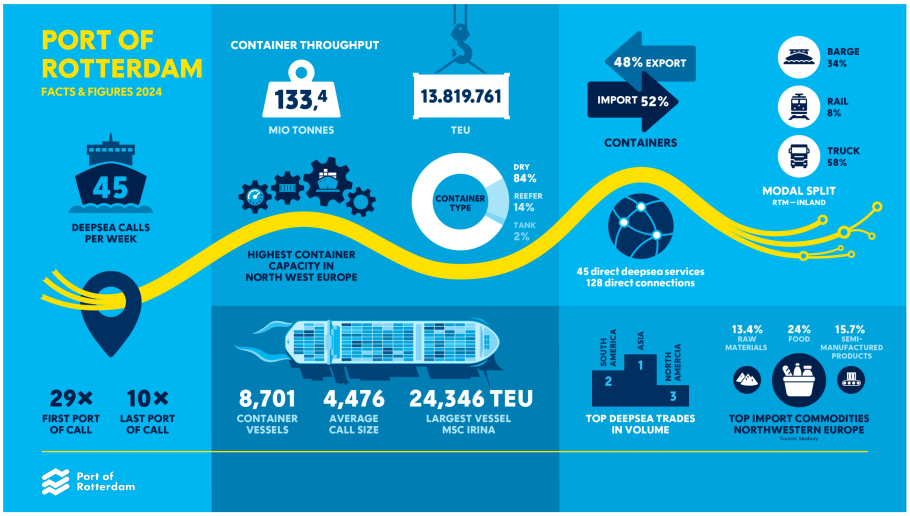

Figure 1.1: Annual container throughput of the Port of Rotterdam [4].

Recent systemic shocks have exposed the vulnerability of this highly interconnected network. The 2023 Red Sea crisis forced widespread vessel rerouting around the Cape of Good Hope, tripling shipping costs in the Netherlands and threatening a GDP contraction of up to 0.9% [5]. Low water levels on the Rhine caused by drought in 2022 reduced inland barge capacity by as much as 75%, leading to severe congestion at critical ports and increased transport costs [6]. Drought are becoming more frequent and the inland waterway transport sector is expected to start facing insurmountable problems associated with low water levels before the end of this century [7]. Recent disruptions in key maritime locations like the attacks on vessels in the Red Sea, drought-induced restrictions in the Panama Canal, and the ongoing Black Sea conflict have

caused sharp drops in vessel transits. Suez Canal traffic has fallen by up to 67%, while Panama Canal transits are down by 49%. These shocks not only disrupt global supply chains but also force higher vessel speeds to maintain schedules, potentially increasing greenhouse gas emissions on routes such as Singapore–Rotterdam by as much as 70% [8].

Moreover, recent crises such as the pandemic, raw material shortages, and disruptions like the war in Ukraine have severely disrupted EU firms' supply chains and exposed their dependence on foreign imports. A study by the European Investment Bank found that 37% of EU firms faced significant obstacles in accessing commodities and raw materials, while 34% were affected by logistics and transport disruptions [9]. With geopolitical tensions and global shocks on the rise, concerns over the security of Europe's economy are growing. This highlights the need for coordinated EU action to improve its resilience against global disruptions.

These events illustrate that ports are not isolated facilities but critical nodes in a complex, interdependent system of sea, port, and hinterland transport. Disruptions at one point in the chain can trigger cascading effects, also known as systemic risks, that propagate through shipping schedules, terminal operations, and inland transport connections. These amplify delays and economic losses far from the original point of failure [10, 11]. Despite growing recognition of these effects, most resilience planning in ports still focuses on localized operational improvements without fully addressing systemic vulnerabilities.

1.1 Problem Statement

The Port of Rotterdam, like other major ports, relies on tightly coupled systems. These include maritime access channels, terminal infrastructure, inland waterways, rail networks, road corridors, and digital coordination platforms. Local disruptions such as labor strikes, infrastructure breakdowns, and climate-induced droughts, directly impact throughput performance and service reliability. Global disruptions on the other hand, can rapidly shift cargo volumes, alter arrival patterns, and overwhelm specific modes or facilities. When these shocks interact, bottlenecks can escalate into widespread performance degradation across the port–hinterland system. The port's ability to withstand or recover from the impact of such disruptions can be key to its competitive position in global trade.

Current research has primarily examined the technical performance of resilience measures in isolated subsystems, such as berth scheduling or yard management. However, there remains a significant gap in understanding how systemic risks emerge from in- and external disruptions, how they propagate through interconnected sea, port, and land operations, and how different resilience strategies influence overall recovery. This study addresses this gap, by evaluating resilience strategies using a hybrid simulation approach that captures both process-level logistics flows and actor-level adaptive decision-making across the full port–hinterland network.

1.2 Research Objective and Questions

The objective of this research is to identify and evaluate resilience strategies that can reduce systemic risks in port operations. This is achieved through simulation modeling of the Port of Rotterdam and its hinterland network under varied disruption scenarios, assessing both the effectiveness and cost-efficiency of different strategies.

Main research question: How can systemic risks in port operations be minimized through resilience-based strategies, identified via a simulation of port disruptions and recovery?

Sub research questions:

- What are the systemic risks and types of disruptions associated with port operations?

- What resilience strategies can mitigate systemic risks in ports, including their sea-, land-, and port-side operations?
- How can simulation modeling be used to evaluate resilience improvement strategies and the impact of disruptive scenarios in port operations?
- How can performance-based metrics from simulations be used to assess systemic resilience in port operations?
- How can the cost-effectiveness of resilience strategies be assessed in terms of systemic risk reduction and investment or operational costs?

Understanding how different resilience strategies influence systemic risk could help port authorities make informed decisions on infrastructure investments, operational changes, and policy development. By identifying measures that limit disruption spillover effects, logistics operators can improve service continuity under stress. The results could also provide evidence-based guidance for policymakers seeking to strengthen the resilience of Europe's maritime gateways.

This research reflects the core of the Management of Technology discipline, where the integration of technological capabilities with strategic decision-making drives competitive advantage. Seaports such as Rotterdam operate in an environment defined by high uncertainty, tight interdependencies and intense global competition. In this context, the ability to leverage digital tools like advanced simulation models becomes a strategic asset.

By using hybrid agent-based and discrete event simulations, this study demonstrates how technology can be applied not only to understand complex operational dynamics, but also to test and refine resilience strategies before they are deployed in reality. These digital tools allow decision-makers to anticipate cascading effects of disruptions, evaluate alternative investment and operational scenarios, and choose solutions that balance efficiency, cost, and robustness.

For a port like Rotterdam, such capabilities can translate directly into improved competitiveness. Faster recovery from disruptions, optimized utilization of infrastructure and data-driven coordination with stakeholders can strengthen its role as Europe's primary logistics hub. This aligns with the MoT vision of using technology as a corporate resource, and by linking technological innovation to strategic objectives, the research offers actionable insights not only for port authorities, but also for the global supply chains that depend on them.

Chapter 2

Literature Review

This chapter reviews existing knowledge on disruptions in nautical supply chains, the resilience strategies developed to address them, and the simulation-based methods used to evaluate performance under systemic shocks. It first examines the types and characteristics of disruptions affecting ports and how these propagate through interconnected maritime and hinterland networks. From there, it discusses resilience definitions and mitigation strategies identified in prior studies.

The chapter then assesses simulation modeling as a decision-support tool for resilience evaluation, comparing methodological approaches and their suitability for capturing complex, system-wide interactions. This includes identifying how different methods vary in their ability to represent both process-level logistics dynamics and actor-level adaptive behaviors.

Finally, the review identifies key gaps in the literature, including the tendency to focus on isolated subsystems rather than the integrated sea–port–land network, and the limited application of scenario-based, comparative assessments across multiple disruption types. These gaps form the basis for the research objectives and questions guiding this study.

By establishing the conceptual and methodological context, this chapter positions the research within the broader academic and practical discourse on port resilience. It connects theoretical frameworks, empirical findings, and technological developments to the specific aim of evaluating resilience strategies through holistic, simulation-based analysis—bridging the gap between abstract resilience concepts and actionable, system-wide interventions.

2.1 Disruptions in Nautical Supply Chains

The global container shipping network (GCSN) is a highly interconnected and complex supply chain, where local disruptions can trigger cascading effects across global trade routes and hinterland connections [10, 12, 13]. When capacity at major ports is reduced, vessels may be rerouted to alternative ports, causing congestion in multiple parts of the network and delays that propagate both upstream and downstream [14–16]. These ripple effects and can result in significant economic losses and systemic shocks, as demonstrated by the 2021 Suez Canal blockage, which was estimated to have cost the European economy around USD 73 billion [1, 5]. Similar impacts have been observed in recent disruptions to shipping routes in the Red Sea, which have caused large-scale shifts in global container flows [14, 17]. This highlights the importance of resilient port infrastructure and operations, as it can lead to an increased competitive advantage in these circumstances over ports which are less prepared [18].

A wide range of external and internal disruptions relevant to port resilience are identified in

existing literature. Prolonged droughts and low water levels significantly reduce the capacity of inland waterways [19], and their occurrence is expected to rise due to climate change [20–22]. Coastal flooding has been identified as the largest hazard to ports in north-western Europe [23], while extreme weather events such as storm surges can disrupt yard operations, vessel access, and quay handling [24]. Geophysical hazards, such as earthquakes or tsunamis, are rare but can cause widespread damage to port infrastructure, leading to long recovery times [25].

Internal operational disruptions can arise from equipment breakdowns, infrastructure damage, or workforce-related issues. Labor strikes are a prominent example, directly reducing quay crane availability, gate processing speeds, and yard handling capacity [26]. Studies also highlight the coupling between external shocks and internal failures: changes in the external environment can trigger or exacerbate internal operational risks, creating complex propagation pathways for disruption [27]. These internal risks, ranging from technical and facility failures to IT disruptions, are direct threats to system stability. Cyberattacks, for instance, can disable routing systems and halt terminal operations, while pandemics affect both capacity, through reduced labor availability, and demand, through changes in trade flows [28–30].

In the literature, disruptions are often classified according to their origin, whether external or internal, their primary effect on capacity or demand, and their scope and duration [31, 32]. External disruptions, such as droughts or route blockages, tend to constrain specific transport modes or lead to periods of demand fluctuations. Internal disruptions, such as strikes or equipment failures, directly reduce operational capacity at port facilities. The severity and frequency of these events vary widely, from frequent, short-term incidents like crane breakdowns to rare but high-impact events such as geopolitical conflicts or major infrastructure damage.

2.2 Port and Supply Chain Resilience

In order to measure and improve resilience, it must first be clearly defined within the port and supply chain ecosystem. In the context of maritime logistics, resilience encompasses multiple dimensions, including the ability to absorb shocks, maintain essential functions, adapt to changing conditions, and recover to a stable state [33] (Figure 2.1).

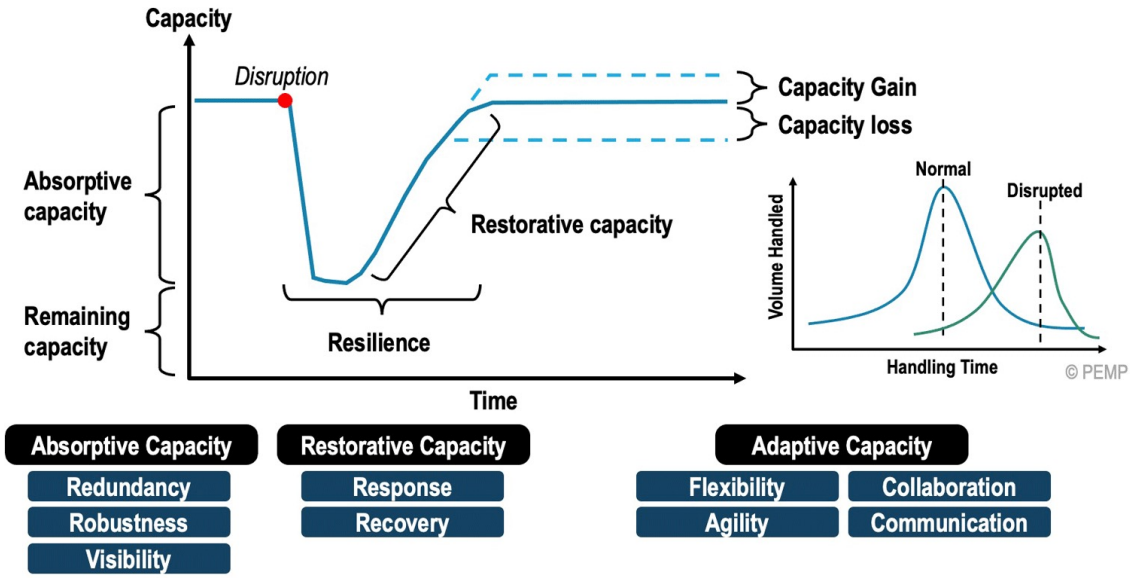

Figure 2.1: Different aspects of resilience in port systems [33].

The way resilience is conceptualized in maritime logistics varies across studies [34]. Some works define resilience through structured frameworks, such as the triplet approach of disruption, functionality, and performance [35], while others classify it into dimensions such as robustness, vulnerability, redundancy, and rapidity, supported by indicators including downtime duration, flexibility, network connectivity, and congestion impacts [36].

Alongside conceptual definitions, a variety of methods are used to operationalize and measure resilience. Probabilistic modelling, simulation-based analyses, and indicator-driven frameworks are common approaches [35–38]. For example, [37] develop a hybrid multimodal simulation that integrates AIS data with a VISSIM-based microscopic traffic model to monitor port throughput, vessel queuing, and traffic flow resilience. Similarly, [38] present a simulation-based model for LNG terminals using P-graph models, Markov chains, and PRF to analyse disruption impacts and predict recovery times.

These studies highlight that resilience in maritime logistics can be assessed through various dynamic performance indicators. Commonly used measures include queue lengths, delay durations, and utilization rates of critical resources such as cranes, transport modes, and storage facilities, tracked over time. These indicators capture a system's capacity to absorb, respond to, and recover from disruptions, while also reflecting changes in operational efficiency during both disruption and recovery phases. Comparing such metrics across different disruption scenarios and resilience strategies allows researchers to evaluate how effectively a port system maintains functionality and adapts under stress.

Improving port resilience benefits a wide range of stakeholders within the port ecosystem. These include transport firms, port labor, local manufacturing industries, end-users of port services, environmental groups, residents, and various levels of government [39]. As the global shipping network becomes more complex, the ability to absorb and recover from disruptions has become increasingly critical [40]. Recent studies have identified several factors that heighten the risk of system failure, including mismatches between technological innovation and system capacities, shortages of warehouse or yard space, and equipment breakdowns [27]. These vulnerabilities underscore the need for targeted strategies that either reduce the system's vulnerability to disruptions, enhance its capacity to adapt, or improve recovery after shocks.

Empirical and simulation-based studies show that enhancing port resilience requires coordinated stakeholder action, proactive planning, resource readiness, and the flexibility to adapt governance and operations during disruptions [40]. Integrated planning, digital transformation, and strong stakeholder relationships enable swift and collective responses to both sudden shocks and long-term changes [33]. These concepts define broader categories which encompass different improvement strategies.

The development of transshipment hubs and hinterland terminals, including sea–rail intermodal transportation systems (SRITS), is a widely discussed resilience strategy for ports. These facilities act as intermediate nodes where cargo can be stored or transferred between transport modes, helping to maintain throughput during localized bottlenecks by redistributing flows away from congested port areas [41, 42]. Examples such as the inland terminals in Alblasserdam [43] and Alphen aan den Rijn [44], as well as proposed projects like the Valburg rail terminal on the Betuwe route [45], demonstrate their potential to relieve pressure on main ports, enhance connectivity, and support modal shifts from road to rail. Effective implementation requires minimizing transshipment costs, selecting strategic locations, ensuring seamless integration with other transport modes, and coordinating operations between ports, railways, and logistics providers [46, 47]. Additional measures, such as reconfiguring terminal layouts, developing rail-connected dry ports, and implementing advanced information systems, can further improve scheduling, equipment allocation, and cargo routing. While inland waterway transport offers high efficiency and environmental benefits compared to road transport, it remains

vulnerable to climate-induced hazards such as low water levels [19, 48].

For high-frequency events, possible measures include temporary capacity boosts and small-scale rerouting [49]. Strategic buffering and yard capacity management have also proven important in both empirical studies and simulation experiments. Creating buffer zones at critical nodes—such as quay areas, inland terminals, or modal hubs—can absorb temporary surges in congestion and prevent delays from propagating through the network. Such buffers can take the form of additional capital equipment (e.g., cranes, dredging equipment, forklifts, reach stackers), redundant facilities (e.g., backup berths, gates, inland terminals with multi-carrier rail access), and energy infrastructure redundancy (e.g., backup generators, fuel storage). Preventive maintenance programs and strong safety management procedures further strengthen absorptive capacity by reducing the likelihood of operational breakdowns during disruptions. Simulation results indicate that adequate yard capacity and container storage space significantly improve a port's resilience by reducing the likelihood that local disruptions escalate into systemic failures [50].

Operational flexibility can also be improved through dynamic rerouting, where cargo flows are reallocated in real time to alternative routes or modes when the primary path is blocked or congested. This may include alternate routing to other transport modes, such as rail if waterways are blocked, or strategic alliances with nearby ports to allow vessel redirection during disruptions. Simulation studies have shown that rerouting can balance loads across the hinterland network and maintain service levels, though its success depends on the availability of alternative capacity and the speed of operational decision-making [50].

Some strategies involve capital-intensive infrastructure and vessel adaptations. Physical modifications such as waterway dredging, reduced vessel drafts, and expanded storage capacity can help mitigate the impacts of extreme weather events, particularly prolonged droughts [7, 51]. These measures expand the operational envelope of inland waterway transport, though their high cost and long lead times often necessitate integration with broader infrastructure investment plans.

Finally, digital tools and automation have emerged as cross-cutting enablers of many resilience measures. Technologies such as Vessel Traffic Systems (VTS) [52], Decision Support Systems (DSS), and digital twins [53] provide real-time monitoring, predictive analytics, and coordination capabilities to support rerouting, buffer management, and slot allocation. Automation of port facilities such as quay cranes and yard trucks can help maintain operations during labor disruptions, though it may introduce new vulnerabilities towards cyberattacks [28, 29].

Overall, these strategies vary widely in investment or operational costs, implementation time, and suitability for different disruption profiles. Their integration in this complex system, rather than isolated application, offers the strongest potential for systemic resilience.

2.3 Simulation Modeling for Resilience Assessment

Simulation modeling is a key tool for evaluating how ports respond to disruption scenarios and for testing the effectiveness of different resilience strategies before real-world implementation. In recent years, the maritime resilience research landscape has expanded to include a wide range of approaches, including multi-criteria decision-making (MCDM), mathematical modeling, simulation-based approaches, Bayesian methods, graph theory, and risk management techniques [36, 54, 55]. Each of these methods offers distinct advantages depending on the research focus: for instance, probabilistic models such as Bayesian networks are well-suited to estimating the likelihood and consequences of disruptions [56], while network-based approaches using graph theory are effective in mapping connectivity and identifying critical links in port–hinterland systems [57].

Data-driven methods have also gained prominence, leveraging real-time and historical information to assess system performance. For example, AIS data has been used to evaluate the resilience of global liner shipping networks by examining how traffic flow disruptions and network fragmentation affect overall system performance [58]. Hybrid approaches have emerged that combine such data with microscopic traffic simulation to model congestion dynamics within ports and their surrounding transport infrastructure [37]. At the operational level, digital decision support systems (DSS) and digital twins have been applied to enable real-time monitoring and adaptive control of port operations [53], although some studies have shown that purely deterministic models can overestimate resilience by failing to capture stochastic and behavioral variability [50]. In parallel, more specialized simulation models—such as the agent-based nautical traffic model for the Port of Rotterdam [59]—have been developed to represent the interaction between operational actors (ships, pilots, tugboats, and port authorities) under varying conditions.

When assessing port resilience, the choice of simulation method is crucial, as it shapes the level of detail, the types of disruptions that can be modeled, and the ability to represent both system-wide processes and the adaptive behavior of individual actors. Graph theory, one of the most established approaches, models port and hinterland networks as nodes and edges, allowing researchers to evaluate routing efficiency, redundancy, and vulnerability to link failures [57]. However, on its own it cannot capture dynamic operational processes or behavioral adaptations without integration into other frameworks. Bayesian networks, by contrast, model probabilistic dependencies among variables, making them valuable for decision-making under uncertainty [50]. Yet, they lack spatial and behavioral representation, which limits their capacity to simulate operational responses to disruptions.

Agent-Based Modeling (ABM) addresses this gap by explicitly representing heterogeneous and autonomous actors, each with individual objectives, constraints, and adaptive behaviors [59, 60]. This makes ABM particularly suitable for resilience studies where emergent system behavior arises from decentralized decision-making, such as rerouting in response to congestion or resource shortages. It is often used to measure recovery and adaptation capacities of resilience, where organizational components play a significant role [61]. Discrete Event Simulation (DES), one of the most widely used methods in logistics and terminal operations, excels at modeling queues, service processes, and shared resource utilization, but does not inherently capture the adaptive decision-making of individual actors.

A recent study has compared mainstream modeling methods for maritime simuation models [62]. Monte Carlo models are often used to generate random traffic flows and evaluate maritime traffic conditions, providing a baseline for traffic and navigation path generation. However, they are rarely applied in isolation, as they lack detailed operational representation. Cellular automata are well-suited for simulating nonlinear traffic phenomena with simple evolution rules. This makes them easy to program and computationally efficient, but they often neglect navigational elements and can suffer from inconsistent accuracy. Multi-agent models have been applied to simulate global shipping networks and study the adaptability of individual actors, though they can involve long computation times and complex programming. Finally, combinations of system simulation and mathematical modeling allow the strengths of multiple approaches to be leveraged, producing targeted solutions for specific problems, but at the cost of limited general applicability.

Given these characteristics, recent literature increasingly supports the use of hybrid simulation approaches for port resilience assessment [59, 62]. By combining ABM with DES, it is possible to capture both the micro-level decision-making of individual actors and the macro-level process flows and capacity constraints that shape system performance. ABM provides the flexibility to model autonomous responses to disruptions, while DES ensures that operational bottlenecks,

queue dynamics, and resource availability are realistically represented. This integrated perspective is particularly valuable for analyzing systemic shock propagation and recovery across complex port–hinterland networks.

2.4 Gaps in Existing Literature

While the literature on port resilience has grown substantially in recent years, several important gaps remain. Many existing studies focus on individual components of the port–hinterland system without fully capturing the interdependencies between sea, port, and land transport. This fragmented perspective limits the ability to assess how disruptions propagate across the entire logistical chain. As a result, cascading failures, where a disturbance in one subsystem triggers performance losses in others, are often overlooked or only partially represented [33].

Another gap lies in the mismatch between the diversity of disruptions observed in reality and the scope of scenarios modeled in research. Although the literature identifies a wide range of external and internal hazards, which range from climate-induced water level changes to labor strikes and cyberattacks [33, 35], most simulation-based studies examine a narrow subset of these. They frequently focus on single-mode disruptions or short-term operational disturbances [50]. This narrow scope constrains the generalizability of findings and may underestimate systemic vulnerability, especially when multiple hazards interact.

From a methodological perspective, the choice of modeling approach also introduces limitations. While methods such as graph theory [63], Bayesian networks [50], and discrete event simulation [64] provide valuable insights into specific aspects of port operations, they often lack the capacity to integrate both process-level logistics dynamics and actor-level adaptive behaviors within the same framework. Hybrid approaches that combine agent-based and process-based simulation have been used in the past but remain underapplied in studies that evaluate resilience across the full sea–port–land interface [36, 62].

Finally, although numerous resilience strategies have been proposed, which include modal diversification, buffer capacity, dynamic rerouting, and digital decision support [36, 38, 54], comparative assessments across multiple disruption types are scarce. Many strategies are evaluated in isolation or under a single disruption scenario, making it difficult to determine how their effectiveness varies under different conditions. This lack of systematic, scenario-based comparison limits the practical guidance that research can offer to policymakers and port authorities.

Addressing these gaps requires a holistic modeling approach that: (i) spans the full port–hinterland chain to capture cascading effects; (ii) incorporates a diverse set of disruption scenarios that reflect both external and internal risks; (iii) integrates actor-level decision-making with system-level process flows; and (iv) systematically compares alternative resilience strategies across different disruption contexts. The present study responds to this need by developing a hybrid agent-based and discrete event simulation of the Port of Rotterdam, designed to evaluate the performance of multiple resilience strategies under varied disruption conditions, with a focus on minimizing systemic shocks and enhancing recovery capabilities.

Chapter 3

Research methodology

This chapter outlines the methodological framework used to evaluate the resilience of the Port of Rotterdam's transport system under disruptive conditions. Building on the literature review, the methodology combines a quantitative, simulation-based exploratory case study with scenario-driven experimentation. This chapter starts by explaining the research design, followed by a description of the simulation model flow and logic. The calibration and validation method is then described followed by the data collection and model input calculation methods. This will also cover the different disruptive scenarios and mitigation strategy settings. Lastly, this chapter will conclude by outlining the performance analysis methods.

3.1 Research Design

Building on identified gaps in literature, this research adopts a quantitative, simulation-based exploratory case study of the Port of Rotterdam. As Europe's largest and most interconnected seaport, Rotterdam provides both the scale and data availability needed to analyse how disruptions propagate across maritime, port, and hinterland transport systems. The quantitative design enables the evaluation of resilience strategies against measurable performance indicators, ensuring objective and comparable results across scenarios. A hybrid agent-based and discrete event simulation is employed to capture both the adaptive behaviors of heterogeneous actors and the process-level logistics flows that shape system performance. This combination is well-suited to replicating the port's complex and interdependent operations, while systematically testing alternative operational strategies under controlled and repeatable conditions. The overall research design is illustrated in Figure 3.1.

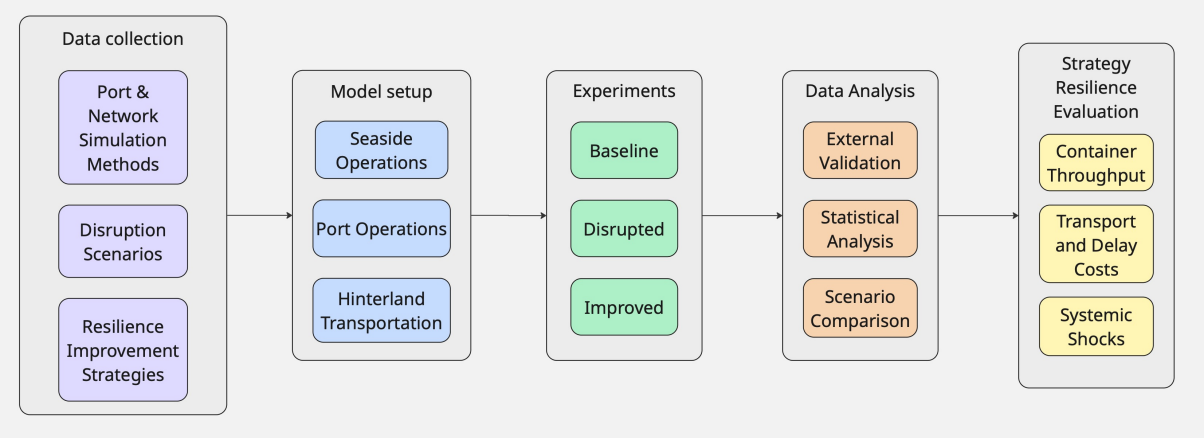

Figure 3.1: Overall Research Design: from Data Collection to Strategy Evaluation.

The scope of the study is defined by different disruptive events with varying durations. This ensures that detailed operational analysis is possible on different timeframes, capturing the real-life variability of disruptions to maritime supply chains. The unit of analysis is the flow of containers across sea-side arrivals, port-side handling operations, and inland transportation up to the national border. The geographical scope is restricted to the Netherlands to focus on national strategic improvement, with international flows represented by aggregated nodes at the network's periphery. Within these boundaries, the model captures both the port's internal handling operations and its dynamic interactions with road, rail, and inland waterway infrastructure.

The research process begins with the development and calibration of a baseline simulation model that reflects real-world operating conditions. Calibration is carried out using empirical data from academic literature, port authority publications, industry reports, and public logistics datasets. Where precise empirical values are not available, parameters are estimated using ranges derived from comparable studies or sector benchmarks, ensuring that the model remains based on realistic performance ranges. Once the baseline is established, three disruption scenarios are implemented, each chosen for its operational relevance, diversity of impact mechanisms, and feasibility of representation in the simulation environment. These include a drought scenario affecting inland waterway capacity, a labor strike scenario reducing port handling capacity, and a sea route change scenario producing demand fluctuations.

Each disruption scenario is paired with targeted mitigation strategies, namely dynamic rerouting, inland transshipment hubs, storage capacity expansion, and autonomous facility upgrades. Synergistic benefits are also explored by combining different strategies. These strategies are built into the model as changes to operational logic, resource availability, or infrastructure capacity. This allows their performance to be evaluated under realistic stress conditions. The effectiveness of these interventions is measured using a set of performance indicators, including time to recovery, port delays, utilization rates of critical resources, and delivery rate distributions.

The model is implemented in AnyLogic, using a hybrid approach that combines agent-based modeling to capture the autonomous behavior of transport actors and discrete-event modeling to represent the sequential, resource-constrained processes of port operations. By combining empirical calibration, scenario-based experimentation, and structured performance evaluation, this research design provides a reproducible and transparent framework for identifying effective resilience strategies in complex maritime logistics networks.

3.2 Simulation Model

This section outlines the structure and functionality of the simulation model developed to analyze the resilience of the Port of Rotterdam's transport system. The model integrates sea-side, port-side, and hinterland operations within a single environment, enabling the study of disruption propagation and the evaluation of mitigation strategies. By implementing this in AnyLogic using a hybrid agent-based and discrete-event approach, it captures both the autonomous decision-making of transport actors and the sequential, resource-constrained processes of port handling. The model is parameterized using empirical data from different sources, like port authority records, industry reports, and academic literature. Assumptions are carefully applied where direct measurements are unavailable. The following subsections describe the model's flow structure, operational logic, and transport network configuration. These together form the foundation for the scenario experiments and performance evaluation.

3.2.1 Simulation Tool Selection

The literature review highlighted that no single simulation method can adequately capture both the operational processes and the adaptive decision-making that drive resilience in port–hinterland systems. Approaches such as discrete event simulation (DES) excel at modeling process flows, capacity constraints, and queuing dynamics, while agent-based modeling (ABM) is better suited to representing the autonomous, adaptive behaviors of individual actors. Given the need to assess systemic risks across the entire sea–port–land interface, a hybrid ABM–DES approach offers the most comprehensive framework. It enables the integration of macro-level operational modeling with micro-level behavioral adaptation.

In this study, the ABM component represents decision-making by transport actors, including inland barges, trucks, and freight trains, while the DES component models the flow of cargo through port terminals and inland facilities, accounting for queues, processing times, and resource constraints. This combination enables a holistic assessment of both behavioral and operational aspects of resilience.

To implement this, AnyLogic was selected as the most suitable modeling environment. First, it supports hybrid simulation, allowing ABM and DES to run within a single simulation framework, which is essential for capturing both system-level process flows and individual actor behaviors. Second, it supports dynamic parameter changes during simulation runs, enabling the modeling of disruption events and adaptive responses in real time. Third, AnyLogic's visual development tools and advanced animation capabilities facilitate efficient model construction and produce clear, communicative simulation outputs. This makes it well-suited for decision-support in complex domains such as maritime logistics and supply chain resilience.

3.2.2 Model Flow Structure

Vessel Generation

The model generates vessels according to a probabilistic distribution of ship classes, reflecting realistic arrival patterns at the Port of Rotterdam. Each vessel's capacity in TEU is sampled based on its type, which also determines its handling time and arrival frequency. Arrival delays are proportional to vessel size, ensuring that larger ships have longer intervals between arrivals. Disruption events modify the scaling factor for arrival intervals, allowing simulation of reduced or increased arrival rates during specific disruption periods. The detailed vessel generation algorithm is provided in Appendix C1.

Port Operations Design

After generating the right amount and size of vessels, they need to be processed through the port infrastructure. This infrastructure will first have to be set-up according to real-world data. A study by [65] reported that the processes which different port actors carry out are inter-dependent. The authors identified three types of inter-dependencies, which are serial (precedence of a process), reciprocal (mutual resource exchange among processes) and pooled inter-dependency (sharing a resource between processes). To capture these dependencies and operational dynamics of a seaport within the simulation environment, the system was modeled using a DES structure. This structure simplifies the system to a series of sequential and resource-constrained port activities. Vessel agents entering the port engage in a series of queue-based processes, where they must seize limited resources such as tug boats, quay cranes, yard trucks, and storage space to complete their unloading, transshipment, and departure operations.

Figure 3.2: Sea-side vessel stages. [66]

An example of the different stages a container ship goes through can be seen in figure 3.2 and 3.3, which were obtained from recent studies [66] [67]. Before berthing, container vessels receive pilots and tugboats to assist them in entering the port area. It was found that tugboat availability is the most critical at this stage [66]. When they are moored and secured to the quay, cranes start unloading the ship. The cargo is transport to and from short-term buffer storage at the terminal by overhead cranes or yard trucks. Cargo is further transported to the gates which function as the gateway towards the hinterland transportation network.

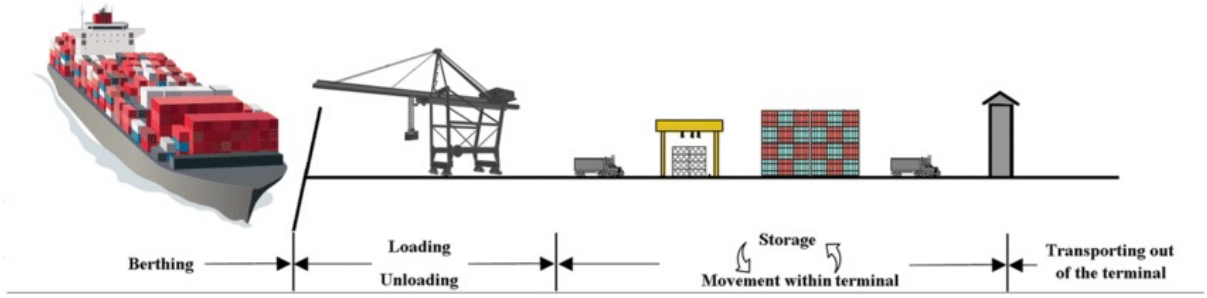

Figure 3.3: Port-side vessel stages. [67]

Each of these resources or facilities used within the port system introduce specific delay times based on the size of the vessel and their accompanying cargo size, which reflects typical operational bottlenecks. The required amount of facilities, like cranes or yard trucks, is also decided by the size of the arriving vessel. This design allows the simulation to account for congestion and competition among vessels for shared facilities, and the analysis of the level of facility utilization.

Hinterland Gate and Transport Network Design

After being unloaded from their vessels, containers are transferred to buffer storage areas before being dispatched to their respective hinterland destinations. The hinterland transportation network is modeled as a system with two primary capacity-limiting stages.

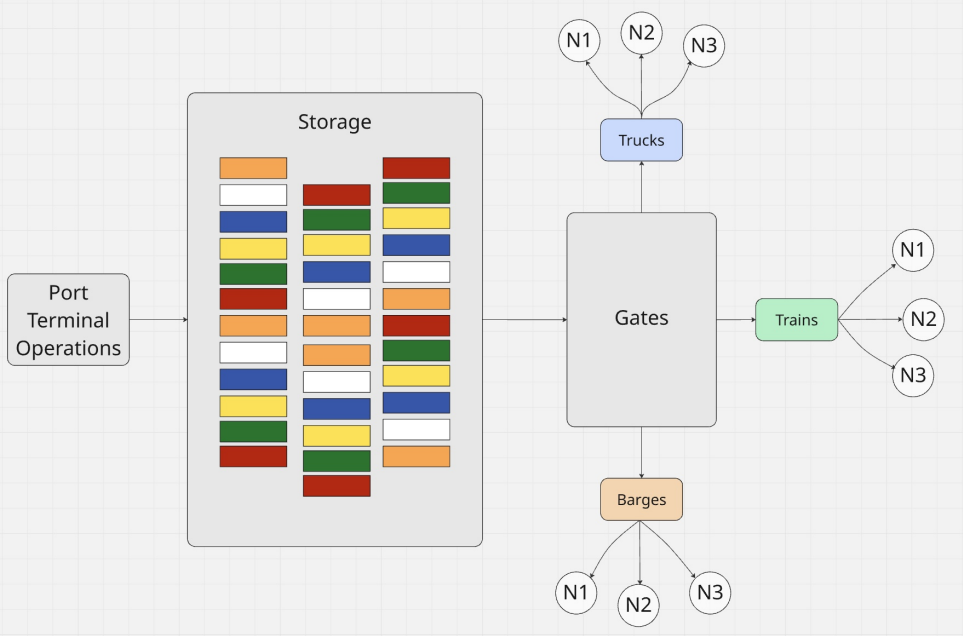

Figure 3.4: Simplified overview of port and hinterland flow.

First, containers are assigned to a transport mode based on the modal split settings. From there, they enter the network via dedicated terminals or gates, each modeled as a queuing system with limited handling capacity. Before entry, the system checks whether sufficient capacity is available at the selected hinterland gate and, if relevant, within the inland network. The logic behind this can be seen in figure 3.5. When rerouting is disabled the check is mode-specific: a shipment is blocked if the assigned mode's terminal or its in-transit capacity is at the limit. When rerouting is enabled, a shipment is only blocked if all modes and their in-transit capacities are simultaneously at their limits. This distinction captures the operational flexibility of multimodal routing while respecting network constraints. The detailed blocking conditions are provided in Appendix C2.

Once a container has been granted access to the hinterland transport network, it enters a routing sequence in a certain transport mode. This sequence includes decision points that determine whether the container remains in its assigned mode queue, is rerouted to an alternative mode, or waits until conditions improve. The process begins with an initial decision block, which checks rerouting status and evaluates queue capacities and destination reachability for barges, trucks, trains or, if activated, the inland hub. Containers are only rerouted if the primary mode is congested and at least one alternative mode with available capacity can reach the same destination. Containers unable to proceed are sent back to the initial decision step to await improved conditions.

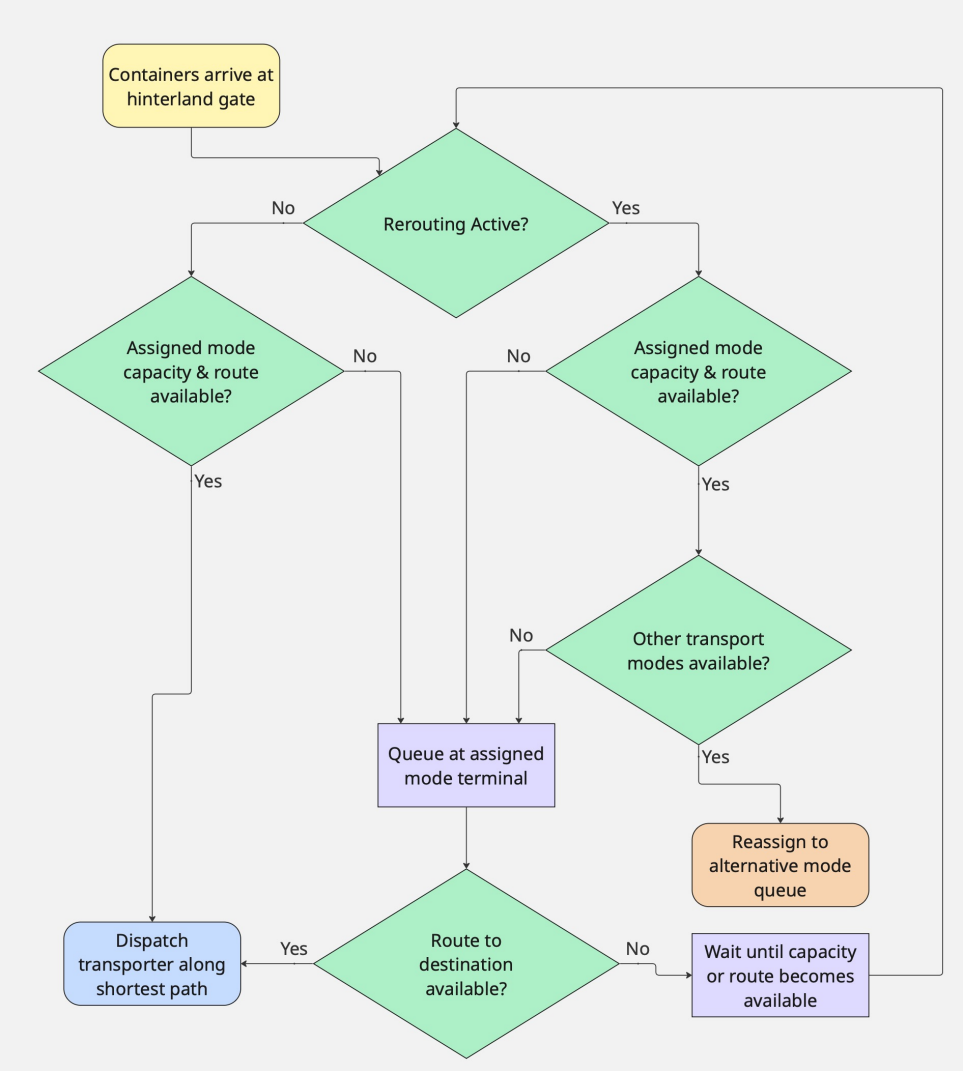

Figure 3.5: Hinterland gate decision-making logic.

After selecting a mode and entering its network queue, containers undergo a final route availability check. Here the system checks if the routes to the specific destination of that transporter are not blocked, and if so it queues the containers to await availability.

Once transporters are assigned and dispatched, they traverse the network by selecting the shortest available route to their destination. Routing within the hinterland transport network is performed using the findShortestPath() function from the AnyLogic Material Handling Library, which applies a shortest-path search consistent with the Dijkstra algorithm [68]. The transport agent then does does a series of checks and makes routing decisions depending on the conditions, the logic for this can be seen in figure 3.6. If no viable route is available due to congestion in the network or through the specific gate reaching its capacity limits, the transporter will block the specific transport mode and destination combination. It will then return to the queue at the network and wait for available routes. This means that the individual transport agents decide on their own if the a route is available, and give a signal to the other transporters with the same destination that there are no routes available. An agent unblocks its route after transport has been completed, allowing new transporters to enter the network. This structure allows the model to capture congestion at multiple levels: during modal allocation at the terminal and within the transportation network itself.

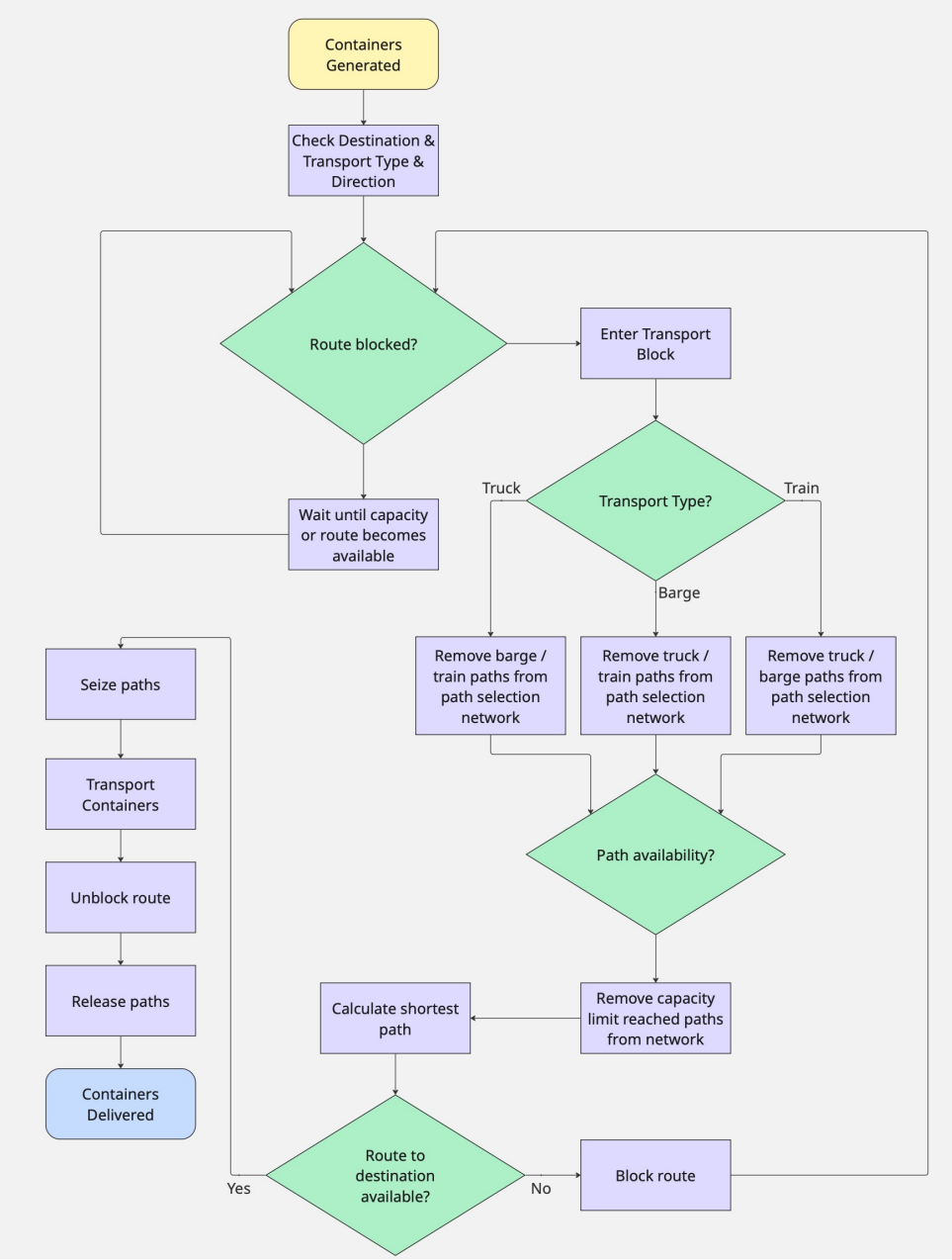

Figure 3.6: Transporter decision-making logic at network entry.

This structure enables the model to capture congestion effects at multiple levels: during modal allocation at terminals and within the transportation network itself. This is important to properly reflect real-world operations of port supply chains, where congestion can occur within the port as well as on mode-specific routes after leaving the port infrastructure.

3.2.3 Transport Network Design

Now that the containers leave the port, they enter the Dutch hinterland transport network through their respective transport modes. The hinterland transport network is modeled as a spatial graph of nodes and edges, where nodes represent terminals or hinterland destinations and edges represent modal connections (road, rail, or inland waterways). The spatial configuration and connectivity are based on official Port of Rotterdam infrastructure data [69] to ensure realism in network topology. This structure enables analysis of multimodal capacity constraints

and congestion dynamics across the full hinterland interface. This gives the model a strong basis of existing real-world infrastructure, which should contribute towards realistic performances.

Figure 3.7 presents the modeled hinterland transport network used in the simulation, based on official infrastructure data visualized through the RoutePlanner platform of the Port of Rotterdam. The network is designed to represent multimodal connectivity between the port and inland destinations across the Netherlands.

The data contains two of the key transport modes, namely the waterway and rail paths. The truck transport paths are not directly listed in the data, but its infrastructure can be seen on the map. The road paths can be set-up by following large Dutch high- and motorways. Each transport mode is represented through a graph-based structure of nodes (locations) and edges (transport connections). The port itself is modeled as a single location node with in- and outbound flows to the hinterland. In order to keep the analysis focused on national strategic improvement, only connections within the Dutch territory are included. Locations around the border of the Netherlands are used as representative entry and exit points, simulating international trade inflows and outflows while keeping the model scope centered on domestic infrastructure.

The simulation has three transport modes modeled with distinct operational characteristics to reflect their real-world behavior in the hinterland network. For each mode, vehicle agents are defined with specific load capacities and average speeds derived from reference values in port logistics studies. Truck and barge movements follow continuous flow logic, where a minimum distance between transporters is maintained based on predefined length settings and headway rules. This ensures congestion effects are realistically captured. Train transport is modeled using capacity densities extracted from the TEN-T rail network data. Fleet capacities for each mode are calculated by aggregating the theoretical throughput of all relevant network paths, based on the infrastructure length and capacity densities.

Figure 3.7: Hinterland transportation network in AnyLogic, based on existing routes from PoR Routeplanner.

The Port of Rotterdam is represented by the central terminal node `T1`, from which all inland transportation flows originate. Surrounding this are nine destination nodes labeled `N1` to `N9`, which are strategically positioned along the national border to represent international and domestic hinterland access points.

Three distinct transportation modes are visualized using color-coded dashed lines:

- **Inland waterways** (orange dashed lines): Represent navigable river and canal routes used for barge transport.
- **Rail infrastructure** (green dashed lines): Show the rail corridors used for freight train movements.
- **Road connections** (blue dashed lines): Indicate the national highway system used for truck transport.

In addition, grey dashed and filled lines denote dummy paths used for the routing logic. These

paths do not represent physical infrastructures but serve functional purposes within the simulation framework. Together, this network forms a spatially bounded, multimodal routing environment through which transportation flows are modeled.

3.2.4 Limitations

The simulation model was developed using the Personal Learning Edition (PLE) of AnyLogic, which imposes several technical constraints that influence the scale and complexity of the study. Most notably, the PLE limits models to 50,000 dynamically generated agents and 200 building blocks, restricting both the number of agents that can be represented and the modularity of flows within the model. This required compact modeling structures and a minimization of block usage, making the inclusion of more detailed internal port operations challenging. The limit on dynamically generated agents also constrains how frequently the model can execute routing decisions. Because the decision-making logic destroys the original agent and creates a new one in the target mode when switching transport modes, excessive mode switching during a simulation run could cause the agent cap to be reached before the experiment finishes. This same restriction also limits the total container demand that can be generated during a run, which in turn constrains the maximum severity of disruption scenarios that can be realistically modelled without further simplification of volumes.

Routing capabilities are restricted to shortest-path algorithms, preventing the exploration of more adaptive or probabilistic routing strategies that might lead to different congestion patterns and resilience outcomes. In addition, the PLE version lacks database connectivity (e.g., SQL, Excel), does not support custom Java classes or external libraries, and omits advanced GIS functionality such as shapefile integration. Models cannot be exported as standalone applications, run on more than one CPU core, or simulate more than five hours per run, which meant that facility and transport speeds needed to be scaled to represent a simulation period of 30 days. While these constraints do not prevent the model from generating meaningful insights, they do set clear boundaries on the behaviours and scenarios that can be tested. A full AnyLogic license would allow for more complex routing logic, dynamic data integration, and expanded scenario capabilities.

3.2.5 Assumptions

To ensure the simulation remains tractable while focusing on key dynamics of port resilience, several assumptions are made in the model. First, route selection for hinterland transport is based on the shortest path among the available routes, without accounting for congestion-aware rerouting or real-time optimization. This simplifies computational complexity but may underestimate the benefits of more adaptive routing strategies in mitigating congestion effects. The port itself is modeled as a sequence of queuing systems, where resources such as tugboats, cranes, and yard trucks are allocated based on availability and capacity constraints. While this captures bottlenecks effectively, it abstracts away from the finer operational details, meaning results should be interpreted at a systems level rather than as predictions of precise operational timings.

The geographic scope of the transport network is limited to the Netherlands, reflecting a national-level focus on hinterland connectivity. Transporters operate in a queue-based system, waiting for paths to become available when occupied, but path capacities remain fixed and do not dynamically adjust to transporter speeds or other real-time variables. Containers are assumed to follow a one-way transport flow; they do not require return trips after delivery. While this reduces complexity, it also excludes the impact of backhaul demand on capacity utilization and resilience outcomes. Port operations and the hinterland gates between sea and land transport are simplified in the model to a sequence of queues and handling facilities. This

abstraction was necessary to remain within the model's block limits, but it omits several layers of operational realism. In practice, container transfers between terminals involve complex interactions such as inter-terminal transport, equipment scheduling, coordination between handling agents, and variability in transfer times. By removing these processes, the model eliminates potential delays and conflicts that could arise from real-world scheduling constraints or resource interactions. While this ensures computational efficiency, it means the representation captures high-level capacity constraints but not the finer operational dynamics. Finally, no additional loading or unloading delays are modeled for hinterland transport modes (e.g., truck, train, barge). This likely overestimates the responsiveness of the hinterland network under disruption scenarios, meaning the resilience benefits of certain strategies may appear slightly more optimistic than in real-world conditions. In general, these simplifications enable a focused investigation of resilience dynamics while simplifying the system in such a way that it can be based on real-world data.

3.3 Model Calibration and Validation

To ensure the representativeness of the simulation results, the model is first compared to real-world port operations data. Calibration involves adjusting key parameters such as vessel arrival patterns, container handling times, and facility capacities. These parameters are checked and adjusted where necessary so that the model's output aligns with observed performance metrics from sources like the Port of Rotterdam and relevant transport studies. Plausibility validation is conducted by comparing the simulated performance during different scenarios to empirical evidence found in literature. The goal is to confirm that the model produces reasonable behavioral outcomes that reflect real-life dynamics under different circumstances. This process enhances confidence in the quality of the model and its ability to evaluate the impact of disruptions and mitigation strategies. The results of the calibration experiment can be found at the start of AppendixB.

3.4 Data Collection and Model Input

This section outlines the data sources and parameter inputs used to construct, calibrate, and run the simulation model and experiments. The model relies on a combination of empirical data from port authority publications, industry reports, academic literature, and public logistics datasets. This ensures that its structure and performance reflect real-world operations of the Port of Rotterdam and its hinterland network. Where direct measurements are unavailable, parameter values are derived from comparable studies or calculated using available data, with assumptions explicitly stated to maintain transparency. The following subsections detail the datasets and estimation methods used for vessel arrivals, throughput volumes, infrastructure capacities, and transport network characteristics, which together define the model's baseline and scenario-specific configurations.

3.4.1 Data Collection

To construct a simulation model which functions as realistically as possible, a combination of commercial, academic and governmental data sources was used. Commercial sources provided information on facility and resource capabilities. The Port of Rotterdam RoutePlanner was used to lay out the core structure of the transport network. Yearly throughput data from the Port Authority offered detailed figures on flow volumes, modal and import / export splits. Available port facilities can also be found on the PoR website. Additionally, information from shipping companies and equipment manufacturers, such as crane and yard truck suppliers, was used to estimate operational delays and facility usage characteristics.

Academic sources supported the quantification of transport mode capabilities and cost structures. Capacity estimates for rail infrastructure were derived from the EU TEN-T network specifications, while barge and truck density values were based on guidelines from TU Delft's traffic flow theory. Transport cost estimation was informed by sector-specific academic reports, which helped benchmark the relative expense of each mode under various conditions.

Finally, both academic literature and governmental reports were reviewed to identify and characterize plausible disruption scenarios and mitigation strategies. This helped ensure that the simulated events align with real-world risks and emerging trends in port and logistics systems. Collectively, these sources form the empirical foundation for the model's inputs, assumptions, and scenario definitions.

3.4.2 Vessel Arrival Pattern

Vessel arrivals at the port are governed by a stochastic generation function that assigns characteristics such as size, cargo volume, and arrival frequency to each vessel. Once the vessel is instantiated with its attributes and delay, it is then injected into the system. This initiates the agent's journey through the ports infrastructure.

To define the arrival rate of sea vessels in the simulation, throughput data from the Port of Rotterdam was used as a basis. The total annual container throughput in 2024 was reported at 13.8 million TEU [4]. To translate this into an arrival rate, an average vessel capacity of 4,476 TEU was assumed based on data from the annual average sea vessel call size.

Using these values, the annual number of vessel arrivals was estimated by dividing total throughput by vessel capacity. This was then converted into a weekly arrival rate, under the assumption of uniform distribution throughout the year. The resulting estimate is approximately 59 fully loaded container vessel arrivals per week.

To model sea vessel arrivals at the port, both the annual throughput and vessel size distribution were considered. Since container vessels vary significantly in capacity, the arrival flow was weighted according to the global distribution of vessel sizes.

The vessel classes and their typical TEU capacities are defined in Table 3.1, based on an industry report [70]. The relative share of each class in the global fleet is shown in Figure 3.8.

Class	**TEU Capacity**
Small	<1,000
Feeder	1,000–3,000
Panamax	3,000–5,100
Post Panamax	5,100–10,000
New Panamax	10,000–15,500
ULCV	>15,500

Table 3.1: Container vessel classification by TEU capacity [70].

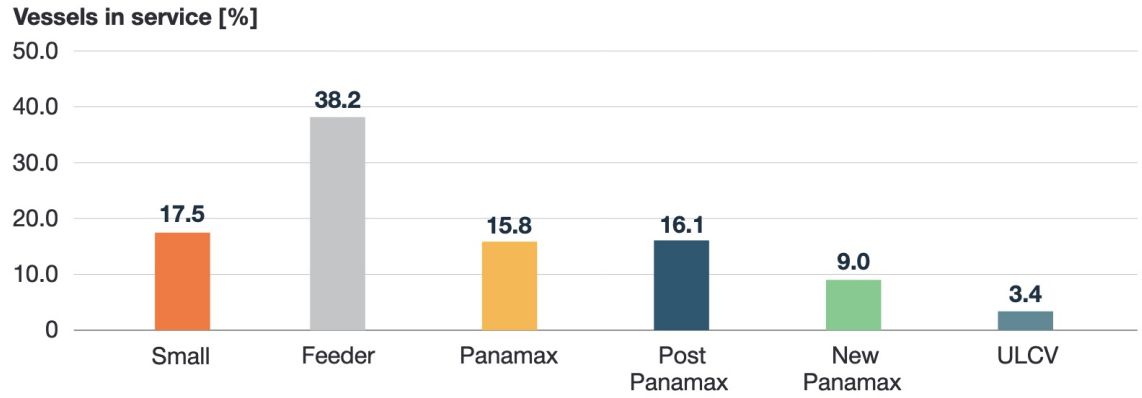

Figure 3.8: Percentage distribution of vessels types in service [70].

3.4.3 Container Throughput and Modal Split

According to the Port of Rotterdam throughput data for 2024 [4], the total container throughput amounts to approximately 13.82 million TEU. This throughput is nearly evenly split between import and export flows, with 52% being import and 48% being export.

In terms of hinterland transport modes, the modal split is distributed as follows:

- **Truck:** 58%
- **Barge:** 34%
- **Rail:** 8%

These shares reflect the relative reliance on road, inland waterway, and rail transport for the movement of containers from and to the port.

3.4.4 Sea-side Capacities

Tugboats, Cranes, and Yard Truck Handling Parameters

To simulate vessel unloading operations at the Port of Rotterdam, handling durations were disaggregated into three operational components: tugboat assistance, quay crane operation, and yard truck transport. The modeling approach is based on throughput formulas using data from [71, 72].

Handling times for each vessel class were computed using the following formulations:

1. **Tugboat Handling Time:**
$$T_{\text{tug}} = \frac{C_{\text{vessel}}}{v_{\text{tug}} \cdot n_{\text{tug}}}$$
2. **Crane Handling Time:**
$$T_{\text{crane}} = \frac{C_{\text{vessel}}}{n_{\text{crane}} \cdot v_{\text{crane}}}$$
3. **Yard Truck Handling Time:**
$$T_{\text{yard}} = \frac{C_{\text{vessel}}}{n_{\text{yt}} \cdot v_{\text{yt}}}$$

The resulting estimated handling times per vessel class are summarized in Table 3.2.

Vessel Class	Capacity (TEU)	Tugboats	Tug Time (h)	Cranes	Crane Time (h)	Yard Trucks	YT Time (h)
Small	750	1	0.22	2	12.52	18	1.68
Feeder	2000	1	0.60	2	33.32	18	4.52
Panamax	4050	2	1.22	3	45.00	27	6.08
Post-Panamax	7550	2	2.26	5	50.32	44	6.80
New Panamax	12750	3	3.82	6	70.84	53	9.56
ULCV	19750	3	5.92	8	82.28	71	11.12

Table 3.2: Simulated unloading times per vessel component (tug, crane, yard truck) by vessel class (converted to hours).

Terminal Crane Capacity and Depot Storage Data

To parameterize the simulation model with realistic infrastructure data, terminal and depot capacity values were extracted from official Port of Rotterdam documents [72]. The number of quay cranes per terminal was counted by reviewing the listed container terminals and summing their available crane equipment. Across fourteen terminals, a total of 137 cranes was identified. The results are summarized in Table 3.3.

Terminal	Cranes	Terminal	Cranes
T1	16	T8	3
T2	15	T9	8
T3	16	T10	2
T4	3	T11	3
T5	14	T12	5
T6	2	T13	14
T7	34	T14	2
Total	**137**		

Table 3.3: Total crane count per container terminal

Similarly, depot storage capacity was obtained by summing the maximum TEU capacity listed for twenty container depots. The total identified storage capacity across these sites amounts to 130,100 TEU, as detailed in Table 3.4.

Depot	TEU Capacity	Depot	TEU Capacity
D1	3,000	D11	22,000
D2	20,000	D12	1,000
D3	12,000	D13	1,500
D4	800	D14	2,000
D5	3,500	D15	4,000
D6	7,000	D16	1,800
D7	15,000	D17	8,000
D8	2,500	D18	5,500
D9	9,000	D19	2,100
D10	7,000	D20	2,400
Total	**130,100**		

Table 3.4: TEU storage capacity across container depots

3.4.5 Port-side Capacities

Transport Terminal Types and Lane Capacity Estimation

The inland barge terminal capacity is calculated similarly as to the methods for the sea vessels, but to prepare for the drought scenario a cargo-based throughput time will be required. This will be based on a constant value per barge and a variable delay based on the loaded cargo. This simulates the standard time required for procedures unrelated to loading and unloading, such as mooring, vessel positioning, and waiting for available facilities. An estimation of the average turnaround time of inland barge terminals can be found in a recent study [73]. By taking the average number of cranes, Rotterdam inland vessel throughput and crane cargo handling speeds the amount of inland terminals can be calculated [4]. The standard time for handling a single barge can be calculated by comparing the throughput capacity against the measured throughput by Wiegmans et al., and compensating that data for 24/7 operation. By doing this, a fixed handling time of 1.3 hours per barge can be calculated and a 2.6 hours crane handling time for an average load of 125 TEU.

According to RST Shortsea Terminal, the typical truck turnaround time is 23 minutes [74]. Along with the required TEU transport per truck per year, the total number of truck gates can be calculated. The available number of terminal rail tracks and average turnaround time of around five hours can be found in public documents, which can be found in [75] and [76].

This results in the following infrastructure estimates:

- **Truck gates:** ≈ 179
- **Barge terminals:** ≈ 27
- **Train tracks:** ≈ 24

These figures were used in the model to parameterize maximum infrastructure capacity for each transport mode.

3.4.6 Land-side Capacities

Path Density Estimation per Transport Mode

Truck Capacity Estimation To estimate the average truck density on hinterland road corridors, the spatial headway between vehicles was derived using the average time headway of 2.83 seconds observed on Dutch highways [77]. Assuming an average cruising speed of 80 km/h, the spatial headway H was calculated as:

$$H = v \cdot t$$

where:

- v = truck speed [m/s]
- t = average time headway [s]

The total occupied space per truck was computed by summing the vehicle length L with the headway:

$$\text{Total spacing} = L + H$$

Truck density k in vehicles per kilometer was then calculated as:

$$k_{\text{truck}} = \frac{1000}{L + H}$$

Using this method with assumed values ($v = 80\,\text{km/h}$, $t = 2.83\,\text{s}$, $L = 16.5\,\text{m}$), the resulting density is approximately 12.6 trucks per kilometer.

Barge Capacity Estimation

Due to limited empirical data on vessel headways in inland navigation, the density of barges per kilometer was estimated using an analogous spacing ratio observed in road freight transport. Specifically, the ratio between spatial headway and vehicle length for trucks was applied to barges. The average speed for loaded vessels on inland waterways was calculated to be around 8 km/h by [78].

Assuming a standard barge length of 105 meters and applying a headway-to-length ratio of 3.81 (based on truck spacing behavior), the estimated barge density is:

$$k_{\text{barge}} \approx 1.98\,\text{barges/km}$$

This value was used to parameterize waterway throughput capacity in the simulation.

Rail Capacity Estimation

To estimate average freight train density on Dutch hinterland rail corridors, data from the Trans-European Transport Network (TEN-T) GIS dataset was utilized [79]. The average speed for international freight trains in Europe was found to be 18 km/h [80] . Key variables extracted for selected high-traffic freight segments include:

- **FRE_23_day:** The average number of freight trains per day on a segment.
- **Shape_Length:** The length of the segment in meters.
- **Train Speed:** A representative average freight train speed of 18 km/h is assumed [80].

The average number of trains present on a track segment at any given time is estimated as:

$$\text{Avg\_trains\_on\_track} = \frac{\text{FRE\_day} \cdot t_{\text{segment}}}{86400} \tag{3.1}$$

where $t_{\text{segment}} = \frac{L}{v}$ is the travel time over the segment, L is segment length [m], and v is average train speed [m/s].

Train density k_{rail} is then given by:

$$k_{\text{rail}} = \frac{\text{Avg\_trains\_on\_track}}{L/1000} \tag{3.2}$$

Based on this method, the estimated rail density is approximately:

$$k_{\text{rail}} = 0.243\,\text{trains/km}$$

By calculating the rail density using the same method as for barge and truck, a density of 0.281 trains/km is calculated. This a only 15% difference in comparison to the calculation based on Ten-T data, meaning that the capacities are somewhat similar.

3.5 Experiment Design

To systematically assess the performance and resilience of the port model, a structured experimental procedure was followed. First, a baseline scenario was executed to establish reference performance metrics under normal operating conditions. Subsequently, a range of disruption scenarios was introduced to simulate adverse events affecting various parts of the port and its transport network. To explore the effectiveness of potential interventions, each disruption scenario was followed by one or more mitigation strategy simulations. This allowed for comparative analysis of system behavior with and without resilience-enhancing measures.

3.5.1 Baseline Scenario

The baseline scenario serves as the reference point for evaluating the performance and resilience of the port system under normal operating conditions. It is constructed using real-world data wherever available to ensure realism and credibility.

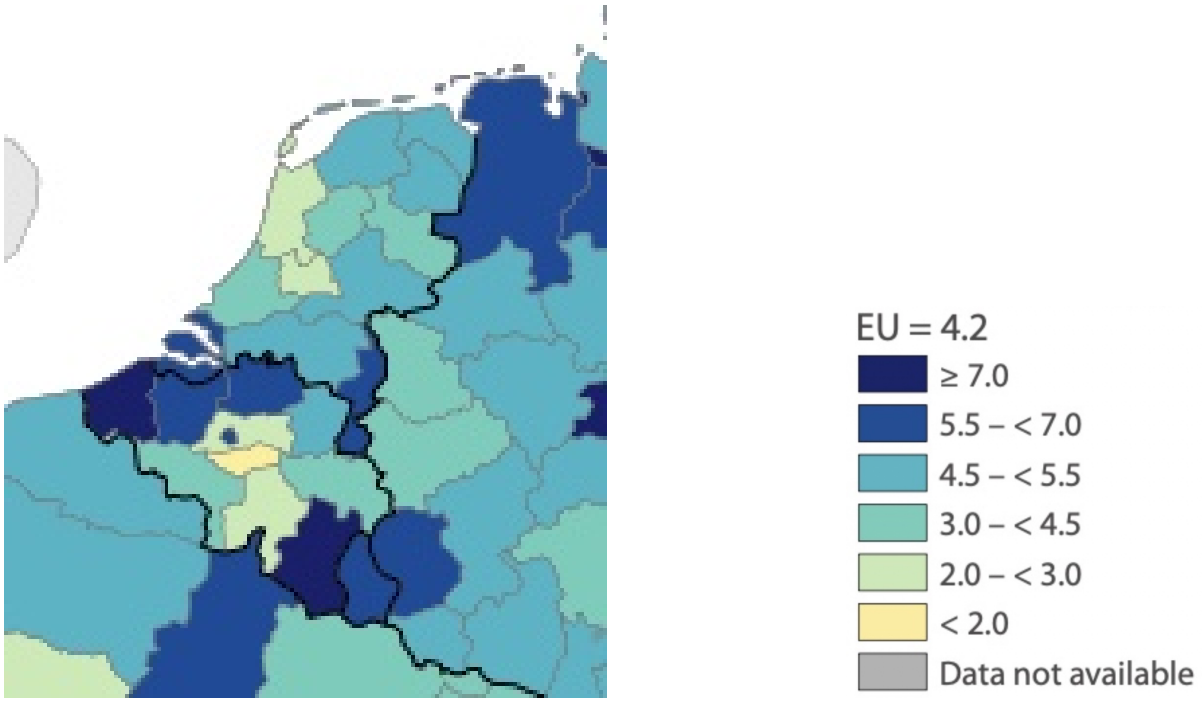

Figure 3.9: Road freight transport in [1000 tonne-km] per region and inhabitant in 2022 [81].

To estimate the distribution of cargo flows across the network in baseline operation, regional demand weights were derived by combining freight transport intensity with population data. Specifically, the Eurostat map on road freight transport in 2022 provided the freight transport performance per region, expressed in thousand tonne-kilometres per inhabitant [81]. This map can be seen in figure 3.9. To translate these relative values into regional demand, population figures for the specific regions and year were used [82]. By multiplying the freight intensity per inhabitant with the respective provincial population, a relative cargo demand was estimated for each region. These demand weights were then used to approximate the share of cargo allocated to each hinterland destination within the simulation, and applied to all three transport types.

Table 3.5: Estimated cargo destination shares and their corresponding model nodes.

Destination Region	Demand Share (%)	Model Node
Antwerp	20%	N2
Venlo	26%	N4
Nijmegen	12%	N5
Enschede	19%	N6
Meppel	6%	N7
Delfzijl	7%	N8
Amsterdam	10%	N9

3.5.2 Disruption Scenario Settings

This section outlines the specific settings and assumptions applied to each disruption scenario used in the simulation. These settings define how disruptions are implemented within the simulation model. Key parameters include their duration, affected components, and operational impact. By clearly specifying these parameters, each scenario remains consistent, reproducible, and aligned with real-world characteristics observed in literature.

3.5.3 Scenario Selection

From the different scenarios explained in Chapter 2, three representative scenarios were selected for implementation in the simulation model: a prolonged drought, a labor strike, and a sudden fluctuation in demand. This selection reflects a deliberate balance between capacity-driven and demand-driven disruptions, and between internally and externally originating events.

The Drought scenario represents a long-duration, externally driven constraint on a single transport mode—in this case, the inland waterway network. Its inclusion is motivated by increasing climate-related variability in water levels [19] and the corresponding impact on barge transport capacity. This type of disruption aligns well with the model's capability to simulate mode-specific capacity reductions and allows for detailed testing of mode-shift resilience strategies.

The Labor Strike scenario captures an internal disruption that directly reduces the operational capacity of key port-side infrastructure, such as quay cranes and yard equipment [26]. This scenario is particularly relevant for testing capacity-enhancing strategies in the model, as the disruption primarily targets terminal-side operations while leaving demand and hinterland connectivity unchanged.

The Demand Fluctuation scenario models the effects of a sudden surge in cargo arrivals caused by changes in sea route availability, such as rerouting around blocked or unsafe regions [1, 5]. This represents a demand-driven, externally induced disruptive scenario that tests the system's ability to handle rapid throughput increases without degrading stability.

By combining these three disruption profiles, each varying in origin, duration, and affected system components, the study ensures coverage of a broad range of operational challenges. This diversity supports the objective described in Chapter 1, where each scenario is paired with different resilience strategies to measure recovery speed, cost performance, systemic stability, and shock propagation. The results of these experiments, presented in Chapter 4 allow for a cross-scenario comparison of strategic effectiveness and trade-offs.

Drought Impact on Barge Speed and Load Capacity

Drought-induced low water depths have a notable impact on both the speed and container carrying capacity of inland waterway vessels. Based on the DST study on ship efficiency, ship speed is significantly influenced by the available water depth [83]. During drought conditions waterlevels can drastically be reduced, which can be seen in a study where they explore the

effects of the 2018 drought on Dutch inland waterways [84]. By looking at their results and selecting the worst month in their data, an estimate for the drought water levels can be taken to calculate new average vessel speeds. The water levels dropped from 6 meters to around 2.5 meters in the worst period of about a month. Using this change in depth, and assuming that average speeds scale the same as the ship speeds from figure 3.10, the new average speed can be calculated to be around 5 km/h.

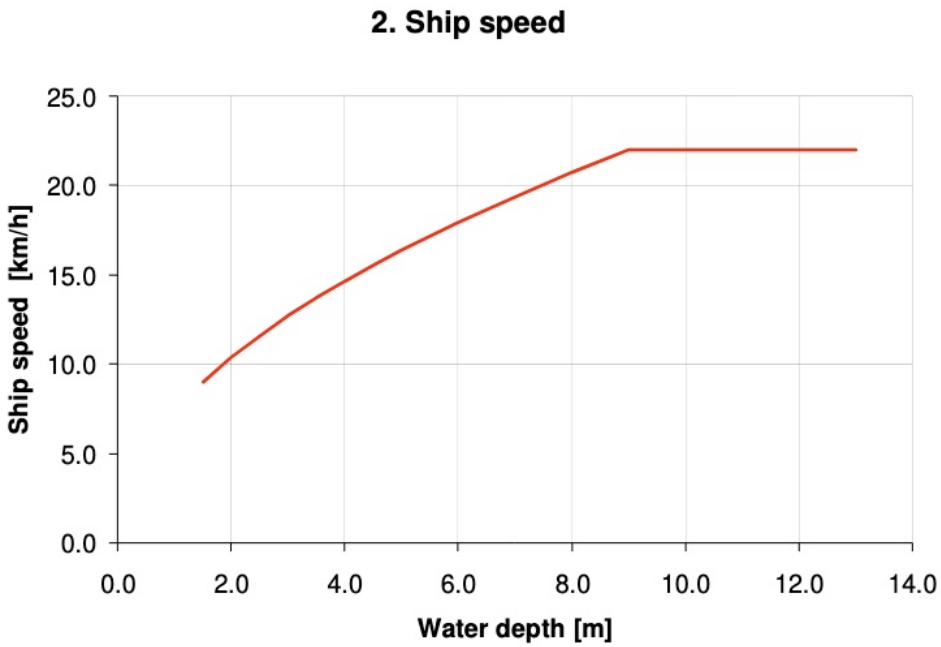

Figure 3.10: Relationship between water depth and ship speed [83].

In addition to speed, drought also impacts cargo capacity. Recent simulation studies into the 2018 Dutch section of the Rhine corridor indicate that for Class V vessels (approximately 105 m in length), only 29% of the original container capacity can be utilized under extreme low water scenarios [85]. This means that instead of a full capacity of 125 TEU per barge, the effective load is reduced to around 36.3 TEU.

This reduced load factor is incorporated into the simulation to capture throughput impacts during prolonged droughts.

Port worker strike impacting port operations

One of the modeled disruptions concerns the ongoing delays and congestion at the Port of Rotterdam, triggered by unexpected labor strikes at the Hutchison Ports Delta II terminal. These strikes have caused a 50% reduction in the terminal's operational capacity, significantly affecting the port's ability to handle container throughput [86].

As a result of this disruption, vessel waiting times have increased sharply, with ocean-going vessels experiencing delays of up to one week for berth allocation. Feeder vessels and barges are also heavily affected, with delays averaging 72 and 76 hours respectively [87]. At the RWG terminal, berth occupancy has reached 80%, with all berths occupied by mainline or feeder vessels, forcing the terminal to reject the return of empty containers. This has resulted in transshipment containers dwelling for up to 12 days. The strike-induced disruption has raised average container dwell time at the port to 9.1 days, making Rotterdam the most congested port in recent years.

To simulate port strike effects like this, a phased disruption in operational capacity was modeled. The disruption starts on day 5 and ends on the 15th day. During the first phase (days 5–10), core terminal operations (e.g. tugboats, cranes, and yard trucks) operate at only 25% of their normal capacity. In the second phase (days 10–15), capacity partially recovers to 50%, before returning to full operational levels from day 15 onward. This progressive recovery reflects realistic strike dynamics and allows analysis of system behavior under constrained conditions and during post-disruption recovery.

Geopolitical Effects on Global Shipping Routes

Geopolitical events such as trade disputes, military conflicts, and accidents in critical maritime chokepoints can exert considerable strain on the global shipping network. These disruptions typically induce short-term volatility in cargo flows, characterized by sudden drops in vessel arrivals followed by pronounced surges once trade routes are restored or diverted. For instance, a 90-day suspension of U.S. tariffs during the trade conflict with China led to a post-delay surge of up to 150% in cargo volumes following an initial dip in activity [88]. Similarly, unpredictable tariff announcements contributed to congestion in major European ports such as Rotterdam, where ship arrival delays of 66 to 77 hours and increased transshipment demand strained available capacity [89] [90]. The 2021 Suez Canal blockage further demonstrated the systemic repercussions of vessel accidents, leading to rerouting via the Cape of Good Hope, and persistent delays in downstream ports such as Rotterdam and Antwerp [91].

Drawing on these real-world observations, this study simulates a geopolitical disruption scenario using a three-phase demand fluctuation pattern:

- Phase 1 — Normal operations (Days 1-7): Normal load on the system
- Phase 2 — Shock (Days 8–14): A temporary surge in throughput to 300% of baseline demand is introduced, representing the backlog of delayed shipments and diverted cargo entering the system within a compressed period.
- Phase 3 — Stabilization (Day 15 onward): Demand normalizes to pre-disruption levels, assuming that the disruption is temporary and corrective actions are taken to restore standard flow.

This time-based disruption profile effectively captures both the suppressive and compensatory dynamics of geopolitical shocks. Implementing this scenario within the simulation allows for a robust assessment of port system resilience under volatile demand conditions.

3.5.4 Strategy Selection

To ensure a targeted and meaningful analysis, the mitigation strategies in this study are selected for their relevance to the three identified disruption scenarios and their feasibility within the simulation model. Each disruption scenario affects distinct components of the port and hinterland network, and therefore requires strategies that address its specific vulnerabilities.

One such strategy is the activation of an inland transshipment hub, which enables the rerouting of flows away from congested or failed rail or waterway links. This is particularly relevant under drought conditions or infrastructure failures. The effectiveness of this strategy depends on dynamic rerouting capabilities within the model, which allow adaptive switching between barge, rail, and truck depending on network availability and congestion levels. dynamic rerouting is also considered as a standalone strategy, as it can alleviate congestion even in the absence of a Transshipment Hub.

Another strategy is the expansion of storage capacity buffers, which can absorb short-term shocks caused by local throughput reductions or terminal congestion, such as those arising from

labor strikes or infrastructure blockages. This approach delays the onset of cascading failures by providing additional operational flexibility. In addition, the deployment of autonomous facilities and digital decision-support tools, such as autonomous quay cranes, yard trucks, and virtual ship pilots, is considered. These technologies can mitigate the effects of labor shortages while enhancing real-time coordination across the network.

Finally, a collaborative strategy is included, combining autonomous facilities with dynamic rerouting in a single configuration. This combined measure is tested under the demand fluctuation scenario to examine the joint effects of improving both port-side processing capacity and inland network flexibility. The demand fluctuation scenario was selected as this stresses the system in the most severe way. The combination is designed to target both infrastructure-oriented improvements, through the automation of key port facilities, operational enhancements, and through the dynamic reallocation of flows based on real-time congestion levels. By simultaneously strengthening internal port operations and the external transport network, the collaborative strategy aims to generate synergetic benefits that exceed the sum of the individual measures.

Each of these strategies is tested under the relevant disruption scenarios to assess their impact on resilience metrics, including total throughput, average delays, queue lengths, and system recovery times. This comparative analysis enables the identification of robust strategies that perform well across multiple disruption contexts, as well as those tailored to specific disturbances.

3.5.5 Mitigation Strategy Settings

This subsection outlines the specific configurations and assumptions applied to each resilience strategy tested within the simulation. These settings define how the strategies alter system behavior and infrastructure in response to disruptions. Key parameters include infrastructure upgrades, routing adjustments, and throughput enhancements. By clearly defining these settings, each strategy remains consistently implemented, reproducible across scenarios, and aligned with plausible interventions found in academic and industry literature.

Dynamic Rerouting

To simulate dynamic rerouting of transport flows, the model continuously monitored both utilization rates and queue levels at gates and terminals. Once a facility reached its capacity, it would block further flow, preventing additional transport from entering. In cases where transport was still directed toward a congested gate, based on its utilization, a secondary mechanism relying on queue size triggered rerouting back to the original or alternative transport modes. This approach ensured that congestion dynamically influenced routing decisions across the network. Similarly, queues at hinterland terminals and gates were monitored using the same logic, allowing the system to reroute transport when all available paths approached or exceeded their maximum capacity. A more detailed description of the rerouting algorithm which injects new transports in Anylogic can be found in Appendix C4.

Transshipment Hub

The inland transshipment hub strategy was implemented using the same dynamic rerouting mechanisms described in the previous section. This is essential, as the model requires transport flows to autonomously redirect based on real-time congestion levels. The distinguishing feature of this strategy is the addition of extra gate capacity specifically for accessing an inland hub.

Rail was selected as the primary transport mode to the hub due to its relatively low disruption risk and suitability for bulk inland movements. The hub was located at node N5, chosen for its central position deep within the hinterland which ensures broad accessibility. To simulate a

meaningful capacity increase, six additional rail tracks were added. This was selected to match the existing infrastructure capacity reported by the RSC terminal [75].

Upon arrival at the inland hub, containers are transshipped to trucks for final delivery to their destinations. Truck was selected due to it's high transport speed and abundance of routes. This indirect routing approach reduces congestion along direct paths by proactively shifting flow upstream, thereby minimizing cumulative delay and enhancing network-wide resilience.

Storage capacity Buffer

The storage capacity buffer strategy was modeled by removing queue size restrictions at the inland terminal gates, effectively allowing an infinite queue. This simulates an expansion of storage and staging areas, enabling terminals to hold significantly more containers during periods of disruption.

This implementation reflects the real-world effect of increased buffer capacity, where terminals can temporarily absorb surges in cargo volumes without immediately rejecting or blocking incoming transport flows. This strategy helps stabilize throughput under stress conditions, by decoupling the transport flows to some extend at these buffer zones. It also reduces the need for emergency rerouting or idle time, allowing for more gradual and coordinated recovery once normal operations resume.

Autonomous Facilities

The autonomous facilities strategy was implemented by reducing the handling time of port equipment like tugboats, cranes, and yard trucks and inland transporter gates by 23%. This figure is based on reported efficiency improvements in automated port operations, as cited by [92]. By accelerating key logistics processes within the port, this strategy aims to reduce delays and improve responsiveness to disruptions. The reduction in delay time represents the operational gains from automation technologies such as autonomous vehicles, automated stacking cranes, and smart yard management systems. These changes were applied uniformly across all vessel classes to simulate a broad implementation of automation throughout the terminal system.

Collaborative Strategy

The collaborative strategy integrates two measures within a single configuration, autonomous facilities and dynamic rerouting. This combined setting is applied to the demand fluctuation scenario to test the joint effects when both port-side processing capacity and inland flexibility are improved. This combination is particularly interesting to experiment with as it brings together both infrastructure-oriented improvements, through the automation of key port equipment and gates, and operational enhancements, through the dynamic reallocation of flows based on real-time congestion levels. By targeting both internal port operations and the external transport network, the configuration has the potential to deliver synergetic benefits that exceed the sum of the individual measures. Whereas the single strategies focus primarily on specific components, such as the port handling chain in the case of automation, or the hinterland network in the case of rerouting, this combined approach addresses capacity and adaptability in parallel.

3.6 Performance Analysis

This section outlines the framework used to evaluate the outcomes of the simulation experiments and determine the relative effectiveness of the tested resilience strategies. The analysis is structured around four key aspects that are examined consistently across all disruption scenarios:

container throughput, transport and delay costs, systemic shock propagation, and cross-scenario evaluation. Together, these perspectives capture both the speed and extent of operational recovery as well as the stability and efficiency of the system during and after disruption events.

3.6.1 Container Throughput

Container throughput is assessed to determine how effectively the system maintains and restores cargo flow under different disruption conditions. Time series outputs of delivery rates are analyzed to identify the immediate impact of the disruption and the subsequent recovery trajectory. Time to Recovery (TTR) is calculated using two complementary approaches to capture both the operational stabilization of the system and the post-disruption recovery phase. In both cases, the TTR represents the elapsed time, in days, from a defined disturbance reference point until the system returns to a stable operating condition.

In the first approach, TTR was measured relative to the end of the disruption. From this point onward, the model checked consecutive time windows of 96 hours to determine when the smoothed container count consistently remained within a fixed tolerance band of ±10,000 TEU around the post-recovery mean. The first time at which this stability criterion was met was recorded as the recovery time, with the TTR being the difference between the two points. In the second approach, the TTR is based on the transport and delay cost rates plotted over the simulated time. This method reflects a delay-focused recovery measure, capturing how long it takes for the system to mitigate delays after the disruption. Combining these two approaches delivers a TTR analysis based on delay dynamics as well as throughput performances.

In addition to recovery speed, throughput patterns over the disruption period are examined to reveal the system's capacity to handle fluctuating demand and the extent to which each strategy prevents prolonged underperformance.

3.6.2 Transport and Delay Costs per TEU

Transport and delay costs provide a monetary measure of disruption severity and the efficiency of mitigation strategies. Delay costs are calculated by tracking the number of containers congested within the port system over time and multiplying these volumes by standardized cost estimates from industry benchmarks. This approach captures the cumulative impact of congestion on stakeholders and highlights the scenarios where strategies most effectively reduce economic losses. In parallel, transport cost changes are monitored to assess the effect of mode shifts and rerouting on overall logistics expenses.

The total costs per TEU in the simulation are calculated for each strategy and scenario. The underlying transport and delay costs are combined to obtain the overall cost per container handled.

Delay Costs

Delay costs are calculated by first tracking the number of containers present in queues at each time step of the simulation. These queues include both port-side facilities (e.g., quay cranes, yard trucks) and hinterland bottlenecks (e.g., gates at inland terminals). For each time step, the number of containers in the queues is accumulated and converted into *container-days*:

$$CD = \sum_{t=1}^{T} \frac{Q_t}{24} \tag{3.3}$$

where Q_t is the total number of containers in queues at time step t (measured hourly), and T is the total number of time steps in the simulation.

The total delay cost C_{delay} is then obtained by multiplying the accumulated container-days by the delay cost rate p_{delay}, which is set to 58.75 €/TEU/day. This value is derived from the average daily demurrage and storage fees for dry 20-foot containers as listed in the Port of Rotterdam local charges [93].

$$C_{\text{delay}} = CD \times p_{\text{delay}} \tag{3.4}$$

Transport Costs

Transport costs are calculated separately for each transport mode based on the simulated transport distances and mode-specific cost parameters. For each mode m, the transport cost per TEU is given by:

$$TC_m = \frac{D_m}{\frac{N_m}{L_m}} \times W \times c_m \tag{3.5}$$

where:

- D_m is the total distance travelled by all vehicles of mode m,
- N_m is the total number of TEUs delivered by mode m,
- L_m is the average load capacity (TEU) of a vehicle of mode m,
- W is the assumed average container weight,
- c_m is the variable cost per tonne-kilometre for mode m, based on the modal cost figures reported by KiM Netherlands Institute for Transport Policy Analysis [94].

The share of each mode in the total delivered containers is then computed:

$$s_m = \frac{N_m}{N_{\text{total}}} \tag{3.6}$$

where N_{total} is the total number of TEUs delivered across all modes.

The average transport cost per TEU, $C_{\text{transport}}$, is obtained by weighting the mode-specific costs by their respective shares:

$$C_{\text{transport}} = \sum_{m \in \{\text{barge, train, truck}\}} s_m \cdot TC_m \tag{3.7}$$

Total Cost per TEU

Finally, the total cost per TEU, C_{total}, is obtained by summing the average transport cost per TEU with the delay cost per TEU:

$$C_{\text{total}} = C_{\text{transport}} + \frac{C_{\text{delay}}}{N_{\text{total}}} \tag{3.8}$$

This metric allows for direct comparison of strategies in terms of combined operational efficiency and delay mitigation effectiveness.

3.6.3 Systemic Shock Propagation

Systemic shock propagation is assessed by analysing delivery rate distributions and capacity utilization patterns across the network. For each scenario and strategy, violin plots of delivery rates are examined to capture both the central tendency and variability in system throughput over time. Wider distributions and larger inter quartile values indicate greater volatility, which can be a sign of instability and the spread of disruption effects beyond the initial impact area.

In addition, the frequency with which key system components—such as port terminals, hinterland gates, and transport modes—reach 100% capacity utilisation is recorded. Persistent or repeated occurrences of full capacity suggest that congestion is propagating through the network, potentially triggering secondary bottlenecks. This dual approach enables the detection of both operational instability (via delivery rate variability) and spatial congestion spread (via capacity saturation events). Together, these measures provide an indication of how effectively each strategy contains or mitigates systemic disruption effects.

3.6.4 Cross-Scenario Evaluation

Finally, a cross-scenario evaluation compares the performance of each mitigation strategy across all disruption types to identify patterns, trade-offs, and context-dependent effectiveness. This approach enables the assessment of whether certain strategies provide consistently strong performance or whether their benefits are contingent on the disruption's nature. The comparison uses a common set of performance indicators, including average delivery rates, time to recovery, delay cost accumulation, delivery rate variability, and systemic shock occurrence, ensuring results are directly comparable between scenarios. By examining differences in both central performance metrics and stability-related measures, the analysis reveals the operational mechanisms that drive strategy effectiveness. This method is particularly valuable for resilience planning, as it highlights not only the best-performing strategy in a given context, but also the potential synergies, trade-offs, and limitations when applied under different disruption conditions.

Chapter 4

Simulation Results

This chapter presents the outcomes of the simulation experiments and directly addresses the main research question: How can systemic risks in port operations be minimized through resilience-based strategies, identified via a simulation of port disruptions and recovery? The analysis also answers sub-questions 3–5 by evaluating the operational performance, cost implications, and systemic stability effects of the tested strategies.

The chapter begins by examining the outcomes of the experiments conducted for each disruption scenario individually. For each scenario, trends and patterns specific to the given conditions are highlighted to explain the underlying system mechanics. The performance of the different resilience strategies is evaluated across four key dimensions. First, cargo throughput patterns are analyzed to understand how delivery rates evolve during and after the disruption, providing insight into processing capability under pressure. Next, recovery times are assessed to determine how long the system takes to return to stable operating conditions following a disruption. Cost performance is then examined by comparing transport and delay costs incurred per TEU, which reflect the operational efficiency and the penalties arising from congestion. Finally, systemic risk behavior is evaluated by analyzing the internal shocks experienced by the system, such as component overloads and delivery volatility, which indicates the degree of resilience under disruptive conditions.

Following the scenario-specific analyses, overarching trends that appear consistently across all three scenarios are discussed. This structure provides a comprehensive view of each strategy's effectiveness under varying conditions and forms the basis for drawing conclusions about the broader implications of the resilience strategies in this study.

4.1 Drought Scenario

The drought scenario simulates a prolonged period of low water levels, severely restricting barge-based inland container transport. This disrupts the capacity of one of the primary transport modes and creates systemic stress within the port system. The goal of this scenario is to evaluate how different resilience strategies—such as rerouting, inland hubs, storage buffers, and autonomous facilities—can maintain system performance when a critical transport mode becomes unreliable.

First the container throughput is considered. The average throughput rates can be seen in figure 4.1. It can be expected that the impact of the barge throughput capacity will have a significant effect on the throughput results of the baseline scenario, and be lower in comparison to the improvement strategies.

However, the average delivery rates are relatively close across strategies, suggesting limited impact of drought-specific interventions on overall throughput. This finding was somewhat unexpected, as the implemented strategies were designed to overcome the limitations imposed by barge constraints. There are some differences in performance, but they could also somewhat be attributed towards run-to-run variability in total container generation, which is inherent in the simulation model. The lack of significant differences in throughput performance across different strategies might be caused by the fact that overloading the barge transports might lead to very efficient use of their capacity, since there is always a queue of containers ready to be transported. These mechanics might lead to higher delays but more efficient throughput, which is the only thing measured by this metric.

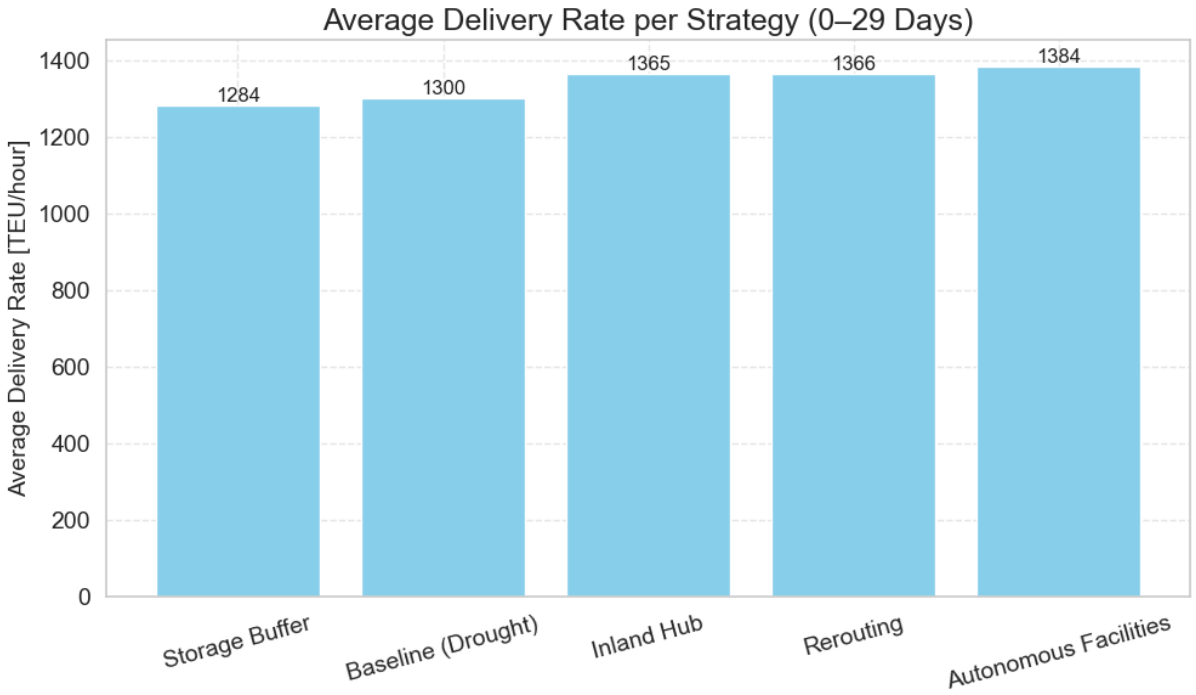

Figure 4.1: Average delivery rate (TEU/hour) of each resilience strategy under drought conditions.

In contrast, when looking at the containers in the system over time, it can be seen that the autonomous facility strategy keeps the lowest amount of containers circulating through the system. It also has the most stable curve, showcasing low variability of the system's throughput performance. The containers in the system over time can be seen in figure 4.2 below.

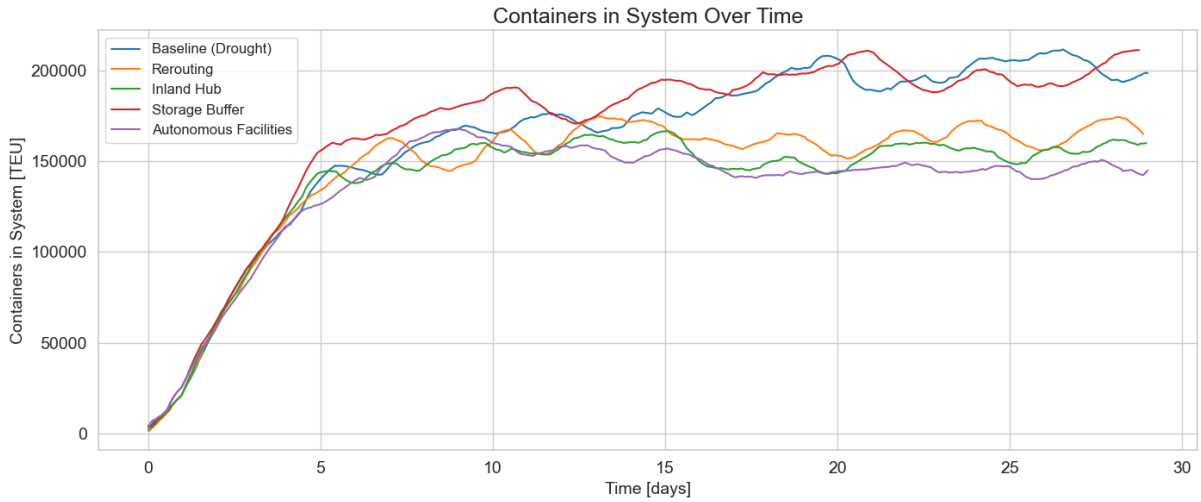

Figure 4.2: Number of containers in the system over time for each strategy under drought, illustrating backlog dynamics.

The figure illustrates that all strategies initially follow a similar trend: a sharp increase in the number of containers in the system, followed by a more gradual plateau as containers are delivered and new shipments are generated. However, the baseline and buffer storage scenarios continue to show a persistent increase in container count throughout the entire simulation period. This observation is supported by the average rate of change in the system from day 10 onward, as presented in table 4.1. The rerouting and inland hub strategies maintain near-zero growth, indicating their ability to meet demand under current conditions. The autonomous facilities strategy even reduces the container count over time, suggesting surplus capacity. In contrast, the baseline and buffer storage strategies exhibit sustained growth, indicating that they are unable to match the inflow of containers with sufficient throughput. This means that while the average throughput rates are similar, the baseline and increased buffer storage scenarios will lead to lower throughput rates across larger timeframes.

Table 4.1: Average change in smoothed containers in system (TEU/hour) from day 10 to 29 under drought conditions.

Strategy	**Average Change [TEU/hour]**
Baseline (Drought)	1731.51
Storage Buffer	1267.59
Rerouting	195.58
Inland Hub	139.91
Autonomous Facilities	-808.30

The delay cost rate over time, shown in Figure 4.3, reinforces this conclusion by illustrating how delay costs in the Baseline and Storage Buffer scenarios continue to rise throughout the simulation period. These costs are calculated based on the number of containers experiencing congestion within the port infrastructure. The Autonomous Facilities strategy does also experience small amounts of delays, but the increased port capacities lead to a more stable performance and thus the costs do not increase significantly over time. In contrast, the Rerouting and Inland Hub strategies generate almost no delay costs, as they effectively distribute shipments across multiple transport modes and rapidly remove containers from the port area, thereby minimizing internal delays.

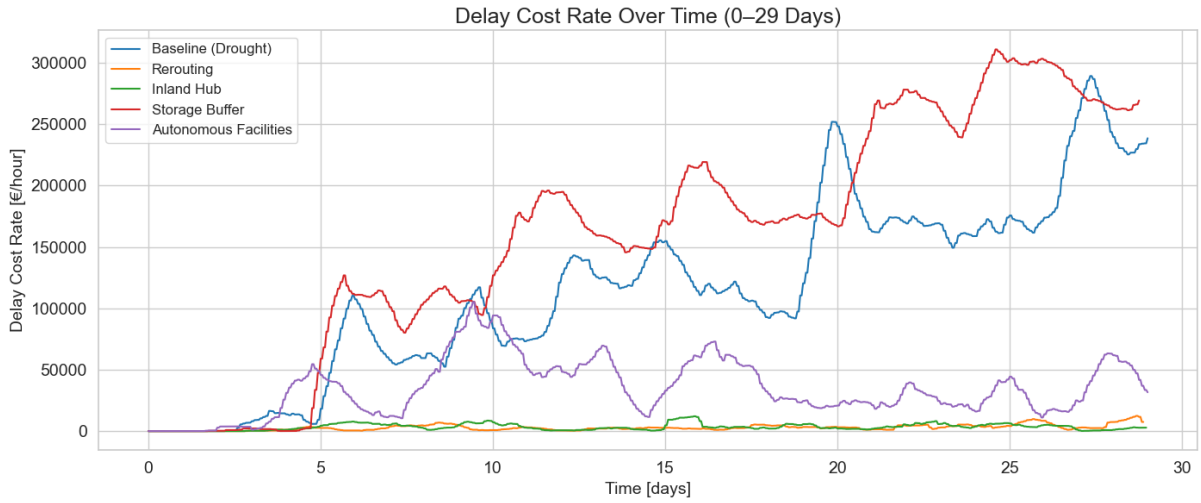

Figure 4.3: Smoothed delay cost rate (€/hour) over time for each strategy in the drought scenario.

By measuring the delay and transport costs between different strategies, insights into their cost efficiency can be gained. The bar plot in figure 4.4 shows the different costs per TEU across the different strategies. These highlight the fact that delays are reduced significantly by spreading load across different transport modes. Not only that, the possible increase in transportation costs caused by using different transport modes does not outweigh the extra distance costs that would have to be covered by loading a single transport mode more extensively.

These findings confirm the expected benefits of dynamically switching resilience strategies. By proactively spreading container flows across truck and rail, these strategies avoid overloading any single transport mode and reduce queuing delays.

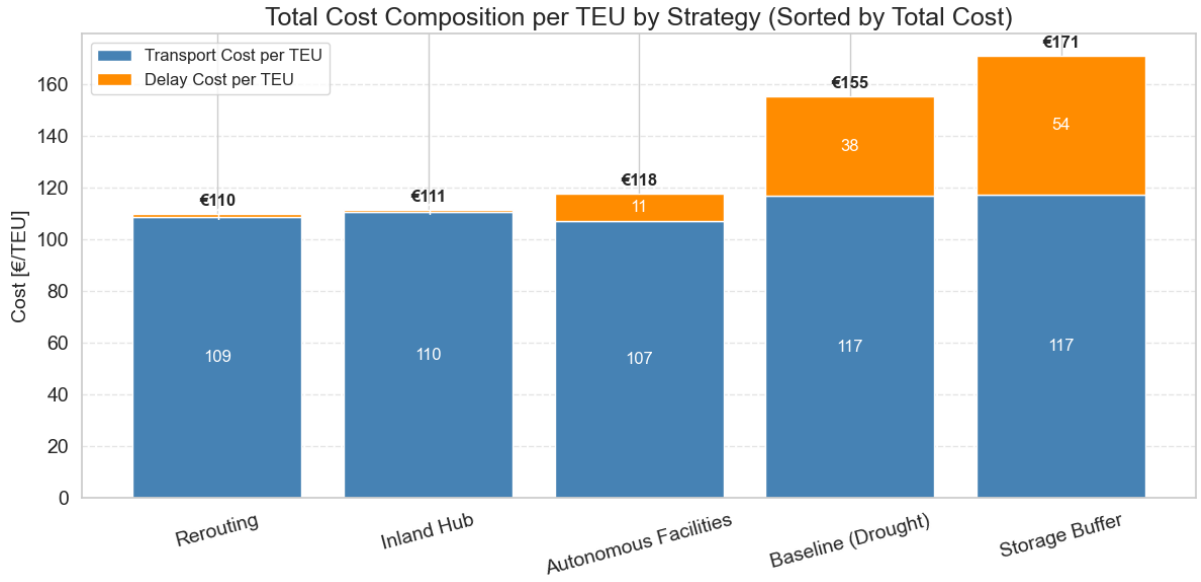

Figure 4.4: Transport and delay costs per TEU for each strategy under drought conditions.

Now while it seems that the Inland Hub and Rerouting strategies are mostly outperforming the others through costs, it is also important to consider their performance regarding systemic shocks. In order to do this, first a violin plot is made of the delivery rates during the simulation

runs, as shown in Figure 4.5. The plot shows that the performance of the Autonomous Facilities strategy is the most stable, with the highest median and a narrow interquartile range. Inland Hub follows with a similarly narrow IQR but a slightly lower median. The Rerouting strategy, while achieving the second-highest median, displays a significantly larger IQR, indicating more volatile performance.

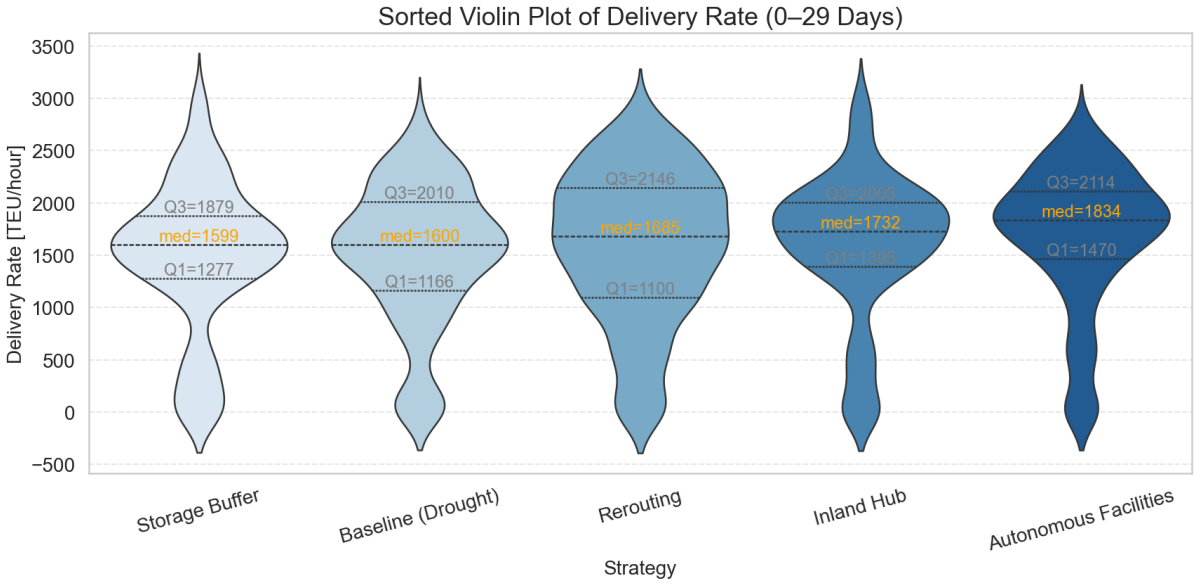

Figure 4.5: Distribution of delivery rates across strategies during the drought scenario.

In this context, stable performance refers to consistent delivery rates with limited fluctuation. Strategies exhibiting this, such as Autonomous Facilities and Inland Hub, could be considered more operationally resilient. The difference between the Rerouting and Inland Hub strategies regarding this distribution could be caused by the tendency of the Inland Hub strategy to favor the train transport mode. This transport mode has extra capacity for inland hub travel in this strategy and thus allows more transports to be redirected to trains when deciding rerouting options, while in the normal Rerouting strategy it might prefer trucks, which are highly volatile due to their transport speeds and low queuing capacities.

This conclusion is further strengthened by considering the average acceleration of the delivery rates of the different scenarios, shown in 4.2 below. Here it can be seen that there's a significant difference between the Rerouting and Inland Hub strategy in this regard, which supports the different violin plot shapes.

Table 4.2: Average Acceleration of the Delivery Rates (Days 10–29)

Strategy	**Avg. Acceleration [TEU/h^2]**
Rerouting	82.9
Autonomous Facilities	78.2
Inland Hub	68.2
Baseline (Drought)	60.5
Storage Buffer	53.6

Furthermore, the number of times a system component reaches a 100% utilization from a lower level indicates how often the maximum capacities were reached. This gives some form of mea-

surement for the systemic shocks that propagate within the system. This was measured throughout the simulation runs and can be seen in figure 4.6 below.

Frequent transitions to full capacity utilization can indicate that capacity limits are often passed onto other components within the system. This is visible in the plot for the Rerouting and Inland Hub strategies, which is to be expected as they reroute cargo across different transport modes until the capacity limits are reached. This lead to a constant switching of transports and frequently hitting capacity limits. On the other hand, the increased throughput speed of the autonomous facilities can also lead to increased frequencies of full capacities being hit, as the system responds more quickly to queues being filled leading to less congestion and more dynamic behavior in the inland terminals.

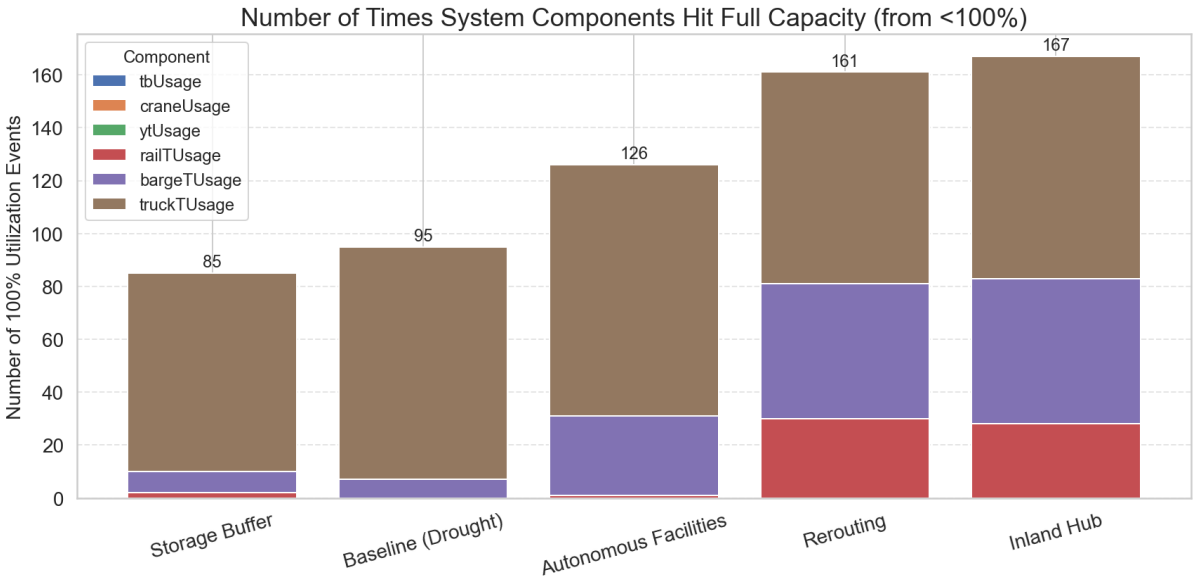

Figure 4.6: Number of full-capacity events per system component under drought conditions.

The stability of the system can further be investigated by looking at the transport mode utilization across different strategies. In figure 4.7 the percentage of time each transport mode was used above 60% capacity can be seen. This plot indicates the share of simulation time during which each mode's utilization exceeded 60% capacity, highlighting operational strain. Rerouting and Inland Hub strategies effectively distribute load across rail, truck, and barge. In contrast, Baseline and Storage Buffer remain highly reliant on barge transport, which is persistently overutilized.

This observation aligns with the delay cost results. Scenarios like Baseline and Storage Buffer, which rely almost exclusively on heavily utilized barge transport, experience persistent congestion and rising delay costs, whereas Rerouting and Inland Hub mitigate these effects by distributing load across multiple transport modes.

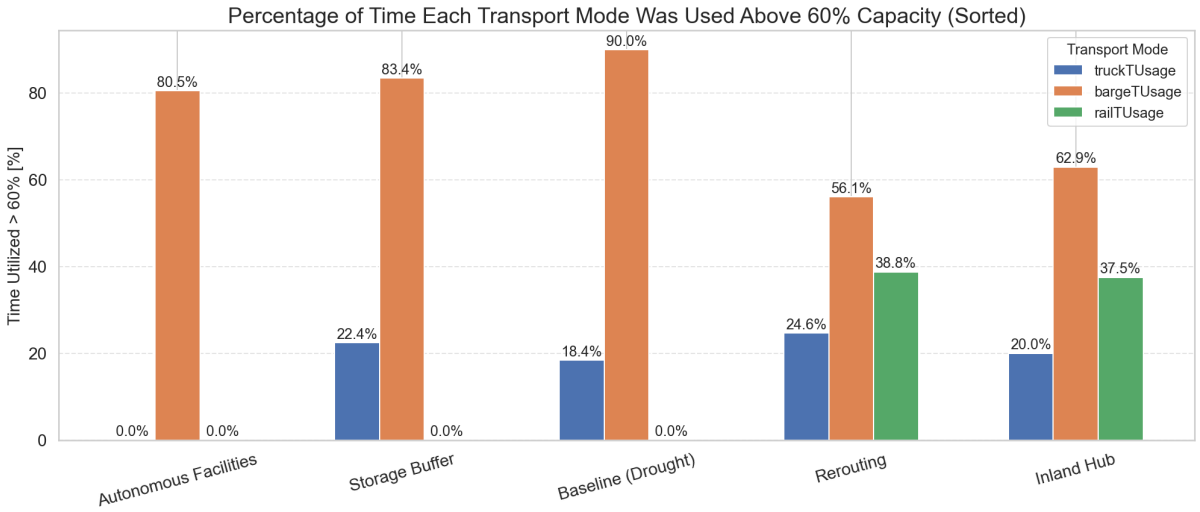

Figure 4.7: Proportion of simulation time each transport mode operated above 60% capacity in the drought scenario.

4.2 Labor Strike Scenario

The labor strike scenario simulates a sudden and severe reduction in port terminal capacity, caused by an unexpected port worker strike affecting key operations such as quay cranes, yard trucks, and tugboats. The disruption is modeled in two distinct phases: a sharp reduction to 25% operational capacity from days 5 to 10, followed by a partial recovery to 50% capacity until day 15. Normal operations resume from day 15 onward.

The goal of this scenario is to assess the resilience of different strategies under a time-bound but intense internal disruption that affects all transport modes at the port interface. Unlike the drought scenario—which limits a single mode (barge)—this scenario creates congestion and queuing across the entire port system by throttling terminal throughput capacity directly.

First, the container throughput is considered to assess whether the labor strike has a lasting impact on delivery performance. Figure 4.8 shows that all strategies experience a rapid buildup of containers in the system once the strike begins on day 5, peaking during the most constrained period of port operations. However, the Autonomous Facilities strategy stands out: it effectively limits the container buildup and stabilizes the system more rapidly than any other strategy. This outcome is expected, as Autonomous Facilities is the only strategy that directly addresses the strike-induced disruption by increasing the capacity of affected port facilities. In contrast, strategies like Rerouting and Inland Hub do not modify the disrupted components directly and therefore cannot prevent the container backlog during the disruption period. This highlights the unique effectiveness of capacity-enhancing interventions in scenarios where port infrastructure is directly impaired. Overall, expect for the autonomous facilities which does not need to recover, the times to recovery are similar across the different scenarios.

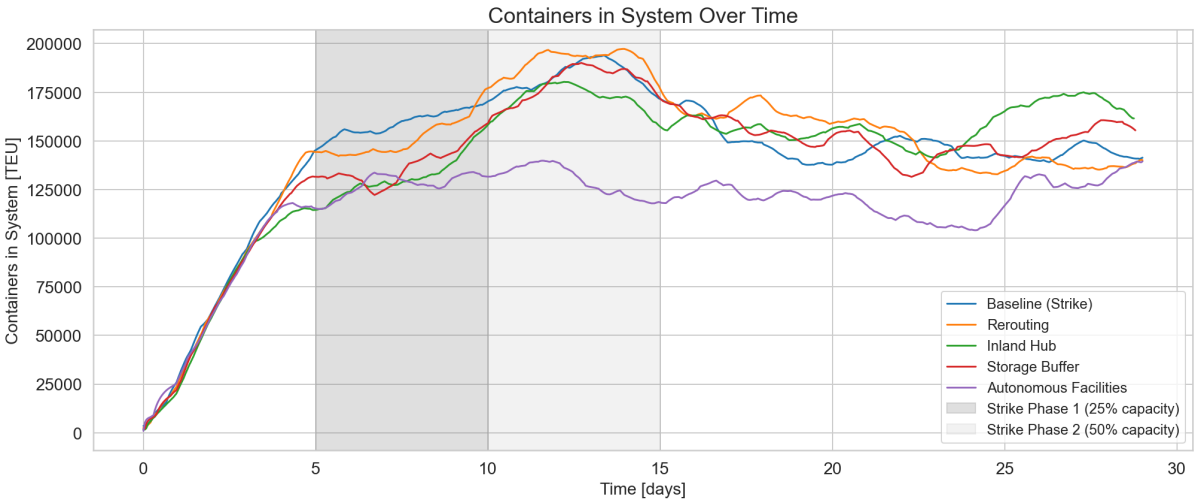

Figure 4.8: Containers in system over time for each strategy during the labor strike scenario.

This is further highlighted by the average delivery rate over time, as shown in Figure 4.9. During the most severe phase of the strike (days 5–10), all strategies experience a noticeable slowdown in delivery rates due to restricted terminal operations. However, Autonomous Facilities shows a clear advantage in recovery: it not only sustains higher throughput during the disruption but also achieves a steeper recovery trajectory once capacity begins to return. Between day 5 to 10, its delivery rate already surpasses that of all other strategies and remains consistently higher for the remainder of the simulation. This performance reinforces the earlier observation that Autonomous Facilities is uniquely positioned to absorb the operational shock of the strike. It highlights the importance of direct capacity enhancement in critical system nodes, especially under port-centric disruptions. The average delivery rates at the end reveal that performance remains nearly identical across all strategies throughout the simulation period. This suggests that the system, despite temporary disruption, is capable of recovering to normal operational throughput levels over time.

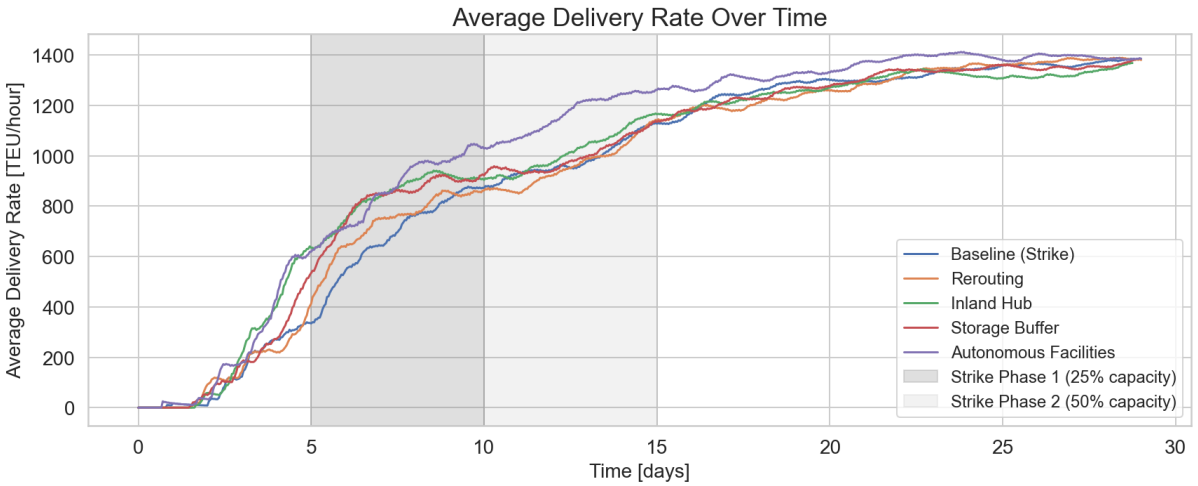

Figure 4.9: Average delivery rate (TEU/hour) over time for each strategy in the labor strike scenario.

The delay cost rate over time plot (Figure 4.10) shows a sharp and simultaneous spike in delay cost rates for all strategies during the first strike phase, highlighting that the system-

wide disruption impacts each strategy with similar speed. However, the Autonomous Facilities strategy maintains the lowest peak, confirming its effectiveness in directly mitigating port-side congestion. Storage Buffer follows with a moderately lower peak compared to the others, while Baseline, Rerouting, and Inland Hub exhibit similarly high cost peaks, indicating insufficient mitigation of internal delays at the terminal level. The effectiveness of the Storage Buffer strategy in limiting quickly rising costs could be caused by removing short congestion at the storage point in the port flow, leading to more efficient flow in the port.

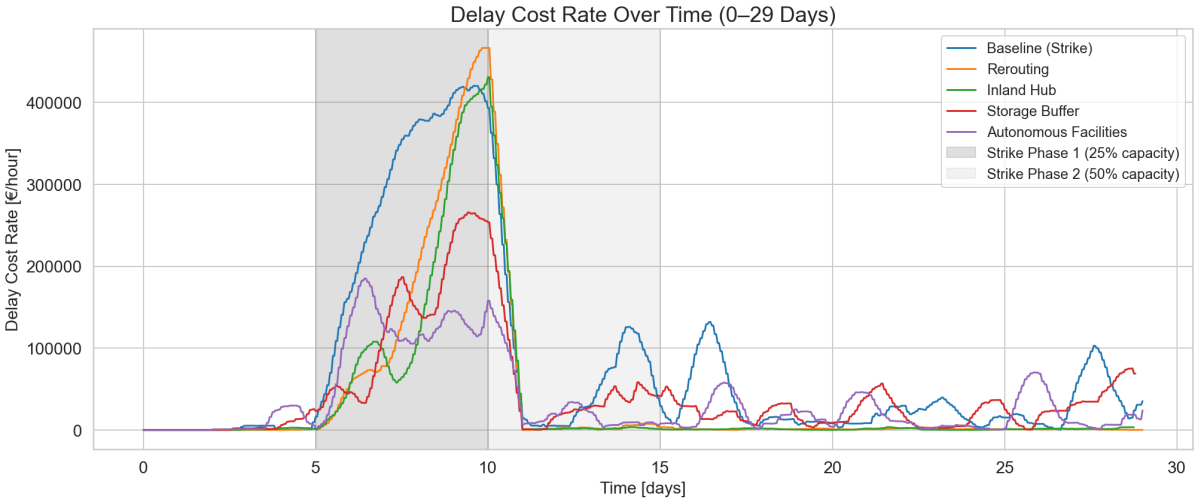

Figure 4.10: Delay cost rate (€/hour) over time for each strategy during the labor strike scenario.

After the initial spike, Baseline is the only strategy to display three additional delay cost peaks, pointing to persistent congestion and delayed system recovery. Meanwhile, Autonomous Facilities and Storage Buffer continue to show some fluctuations above zero, suggesting ongoing inefficiencies, albeit at a lower level. In contrast, Rerouting and Inland Hub maintain near-zero delay costs after the disruption period, indicating their effectiveness in diverting flows away from the strained terminal. However, their inability to reduce the initial peak shows that external rerouting alone cannot fully mitigate an internally concentrated shock like a labor strike.

The total delay costs per TEU, shown in Figure 4.11, align with the patterns observed in the delay cost rate plot. Scenarios that exhibited sharp spikes and prolonged delay cost activity, like Baseline and Buffer Storage, also score high in total delay costs. In contrast, Rerouting and Inland Hub strategies, which have high initial cost peaks nearly eliminate delay cost rates after the disruption phase, achieve some of the lowest total delay costs (€13 and €11 per TEU respectively). Although the Autonomous Facilities strategy shows some ongoing delay costs in the rate plot, its proactive capacity increase keeps both peaks and cumulative delay cost impact minimal, resulting in the most cost-effective outcome (€11 per TEU). This underscores how short-term control of disruption-induced delays translates directly into better cost performance across the entire simulation.

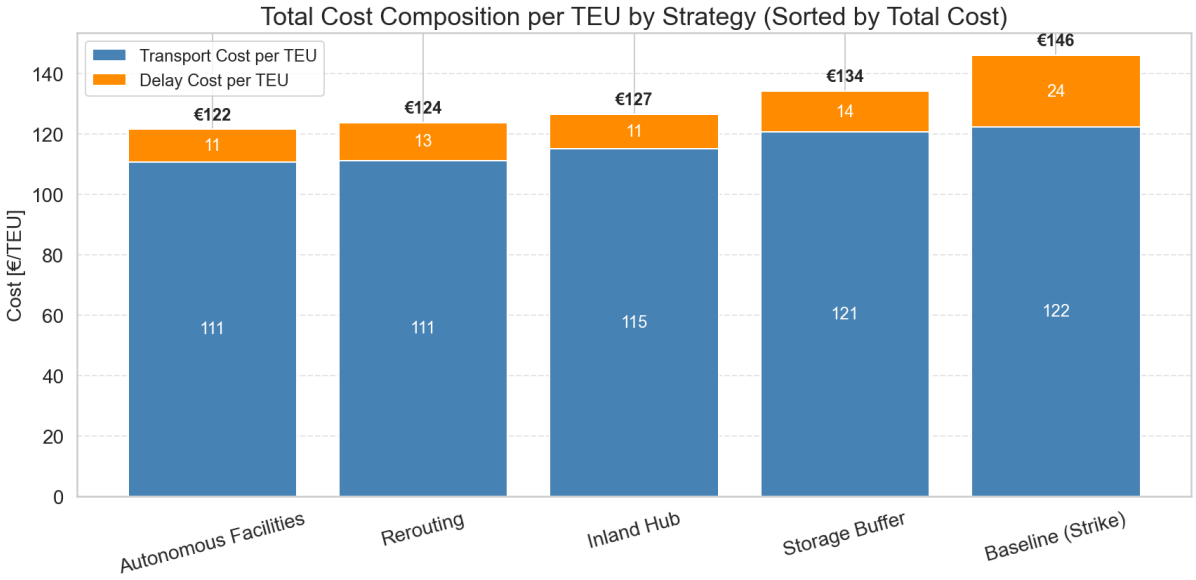

Figure 4.11: Total delay cost per TEU for each strategy in the labor strike scenario.

To better understand the origins of the observed cost differences, it is important to examine how frequently system components were pushed to their operational limits. While the cost analysis revealed meaningful differences in both transport and delay cost contributions, these outcomes are often linked to how resilient each strategy is under pressure. Figure 4.12 shows how often various critical components reached full capacity throughout the simulation. Here it can be seen that there's a relatively similar number of events in which system components hit full capacity (ranging from 114 to 133 occurrences) across strategies. This gives evidence towards the conclusion that the strike scenario is not severe enough to cause major differences in stability or systemic shocks between the different strategies.

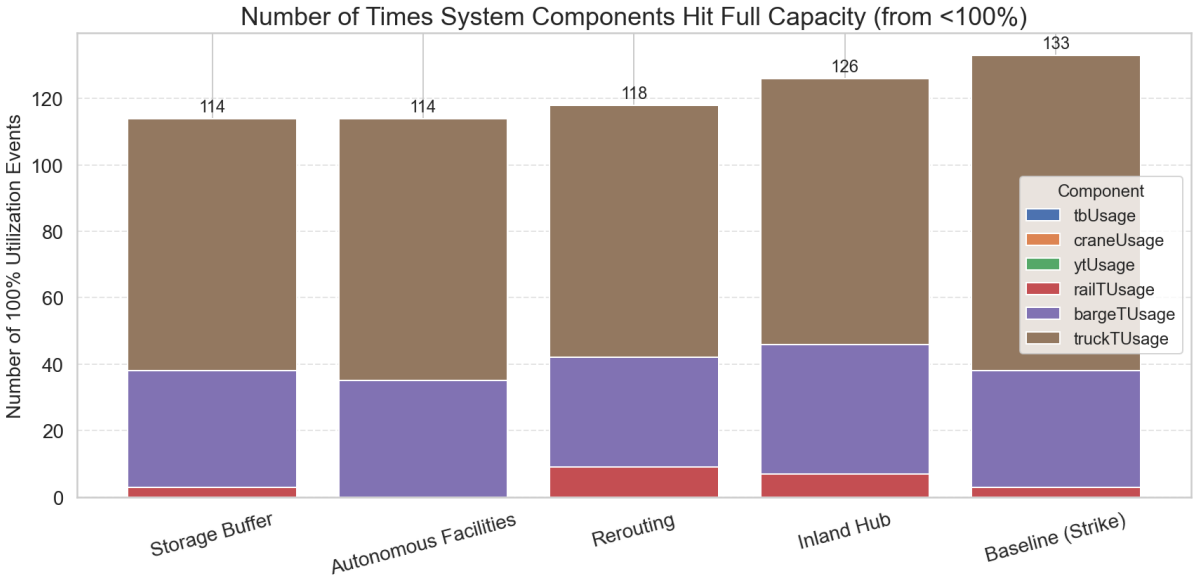

Figure 4.12: Number of full-capacity events per component during the labor strike scenario.

4.3 Demand Fluctuation Scenario

The demand fluctuation scenario simulates a short-term but intense surge in container arrivals resulting from a geopolitical disruption in global shipping routes. Following a short period of normal operations, the system experiences a sudden influx of cargo. This scenario introduces an entirely different type of disruption compared to the drought and labor strike cases: rather than restricting infrastructure or transport capacity, it directly challenges the system's ability to absorb and process a massive influx of demand within a short time frame. Consequently, all components of the port system are expected to experience temporary overload conditions. Queuing, congestion, and delayed handling are likely outcomes during the surge, followed by a recovery phase where the system works through accumulated backlogs.

In short, the scenario serves as a stress test for each strategy's capacity to buffer, adapt, and recover from an acute demand-side shock.

Figure 4.13 shows the number of containers in the system over time during the demand fluctuation scenario. The plot also shows the calculated TTRs per scenario to further analyse performances with the vertical dotted lines. The time to recovery is defined as the time it takes for the number of containers in the system to return to a stable level. This stable level was determined to require a 96-hour window with the amount of containers in the system within a 10,000 TEU tolerance. As expected, all strategies experience a significant rise in system load during the disruption period (days 7–14), when demand spikes to 300% of baseline levels. Among the strategies, Autonomous Facilities is the most effective at containing the backlog during the surge, reaching the lowest peak container count. This confirms its ability to absorb excess demand through added capacity at critical nodes. It also shows the most immediate response once the disruption ends, with a visibly sharper decline in container count starting immediately after day 14.

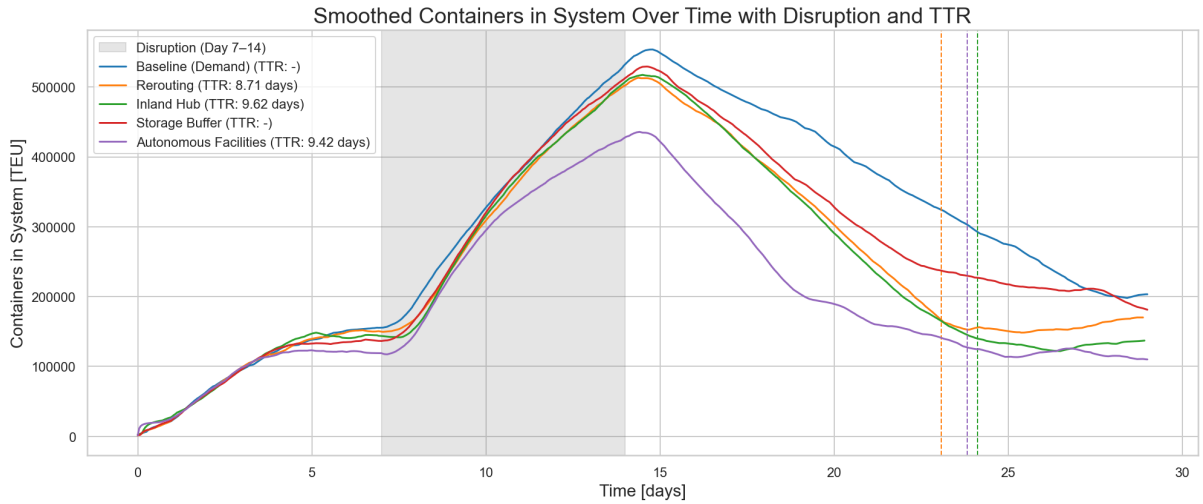

Figure 4.13: Containers in system over time with TTR annotations for each strategy under demand surge conditions.

However, the Rerouting strategy recovers the fastest while being slightly ahead of Autonomous Facilities strategy. While Autonomous Facilities reduces the container count more aggressively after the disruption due to it's increased throughput performance, it still develops delay issues due to congestion at the barge gate. This can be seen in figure 4.13, where at around 18 days the number of containers in the system starts to decrease less quickly. This is the point where the throughput is limited by the barge performance, and the other transport modes throttle

down due to the lack of demand. This is shows a clear vulnerability caused by the inability to switch transport modes. In contrast, Rerouting achieves a steadier final state more quickly, even if its overall peak backlog is higher and its initial response slower. The Inland Hub strategy performs well in terms of TTRs but falls short compared to the Rerouting strategy. This is likely because it relies more heavily on train transport, whereas the Rerouting strategy favors trucks. The reason for this is that the additional hub capacity is located where train rerouting occurs, thus the Inland Hub strategy sends more transport towards the train gate. This preference is confirmed by looking at figure 4.14, which shows that the train utilization rates are higher in the Inland Hub strategy than in the Rerouting strategy. Given that trains are slower than trucks in this context, this reliance likely contributes to the reduced performance observed.

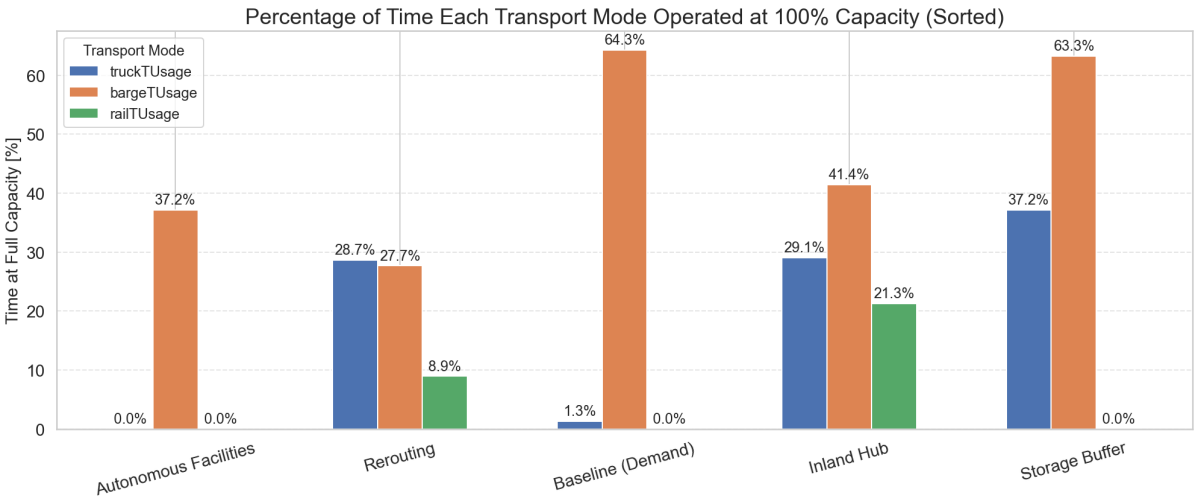

Figure 4.14: Number of full-capacity events per component under the demand fluctuation scenario.

To further investigate the system responses of the different strategies, the delay cost rate plot (Figure 4.15) is examined alongside the containers-in-system curve. Here the TTR is shown as the moment where the cost rate is zero for at least 96 hours, indicating that the system might have reached stability. This figure reinforces the patterns observed earlier: Autonomous Facilities achieves the lowest peak in system congestion and maintains relatively low delay costs throughout the disruption. However, despite its strong overall performance, its Time to Recovery (TTR) in terms of delay costs is slightly slower than that of the Rerouting and Inland Hub strategies. This suggests that while the system increases its container flow relatively quickly, it does face residual queues at the inland transport gates leading to higher delay costs. Notably, the Inland Hub strategy outperforms the Autonomous Facilities strategy in this regard. This is likely because, similar to the Rerouting strategy, it evenly distributes the load across different transport types. This reduces internal delays in the port which has a greater impact on the cost-based TTR than on the TTR based on container volumes, as the latter also considers the time required to transport cargo to its final destinations. Nevertheless, both plots consistently identify Rerouting, Inland Hub and Autonomous Facilities as the most effective strategies, delivering faster stabilization, lower cumulative delay costs, and reduced systemic strain under volatile demand conditions.

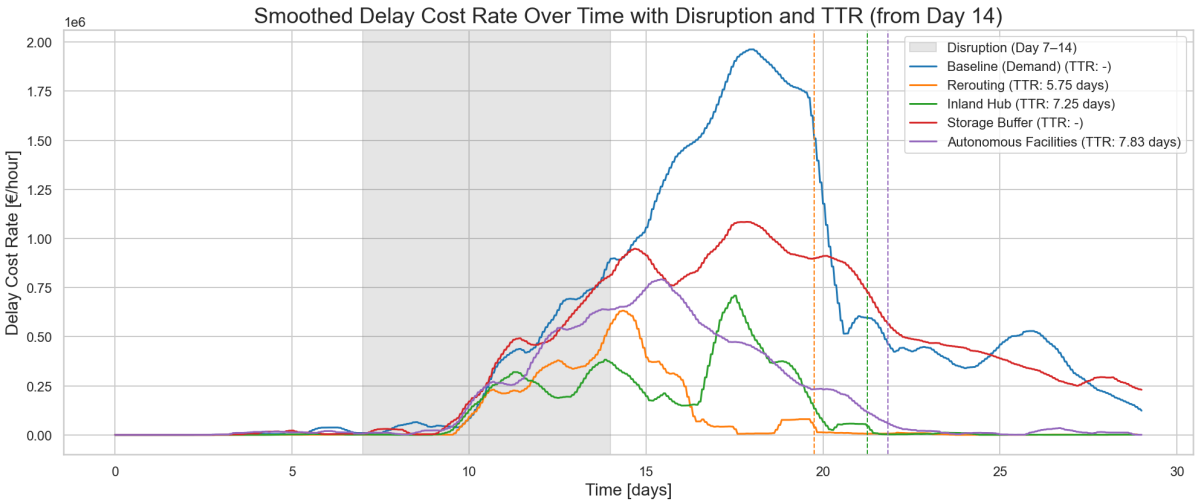

Figure 4.15: Delay cost rate (€/hour) over time with TTR annotations in the demand fluctuation scenario.

It is important to note the distinction between the Time to Recovery (TTR) based on delay costs and that based on containers in the system. While delay costs reflect congestion and queuing within the port infrastructure, they do not capture delays occurring during longer or slower transport outside the port. As a result, delay costs may return to normal even though a backlog of containers remains in transit or awaiting final delivery. This explains why some strategies show a faster TTR in terms of delay costs, while still requiring more time to fully clear the system and reduce the total container count. The two TTR measures therefore capture complementary dimensions of recovery: operational efficiency versus complete throughput normalization.

To further analyze the different strategies, their costs must also be considered. Figure 4.16 presents the total cost composition per TEU across strategies, distinguishing between transport and delay costs. Rerouting and Inland Hub clearly outperform the other strategies in terms of delay cost efficiency. In contrast, Baseline and Storage Buffer accumulate significant delay costs due to prolonged congestion and slower recovery. Additionally, transport costs are highest for Baseline and Storage Buffer strategies. This is likely driven by the overuse of single transport modes, resulting in longer average transport distances and reduced efficiency. This emphasizes the benefit of flexible routing and diversified mode utilization in managing both disruption-induced delays and transport overhead.

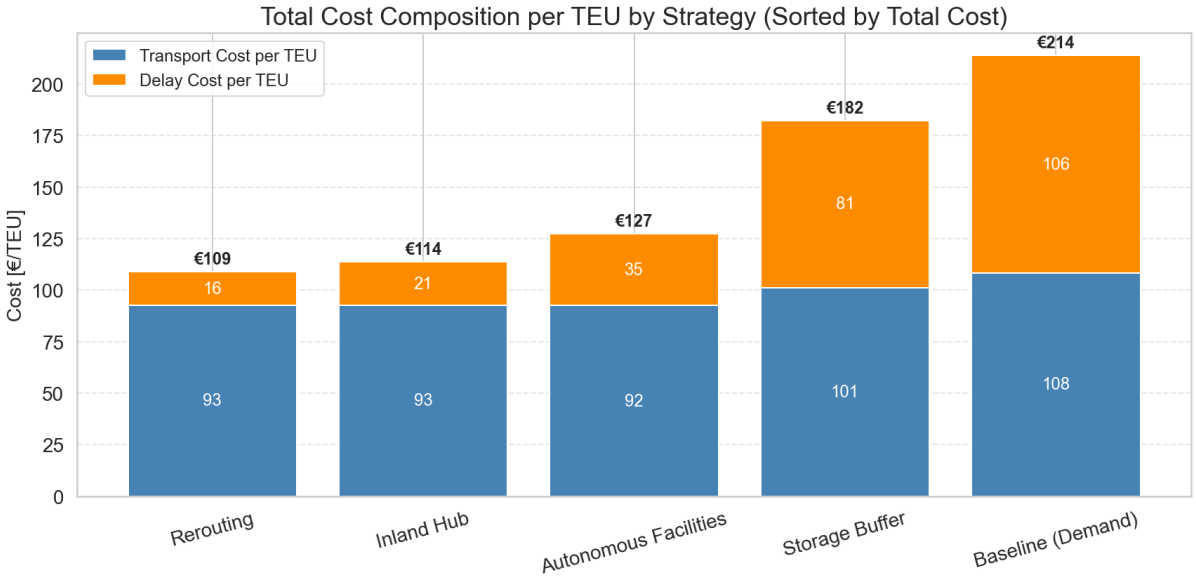

Figure 4.16: Total cost composition per TEU—transport vs. delay costs—for each strategy during the demand surge.

Figure 4.17 compares the distribution of delivery rates across strategies, providing insight into performance stability. Stability is assessed based on the compactness of the interquartile range (IQR), the position of the lower quartile (Q1), and the extent of distribution tails.

The IQRs reveal meaningful differences in the consistency of delivery performance across strategies. The Baseline scenario has the narrowest IQR, while Storage Buffer, Autonomous Facilities, Rerouting, and Inland Hub show progressively wider spreads. Although the Baseline has the most compact IQR, its pronounced lower tail suggests greater volatility and a higher likelihood of systemic underperformance. In contrast, the Rerouting and Inland Hub strategies exhibit the widest IQRs, implying more fluctuation in delivery rates and potentially less stable behavior under varying conditions. This further confirms earlier results, highlighting that the dynamic rerouting mechanisms of these strategies lead to more frequent performance fluctuations. Increased buffer capacities in the Storage Buffer strategy or more efficient facilities like in the Autonomous Facilities strategies do the opposite.

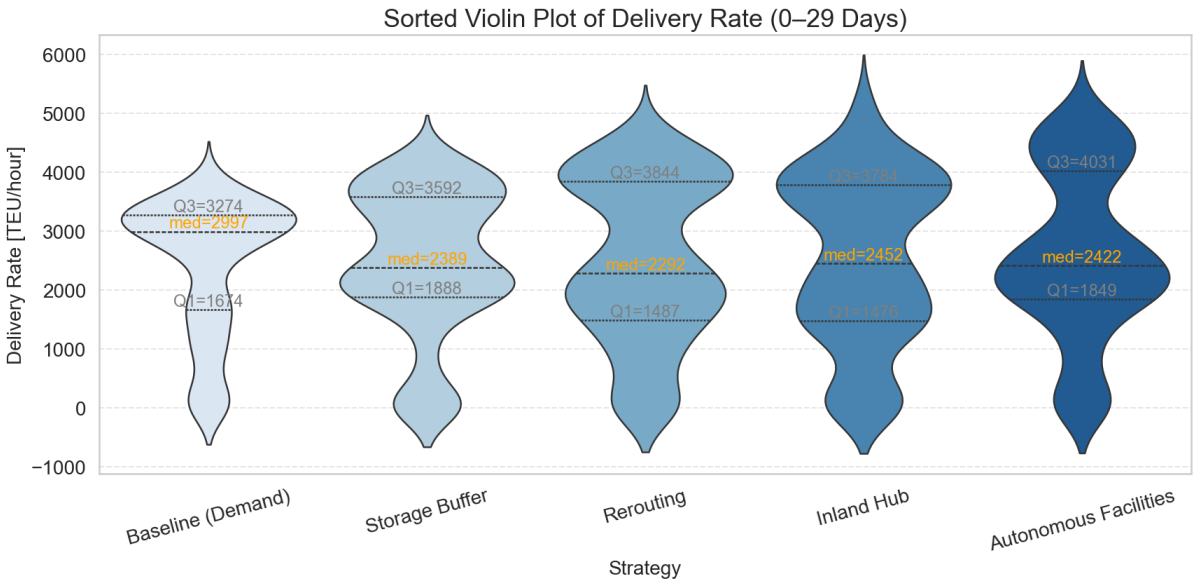

Figure 4.17: Distribution of delivery rates across strategies in the demand fluctuation scenario.

To further understand the underlying stability of the system performance, two aspects of transport system utilization are evaluated: the number of full capacity events per component (Figure 4.18) and the percentage of time each transport mode operates above 60% capacity (Figure 4.19).

Figure 4.18 shows that the highest number of full capacity events occurs in the Autonomous Facilities and Baseline (Demand) strategies, mainly due to repeated saturation of truck transport capacity. Interestingly, strategies like Rerouting and Inland Hub, which showed the highest number of full capacity events under the drought scenario, now exhibit fewer such events. This contrast can be attributed to the way excess demand is handled. In strategies without rerouting mechanisms, barge transport is frequently overloaded. Once barge capacity is reached, it periodically releases and re-accumulates load, leading to repeated spikes in utilization. This cycling behavior results in a high frequency of components hitting 100% utilization.

In contrast, rerouting strategies like Inland Hub and Rerouting can distribute excess demand more evenly across available modes and infrastructure. This buffering effect prevents extreme pressure on any single component.

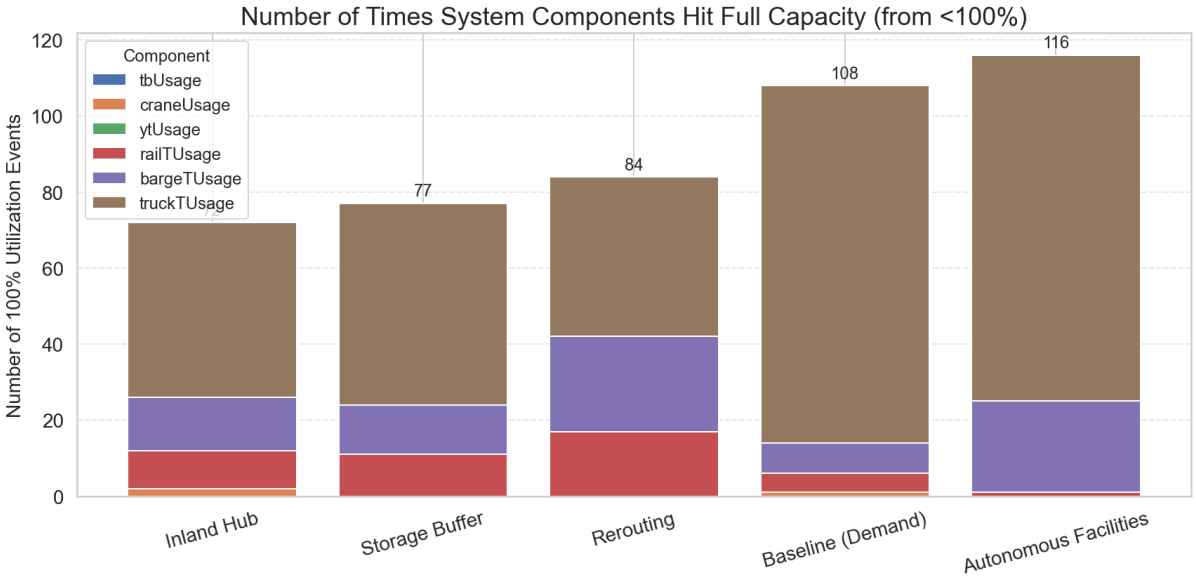

Figure 4.18: Frequency of full-capacity utilization events per component under the demand fluctuation scenario.

Complementing this, Figure 4.19 shows the share of time transport modes operated above 60% capacity. Storage Buffer and Baseline scenarios exhibit especially high utilization of barge and truck transport, which aligns with the congestion levels observed in earlier cost and delay analyses. Notably, strategies like Rerouting and Inland Hub display more balanced modal utilization, spreading demand more effectively across rail, barge, and truck. The Autonomous Facilities strategy shows relatively lower high-utilization time shares despite having the highest number of full capacity events, suggesting that it experiences acute but short-lived spikes rather than sustained overload.

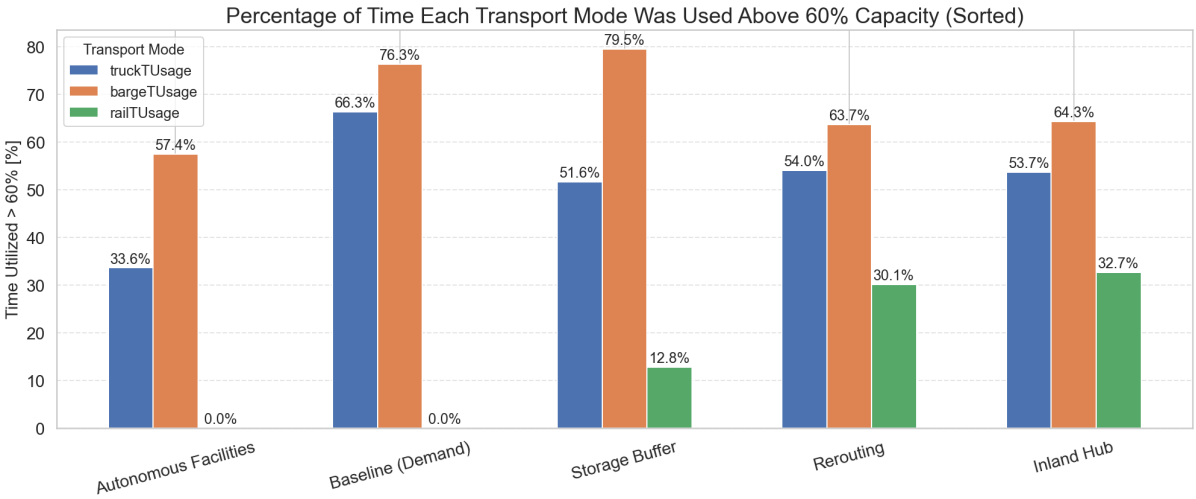

Figure 4.19: Share of time each transport mode operated above 60% capacity during the demand fluctuation scenario.

Overall, these results highlight that not just throughput capacity but also how that capacity is distributed and utilized across transport modes plays a key role in reducing systemic risk and enhancing resilience under volatile conditions.

4.3.1 Collaborative Strategy

While the previous analyses assessed each resilience strategy in isolation, real-world resilience planning often involves coordinated interventions between multiple stakeholders. To explore the potential benefits of such collaboration, an additional experiment was conducted combining the Autonomous Facilities and Rerouting strategies. This setup simulates a scenario in which port authorities invest in capacity-enhancing measures at critical terminals while simultaneously coordinating with inland transport operators to dynamically reallocate flows across truck, rail, and barge in response to congestion. The demand fluctuation scenario was selected for this experiment, as it represents a challenging, high-intensity disruption in which both port-side throughput and inland transport flexibility play critical roles in recovery.

In figure 4.20 the resulting amount of containers in the system over time can be seen, along with the recovery time. This set-up is the same as in the demand scenario results, but with the added collaborative strategy. The figure shows that the collaborative strategy achieves the lowest peak container count of all tested approaches during the demand surge, indicating improved absorption of the disruption through the combined effects of port-side capacity expansion and adaptive inland routing. The approach also delivers the fastest time to recovery and steepest post-disruption decline, suggesting that the strategy mitigates both port-side and inland transport bottlenecks. This is reflected by the fact that the strategy doesn't have a second slower delivery rate like the Autonomous Facilities strategies, which was caused by the barge congestion. By addressing capacity constraints in both sections simultaneously, the collaborative strategy avoids the residual congestion observed when each measure is applied in isolation.

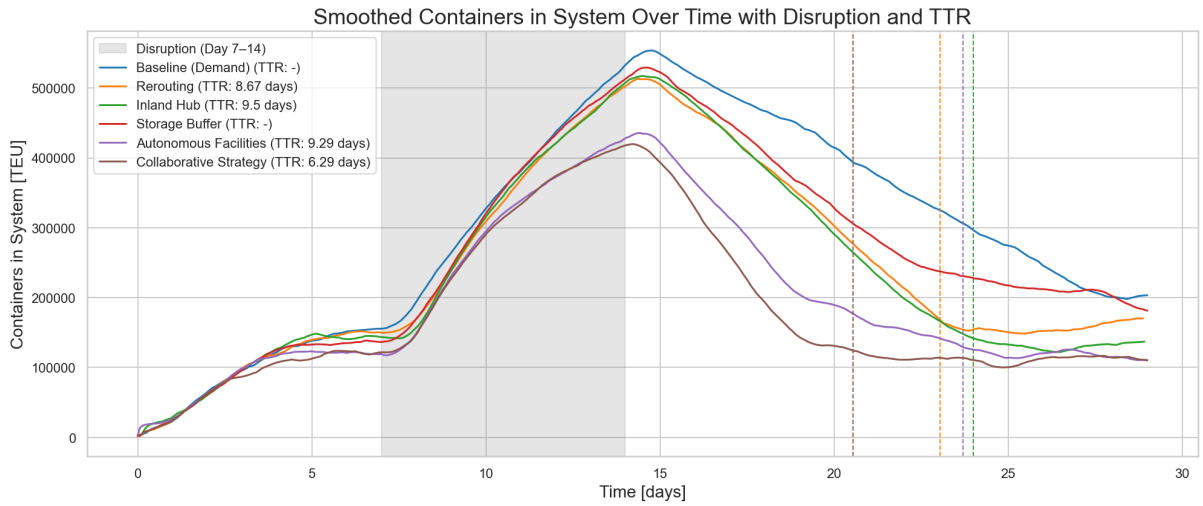

Figure 4.20: Container count in the system over time for all strategies under demand fluctuation.

Figure **??** further demonstrates the increase in performance, by highlighting that the Collaborative strategy maintains the lowest delay cost rates throughout the disruption and recovery phases. It remains well below the peaks observed in all other strategies, showing almost zero delay cost increases throughout the experiment. The Collaborative strategy not only minimizes the magnitude of the cost peaks but also achieves the fastest cost-based recovery, with only one small peak after the disruption.

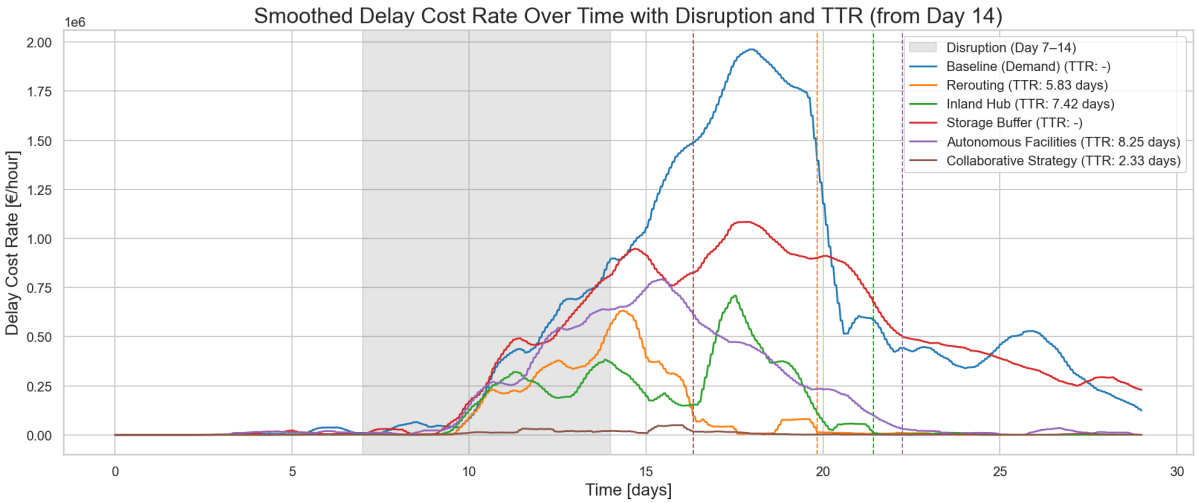

Figure 4.21: Delay cost rate over time for all strategies.

To further evaluate the Collaborative strategy, its performance in terms of stability and systemic shock mitigation is examined. The delivery rate distribution in Figure **??** shows that the strategy achieves a competitive median delivery rate alongside a relatively narrow interquartile range, indicating consistent throughput under fluctuating demand. This represents an improvement over the underlying single strategies, which achieve higher medians but exhibit wider IQRs and a pronounced two-tier distribution, indicating prolonged periods at fixed performance levels. In the collaborative setup, this pattern is less prominent, suggesting that the combination of increased throughput from Autonomous Facilities and adaptive load balancing from Rerouting enables smoother transitions between operating states and greater overall stability.

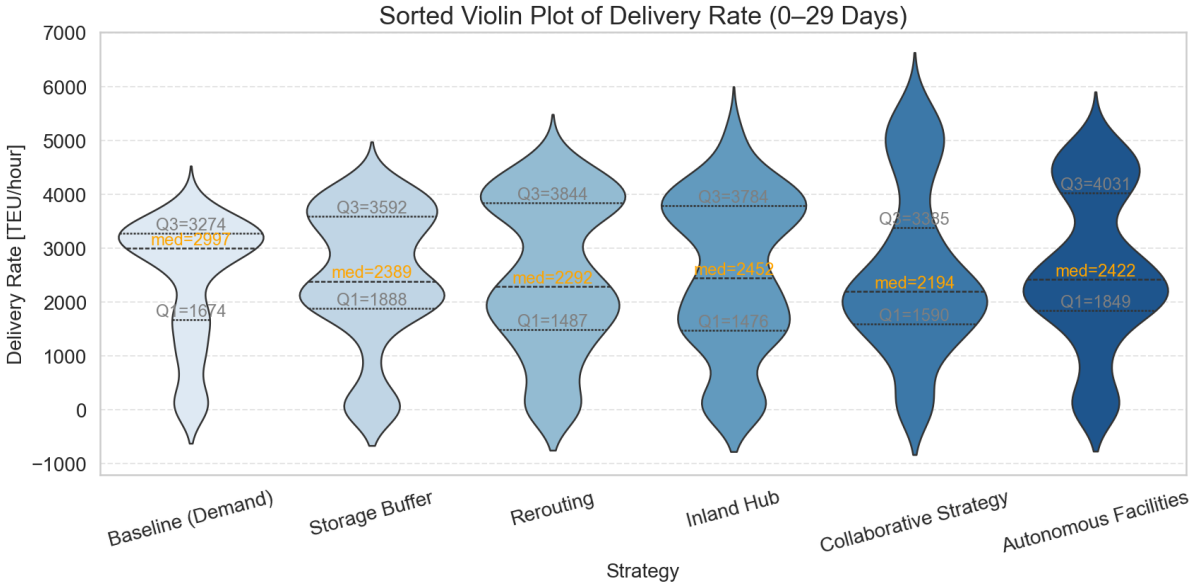

Figure 4.22: Distribution of delivery rates (0–29 days).

In contrast to the findings in the violin plot regarding systemic shock behavior, figure 4.23 reveals that the collaborative strategy records the highest number of full-capacity events (137) among all strategies. This indicates that while the strategy accelerates recovery and sustains high throughput, it also drives the system to operate near its capacity limits more often. This

is expected, as the increased processing speed from the Autonomous Facilities and the capacity-triggered decision-making of the Rerouting strategy reinforce each other, enabling the system to reach and utilize its maximum capacity more frequently. This in turn results in a higher number of full-capacity events and suggests a trade-off: the collaborative approach effectively clears backlogs and maintains performance, but does so by operating with high intensity across transport modes, leading to short-lived yet frequent peaks in component load. Changing the simulation model to make decisions before hitting capacity limits could mitigate this phenomenon and make the strategy the most stable and best performing set-up yet.

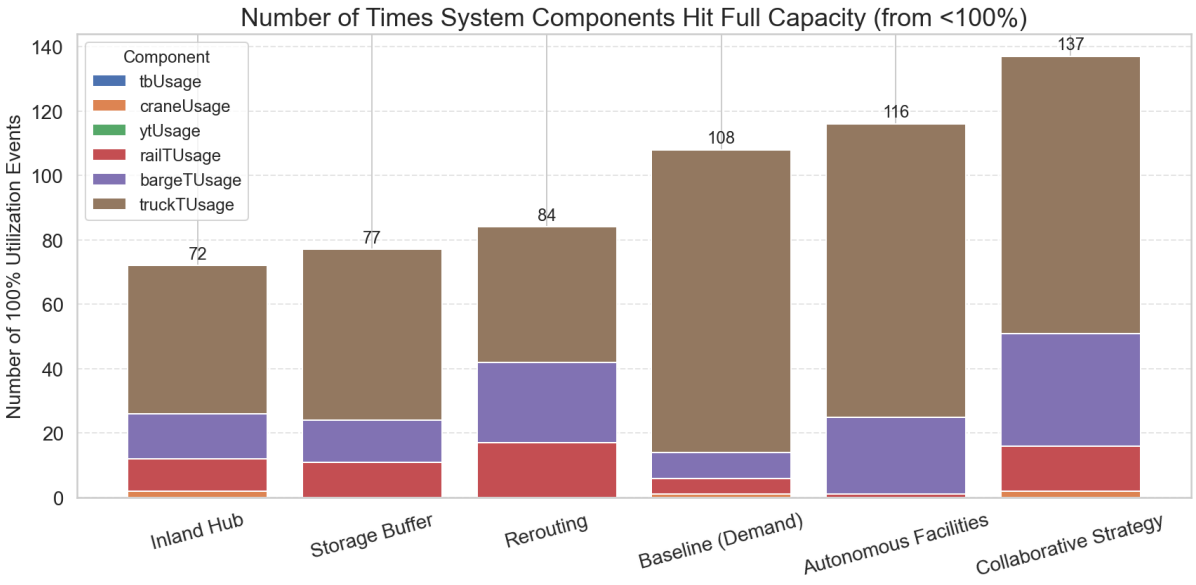

Figure 4.23: Number of full-capacity events per system component.

4.4 Cross-Scenario Evaluation

The simulations across the scenarios reveal that strategy effectiveness is dependent on the nature of the disruption, with each approach offering distinct advantages and trade-offs. While average delivery rates across strategies during these experiments are often similar, the underlying system dynamics concerning recovery speed, delay cost accumulation, variability in performance, and systemic shocks vary considerably. Longer simulated runtimes or more severe disruption settings might lead to larger differences in throughput performance, as some scenarios showed increasing delays throughout the simulation for certain strategies.

The storage buffer strategy offers modest but reliable improvements across all scenarios by smoothing flows at the port interface. In the drought scenario, the lack of extra gate speeds or the inability to switch transport modes causes it to be unable to keep up with demand, similar to the baseline scenario. It does, however, help contain delay costs in short disruptions, such as the labor strike, and maintains relatively stable performance under demand surges. Nevertheless, it lacks the throughput and recovery advantages of the more adaptive or capacity-enhancing strategies, leading to its inability to recover from the drought and demand fluctuation scenarios. Its relative improvement over the baseline also suggests that by moving more cargo to the inland transport gates and maintaining higher queues there, the strategy enables more consistent utilization of hinterland transport capacity.

The autonomous facilities strategy demonstrates consistently high delivery performance and rapid backlog reduction, particularly when disruptions directly affect port infrastructure, as in the labor strike scenario. This is to be expected, as the improvement directly targets the

disrupted components. By increasing capacity at critical nodes, it minimizes peak congestion and stabilizes throughput, achieving the lowest delay cost peaks in both the labor strike and drought scenarios. Its delivery rate distributions are compact, indicating stable performance. However, in the demand-side disruption it recovered slightly slower than the rerouting strategy due to residual internal delays. In this scenario, it also reached full capacity more frequently, which is in contrast to the other scenarios where it performed better regarding stability. The slower recovery speed and increased instability in this scenario suggest that the demand-side disruption overloads the system to such an extent that, without the ability to switch transport modes, congestion persists even when throughput capacity at key components is increased.

The rerouting strategy excels in external disruptions, especially demand surges and drought conditions. By dynamically shifting flows across transport modes, it achieves the fastest recovery times in the demand fluctuation scenario and near-zero delay costs in drought conditions. However, its high variability in delivery rates reflects greater operational volatility, and its performance advantage diminishes in internal disruptions like the labor strike. This is likely caused by rerouting delays and less efficient use of single transport modes, due to switching of cargo and smaller queue sizes.

The inland hub strategy mirrors many of rerouting's advantages, particularly in controlling delay costs under external disruptions. It shows stable recovery in both drought and demand surge scenarios, but its greater reliance on slower train transport and longer routes often results in slightly longer recovery times compared to rerouting. Similar to rerouting, its impact during internal disruptions is limited.

Across all scenarios, a clear trade-off emerges between stability and flexibility. Capacity-enhancing strategies like autonomous facilities provide stability and strong performance under infrastructure constraints but can be less agile in restoring full system equilibrium after demand-side shocks. Flexible routing strategies like rerouting and inland hub recover faster from demand surges but introduce greater operational variability. Cost performance was most consistently strong in the Rerouting and Inland Hub strategies during external disruptions, and in autonomous facilities during internal disruptions, with the baseline scenario and storage buffer strategy incurring the highest cumulative delay costs.

The collaborative strategy, combining autonomous facilities and rerouting, demonstrates that joint implementation of capacity expansion and flexible routing can outperform each measure in isolation. It achieves the lowest peak container counts, fastest recovery times, and lowest delay costs of all tested strategies, while maintaining a relatively narrow interquartile range in delivery rates. This indicates improved stability compared to the single strategies. However, this comes with a notable trade-off: the approach records the highest number of full-capacity events across scenarios, reflecting a tendency to operate at or near system limits more frequently. While this high-intensity utilization accelerates backlog clearance and sustains high throughput, it may also require more robust operational coordination. These results suggest that the collaborative strategy is particularly well-suited for severe disruptions where both port-side capacity and inland transport flexibility are simultaneously stressed, though further model refinement could improve its performance in stability-sensitive contexts.

These findings suggest that no single strategy is universally optimal. Effective resilience planning for the Port of Rotterdam, and similar large-scale multimodal hubs, requires a combination of interventions that can be matched to the nature of the disruption. Infrastructure-focused measures are best suited for internal capacity losses, flexible multi-modal routing is more effective for external transport bottlenecks or demand surges, and buffering capacity offers a relatively simple yet effective means of enhancing performance. The results of the collaborative strategy further highlight the potential of integrated multi-stakeholder approaches, showing that combining complementary measures can yield superior recovery speeds, lower delay costs,

and greater stability. But this might come with the need to manage the increased operational complexity.

Chapter 5

Discussion

This chapter reflects on the performance of the developed simulation model, the outcomes of the evaluated resilience strategies, and their broader implications for port operations and resilience planning. The discussion links the findings directly to specific results presented in Chapter 4, considers stakeholder perspectives, and incorporates cost–benefit reflections. It concludes with remarks on generalizability, relevance to literature, and future research directions.

The simulation results reveal several structural characteristics of the model that shape the interpretation of strategy performance. Improvements in throughput capacity, most evident in the autonomous facilities strategy, enhance not only operational efficiency but also the accuracy of downstream routing logic. By processing the agents faster, downstream availability is updated sooner, allowing more frequent routing decisions. This effect was particularly visible in the drought scenario, where autonomous facilities could keep up with dynamic rerouting strategies while being limited by a single transport mode. Conversely, the routing and blocking logic depends on queue sizes and utilization thresholds, which in highly dynamic flow situations can lead to premature unloading before downstream constraints are accounted for. In the rerouting and inland hub strategies under the Labor Strike scenario, this contributed to short-lived congestion spikes and slightly reduced throughput, highlighting the model's sensitivity to delayed capacity feedback.

Certain resources, notably tugboats and yard trucks, were rarely stressed across all scenarios, suggesting a possible overestimation of their availability or underrepresentation of their handling time variability. Inland terminal capacity consistently emerged as a major bottleneck, even in the drought scenario where barge operations were directly impaired. Congestion concentrated at inland terminals rather than along the waterway, whereas in reality, additional downstream constraints—such as lock scheduling or regional infrastructure capacity limits—could further exacerbate delays. These factors, combined with the idealized handling speeds and lack of stochastic variability in operations, suggest that the model may slightly overestimate the real-world throughput potential of the Port of Rotterdam. More granular calibration, disruption case studies, and expert validation would enhance representativeness.

The comparative performance analysis underscores that no single strategy is universally optimal. Effectiveness depends on the disruption type, with each approach offering distinct advantages and trade-offs. From a port authority perspective, infrastructure-focused measures like autonomous facilities offer clear benefits under internal disruptions by directly addressing port-side capacity limitations. However, these measures require significant capital investment and show diminishing returns in demand-side disruptions where inland capacity becomes the limiting factor. From the perspective of terminal operators, buffering measures such as storage capacity buffer provide a relatively low-cost method to smooth flows and contain delay costs

in short, sharp events. Yet, they lack the flexibility to handle prolonged or multi-modal disruptions. Logistics providers and carriers benefit more from flexible routing measures, such as rerouting and inland hub, which proved most effective in external disruptions like demand fluctuation and drought by bypassing bottlenecks and reducing recovery times. However, these strategies can increase operational variability, and may in practice lead to higher transport costs.

The collaborative strategy, combining autonomous facilities and rerouting, demonstrated that joint implementation of capacity expansion and flexible routing can outperform each measure in isolation. Across all strategies, it achieved the lowest peak delays, fastest recovery times, and relatively stable delivery rate distributions. Yet, it also recorded the highest frequency of full-capacity events, indicating that while backlogs were cleared rapidly, the system operated closer to its limits. For stakeholders, this implies both faster recovery and a potential increase in operational risk if disruptions escalate, underscoring the importance of robust coordination mechanisms when deploying high-intensity strategies.

Although this study evaluates strategies based on operational performance, cost considerations remain crucial for real-world decision-making. The autonomous facilities strategy involves substantial capital expenditure, potentially running into hundreds of millions of euros for full-scale automation [92]. Recent studies have also shown that the costs of automated port equipment are not necessarily well-covered by the performance improvements [95]. Dynamic rerouting requires comparatively lower upfront investments but may lead to higher variable transport costs. These differences are particularly relevant given that variable transport costs per mode, as reported in [94], vary significantly and can influence the net benefits of rerouting-heavy strategies. Switching costs between transport modes have also been excluded in this analysis. It is notable to mention that using the transport type with the lowest distance based cost might not necessarily be the cheapest option, as increased network utilization might lead to longer routes. Delay costs can offset higher transport costs in severe disruptions, but only when the avoided delays are substantial. A full cost–benefit analysis would be needed to assess the economic feasibility of each strategy in operational practice.

These findings are consistent with resilience literature that distinguishes between absorptive capacity, such as buffering and storage, and adaptive capacity, such as rerouting, both of which are essential for maintaining performance under disruption [36, 40]. The strong performance of the collaborative strategy reflects the integrated approach to resilience described in [33], where combining capacity expansion with flexible routing enhances both robustness and adaptability. Nevertheless, the generalizability of these results is shaped by the model's calibration to the Dutch national territory and the specific operational and infrastructural characteristics of the Port of Rotterdam. While the tested mechanisms are conceptually relevant to other large multimodal ports, absolute performance outcomes will depend on local geographic, infrastructural, and regulatory contexts.

The study's main limitations stem from its simplified operational processes, the reactive nature of routing logic, and the underrepresentation of certain constraints such as customs clearance, scheduling or network path congestion at points further downstream. Furthermore, the absence of an comprehensive cost–benefit model means that strategy prioritization remains focused on operational resilience rather than full economic viability. Addressing these limitations would involve integrating predictive routing algorithms, calibrating model parameters with historical disruption data, and expanding the representation of hinterland transport constraints.

Future research could focus on incorporating a more comprehensive model for the port operations while retaining the holistic view of sea-, port and land aspects. Dynamically responsive models which predict utilization levels before hitting capacity limits would also be beneficial. Incorporating a more comprehensive economic evaluation into resilience strategy assessment,

and exploring stakeholder-driven scenario weighting to align priorities with risk tolerance would also improve the assessment of the strategy performances. By doing so, decision-making for resilience planning could shift from purely operational optimisation towards strategies that balance performance, cost-effectiveness, and practical feasibility.

Overall, the results confirm that resilience in complex port–hinterland systems is multi-faceted. Infrastructure measures provide stability during capacity-limited disruptions, routing measures excel in demand-side shocks, and buffering offers low-cost baseline improvements. Combining complementary strategies, particularly capacity enhancement and routing flexibility, can deliver superior resilience outcomes, but also increases operational intensity. These trade-offs highlight the need for integrated, stakeholder-informed, and economically grounded resilience planning for large multimodal ports such as Rotterdam.

Chapter 6

Conclusion

This research set out to determine how systemic risks in port operations can be minimized through resilience-based strategies, identified via a simulation of port disruptions and recovery. The study began by identifying key systemic risks and disruption types in port–hinterland systems, including capacity constraints, demand surges, and infrastructure failures affecting sea-, port-, and land-side operations. These risks were addressed through resilience strategies derived from the literature, reflecting both absorptive measures, such as storage buffers, and adaptive measures, such as dynamic rerouting and inland hub activation, alongside capacity-enhancing measures like autonomous facilities.

To evaluate these strategies, a hybrid agent-based and discrete-event simulation model was developed, representing the operational flow of containers and the decision-making of transport actors in a multimodal network. The model was used to simulate multiple disruption scenarios and quantify their impact through performance-based metrics, including time to recovery, delivery rate stability, delay costs, and total costs per TEU. These metrics enabled a systematic comparison of strategies and revealed how performance varied according to disruption type and severity.

The results show that no single strategy is universally optimal. Autonomous facilities delivered the greatest benefits when port-side capacity was the limiting factor, while routing-based measures performed best when inland bottlenecks or external shocks dominated. Storage capacity buffers provided consistent but modest benefits in short disruptions, though they lacked adaptability for longer or more complex events. The collaborative strategy—combining autonomous facilities with dynamic rerouting—consistently outperformed individual measures, delivering faster recovery, lower peak delays, and more stable throughput. However, this came at the cost of operating closer to capacity limits, which may heighten vulnerability under extreme conditions.

Finally, while the cost-effectiveness analysis in this study was indicative rather than comprehensive, it highlighted the trade-offs between high-capital strategies with stable long-term benefits and lower-investment measures with higher operational variability. Delay cost reductions can offset increased transport costs in severe disruptions, but this depends on disruption characteristics and the scale of avoided delays.

Overall, the study concludes that systemic risk reduction in port operations is best achieved through a tailored mix of strategies matched to disruption type, supplemented by integrated approaches that combine capacity expansion with operational flexibility. The simulation-based framework developed here provides a transferable method for assessing such strategies, though absolute performance outcomes will depend on local infrastructure, geography, and governance contexts.

Bibliography

[1] T. Gokan *et al.*, "Economic impacts of the blockage of the suez canal: An analysis by ide-gsm," *IDE Discussion Papers*, no. 919, 2024. [Online]. Available: https://www.ide.go.jp/English/Publish/Reports/Dp/919.html.

[2] M. Christiansen, E. Hellsten, D. Pisinger, D. Sacramento, and C. Vilhelmsen, "Liner shipping network design," *European Journal of Operational Research*, vol. 286, no. 1, Oct. 2020. [Online]. Available: https://linkinghub.elsevier.com/retrieve/pii/S0377221719308148 (visited on 01/20/2025).

[3] Port of Rotterdam Authority. "Facts and figures." (2025), [Online]. Available: https://www.portofrotterdam.com/en/experience-online/facts-and-figures.

[4] Port of Rotterdam Authority, *Port of rotterdam facts & figures 2024*, 2024. [Online]. Available: https://www.portofrotterdam.com/en/news-and-press-releases/facts-and-figures.

[5] MFAT, "Implications of shipping disruptions in the red sea: A view from europe," *MFAT Market Reports*, 2024. [Online]. Available: https://www.mfat.govt.nz/en/trade/mfat-market-reports/implications-of-shipping-disruptions-in-the-red-sea-february-2024/.

[6] E. Thomson. "Droughts are creating new supply chain problems. this is what you need to know." (Oct. 2023), [Online]. Available: https://www.weforum.org/stories/2023/10/drought-trade-rivers-supply-chain/.

[7] M. Riquelme-Solar, E. van Slobbe, and S. E. Werners, "Adaptation turning points on inland waterway transport in the rhine river," *Journal of Water and Climate Change*, vol. 6, no. 4, pp. 670–682, 2015. DOI: 10.2166/wcc.2014.091.

[8] UNCTAD. "Unprecedented shipping disruptions raise risk to global trade, UNCTAD warns." Accessed: 2025-08-15. (Feb. 2024), [Online]. Available: https://unctad.org/news/unprecedented-shipping-disruptions-raise-risk-global-trade-unctad-warns.

[9] André, Marine Charlotte and Delanote, Julie and Gutierrez, Dominique Aira and Haraszti, Péter and Weiss, Christoph, "Navigating supply chain disruptions: New insights into the resilience and transformation of eu firms," European Investment Bank (EIB), Technical Report QH-01-24-002-EN-N, Oct. 2024, Accessed: 2025-08-15, p. 52. DOI: 10.2867/3765519. [Online]. Available: https://www.eib.org/en/publications/20240179-navigating-supply-chain-disruptions.

[10] Y. Xu, P. Peng, C. Claramunt, F. Lu, and R. Yan, "Cascading failure modelling in global container shipping network using mass vessel trajectory data," *Reliability Engineering and System Safety*, vol. 249, p. 110 231, 2024. DOI: 10.1016/j.ress.2024.110231. [Online]. Available: https://linkinghub.elsevier.com/retrieve/pii/S0951832024003041.

[11] J. Verschuur, R. Pant, E. Koks, and J. Hall, "A systemic risk framework to improve the resilience of port and supply-chain networks to natural hazards," *Maritime Economics & Logistics*, pp. 1–18, 2022. DOI: 10.1057/s41278-021-00204-8. [Online]. Available: https://www.semanticscholar.org/paper/34cc52cc9c38929cae9e89fd14e6862db19c1c85.

[12] Y. Cao *et al.*, "Data-driven resilience analysis of the global container shipping network against two cascading failures," *Transportation Research Part E: Logistics and Transportation Review*, vol. 193, p. 103 857, 2025. DOI: 10.1016/j.tre.2024.103857. [Online]. Available: https://linkinghub.elsevier.com/retrieve/pii/S1366554524004484.

[13] V. Wendler-Bosco and C. Nicholson, "Port disruption impact on the maritime supply chain: A literature review," *Sustainable and Resilient Infrastructure*, vol. 5, no. 6, 2020. DOI: 10.1080/23789689.2019.1600961. [Online]. Available: https://www.researchgate.net/publication/333057542_Port_disruption_impact_on_the_maritime_supply_chain_a_literature_review.

[14] U. N. C. on Trade and Development, *Navigating the red sea crisis: Impacts on global trade and shipping routes*, 2024. [Online]. Available: https://unctad.org.

[15] I. T. F. (OECD), "The red sea crisis: Impacts on global shipping and the case for international co-operation," *OECD/ITF Report*, 2024.

[16] Maersk. "The ongoing ripple effects of red sea shipping disruptions." (2024), [Online]. Available: https://www.maersk.com/insights/resilience/2024/07/09/effects-of-red-sea-shipping.

[17] I. M. Fund. "Red sea attacks disrupt global trade." (2024), [Online]. Available: https://www.imf.org/en/Blogs/Articles/2024/03/07/Red-Sea-Attacks-Disrupt-Global-Trade.

[18] O. for Economic Co-operation and Development, *The competitiveness of global port-cities: Synthesis report*, 2014. DOI: 10.1787/9789264205277-en. [Online]. Available: https://www.oecd.org/content/dam/oecd/en/publications/reports/2013/09/the-competitiveness-of-global-port-cities-synthesis-report_g17a2367/5k40hdhp6t8s-en.pdf.

[19] O. Jonkeren and P. Rietveld, *Impacts of low and high water levels on inland waterway transport: Literature review for Kennis voor Klimaat*, 2009.

[20] I. P. on Climate Change, "Europe," in *Climate Change 2022: Impacts, Adaptation and Vulnerability*, Cambridge University Press, 2022. DOI: 10.1017/9781009325844.015. [Online]. Available: https://www.ipcc.ch/report/ar6/wg2/chapter/technical-summary/.

[21] A. Christodoulou and H. Demirel, "Impacts of climate change on transport: A focus on airports, seaports and inland waterways," European Commission, Joint Research Centre, Tech. Rep., 2018. DOI: 10.2760/67775. [Online]. Available: https://publications.jrc.ec.europa.eu/repository/handle/JRC108865.

[22] C. C. C. Service, *European state of the climate 2024*, 2024. [Online]. Available: https://climate.copernicus.eu.

[23] J. Verschuur, "Multi-hazard risk to global port infrastructure and resulting trade and logistics losses," 2023, DOI: 10.1038/s43247-022-00656-7.

[24] Z. Yang, "Port resilience to climate change in the greater bay area," *Journal of Shipping and Trade*, 2025.

[25] J. Verschuur, M. Haraguchi, and S. Hallegatte, "Multi-hazard risk to global port infrastructure and resulting trade risk," *Communications Earth & Environment*, vol. 3, no. 125, 2022.

[26] Maersk, *Slow operations at hutchinson port delta ii in rotterdam*, 2025. [Online]. Available: https://www.maersk.com/news/articles/2025/02/11/slow-operations-at-hutchinson-port-delta-in-rotterdam.

[27] M. Wang and H. Wang, "Exploring the failure mechanism of container port logistics system based on multi-factor coupling," *Journal of Marine Science and Engineering*, vol. 11, no. 5, p. 1067, 2023. DOI: 10.3390/jmse11051067. [Online]. Available: https://www.mdpi.com/2077-1312/11/5/1067.

[28] A. Greenberg, *The untold story of notpetya, the most devastating cyberattack in history*, 2018. [Online]. Available: https://www.wired.com/story/notpetya-cyberattack-ukraine-russia-code-crashed-the-world/.

[29] A. B. Corporation, *Dp world cyberattack disrupts australian port operations*, 2023. [Online]. Available: https://www.abc.net.au/news.

[30] C. Guan and C. Wooldridge, "The impact of covid-19 on the global maritime transport and port industry," *Maritime Economics & Logistics*, 2021.

[31] M. Rinaldi *et al.*, "A systematic review of disruption and resilience research in supply chains," *International Journal of Production Research*, vol. 60, no. 13, pp. 4054–4078, 2022. DOI: 10.1080/00207543.2021.2002941.

[32] J. B. Rice, F. Caniato, and E. Brandon-Jones, "The resilience framework: A supply chain perspective," *International Journal of Production Research*, vol. 57, no. 22, pp. 7123–7138, 2019. DOI: 10.1080/00207543.2019.1629674.

[33] UNCTAD, *Resilient ports: Key to a resilient maritime supply chain*, 2023. [Online]. Available: https://resilientmaritimelogistics.unctad.org/guidebook/2-resilient-ports-key-resilient-maritime-supply-chain.

[34] R. Pant, K. Barker, and C. W. Zobel, "Supply chain resilience and sustainability: A comparative analysis of current literature," *International Journal of Production Research*, vol. 52, no. 18, pp. 5367–5383, 2014. DOI: 10.1080/00207543.2013.859116.

[35] M. Yang, H. Sun, and S. Geng, "On the quantitative resilience assessment of complex engineered systems," *Process Safety and Environmental Protection*, vol. 174, pp. 941–950, 2023. DOI: 10.1016/j.psep.2023.05.019. [Online]. Available: https://linkinghub.elsevier.com/retrieve/pii/S0957582023003865.

[36] K. X. Li, H. Wang, Y. Yang, and M. Li, "Resilience in maritime logistics: Theoretical framework, research methodology, and indicator system," *Ocean & Coastal Management*, vol. 259, p. 107 465, 2024. DOI: 10.1016/j.ocecoaman.2024.107465. [Online]. Available: https://linkinghub.elsevier.com/retrieve/pii/S0964569124004502.

[37] M. Dhanak, S. Parr, E. I. Kaisar, P. Goulianou, H. Russell, and F. Kristiansson, "Resilience assessment tool for port planning," *Environment and Planning B: Urban Analytics and City Science*, vol. 48, no. 5, pp. 1126–1143, 2021. DOI: 10.1177/2399808321997824. [Online]. Available: https://journals.sagepub.com/doi/10.1177/2399808321997824.

[38] H. Sun *et al.*, "A simulation-based approach for resilience assessment of process system: A case of lng terminal system," *Reliability Engineering and System Safety*, vol. 249, p. 110 207, 2024. DOI: 10.1016/j.ress.2024.110207. [Online]. Available: https://linkinghub.elsevier.com/retrieve/pii/S0951832024002801.

[39] N. Vanlaer, S. Albers, A. Guiette, S. Van Den Oord, and H. Marynissen, "100% operational! an organizational resilience perspective on ports as critical infrastructures," *Case Studies on Transport Policy*, vol. 10, no. 1, pp. 57–65, 2022. DOI: 10.1016/j.cstp.2021.11.002. [Online]. Available: https://linkinghub.elsevier.com/retrieve/pii/S2213624X21001772.

[40] T. Notteboom and J. S. L. Lam, "Dealing with uncertainty and volatility in shipping and ports," *Maritime Policy & Management*, vol. 41, no. 7, pp. 611–614, 2014. DOI: 10.1080/03088839.2014.965297. [Online]. Available: http://www.tandfonline.com/doi/abs/10.1080/03088839.2014.965297.

[41] V. Roso, J. Woxenius, and K. Lumsden, "The dry port concept: Connecting container seaports with the hinterland," *Journal of Transport Geography*, vol. 17, no. 5, pp. 338–345, 2009. DOI: 10.1016/j.jtrangeo.2008.10.008.

[42] T. E. Notteboom and J.-P. Rodrigue, "Port regionalization: Towards a new phase in port development," *Maritime Policy & Management*, 2005. DOI: 10.1080/03088830500139885. [Online]. Available: https://www.tandfonline.com/doi/full/10.1080/03088830500139885.

[43] M. Courant, *Containertransferium alblasserdam groeit als kool*, 2021. [Online]. Available: https://maritiemmedia.nl/containertransferium-alblasserdam-groeit-als-kool/.

[44] TNO, "Binnenhaven alphen aan den rijn," TNO, Tech. Rep., 2004. [Online]. Available: https://www.tno.nl.

[45] P. Gelderland, *Railterminal gelderland*, 2020. [Online]. Available: https://www.gelderland.nl/projecten/railterminal-gelderland/achtergrond.

[46] H. Flämig and M. Hesse, "Placing dryports. port regionalization as a planning challenge – the case of hamburg, germany, and the süderelbe," *Research in Transportation Economics*, vol. 33, no. 1, pp. 42–50, 2011, ISSN: 0739-8859. DOI: 10.1016/j.retrec.2011.08.005. [Online]. Available: https://doi.org/10.1016/j.retrec.2011.08.005.

[47] T. Abu-Aisha, J.-F. Audy, and M. Ouhimmou, "Toward an efficient sea-rail intermodal transportation system: A systematic literature review," *Journal of Shipping and Trade*, vol. 9, p. 23, 2024. DOI: 10.1186/s41072-024-00182-z. [Online]. Available: https://doi.org/10.1186/s41072-024-00182-z.

[48] F. Vinke, M. van Koningsveld, C. van Dorsser, F. Baart, P. van Gelder, and T. Vellinga, "Cascading effects of sustained low water on inland shipping," *Transport Policy*, vol. 116, pp. 98–110, 2022. DOI: 10.1016/j.tranpol.2021.12.005.

[49] J. Verschuur, E. E. Koks, and J. W. Hall, "Port disruptions due to natural disasters: Insights into port and logistics resilience," *Transportation Research Part D: Transport and Environment*, vol. 85, p. 102 393, 2020. DOI: 10.1016/j.trd.2020.102393. [Online]. Available: https://linkinghub.elsevier.com/retrieve/pii/S1361920920305800.

[50] N. U. I. Hossain, F. Nur, S. Hosseini, R. M. Jaradat, M. Marufuzzaman, and S. Puryear, "A bayesian network based approach for modeling and assessing resilience: A case study of a full service deep water port," *Reliability Engineering & System Safety*, vol. 189, pp. 378–396, 2019. DOI: 10.1016/j.ress.2019.04.037.

[51] U. N. E. C. for Europe, *Climate change impacts and adaptation for transport networks and nodes*, 2021. [Online]. Available: https://unece.org.

[52] G. Praetorius, E. Hollnagel, and J. Dahlman, "Modelling vessel traffic service to understand resilience in everyday operations," *Reliability Engineering and System Safety*, vol. 141, pp. 10–21, 2015. DOI: 10.1016/j.ress.2015.03.020.

[53] C. Zhou *et al.*, "Analytics with digital-twinning: A decision support system for maintaining a resilient port," *Decision Support Systems*, vol. 143, p. 113 496, 2021. DOI: 10.1016/j.dss.2021.113496. [Online]. Available: https://linkinghub.elsevier.com/retrieve/pii/S0167923621000063.

[54] R. Pant, K. Barker, and C. W. Zobel, "Supply chain resilience and the management of disruption risk in port–hinterland transport networks," *Transportation Research Part E: Logistics and Transportation Review*, vol. 72, pp. 282–298, 2014. DOI: 10.1016/j.tre.2014.10.003.

[55] O. Berle, B. E. Asbjørnslett, and J. B. Rice Jr, "A vulnerability framework for analyzing resilience in maritime logistics," *International Journal of Production Economics*, vol. 147, pp. 455–464, 2013, Proposes absorptive, adaptive, and restorative capacity as core resilience dimensions. DOI: 10.1016/j.ijpe.2013.08.029.

[56] N. Wang, M. Wu, and K. F. Yuen, "Assessment of port resilience using bayesian network: A study of strategies to enhance readiness and response capacities," *Reliability Engineering & System Safety*, vol. 237, p. 109 394, 2023. DOI: 10.1016/j.ress.2023.109394. [Online]. Available: https://linkinghub.elsevier.com/retrieve/pii/S0951832023003083.

[57] Q. Liu, Y. Yang, A. K. Ng, and C. Jiang, "An analysis on the resilience of the european port network," *Transportation Research Part A: Policy and Practice*, vol. 170, p. 103 778, 2023, ISSN: 0965-8564. DOI: 10.1016/j.tra.2023.103778. [Online]. Available: https://doi.org/10.1016/j.tra.2023.103778.

[58] X. Bai, Z. Ma, and Y. Zhou, "Data-driven static and dynamic resilience assessment of the global liner shipping network," *Transportation Research Part E*, vol. 170, p. 103 016, 2023. DOI: 10.1016/j.tre.2023.103016.

[59] R. W. Fransen and I. Y. Davydenko, "Empirical agent-based model simulation for the port nautical services: A case study for the port of rotterdam," *Maritime Transport Research*, vol. 2, p. 100 040, 2021. DOI: 10.1016/j.martra.2021.100040. [Online]. Available: https://linkinghub.elsevier.com/retrieve/pii/S2666822X21000319.

[60] L. Zhen *et al.*, "An agent-based simulation approach for the yard truck scheduling problem in container terminals," *Maritime Economics & Logistics*, vol. 21, no. 2, pp. 266–288, 2019. DOI: 10.1057/s41278-017-0084-0.

[61] W. Bi, K. MacAskill, and J. Schooling, "Old wine in new bottles? understanding infrastructure resilience: Foundations, assessment, and limitations," *Transportation Research Part D: Transport and Environment*, vol. 120, p. 103 793, 2023. DOI: 10.1016/j.trd.2023.103793. [Online]. Available: https://doi.org/10.1016/j.trd.2023.103793.

[62] D. Han, X. Cheng, H. Chen, C. Xiao, Y. Wen, and Z. Sui, "Simulation modeling for ships entering and leaving port in qiongzhou strait waters: A multi-agent information interaction method," 2023.

[63] L. Li, C. Wei, J. Liu, J. Chen, and H. Yuan, "Assessing port cluster resilience: Integrating hypergraph-based modeling and agent-based simulation," *Transportation Research Part D: Transport and Environment*, vol. 136, p. 104 459, 2024. DOI: 10.1016/j.trd.2024.104459. [Online]. Available: https://linkinghub.elsevier.com/retrieve/pii/S1361920924004164.

[64] P. Srisurin, P. Pimpanit, and P. Jarumaneeroj, "Evaluating the long-term operational performance of a large-scale inland terminal: A discrete event simulation-based modeling approach," *PLOS One*, vol. 17, no. 12, e0278649, 2022. DOI: 10.1371/journal.pone.0278649. [Online]. Available: https://doi.org/10.1371/journal.pone.0278649.

[65] T. Vitsounis and A. Pallis, "Port value chains and the role of interdependencies," *Maritime Logistics: Contemporary Issues*, pp. 155–173, Jan. 2012.

[66] S. Nikghadam, R. Vanga, J. Rezaei, and L. Tavasszy, "Cooperation between vessel service providers in ports: An impact analysis using simulation for the port of rotterdam," *Maritime Transport Research*, vol. 4, Jun. 2023, ISSN: 2666822X. DOI: 10.1016/j.martra.2023.100083. [Online]. Available: https://linkinghub.elsevier.com/retrieve/pii/S2666822X23000023.

[67] X. Gou and J. S. L. Lam, "Risk analysis of marine cargoes and major port disruptions," *Maritime Economics & Logistics*, vol. 21, no. 4, pp. 497–523, 2019.

[68] The AnyLogic Company, *Road traffic library webinar q&a*, 2018. [Online]. Available: https://www.anylogic.com/upload/models/rtl_webinar_qna.pdf.

[69] Port of Rotterdam Authority, *Port of rotterdam transport network routes*, 2024. [Online]. Available: https://www.portofrotterdam.com/nl/logistiek/verbindingen.

[70] M. E. Solutions, "Propulsion trends in container vessels," 2025.

[71] Maersk, *How are containers unloaded from a vessel?* 2024. [Online]. Available: https://www.maersk.com/logistics-explained/transportation-and-freight/2024/08/13/unloading-a-vessel.

[72] Port of Rotterdam Authority, *Container terminals and depots in the rotterdam port area*, 2021. [Online]. Available: https://www.portofrotterdam.com/sites/default/files/2021-06/container-terminals-and-depots-in-the-rotterdam-port-area.pdf.

[73] B. Wiegmans and P. Witte, "Efficiency of inland waterway container terminals: Stochastic frontier and data envelopment analysis to analyze the capacity design- and throughput efficiency," *Transportation Research Part A: Policy and Practice*, vol. 106, pp. 12–21, 2017. DOI: 10.1016/j.tra.2017.09.007. [Online]. Available: https://doi.org/10.1016/j.tra.2017.09.007.

[74] APM Terminals Maasvlakte II, *Truck Turn Times*, https://www.apmterminals.com/nl/maasvlakte/e-tools/truck-turn-times, 2025.

[75] RSC Rotterdam. "Trains summary." (2024), [Online]. Available: https://www.rscrotterdam.nl/trains-summary/.

[76] Europe Container Terminals (ECT), *Rail Related Services – Hutchison Ports ECT Rotterdam*, https://www.ect.nl/sites/www.ect.nl/files/documenten/publicaties/rail_related_services_ect_rotterdam.pdf, Version 3.0, January 4, 2024, 2024.

[77] G. Schermers, *Dutch evaluation of chauffeur assistant version 3.25*, https://www.rijksoverheid.nl/documenten/publicaties/2024/05/01/dutch-evaluation-of-chauffeur-assistant-version-3-25, 2004.

[78] O. Jonkeren, P. Rietveld, and J. Van Ommeren, "Modal-split effects of climate change: The effect of low water levels on the competitive position of inland waterway transport in the river rhine area," *Transportation Research Part A: Policy and Practice*, vol. 45, no. 10, pp. 1007–1019, 2011. DOI: 10.1016/j.tra.2009.01.004.

[79] E. Commission, *Trans-european transport network (ten-t)*, 2024. [Online]. Available: https://transport.ec.europa.eu/transport-themes/infrastructure-and-investment/trans-european-transport-network-ten-t_en.

[80] *Rail freight transport in the EU: still not on the right track; Special Report No 08, 2016*, Luxembourg, 2016, ISBN: 978-92-872-4610-3. DOI: 10.2865/53961.

[81] Eurostat, *Road freight transport 2022, by nuts 2 region of loading / unloading*, 2022. [Online]. Available: https://ec.europa.eu/eurostat/statistics-explained/index.php?title=Transport_statistics_at_regional_level#Road_transport_and_accidents.

[82] C. B. voor de Statistiek (CBS), *Inwonertal per provincie, 1 september 2022*, 2022. [Online]. Available: https://www.cbs.nl/nl-nl/maatwerk/2023/07/inwonertal-per-provincie-1-september-2022.

[83] T. Guesnet, "Energy efficiency of inland water ships – and how to improve it," 2013, Presented at the Workshop Inland Navigation CO emissions. [Online]. Available: https://www.dst-org.de/wp-content/uploads/2021/06/2013-11-21_EUSDR_PA1A_SG_CO2_emissions_DST.pdf.

[84] F. Vinke, M. van Koningsveld, C. van Dorsser, F. Baart, P. van Gelder, and T. Vellinga, "Cascading effects of sustained low water on inland shipping," *Journal of Waterway, Port, Coastal, and Ocean Engineering*, 2022, Available online 24 January 2022, Version of Record 27 January 2022.

[85] C. van Dorsser, F. Vinke, R. Hekkenberg, and M. van Koningsveld, "The effect of low water on loading capacity of inland ships," *European Journal of Transport and Infrastructure Research*, vol. 20, no. 3, pp. 47–70, 2020. [Online]. Available: https://journals.open.tudelft.nl/ejtir/article/view/3981/4788.

[86] SeaRates, *Delays in singapore, rotterdam, and other european ports: Causes and impacts*, 2024. [Online]. Available: https://www.searates.com/blog/post/delays-in-singapore-rotterdam-and-other-european-ports-causes-and-impacts.

[87] Mainfreight, *Congestion rotterdam and antwerp ports*, 2024. [Online]. Available: https://www.mainfreight.com/en-nz/congestion-rotterdam-and-antwerp-ports.

[88] C. S. H. Vienna, *90-day tariff pause causes major shipping disruption, study finds*, 2025. [Online]. Available: https://phys.org/news/2025-05-day-tariff-major-shipping-disruption.html.

[89] MFAME, *Trump tariffs spark congestion at overflowing european ports*, 2024. [Online]. Available: https://mfame.guru/trump-tariffs-spark-congestion-at-overflowing-european-ports/.

[90] Industry Intelligence, *European ports face worst supply chain congestion since pandemic due to erratic us tariffs, low river rhine water levels*, 2024. [Online]. Available: https:

//www.industryintel.com/news/european-ports-face-worst-supply-chain-congestion-since-pandemic-due-to-erratic-us-tariffs-low-river-rhine-water-levels-container-schedules-are-disrupted-overloading-major-hubs-like-rotterdam-antwerp-and-hamburg-and-causing-ship-delays-of-66-77-hours-171596277960.

[91] UNCTAD, *Case study - the suez canal blockage*, *Resilient Maritime Logistics Guidebook*, UNCTAD, 2023. [Online]. Available: https://resilientmaritimelogistics.unctad.org/guidebook/case-study-3-port-port-said-egypt.

[92] T. Notteboom, S. Roux, and F.-X. Delenclos, *The future of automated ports*, https://www.mckinsey.com/industries/logistics/our-insights/the-future-of-automated-ports, 2018. [Online]. Available: https://www.mckinsey.com/industries/logistics/our-insights/the-future-of-automated-ports.

[93] WEC Lines, *Local charges – port of rotterdam*, 2025. [Online]. Available: https://www.weclines.com/local-charges/.

[94] KiM Netherlands Institute for Transport Policy Analysis, *Cost figures for freight transport*, 2023. [Online]. Available: https://www.kimnet.nl/publicaties/rapporten/2023/06/15/cost-figures-for-freight-transport.

[95] S. Gailus, L. Liu, and L. Ni, "The future of automated ports," European Commission, SIPOTRA, Technical Report, Apr. 2019, Accessed: 2025-08-15. [Online]. Available: https://www.sipotra.it/wp-content/uploads/2019/04/The-future-of-automated-ports.pdf.

Appendix A

Appendix A

A.1 Road Freight Calculation

Table A.1: Population of the Netherlands by Province as of 1 September 2022

Province	**Number of People**
Groningen	595,011
Friesland	658,747
Drenthe[1)]	501,327
Overijssel	1,181,720
Flevoland	441,874
Gelderland	2,127,493
Utrecht	1,382,302
North Holland	2,941,163
South Holland	3,787,452
Zeeland	390,636
North Brabant	2,617,331
Limburg	1,124,206
Total Netherlands	**17,749,262**

Source: Statistics Netherlands (CBS).
[1)] Legally established population for administrative purposes under the Provinces Act.

Table A.2: Road Freight Transport per Dutch Province (in 1000 tonne-km)

Province	**1000 tonne-km/inhabitant**	**Inhabitants**	**1000 tonne*km**	**% of Total**
Groningen	4.8	595,011	2,856,053	3.8%
Drenthe	5.0	501,327	2,506,635	3.3%
Friesland	4.5	658,747	2,964,362	4.0%
Overijssel	4.4	1,181,720	5,199,568	6.9%
Flevoland	4.2	441,874	1,855,871	2.5%
Gelderland	4.6	2,127,493	9,786,468	13.1%
Utrecht	2.2	1,382,302	3,041,064	4.1%
Noord-Holland	2.7	2,941,163	7,941,140	10.6%
Zuid-Holland	4.3	3,787,452	16,286,044	21.7%
Zeeland	5.7	390,636	2,226,625	3.0%
Noord-Brabant	5.3	2,617,331	13,871,854	18.5%
Limburg	5.7	1,124,206	6,407,974	8.6%
Total			74,943,658	100.0%

Table A.3: Cargo Share Distribution per Node

Node	**Cargo Share (%)**
N2	20%
N4	26%
N5	12%
N6	19%
N7	6%
N8	7%
N9	10%

Appendix B

Appendix B

B.1 Model Calibration and Validation

To ensure the model adequately reflects port operations, an initial calibration was performed under baseline conditions. The first run produced an average truck terminal queue of 11,374 TEU per day (Figure B.1), combined with an average gate utilization of 85% (Figure B.2). Considering that containers typically require three days to reach the truck terminal, this result indicates that the modeled terminal capacity was underestimated. The aggregation of 100 trucks into a single agent is a likely cause of this congestion effect, as it reduces the model's ability to distribute flows smoothly.

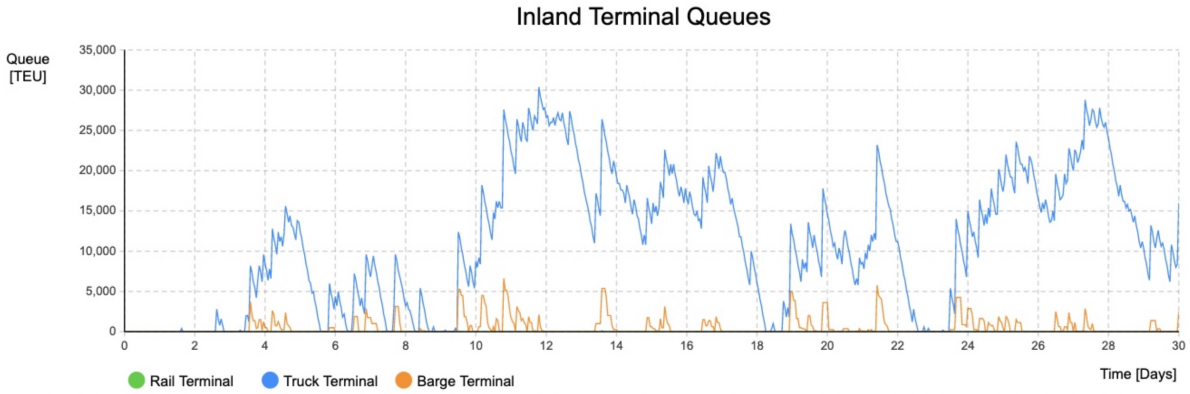

Figure B.1: Baseline run: inland terminal queues.

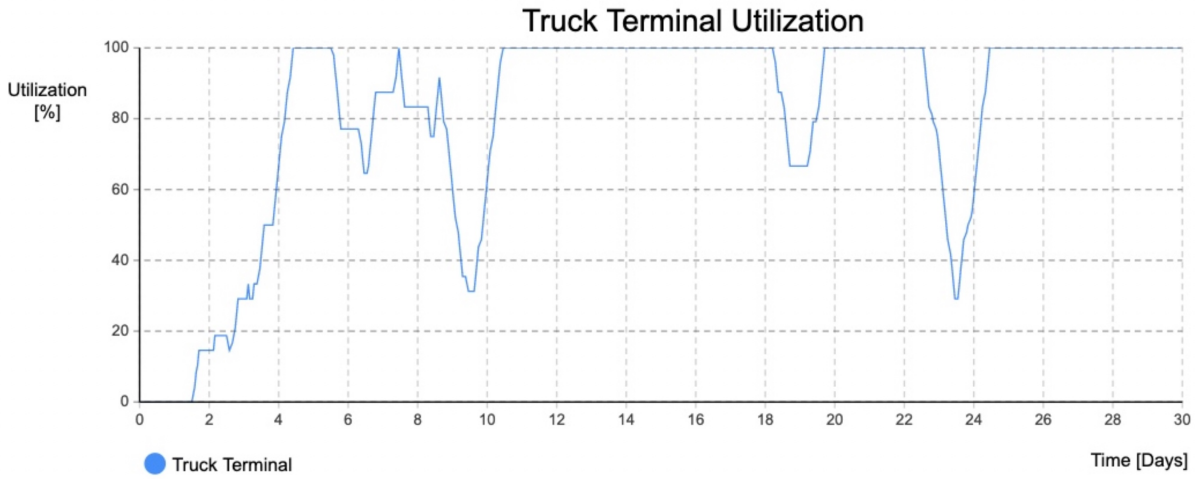

Figure B.2: Baseline run: truck terminal gate utilization.

Increasing the number of truck agents would raise computational requirements and risk reaching the AnyLogic dynamic agent limit. Therefore, the calibration strategy chosen was to increase the modeled terminal capacity. Doubling truck terminal capacity reduced the average utilization to 43% and decreased the average truck terminal queue to 1,189 TEU per day—around 10% of the original baseline level (Figures B.3 and B.4).

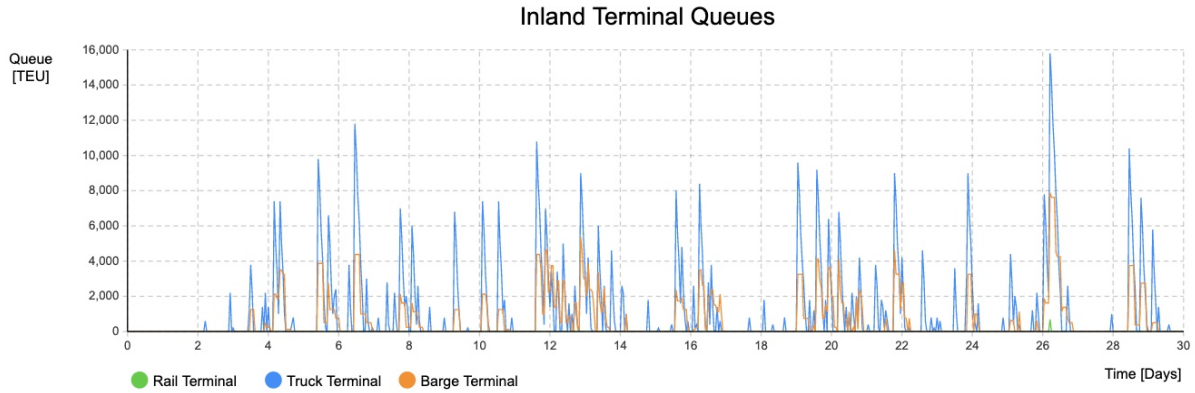

Figure B.3: Calibrated run: inland terminal queues.

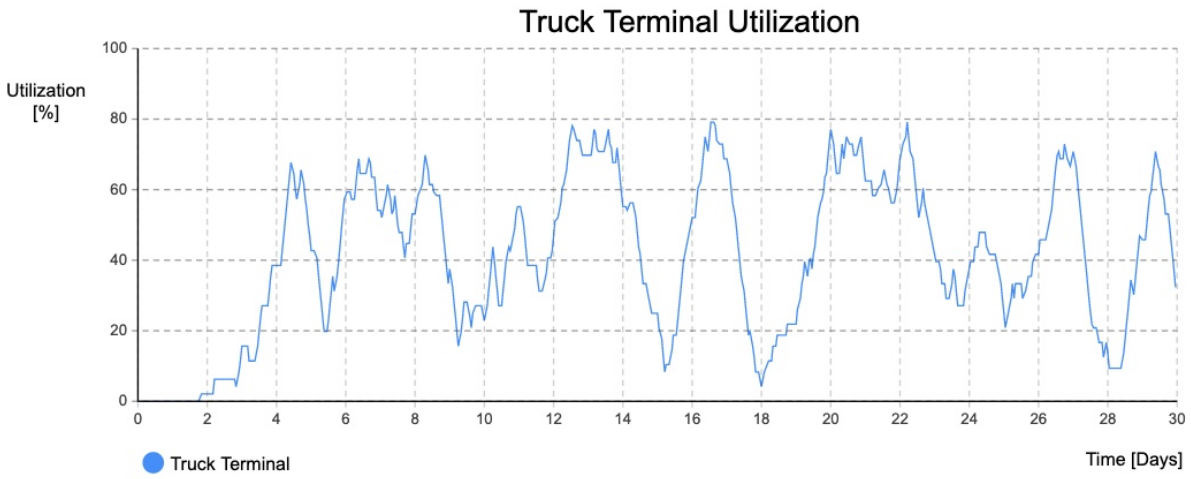

Figure B.4: Calibrated run: truck terminal gate utilization.

The calibrated model delivered approximately 1.01 million TEU during the full simulation horizon. Adjusting for the three-day start-up period required for the first vessels to reach the inland network, this corresponds to an average throughput of about 1.11 million TEU per month. This result is within 5% of the reported Port of Rotterdam monthly throughput of 1.15 million TEU [4], indicating a close match.

Validation statement. On this basis, the model can be considered adequately calibrated for throughput and terminal utilization, providing a realistic foundation for strategy evaluation. However, it must be noted that aggregation of truck agents introduces simplifications in queue dynamics. While this does not significantly affect system-level throughput, it may smoothen micro-level variations in waiting times.

Limitations. The calibration approach—scaling terminal capacity instead of disaggregating truck agents—improves computational efficiency but may understate the fine-grained congestion effects at truck gates. These limitations should be considered when interpreting results on queue distributions, though overall throughput patterns remain robust.

B.2 Complete Experiment Results

This chapter presents the outcomes of the simulation experiments conducted to evaluate the resilience of the Port of Rotterdam under different disruption scenarios and mitigation strategies. Building on the methodology and model design described earlier, each subsection provides a structured overview of the results for one scenario.

For every experiment, the figures are organized into four categories: (i) *settings and flow overview*, which shows the configuration of the experiment and main container flows; (ii) *network metrics and throughput*, capturing how disruptions and strategies influenced container movement through the port–hinterland system; (iii) *delays and general performance metrics*, showing systemic impacts on service levels; and (iv) *facility utilization*, highlighting how resources were stressed or rebalanced during the disruption and recovery periods.

The results are grouped by disruption type: Drought, labor strike, and demand fluctuation. Within each group, baseline performance under disruption is followed by strategy-specific results, including facility automation, hub activation, rerouting, storage buffers, and in the case of demand fluctuations, a combined collaboration strategy. This structure enables both a scenario-specific analysis and a cross-strategy comparison, showing how different measures alter system

behavior under varying disruption conditions.

The following sections present these results in detail, supported by visualizations of key performance indicators and system dynamics.

B.2.1 Drought

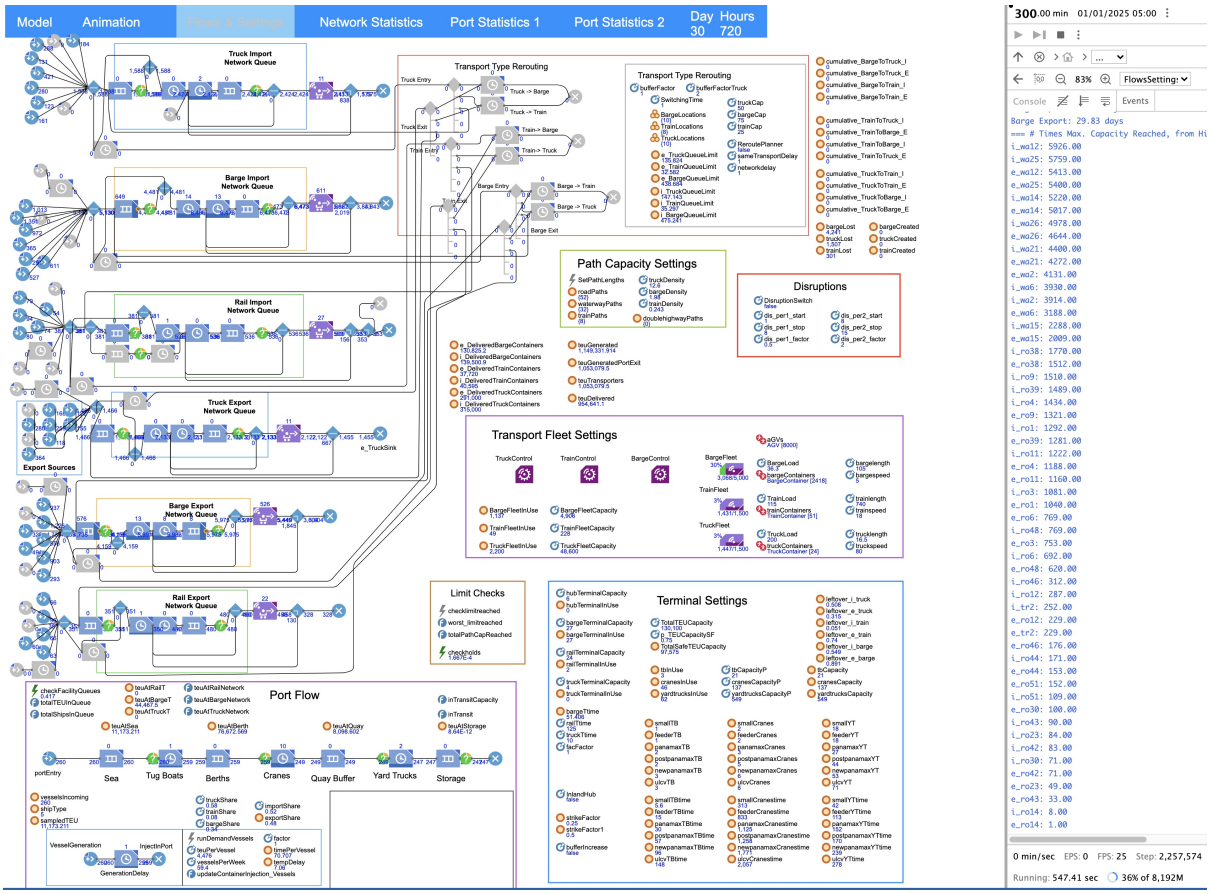

Figure B.5: Drought — experiment settings and flow overview

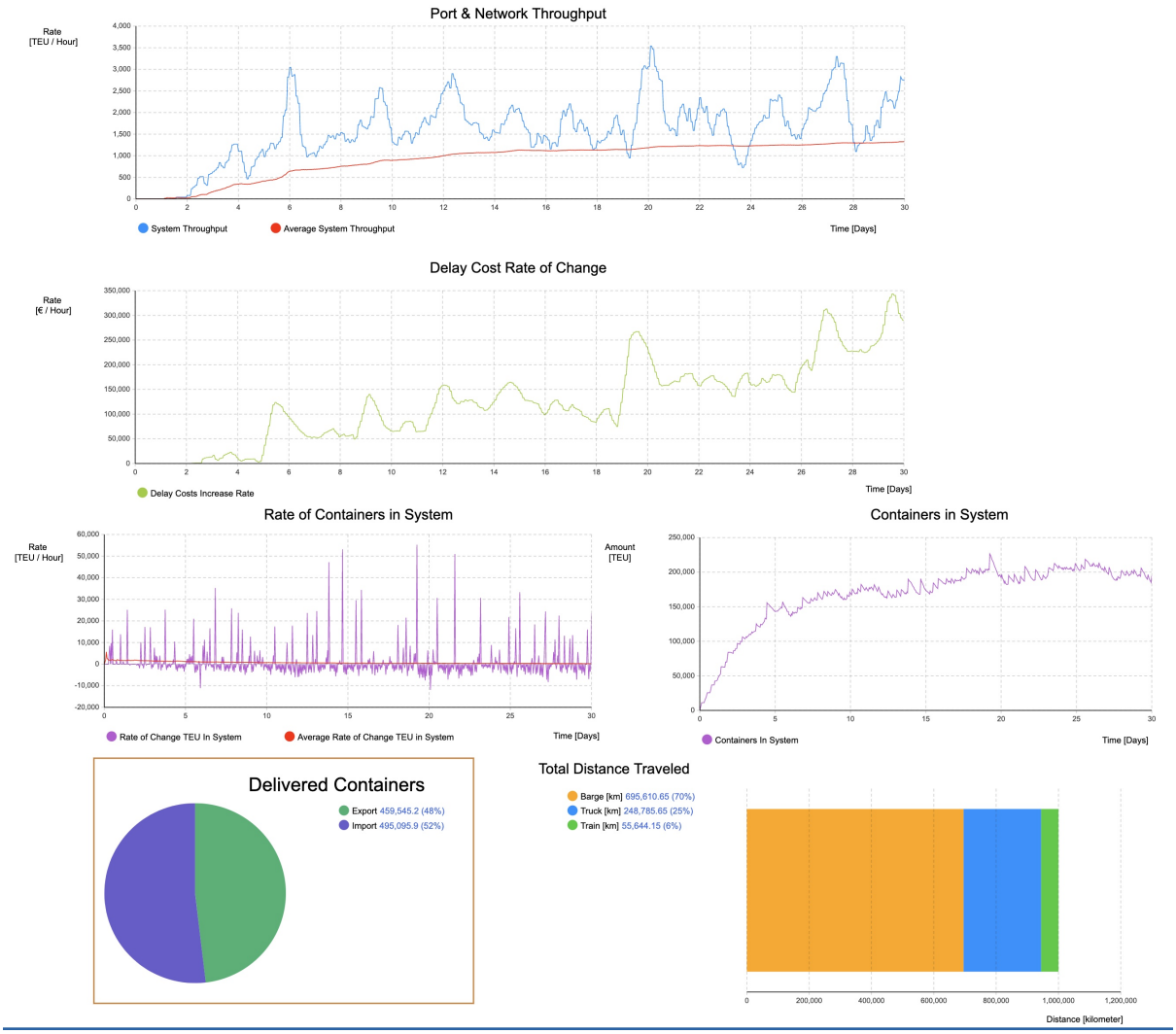

Figure B.6: Drought — network metrics and container throughput

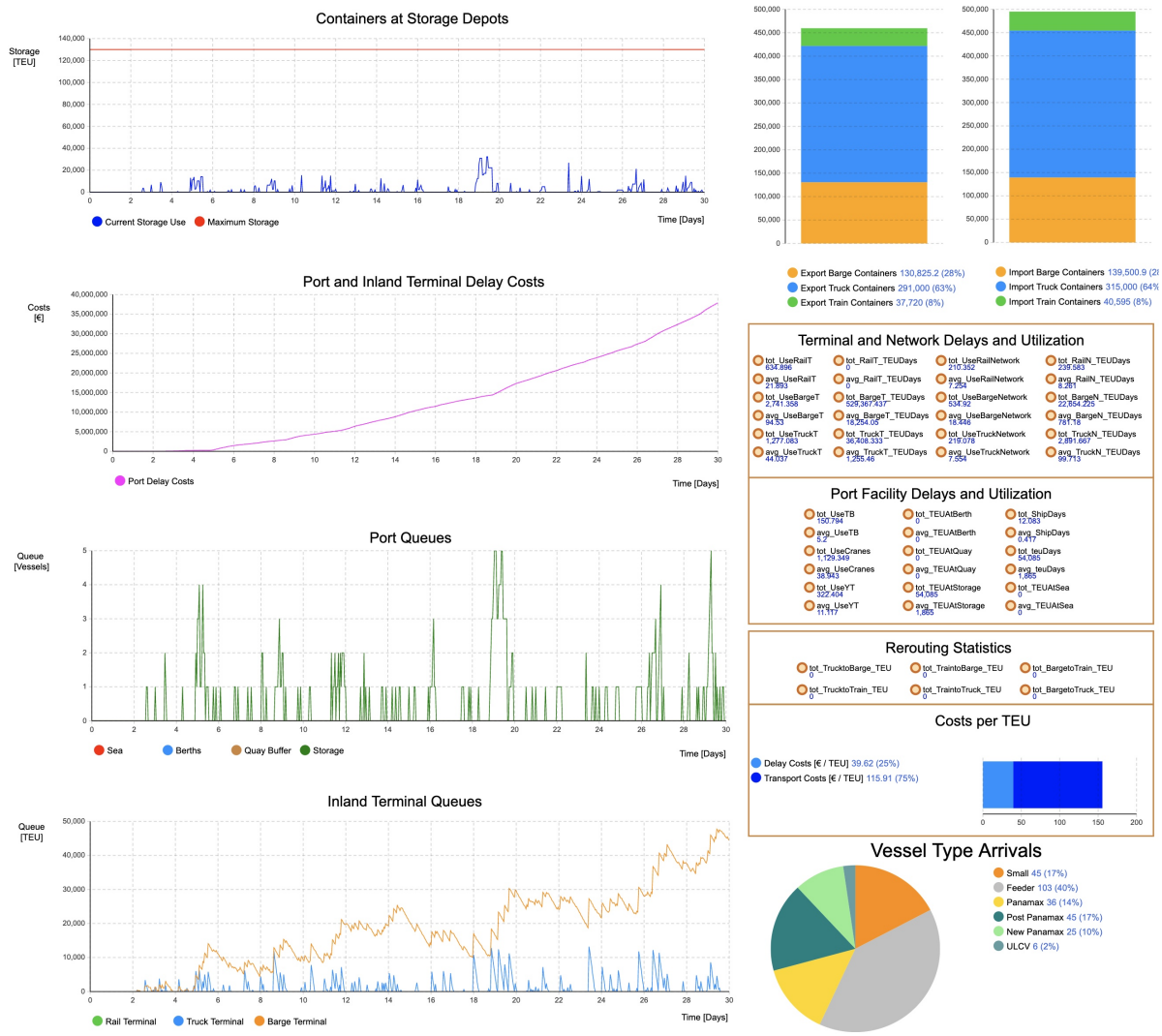

Figure B.7: Drought — delays in port system and general metrics

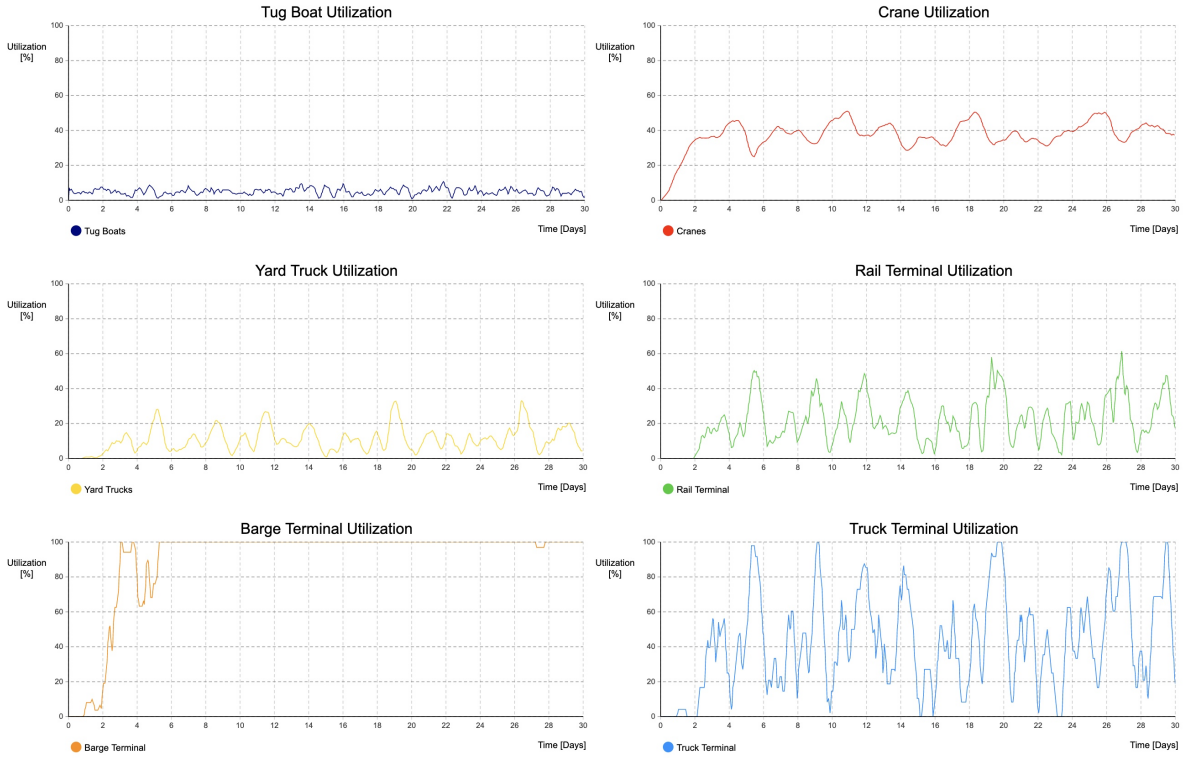

Figure B.8: Drought — utilization levels of facilities

B.2.2 Drought - Facility

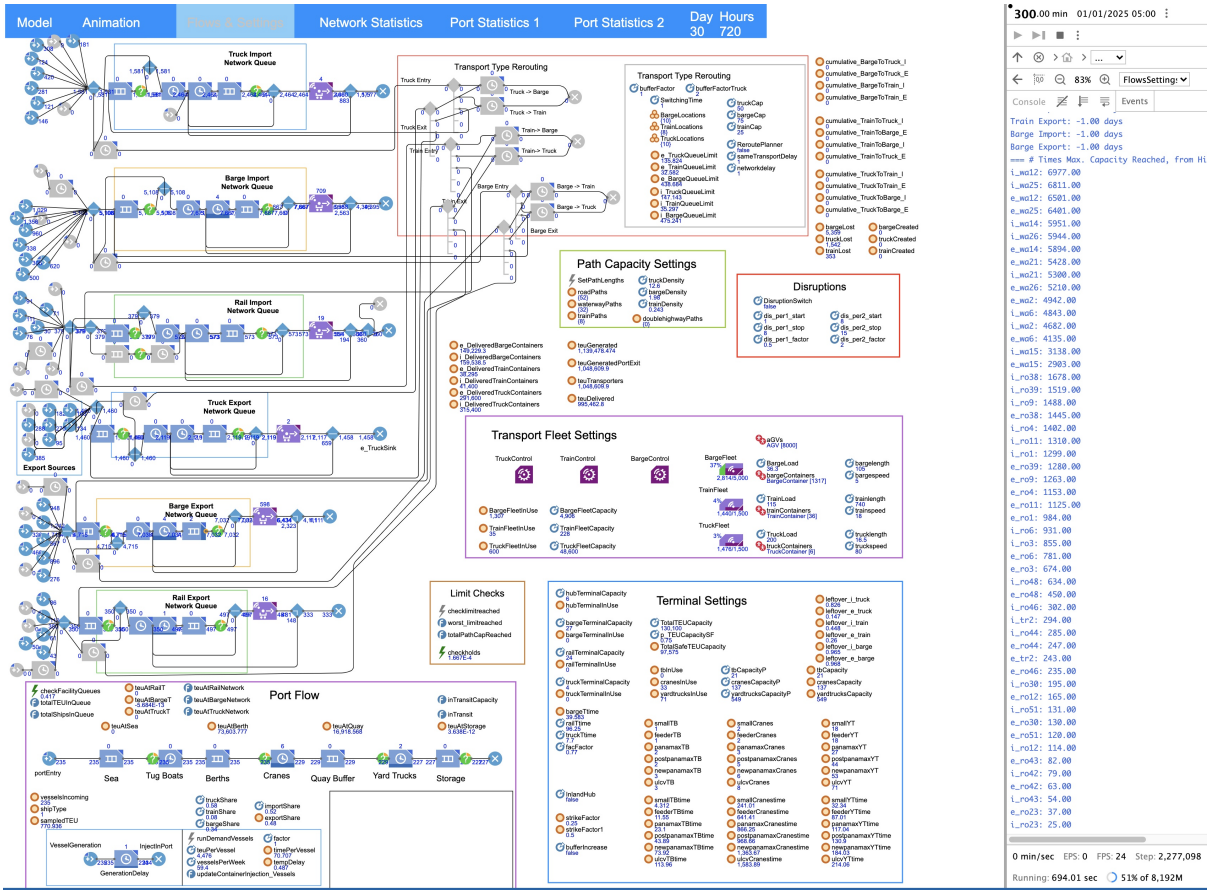

Figure B.9: Drought–Facility — settings and flow overview

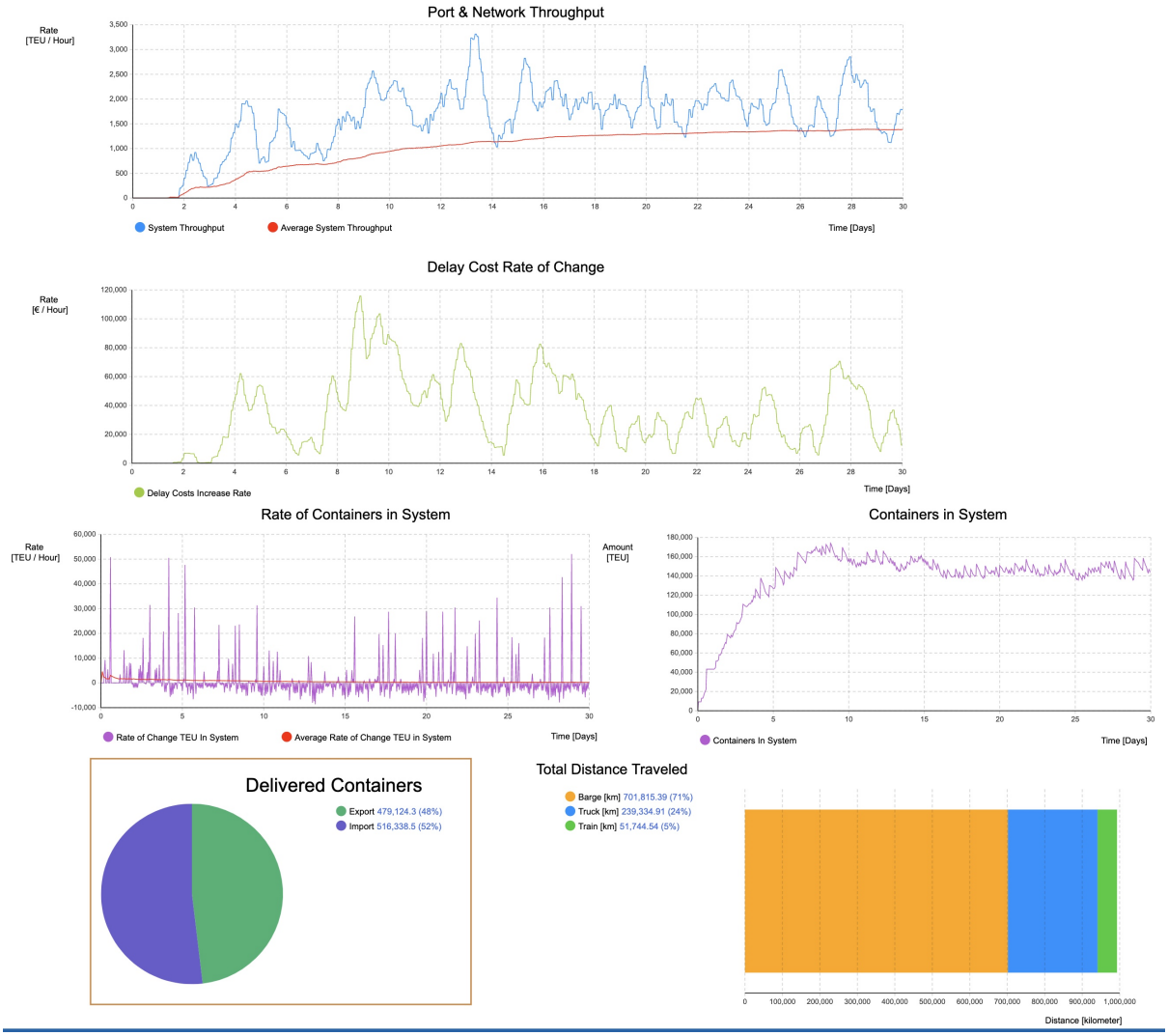

Figure B.10: Drought–Facility — network metrics and container throughput

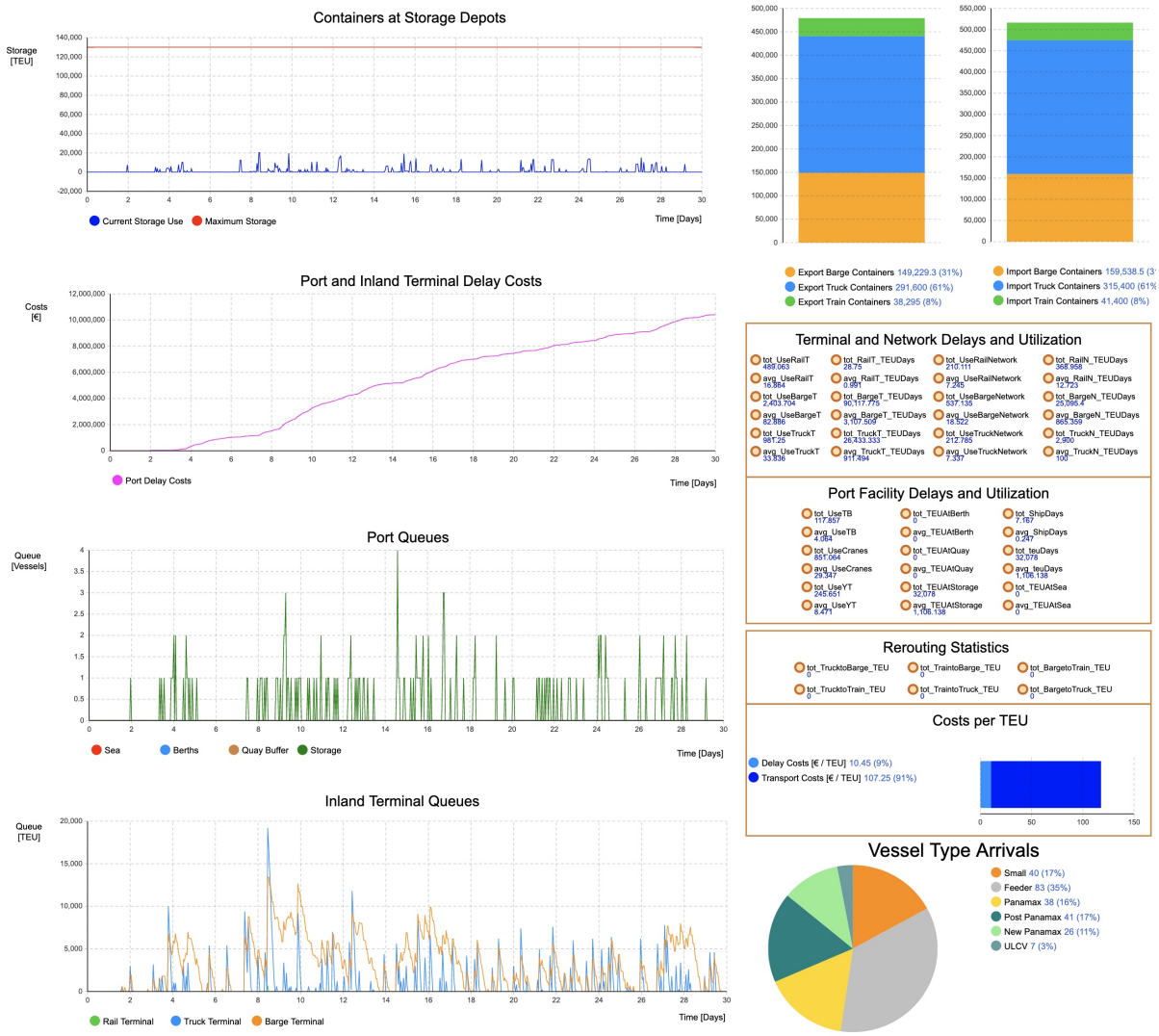

Figure B.11: Drought–Facility — delays in port system and general metrics

Figure B.12: Drought–Facility — utilization levels of facilities

B.2.3 Drought - Hub

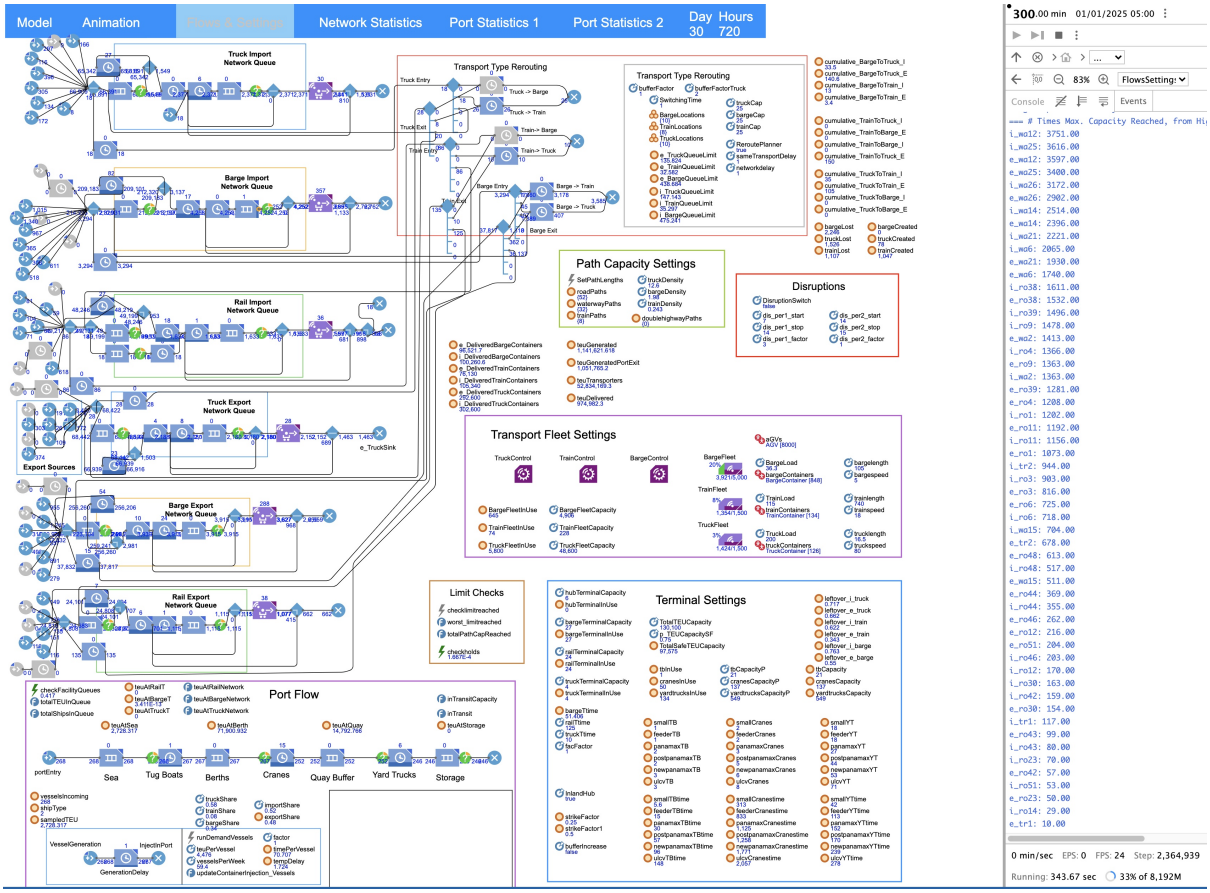

Figure B.13: Drought–Hub — settings and flow overview

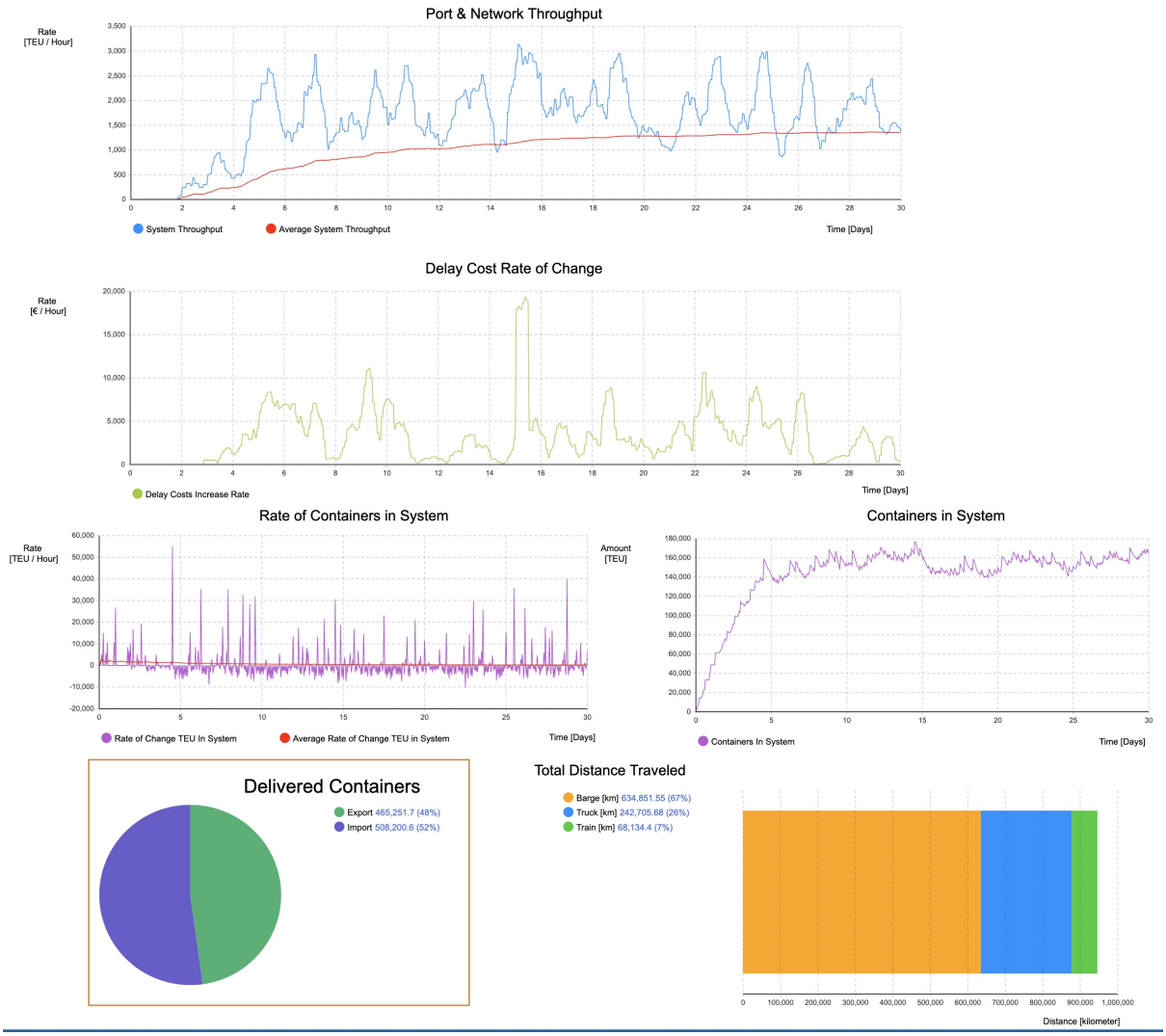

Figure B.14: Drought–Hub — network metrics and container throughput

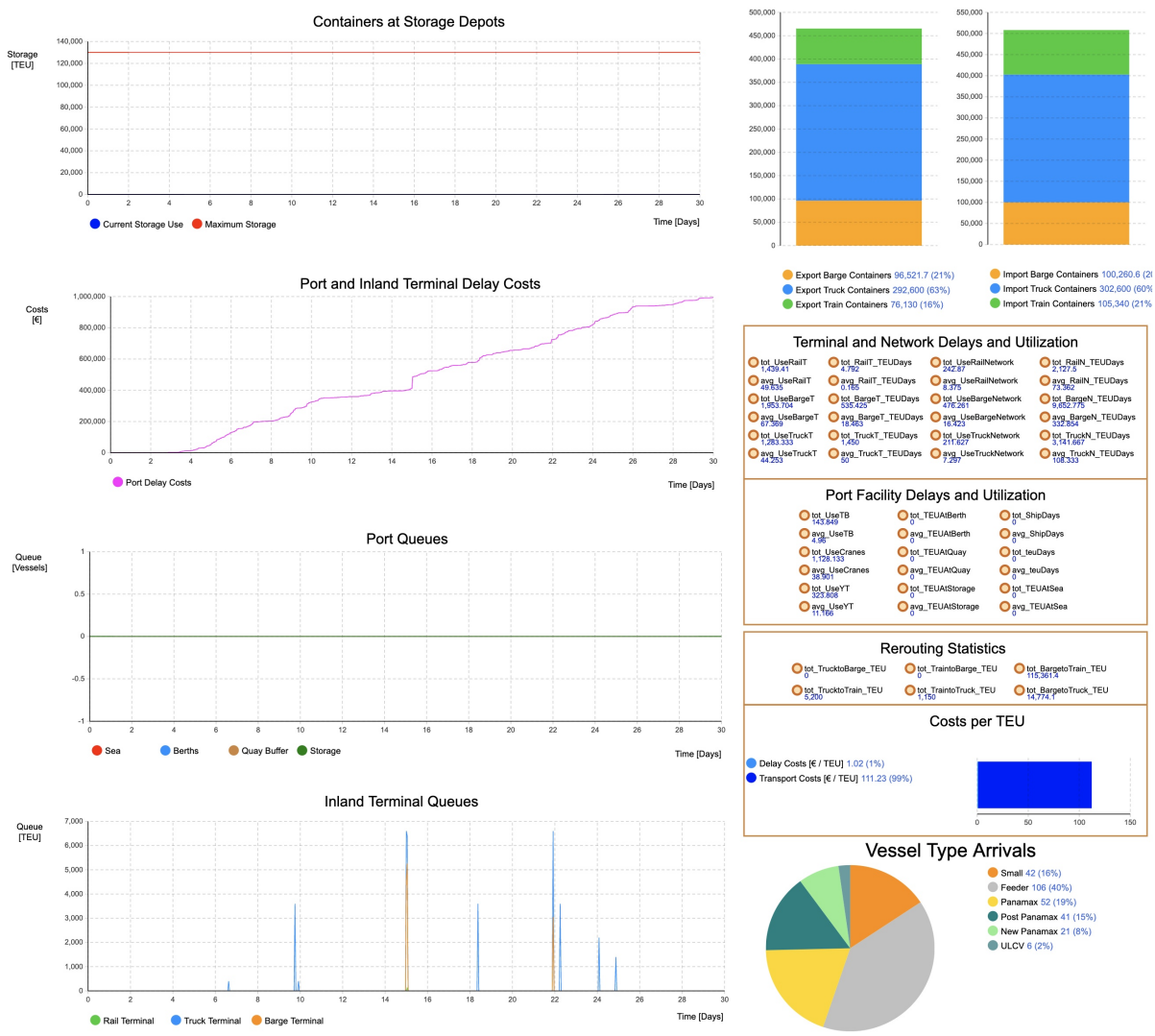

Figure B.15: Drought–Hub — delays in port system and general metrics

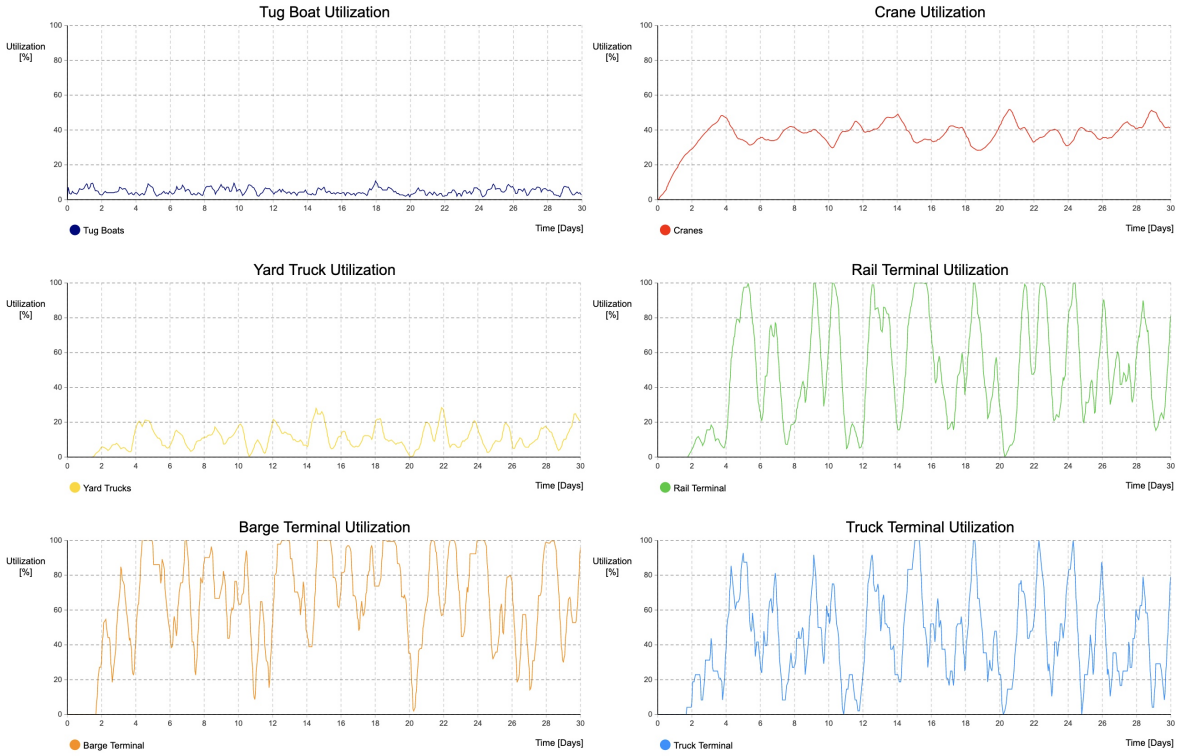

Figure B.16: Drought–Hub — utilization levels of facilities

B.2.4 Drought - Reroute

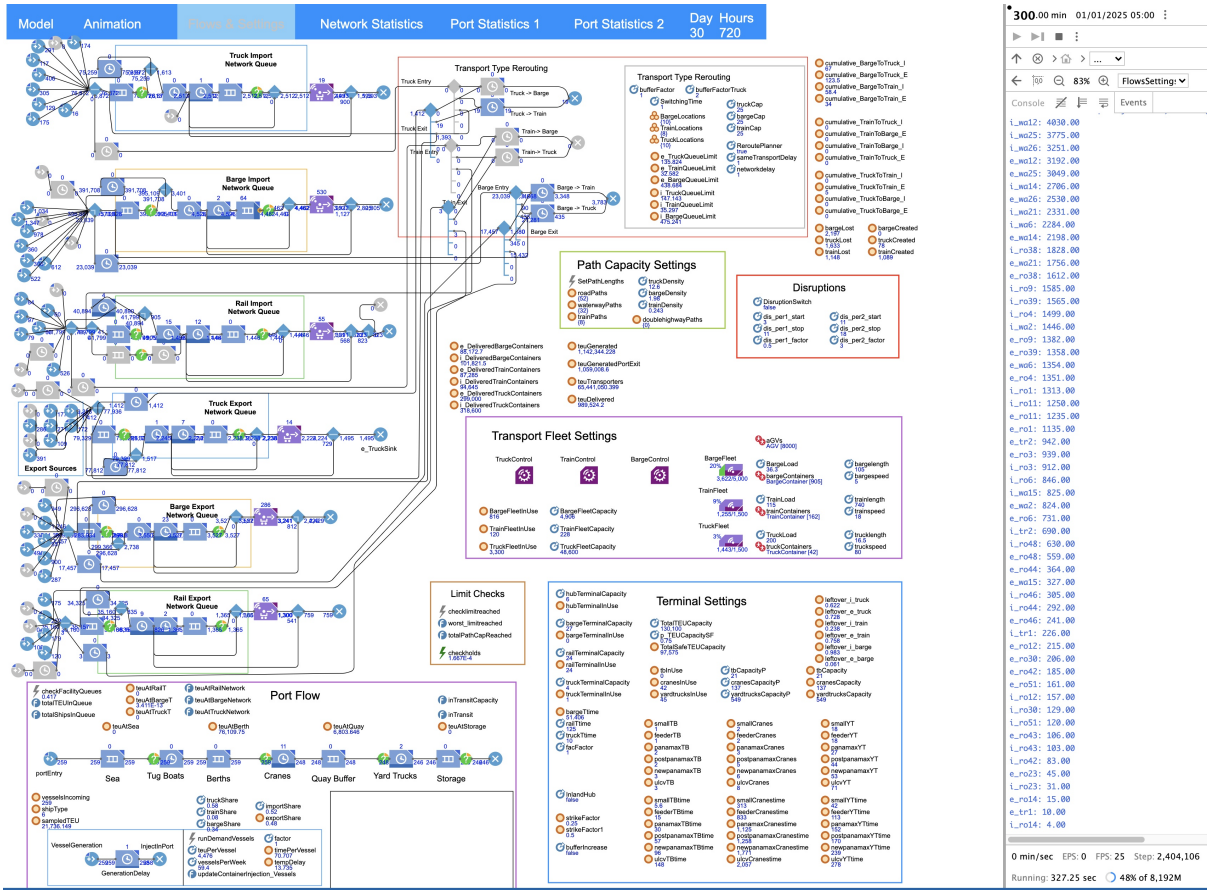

Figure B.17: Drought–Reroute — settings and flow overview

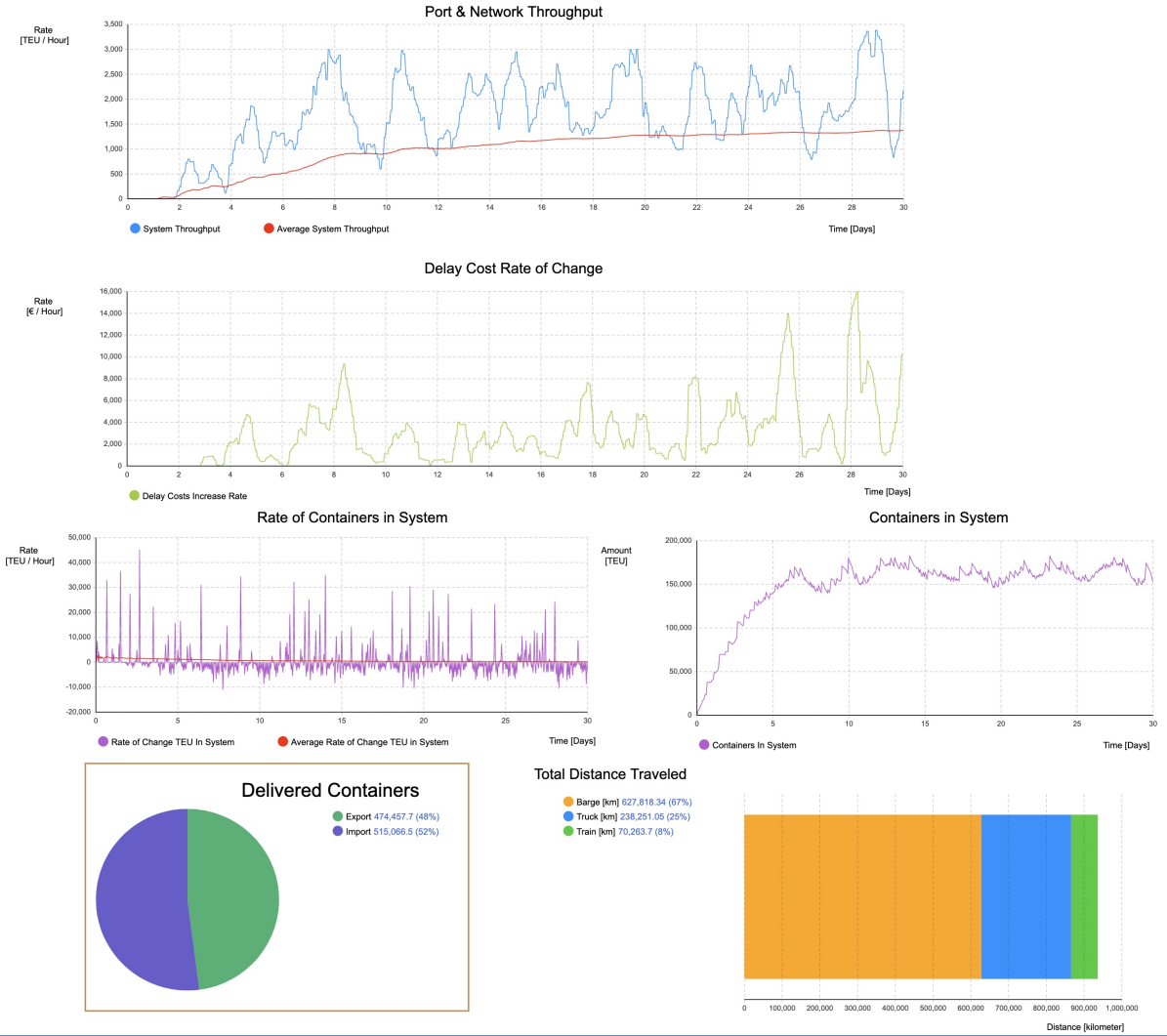

Figure B.18: Drought–Reroute — network metrics and container throughput

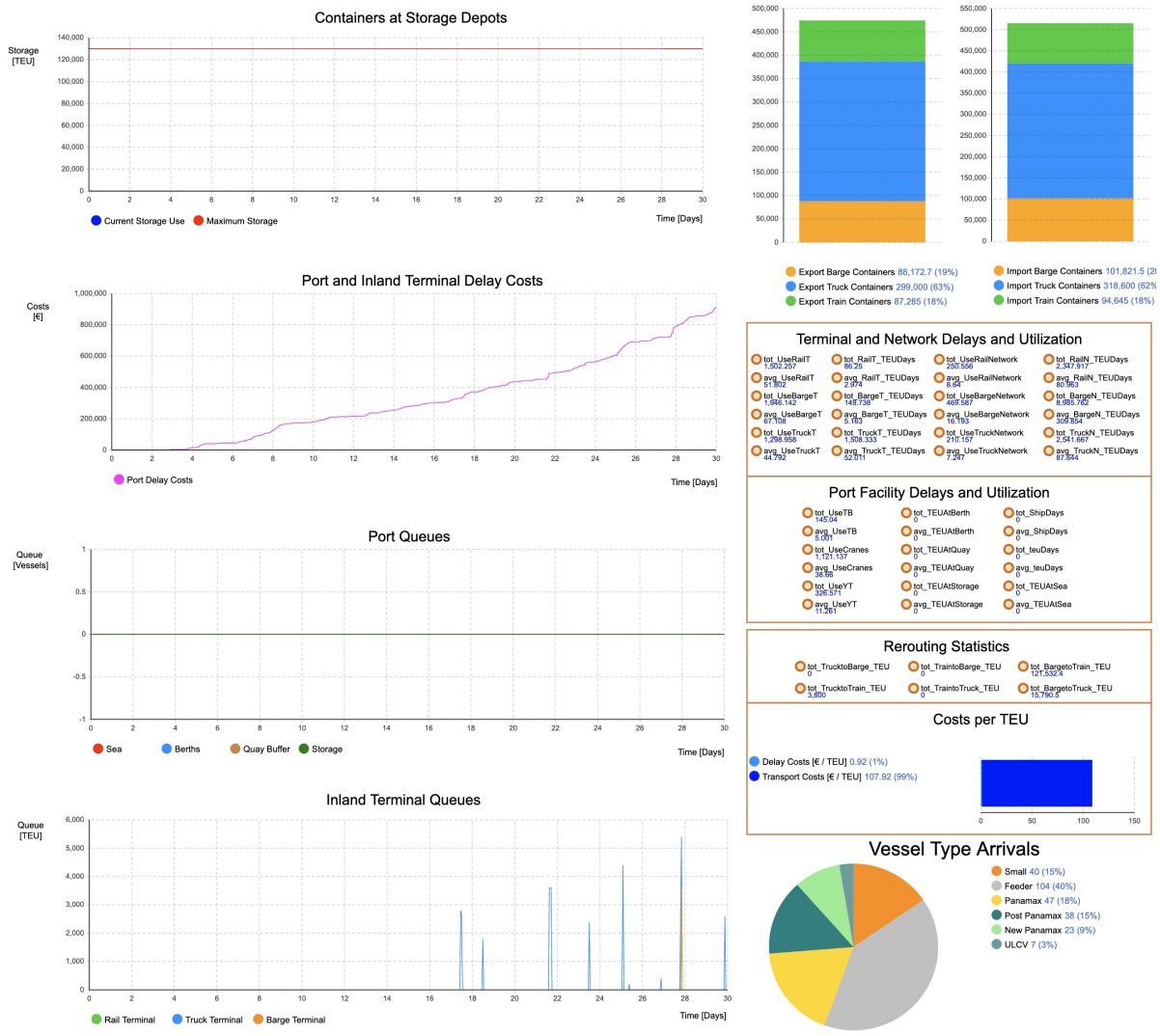

Figure B.19: Drought–Reroute — delays in port system and general metrics

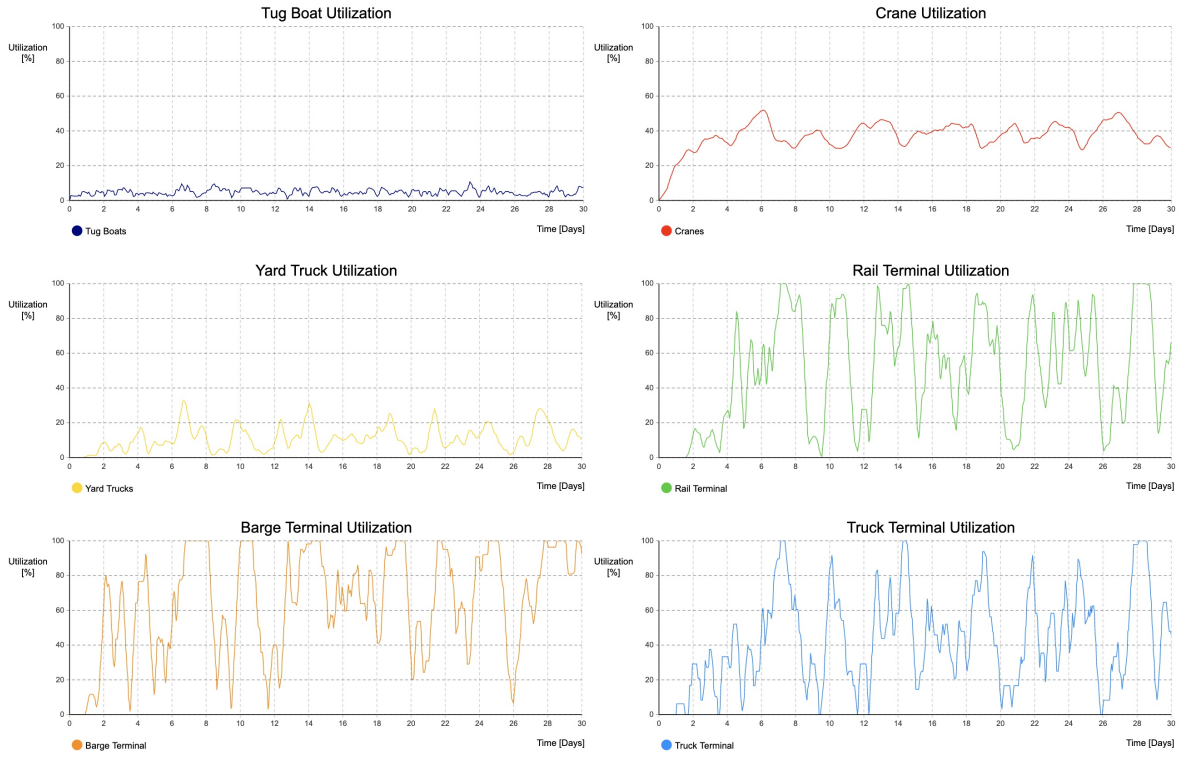

Figure B.20: Drought–Reroute — utilization levels of facilities

B.2.5 Drought - Storage

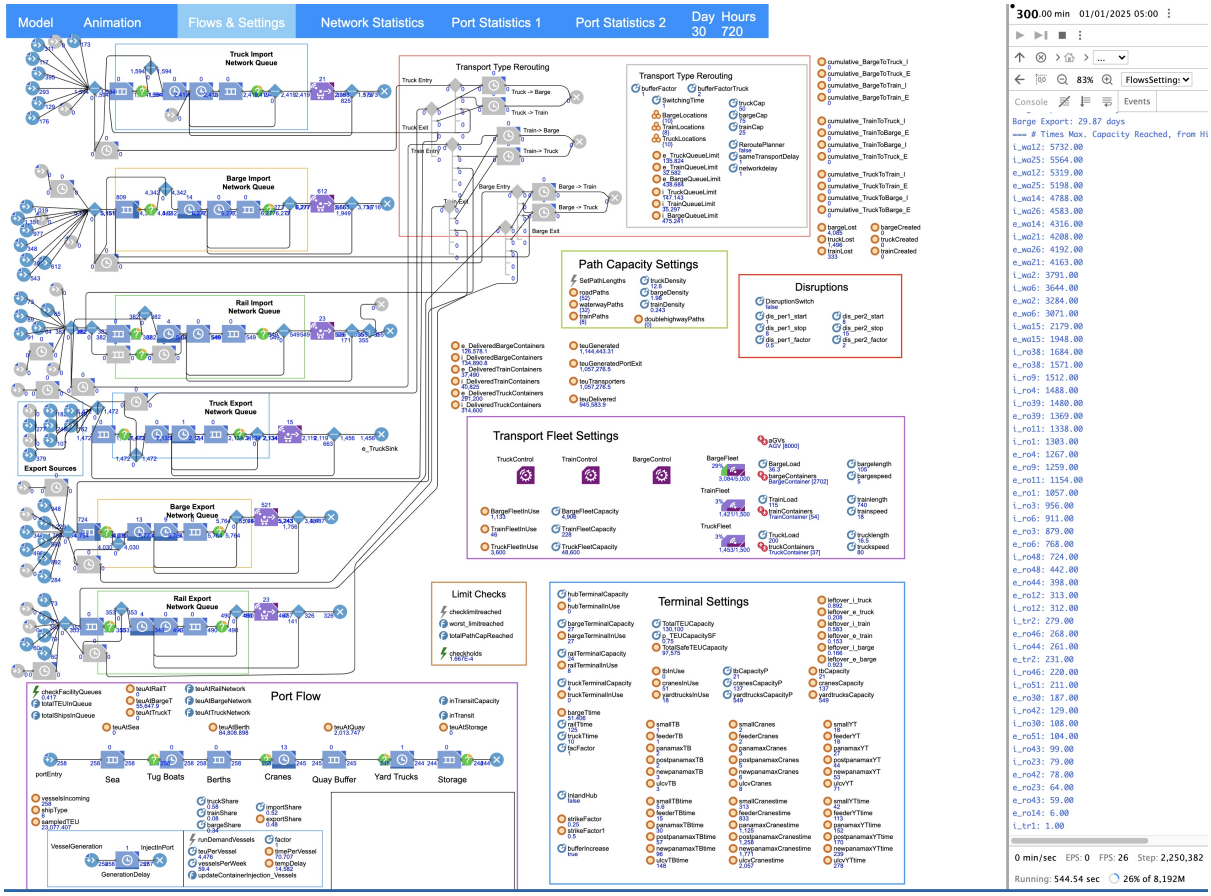

Figure B.21: Drought–Storage — settings and flow overview

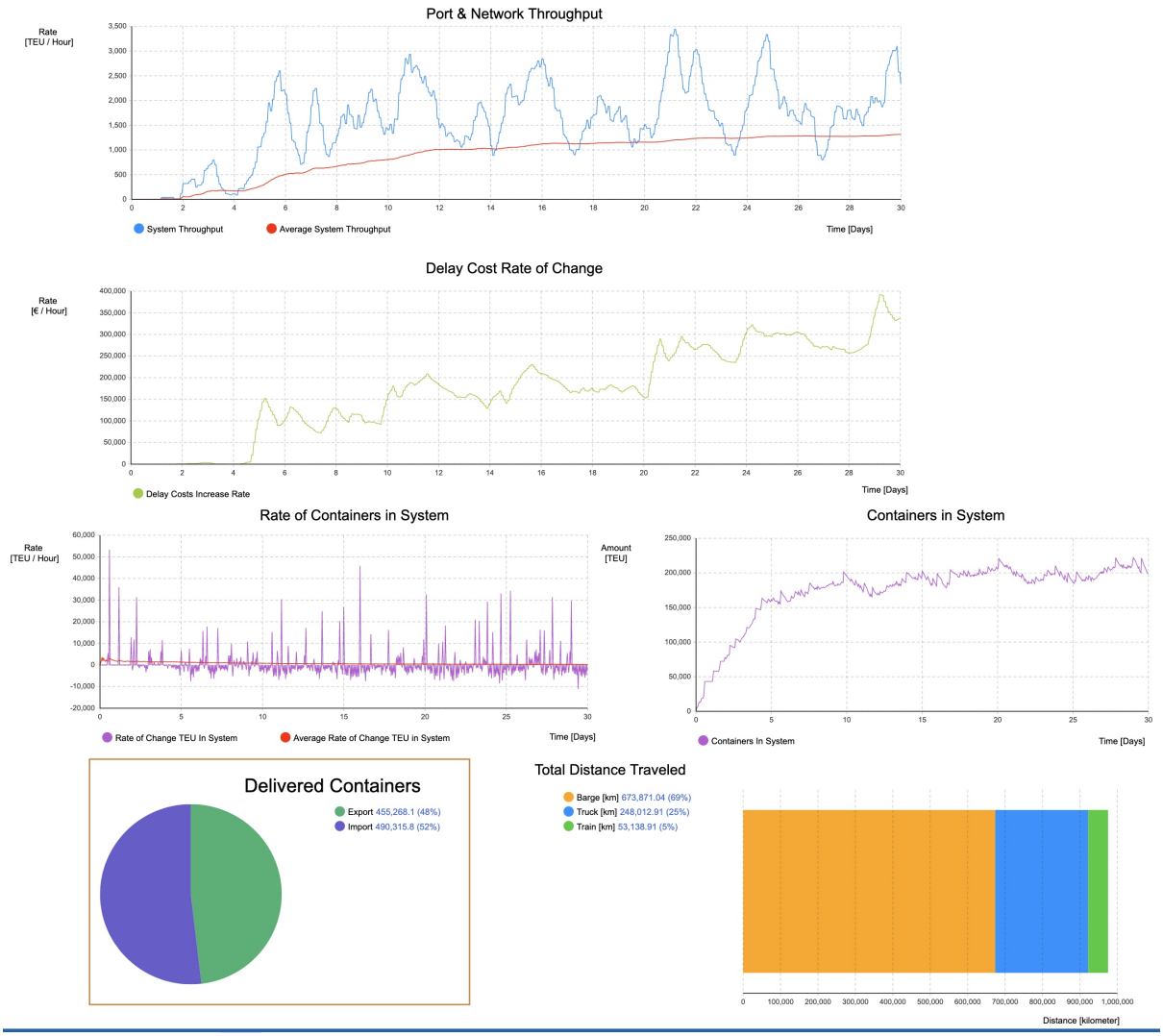

Figure B.22: Drought–Storage — network metrics and container throughput

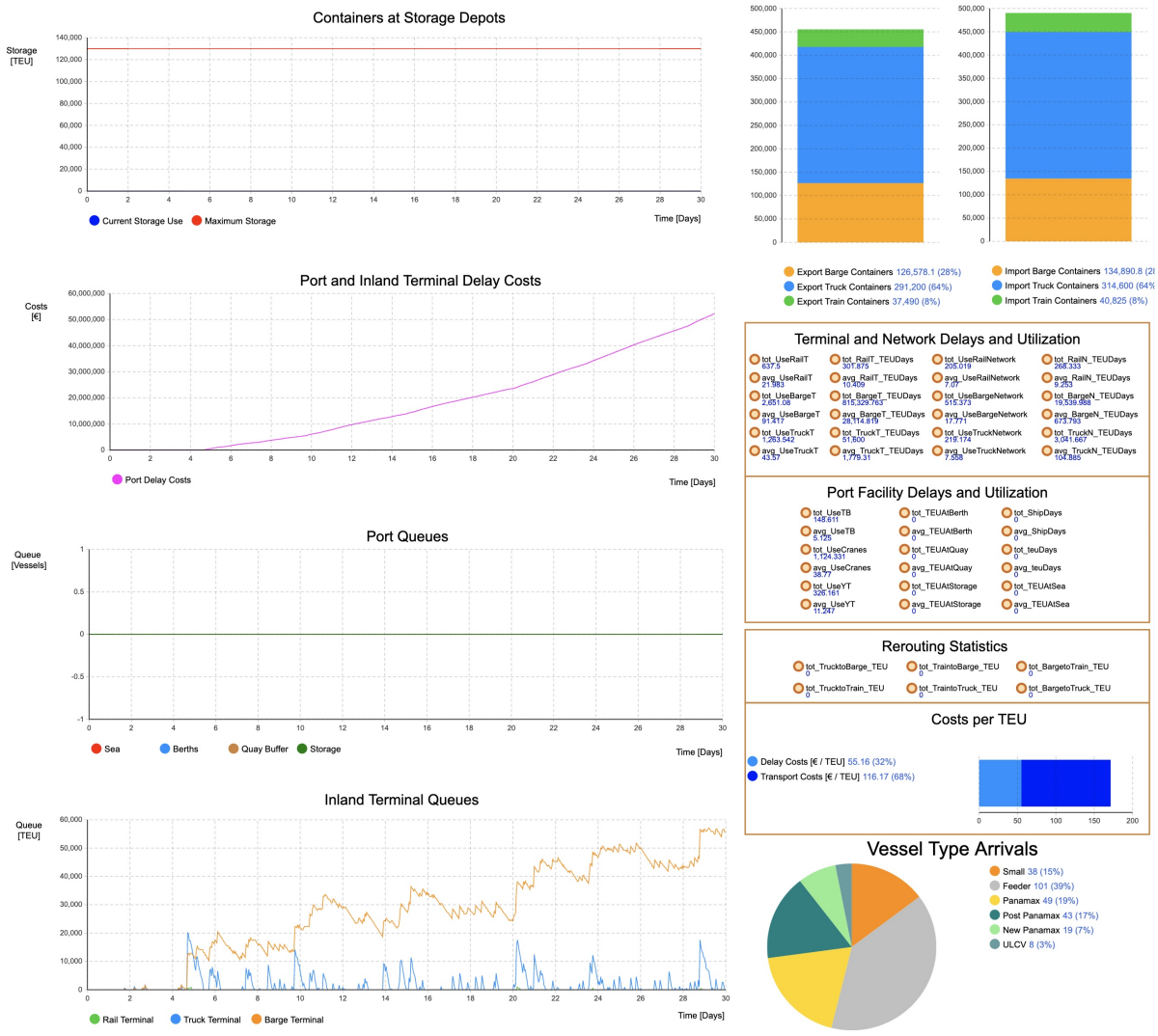

Figure B.23: Drought–Storage — delays in port system and general metrics

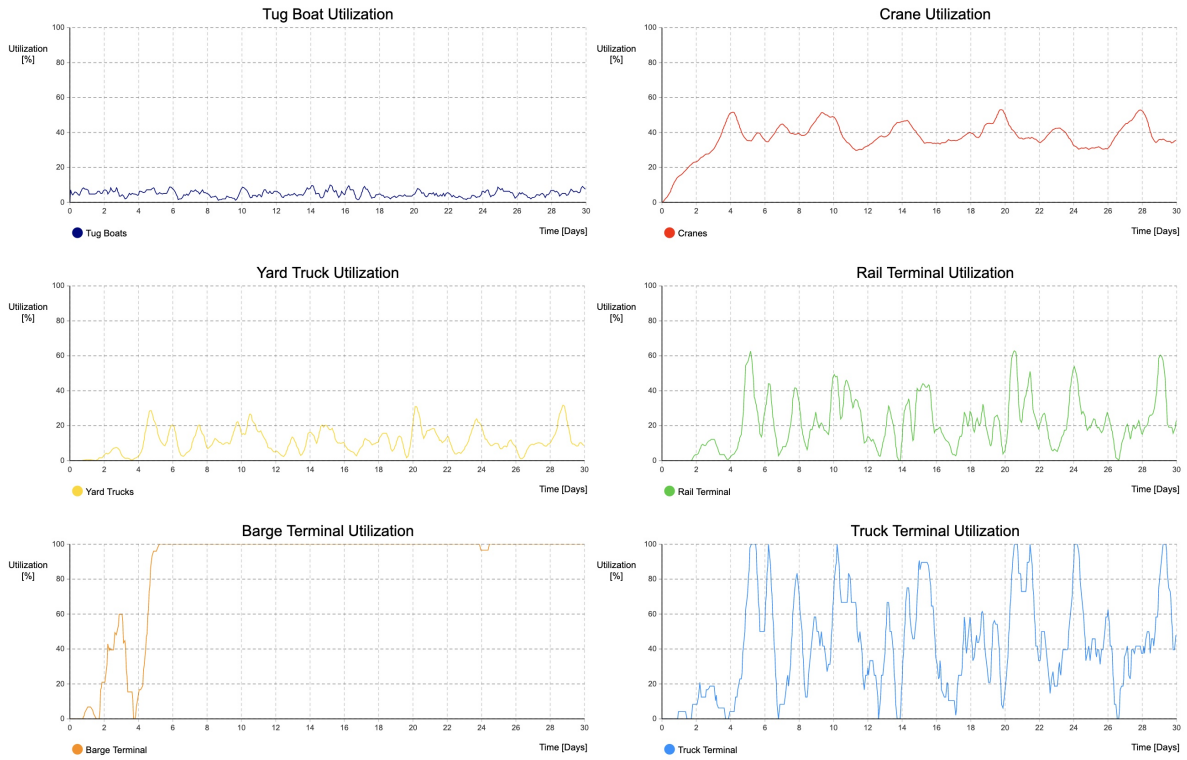

Figure B.24: Drought–Storage — utilization levels of facilities

B.2.6 Strike

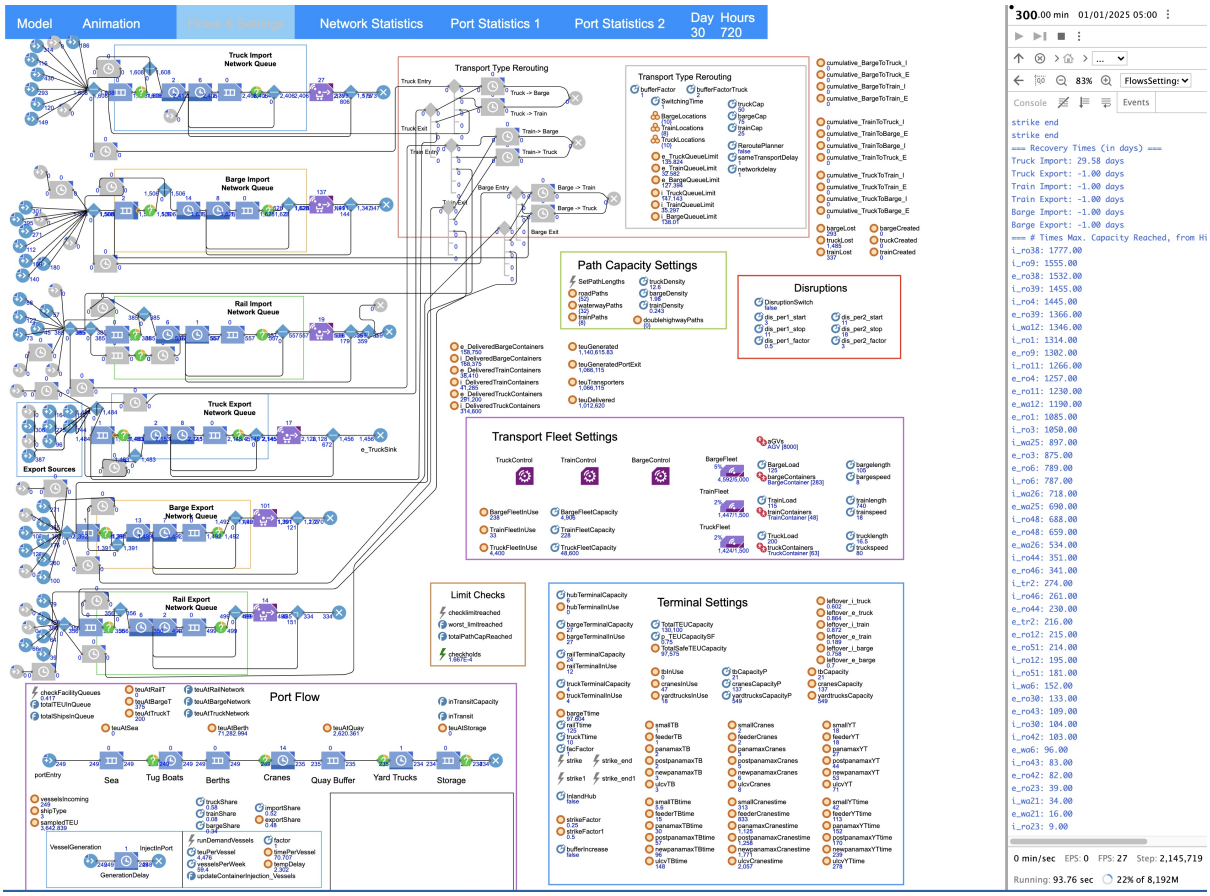

Figure B.25: Strike — experiment settings and flow overview

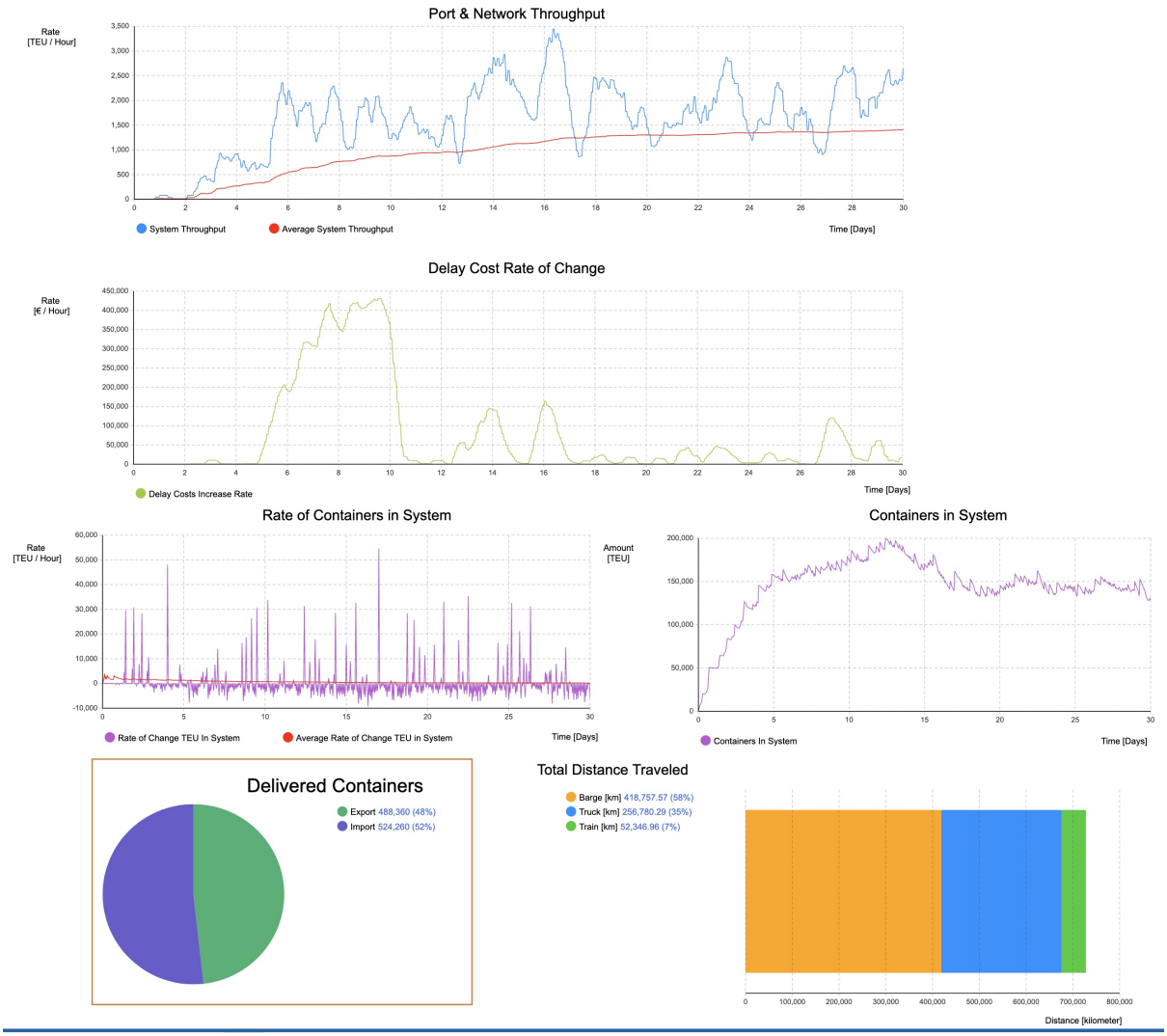

Figure B.26: Strike — network metrics and container throughput

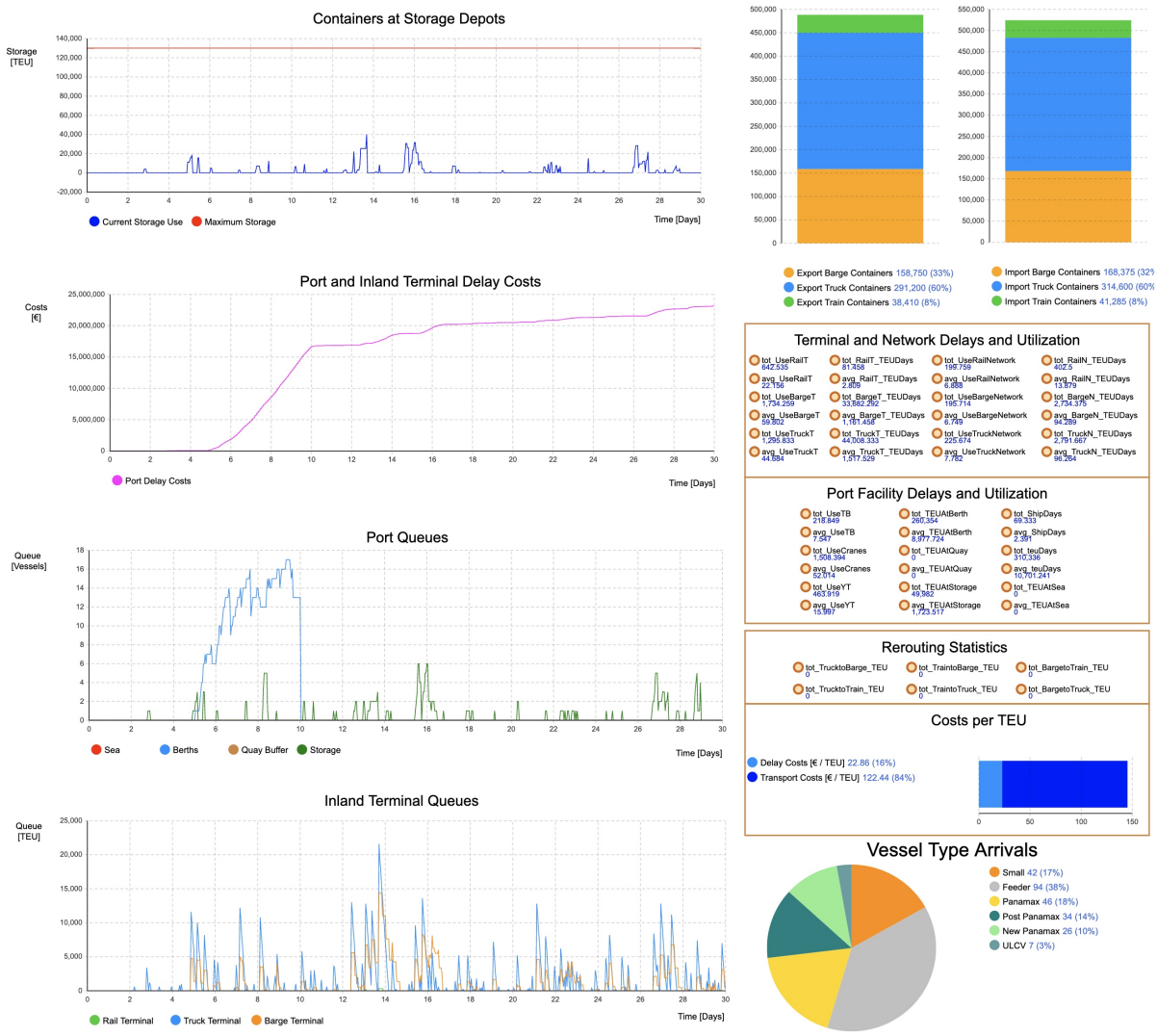

Figure B.27: Strike — delays in port system and general metrics

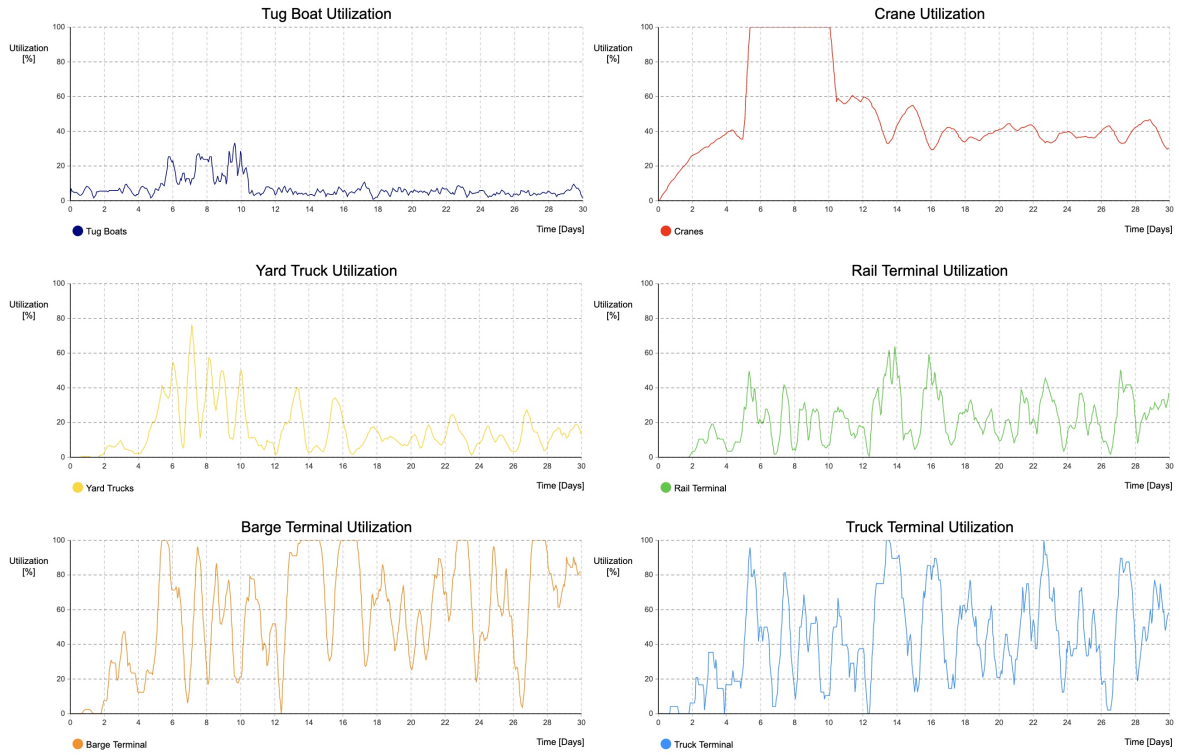

Figure B.28: Strike — utilization levels of facilities

B.2.7 Strike - Facility

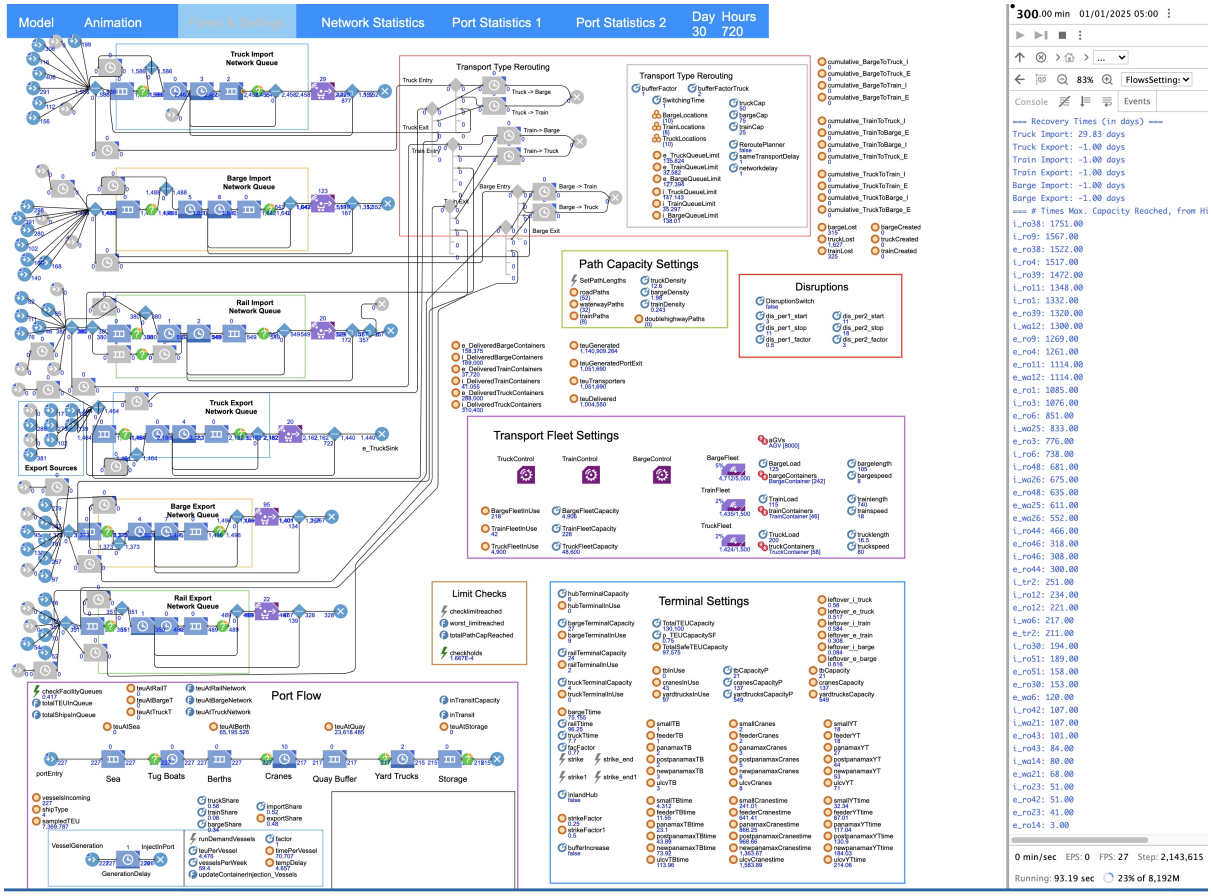

Figure B.29: Strike–Facility — settings and flow overview

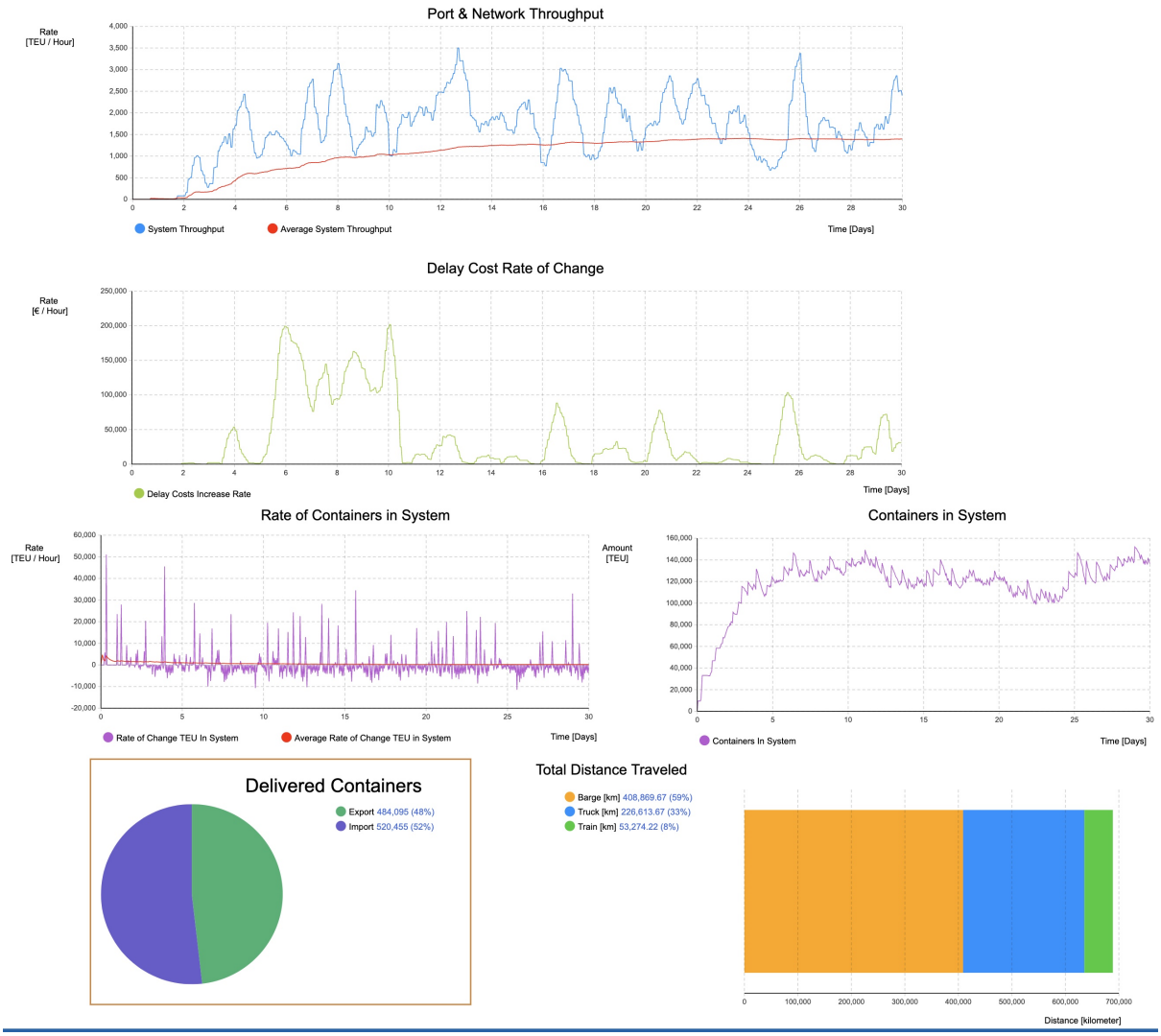

Figure B.30: Strike–Facility — network metrics and container throughput

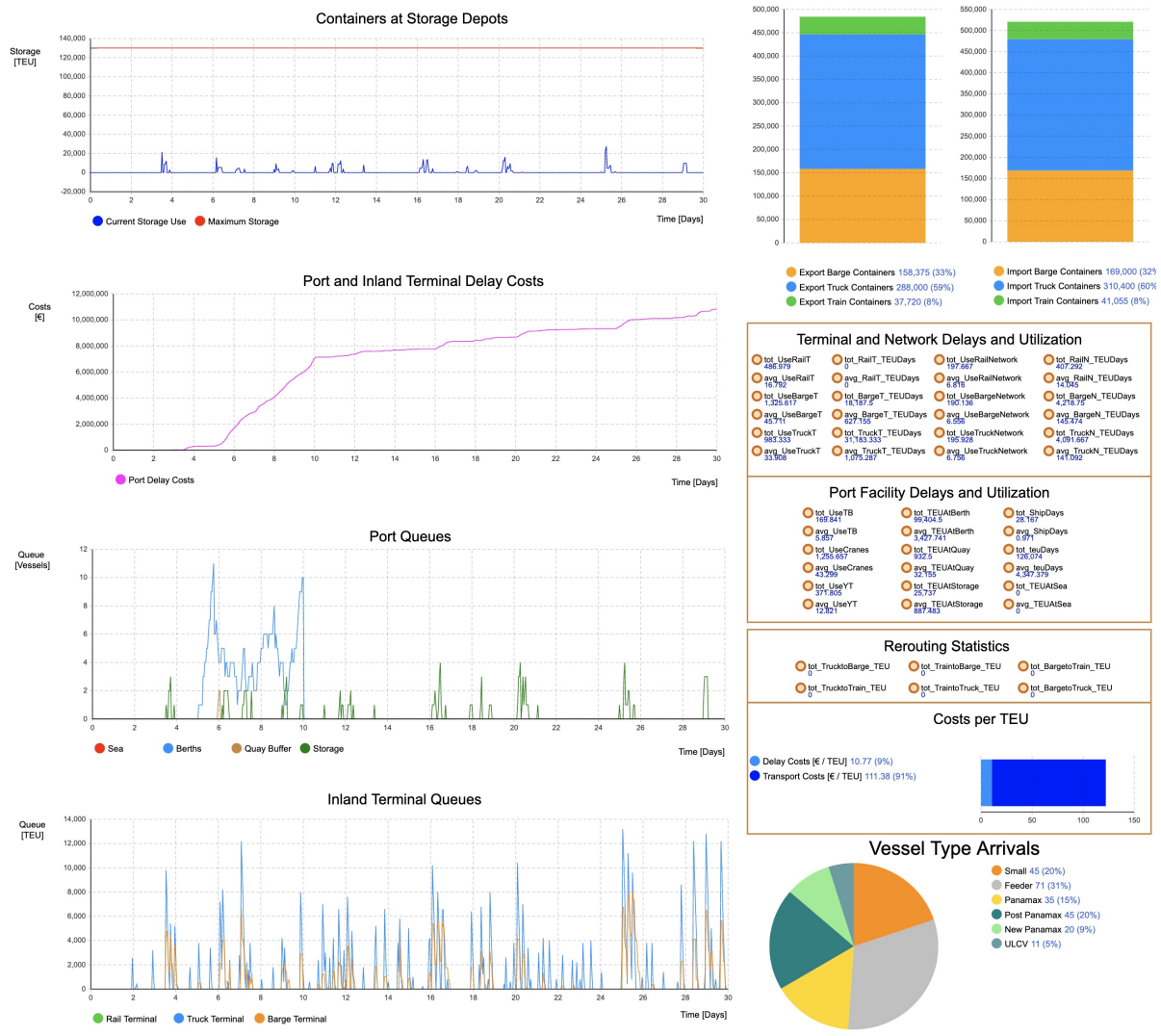

Figure B.31: Strike–Facility — delays in port system and general metrics

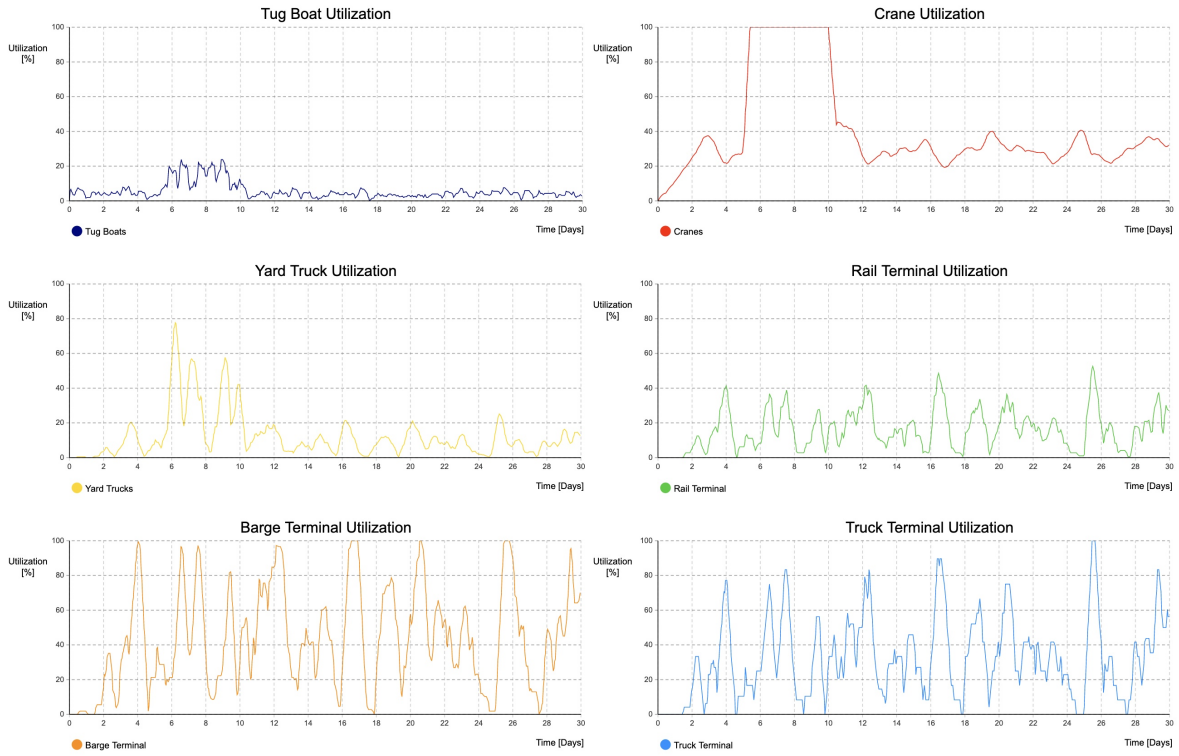

Figure B.32: Strike–Facility — utilization levels of facilities

B.2.8 Strike - Hub

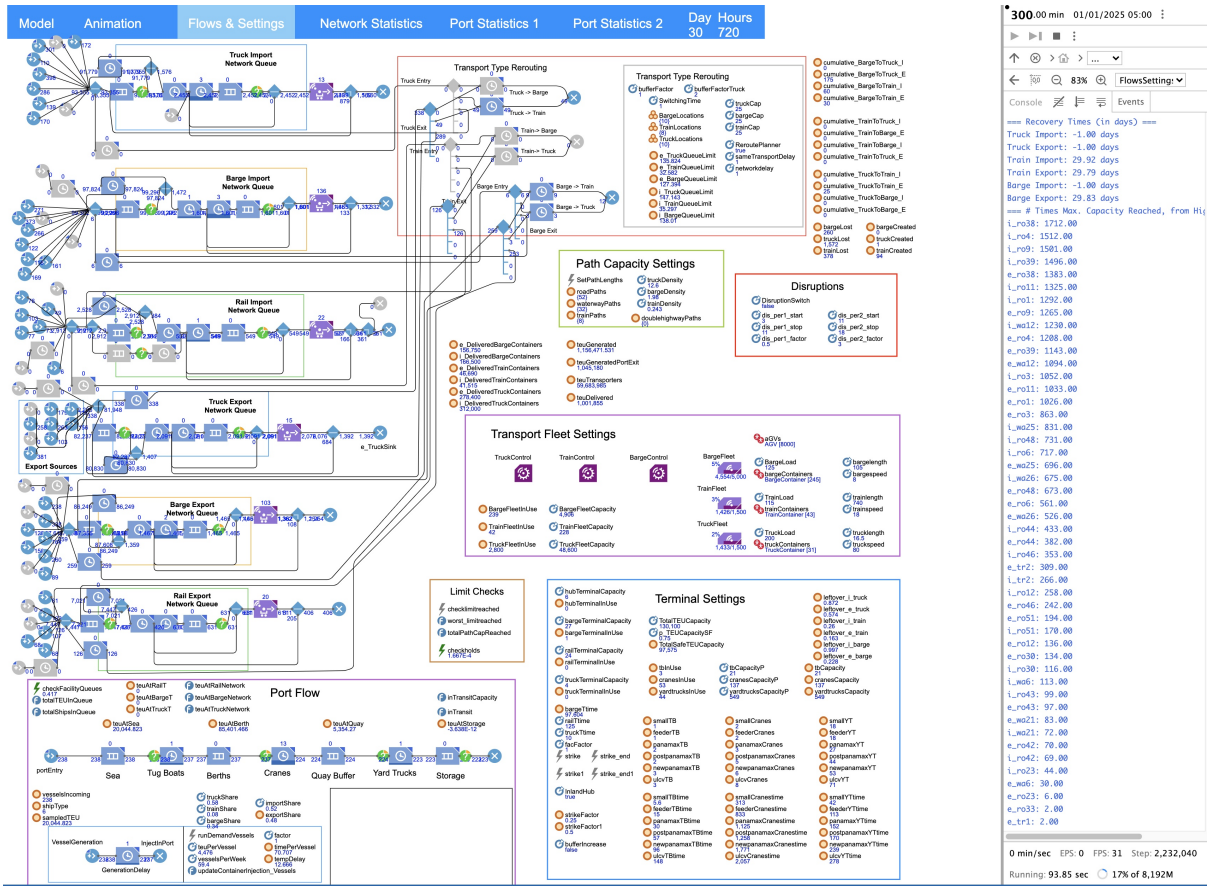

Figure B.33: Strike–Hub — settings and flow overview

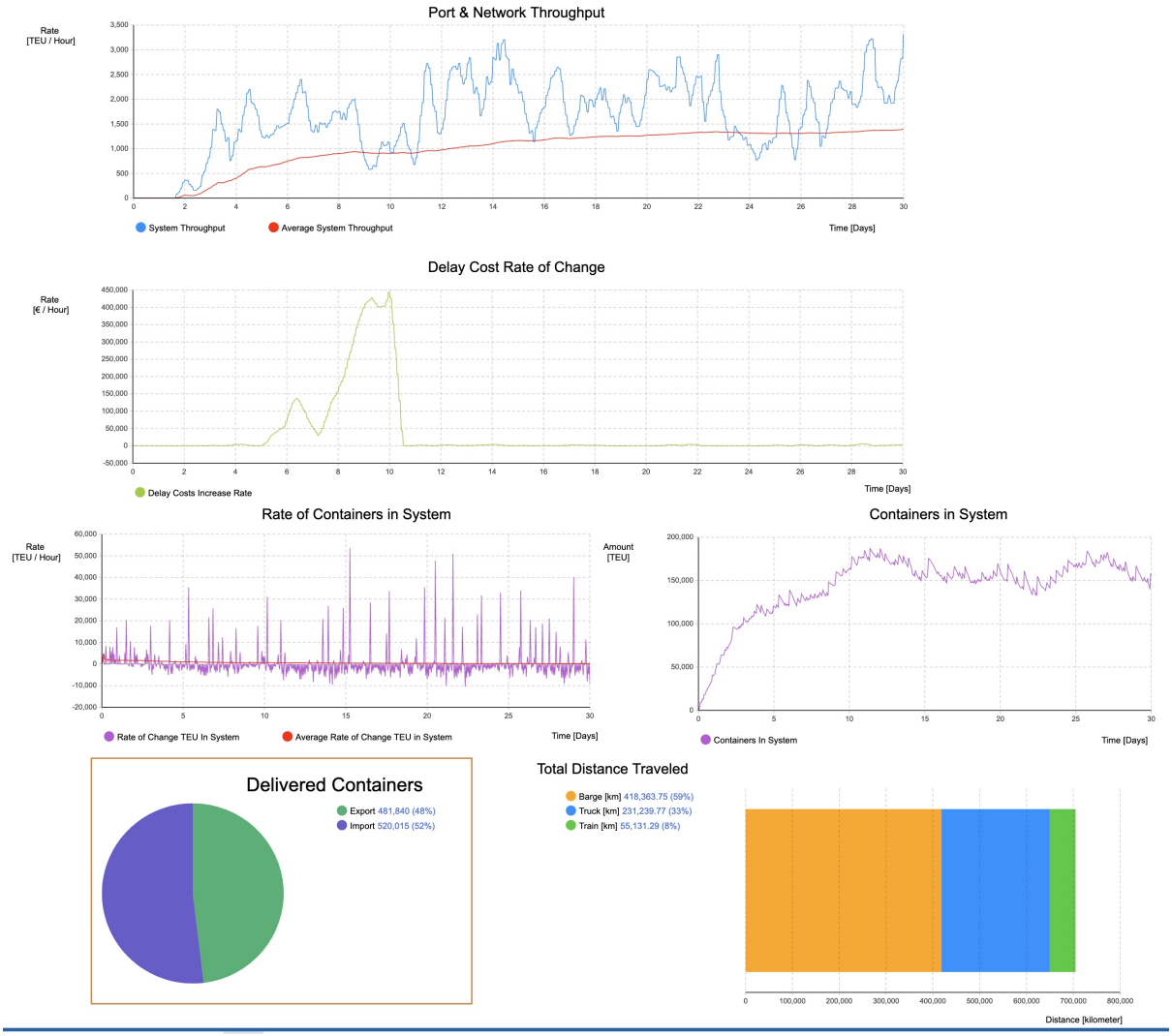

Figure B.34: Strike–Hub — network metrics and container throughput

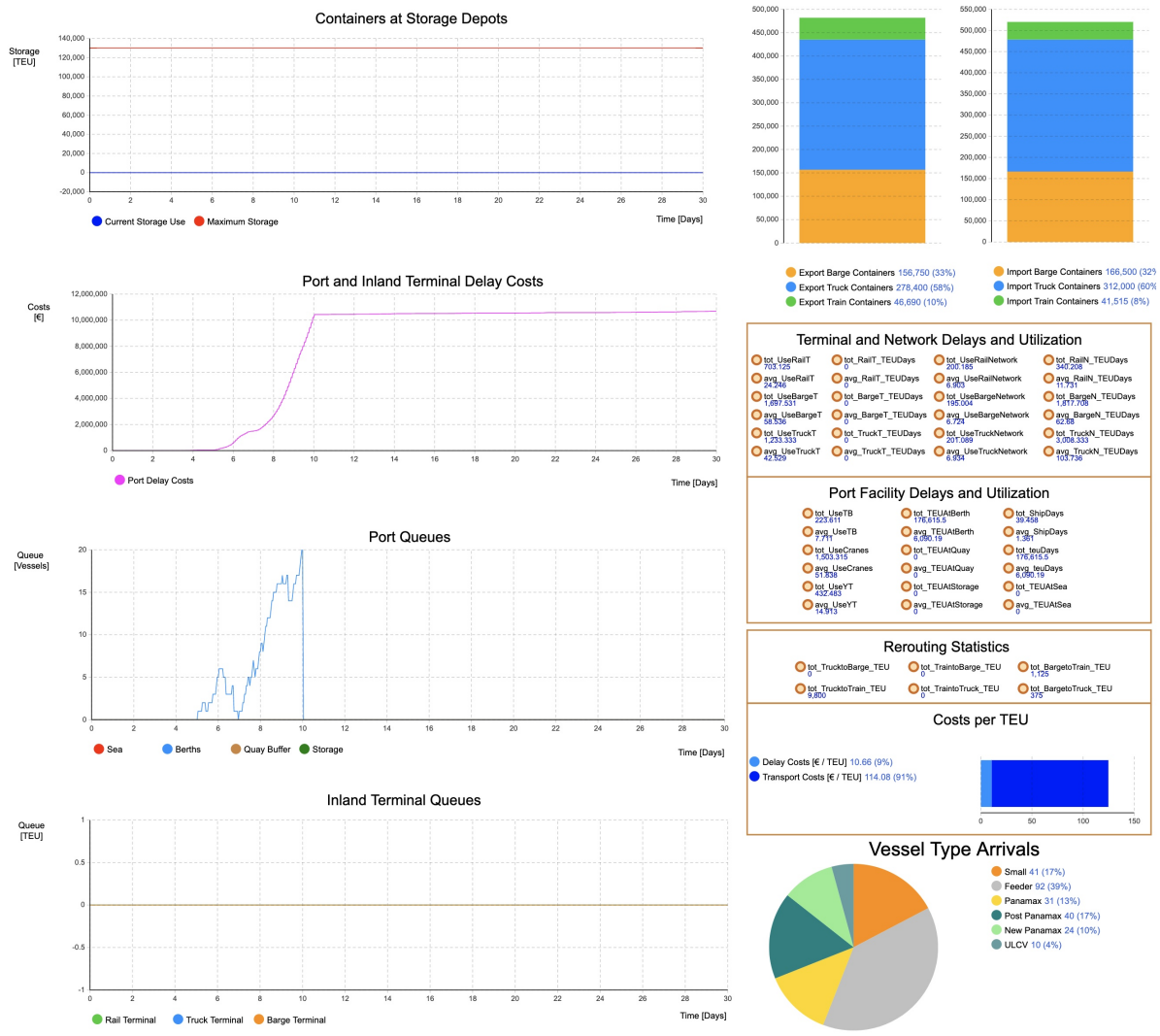

Figure B.35: Strike–Hub — delays in port system and general metrics

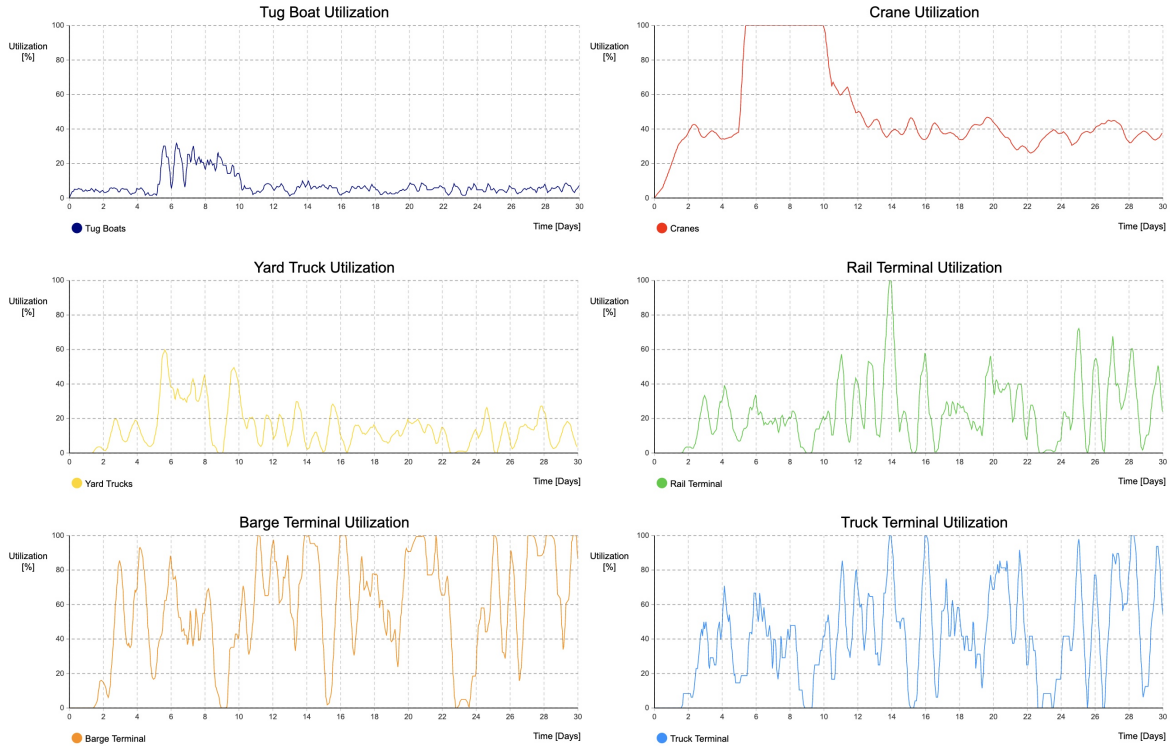

Figure B.36: Strike–Hub — utilization levels of facilities

B.2.9 Strike - Reroute

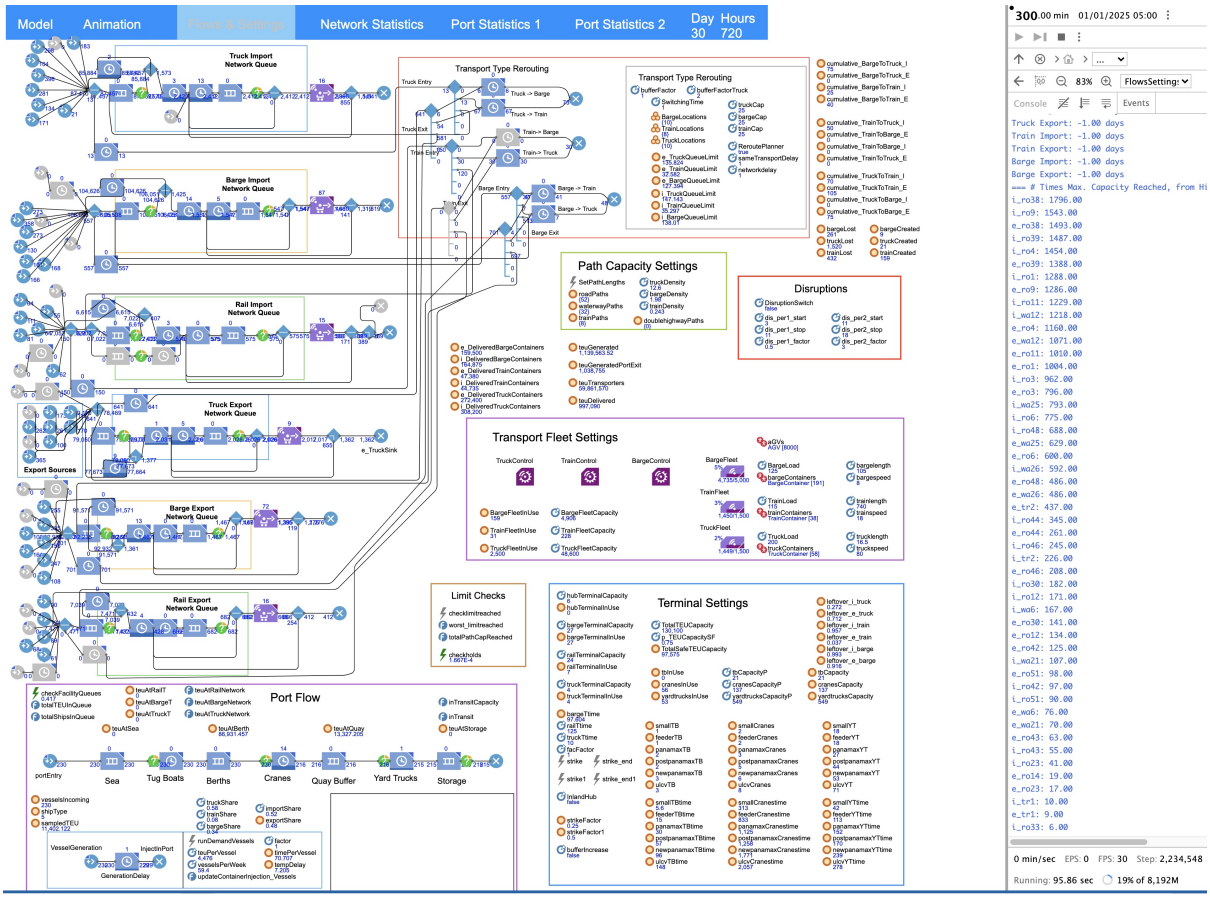

Figure B.37: Strike–Reroute — settings and flow overview

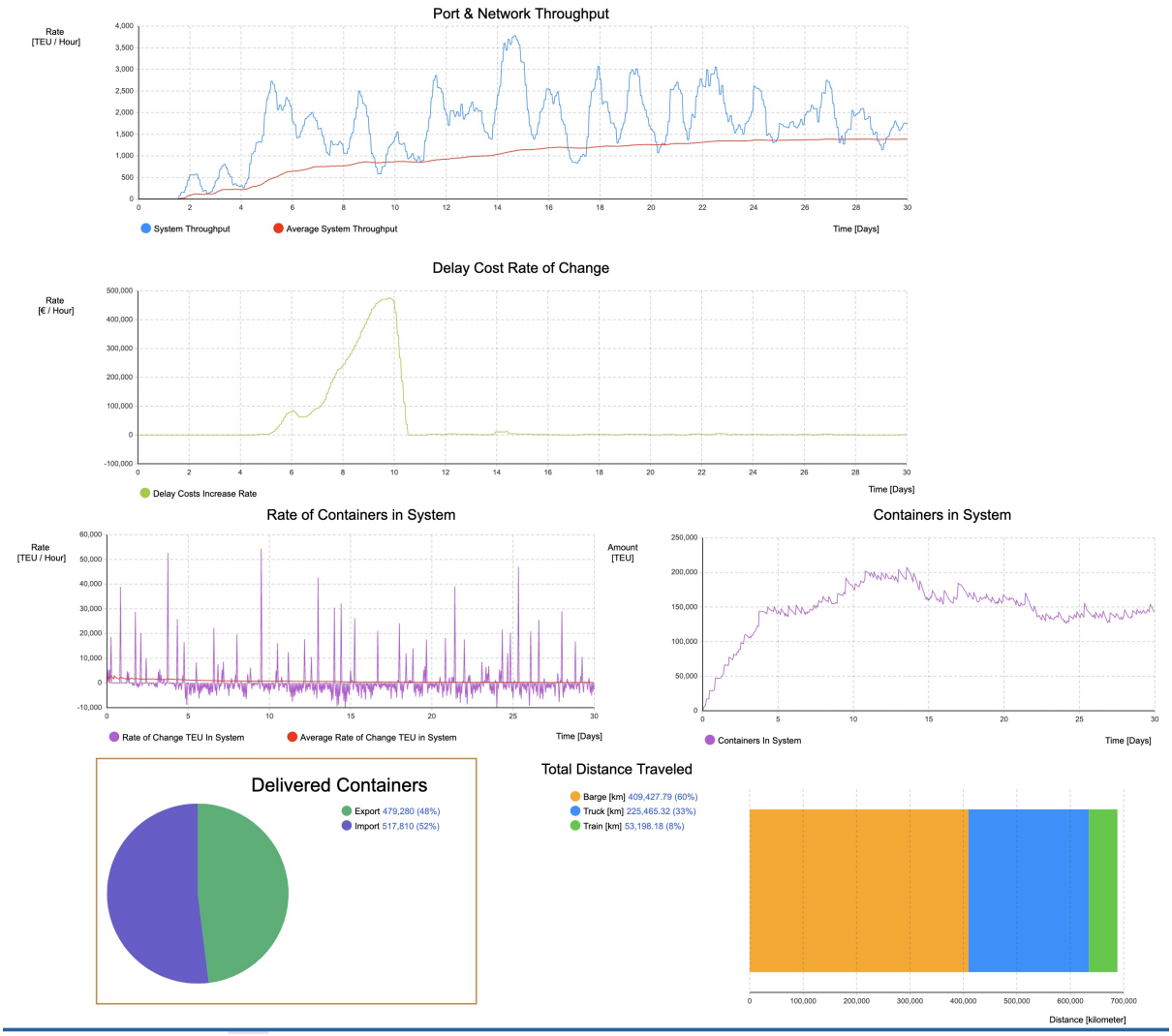

Figure B.38: Strike–Reroute — network metrics and container throughput

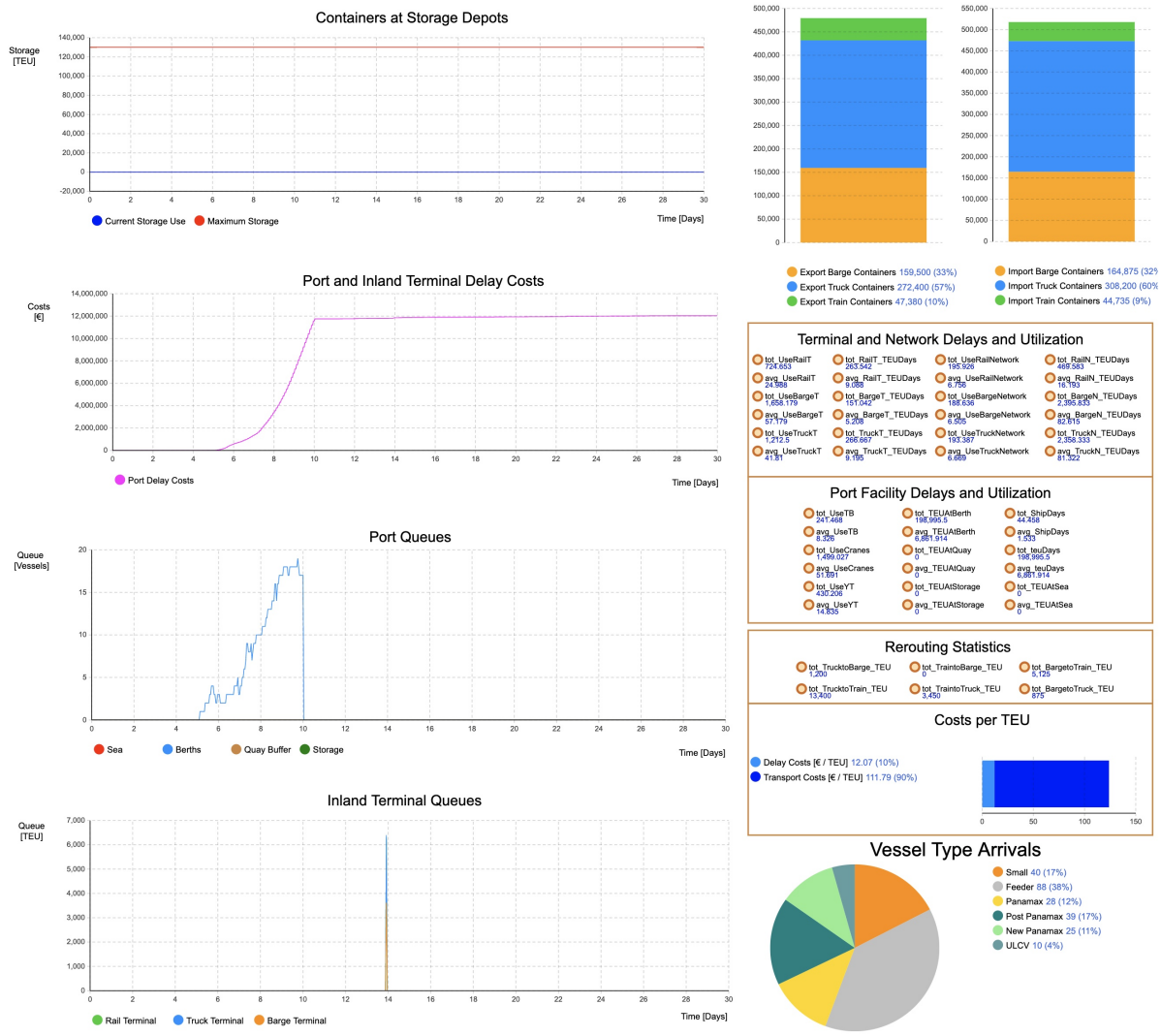

Figure B.39: Strike–Reroute — delays in port system and general metrics

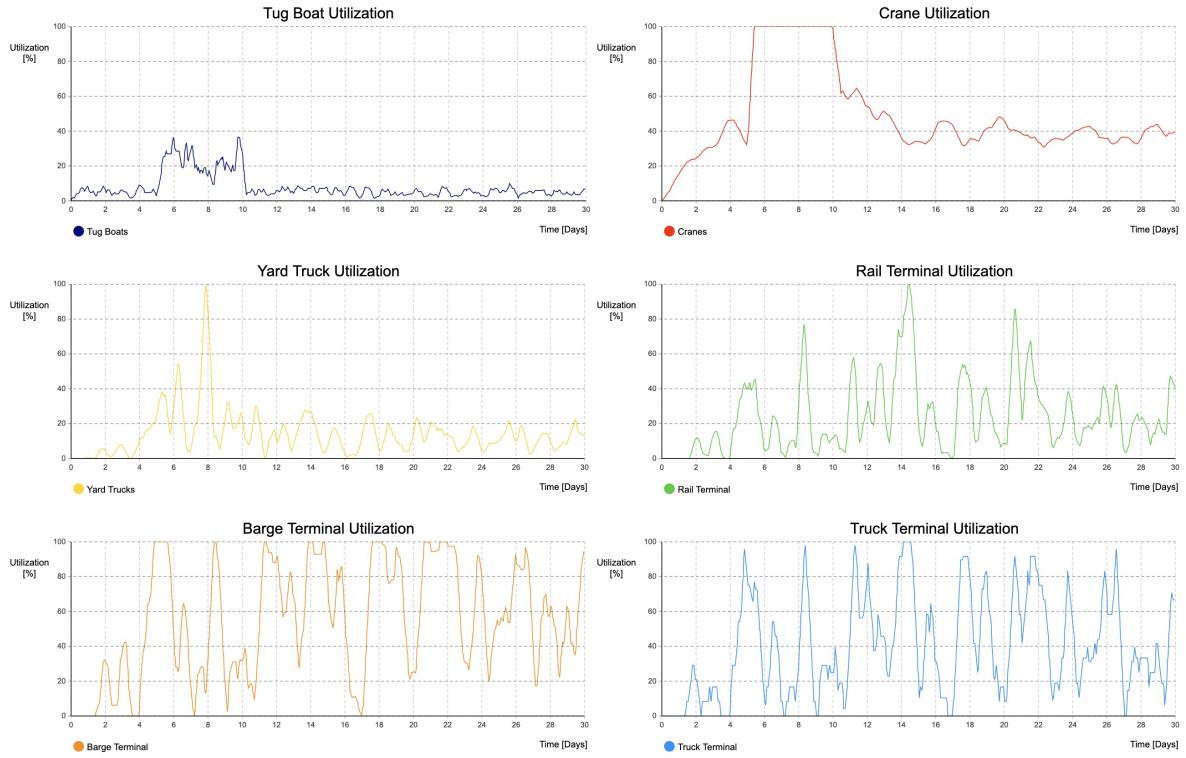

Figure B.40: Strike–Reroute — utilization levels of facilities

B.2.10 Strike - Storage

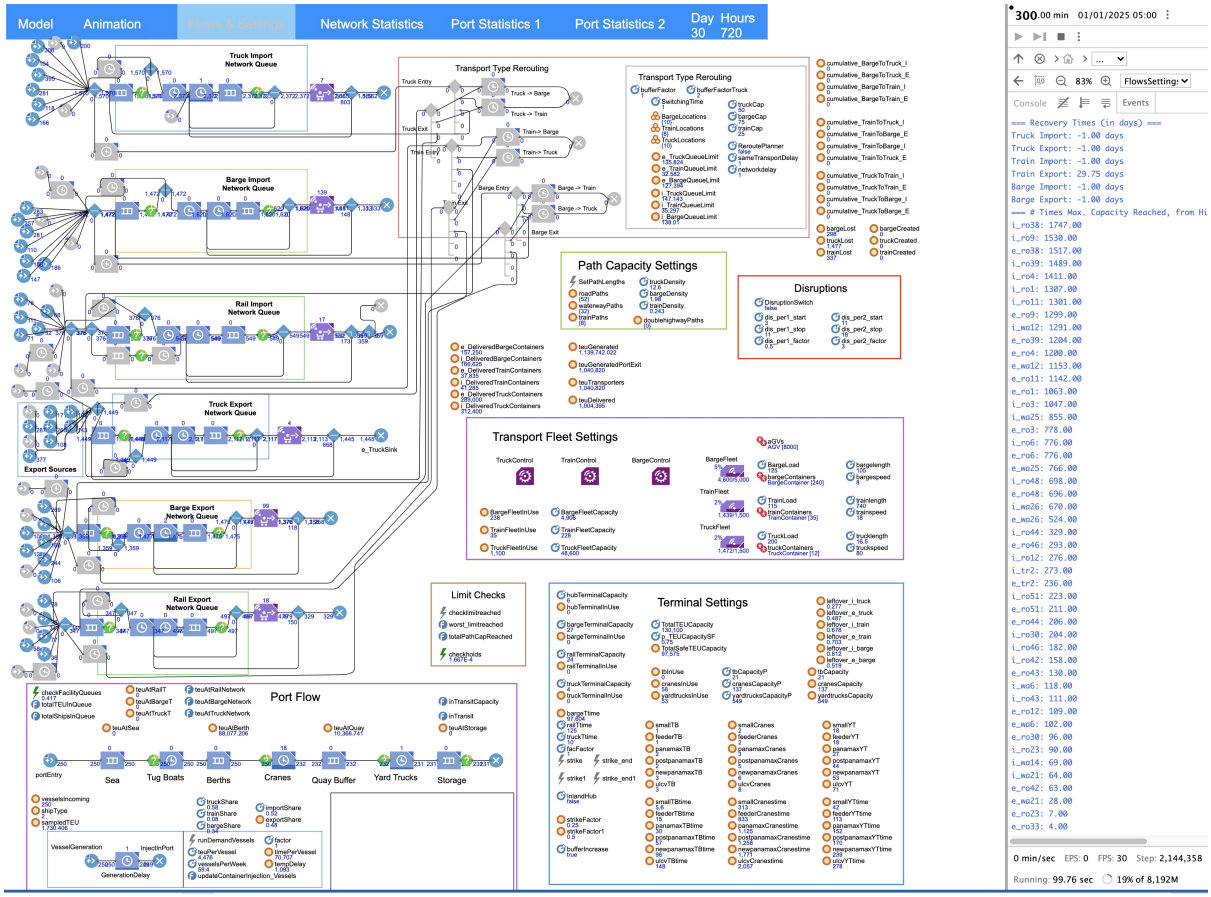

Figure B.41: Strike–Storage — settings and flow overview

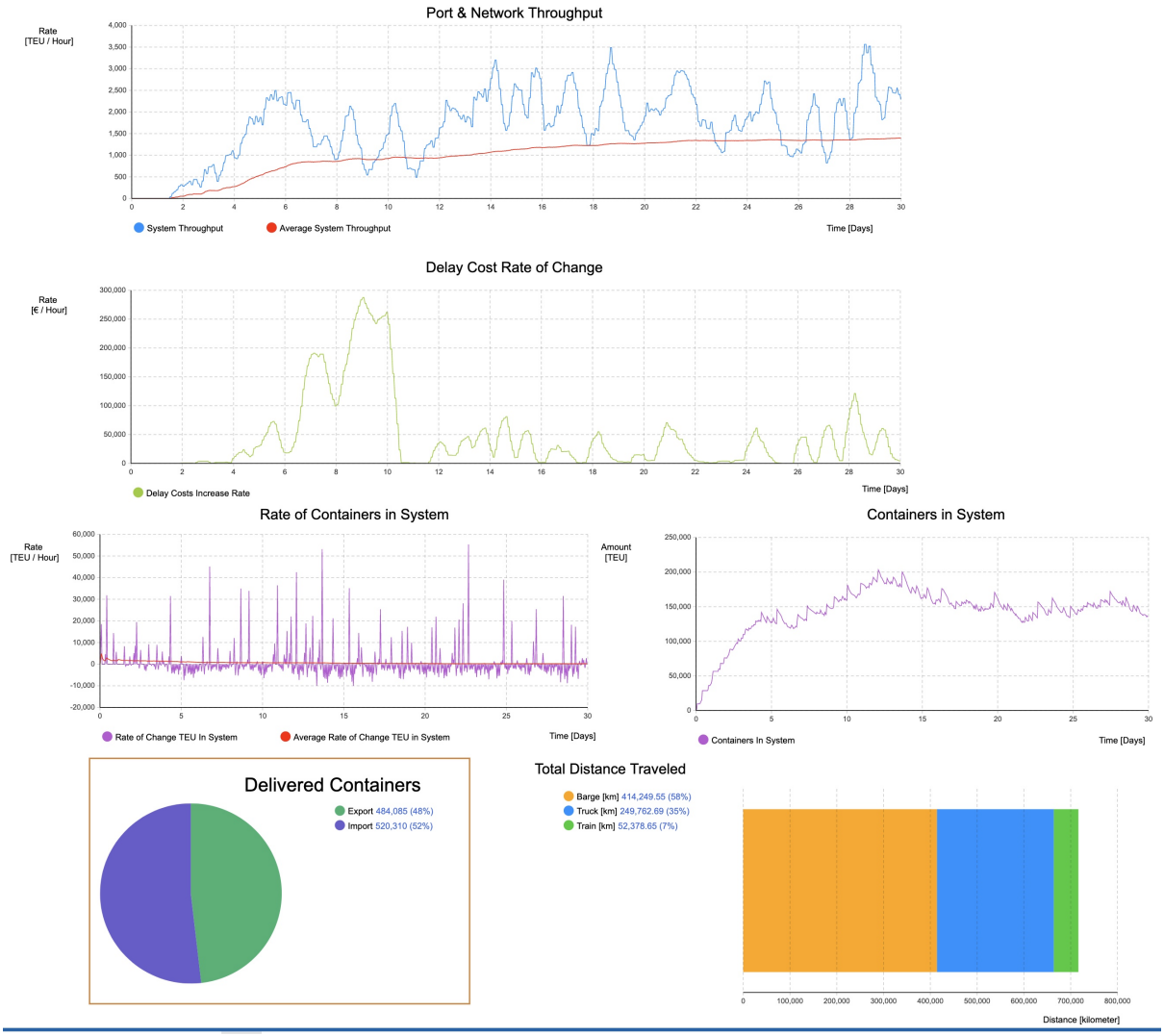

Figure B.42: Strike–Storage — network metrics and container throughput

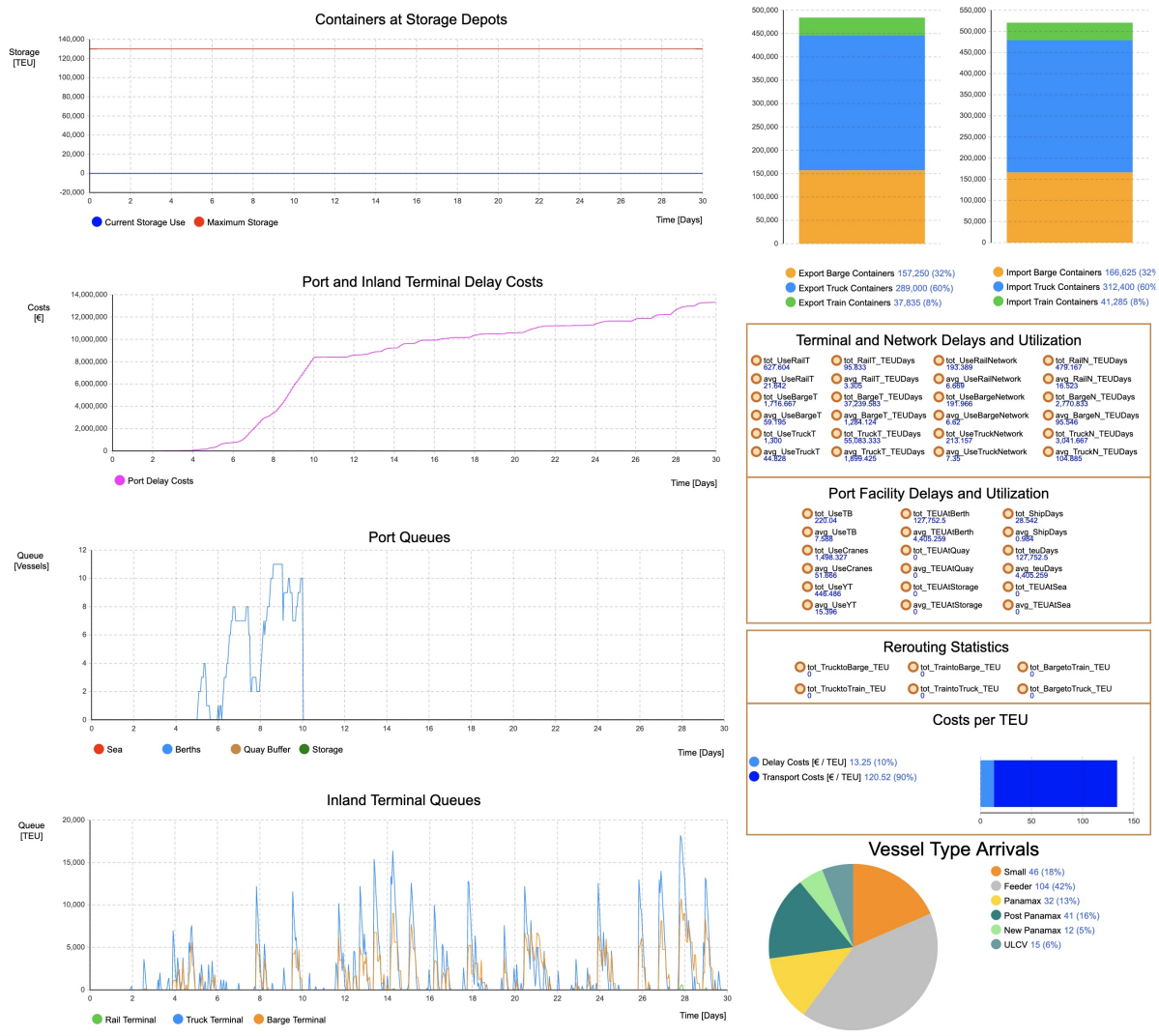

Figure B.43: Strike–Storage — delays in port system and general metrics

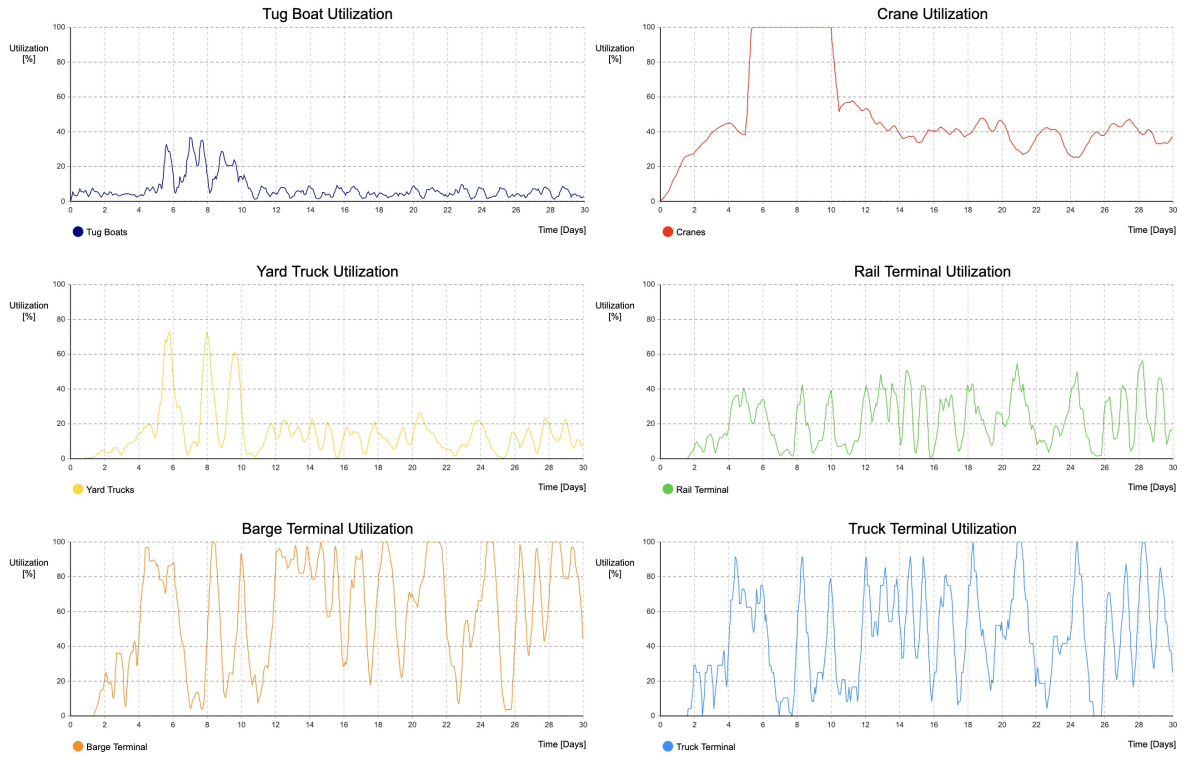

Figure B.44: Strike–Storage — utilization levels of facilities

B.2.11 Demand

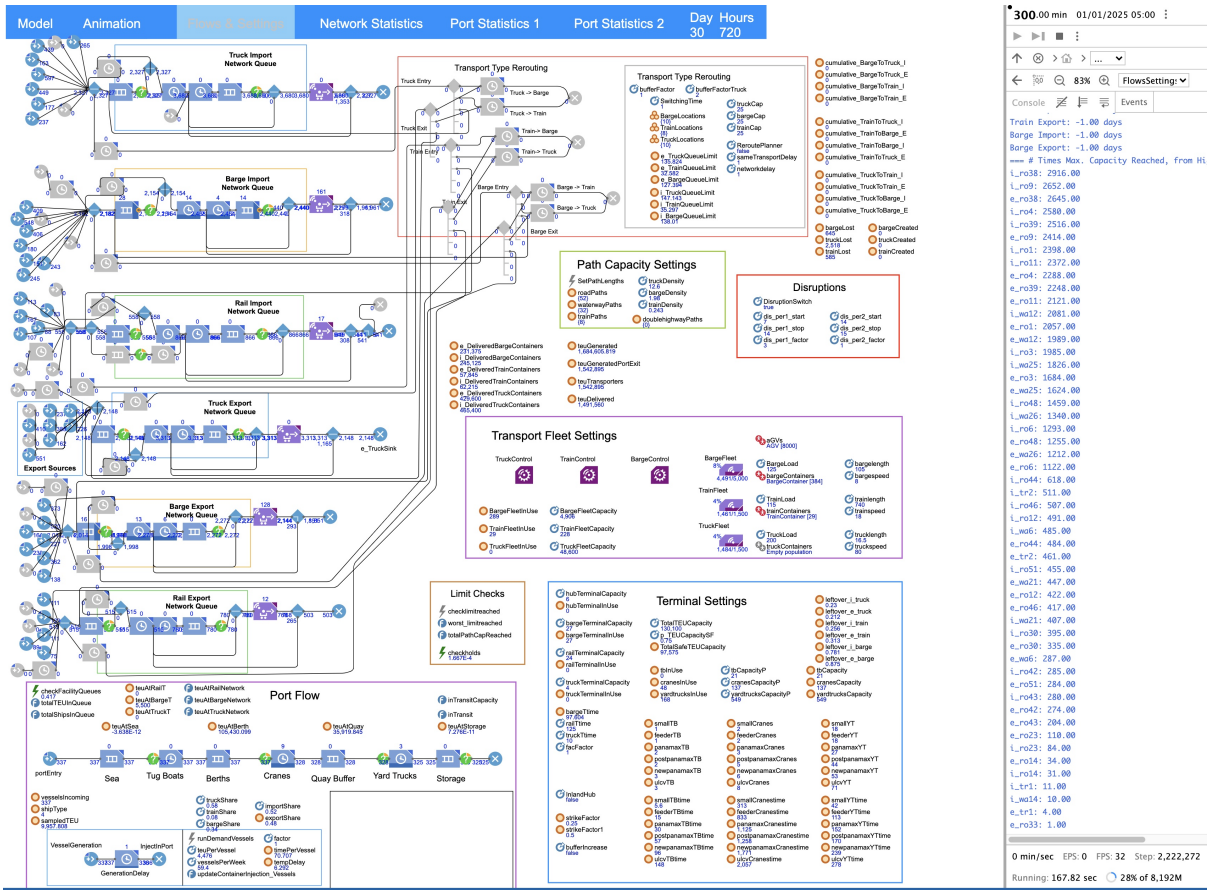

Figure B.45: Demand — experiment settings and flow overview

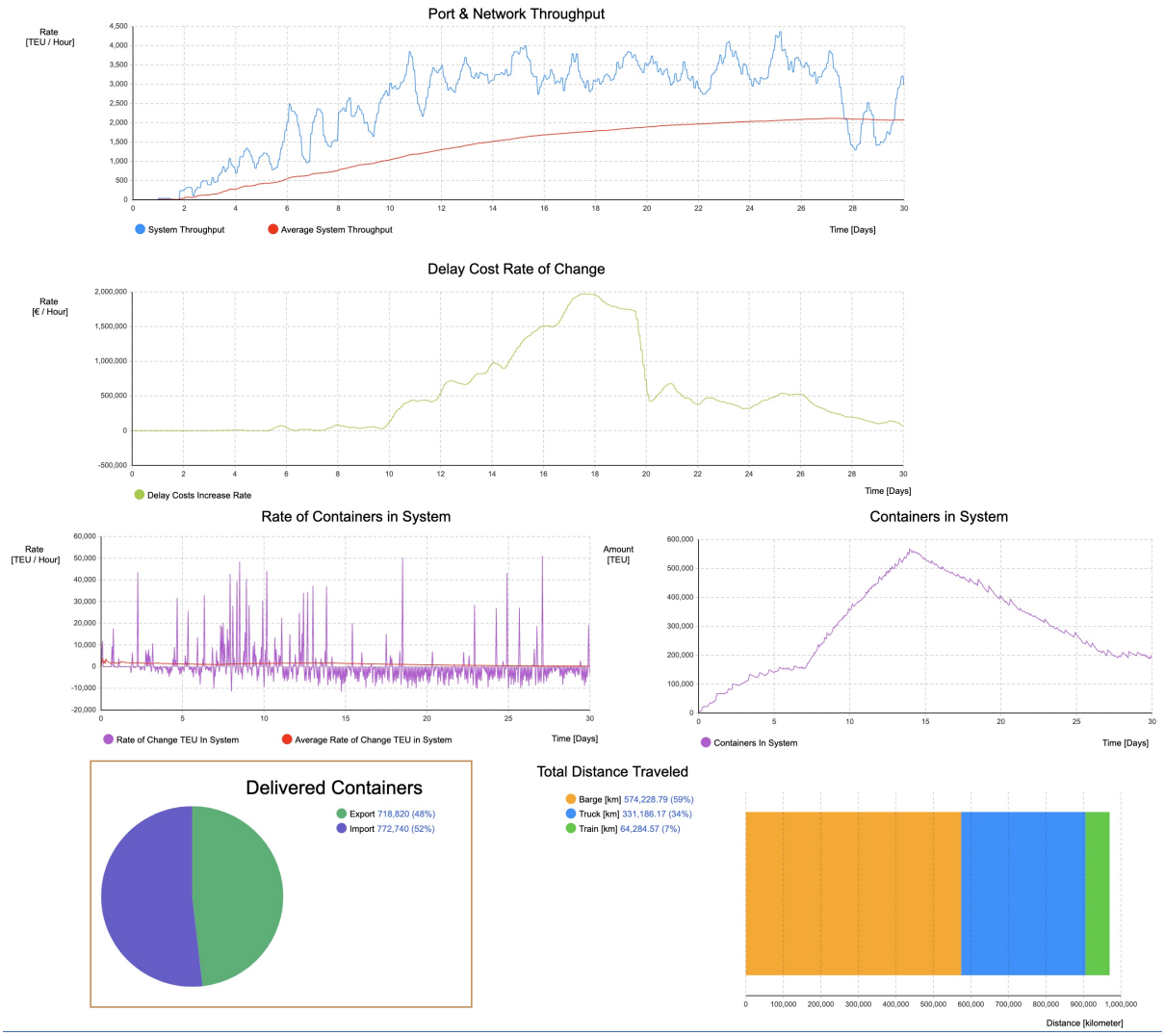

Figure B.46: Demand — network metrics and container throughput

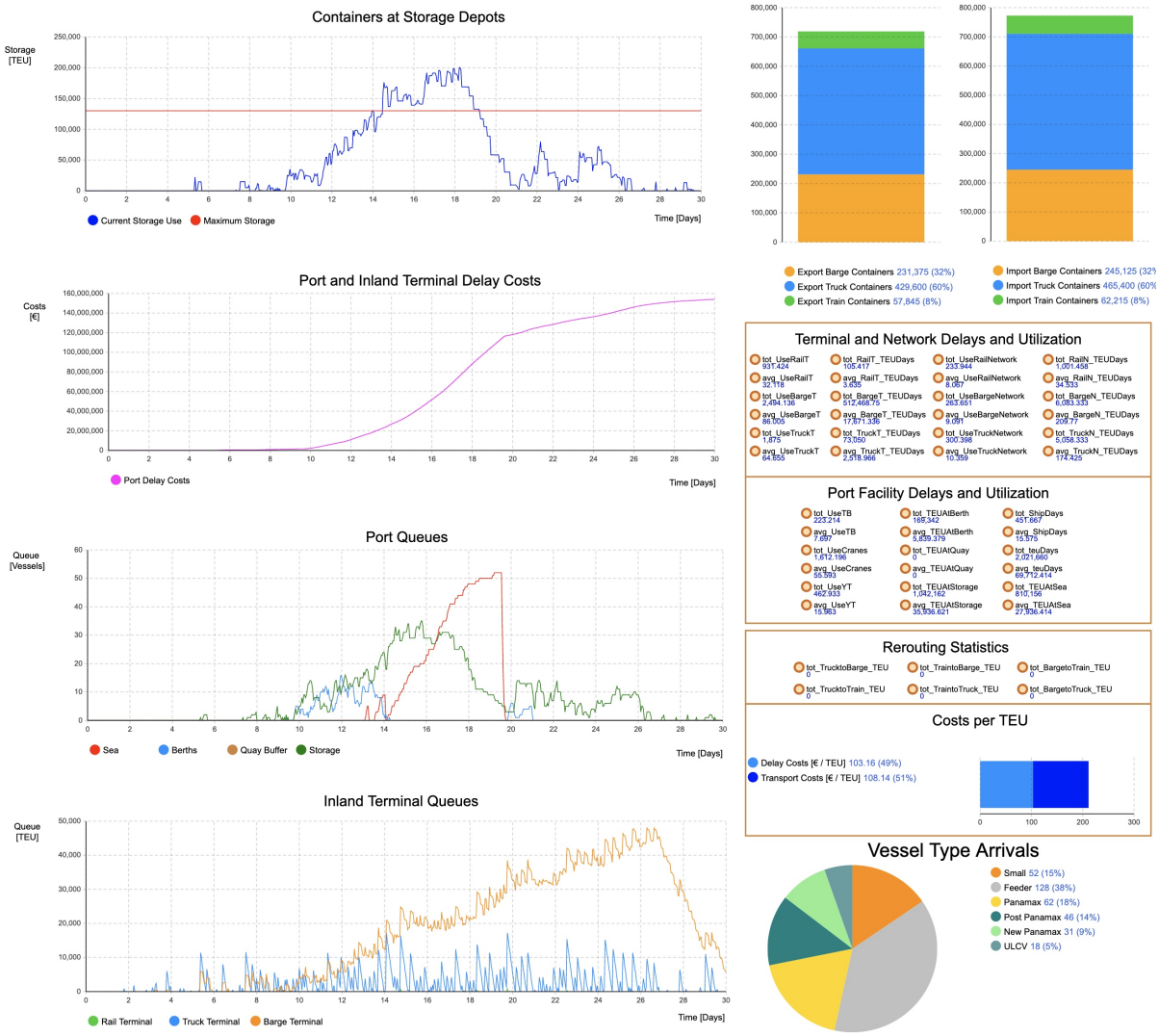

Figure B.47: Demand — delays in port system and general metrics

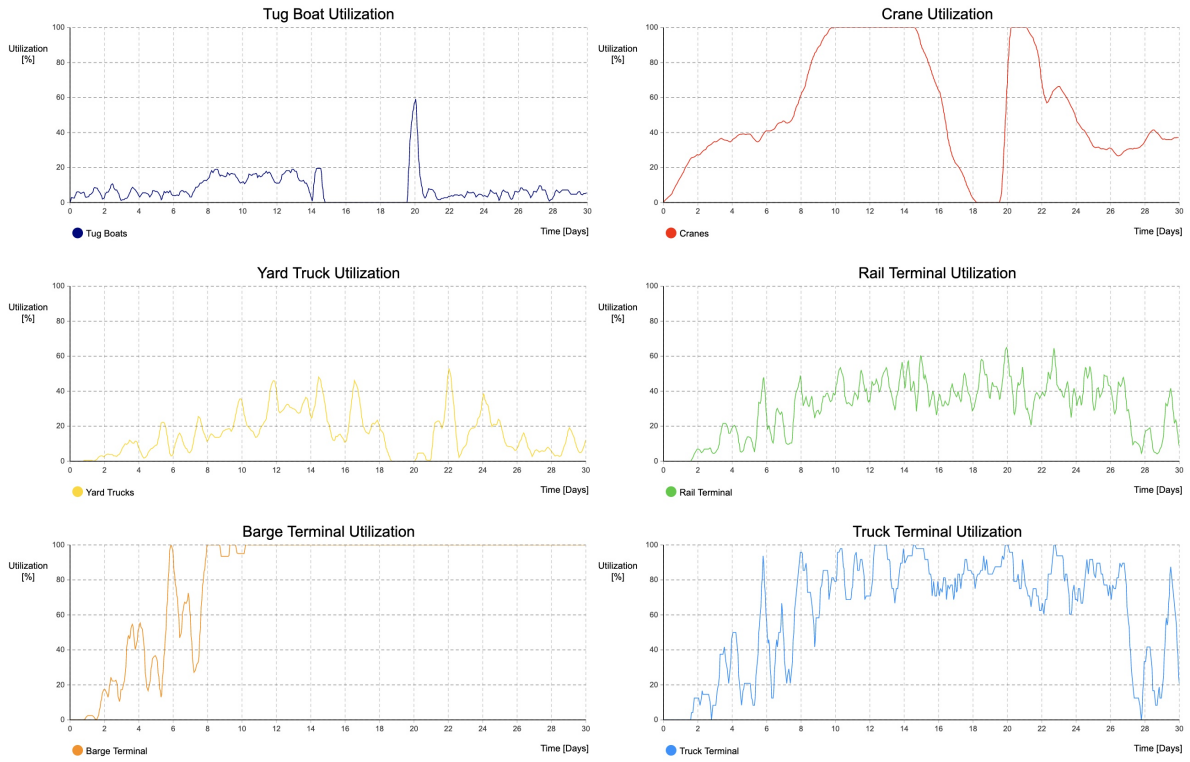

Figure B.48: Demand — utilization levels of facilities

B.2.12 Demand - Facility

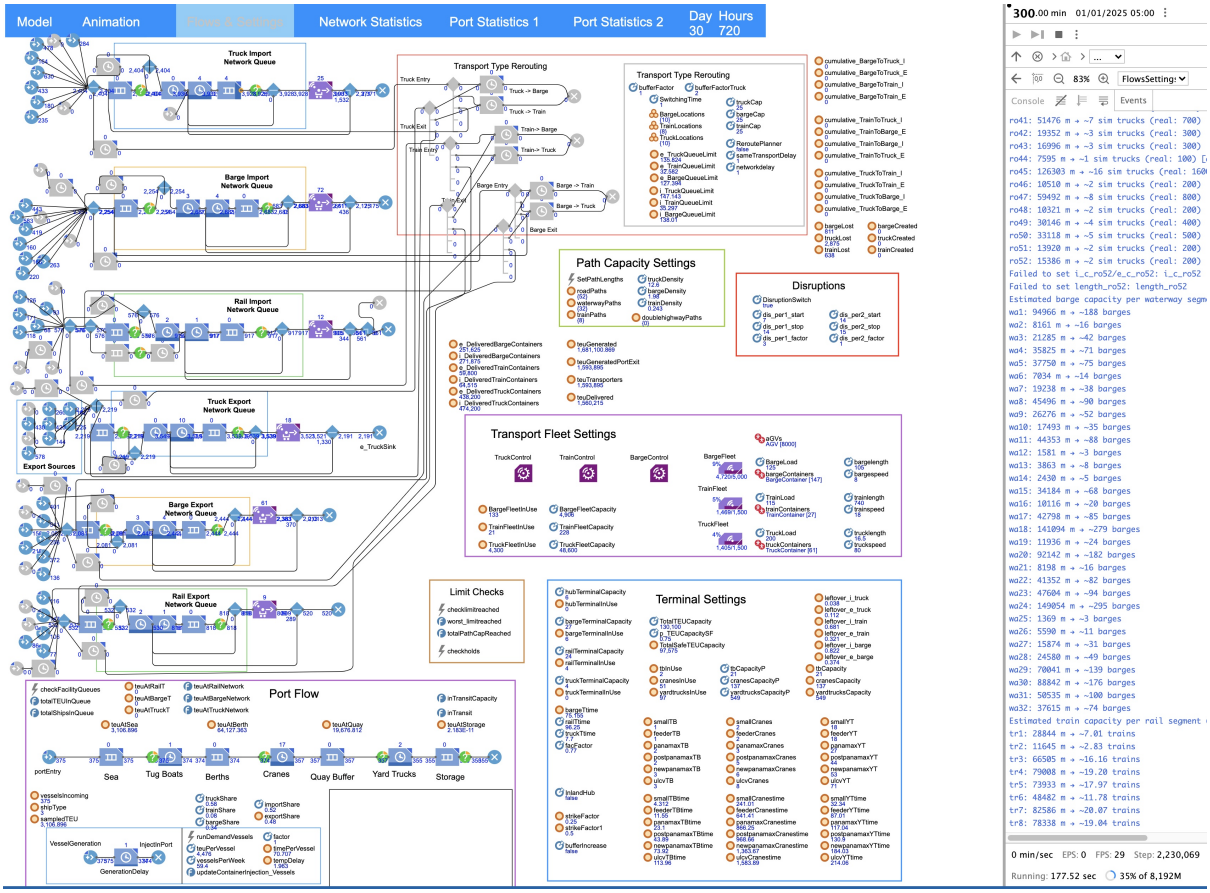

Figure B.49: Demand–Facility — settings and flow overview

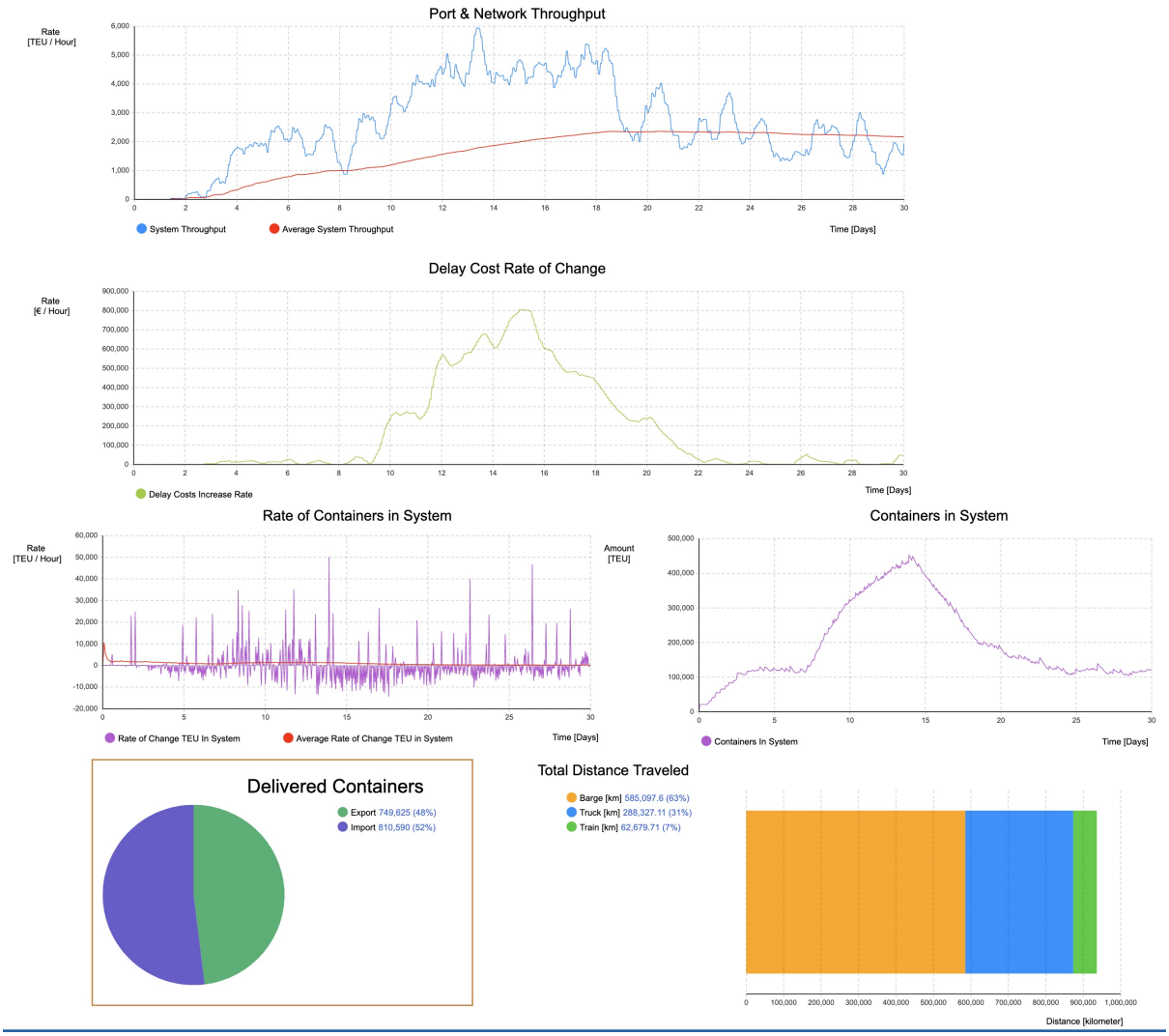

Figure B.50: Demand–Facility — network metrics and container throughput

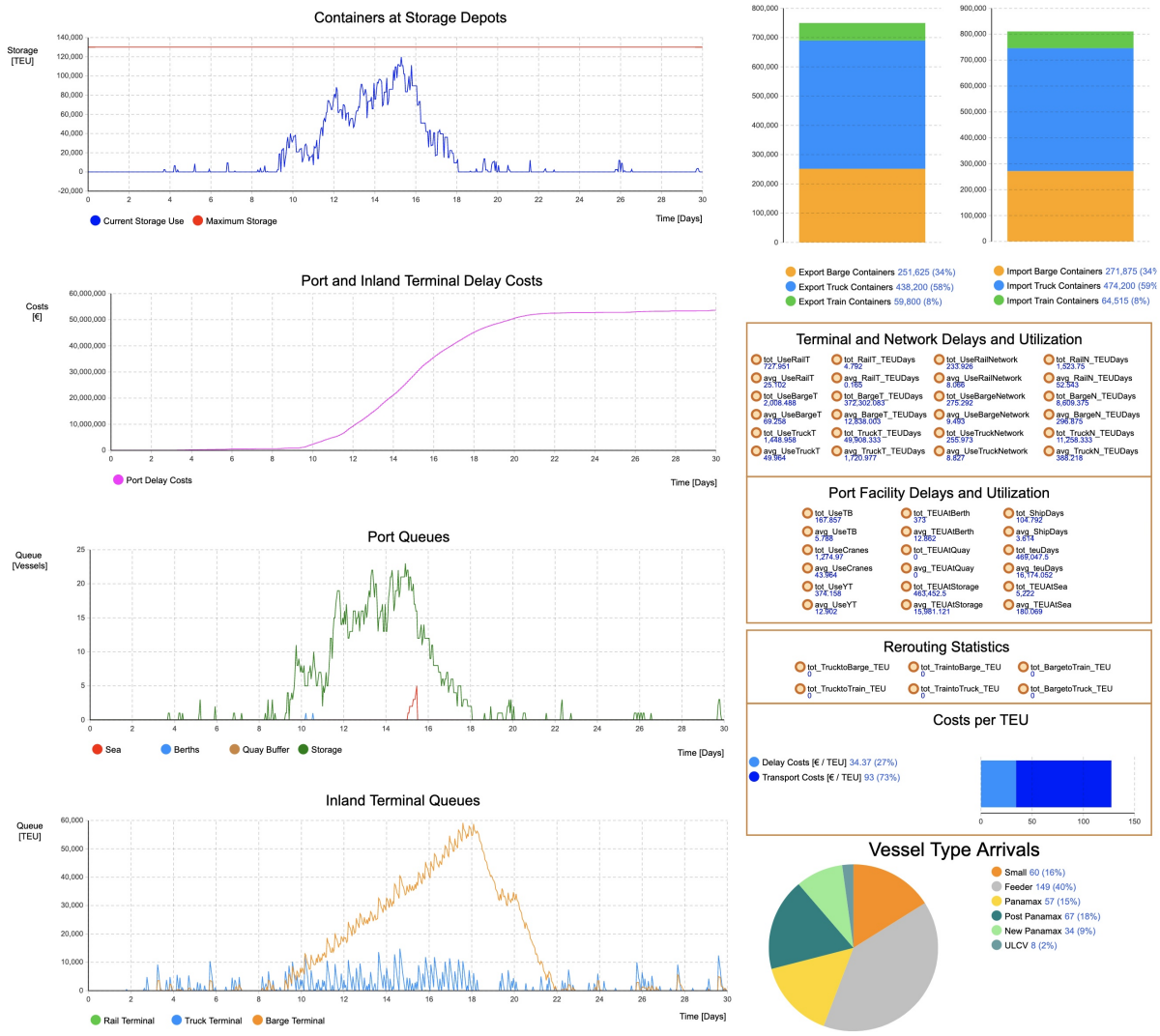

Figure B.51: Demand–Facility — delays in port system and general metrics

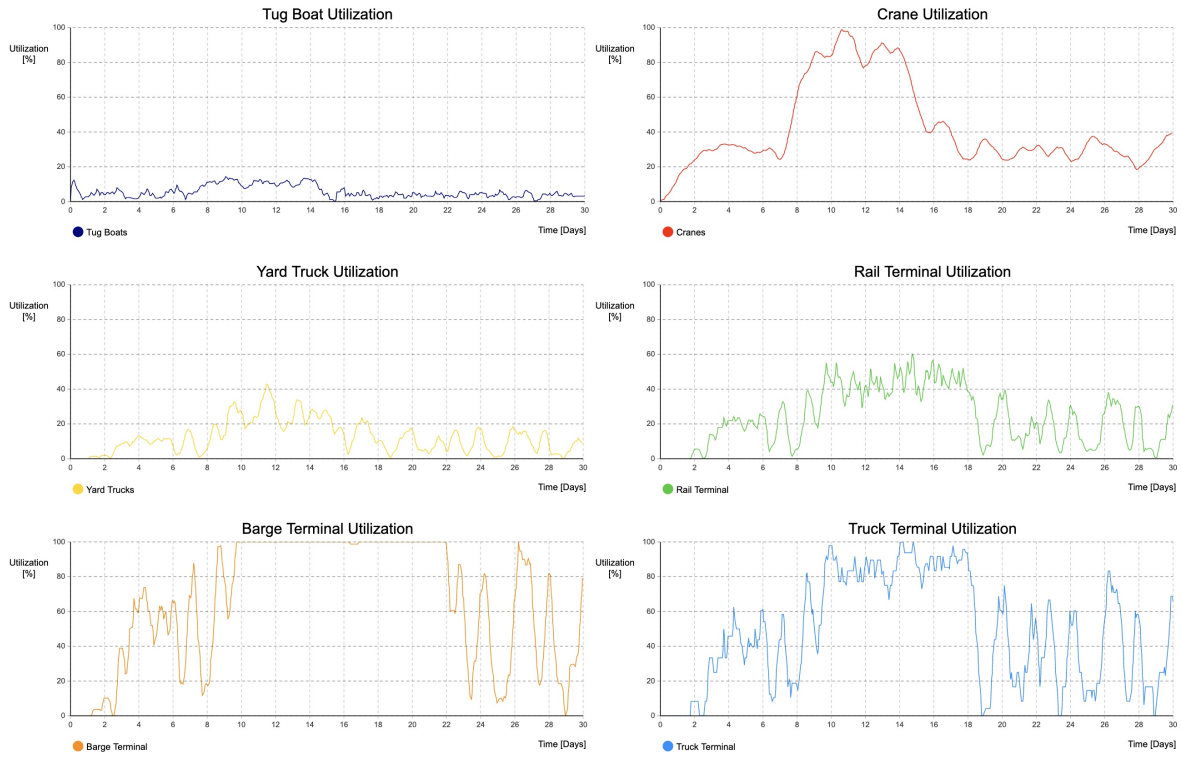

Figure B.52: Demand–Facility — utilization levels of facilities

B.2.13 Demand - Hub

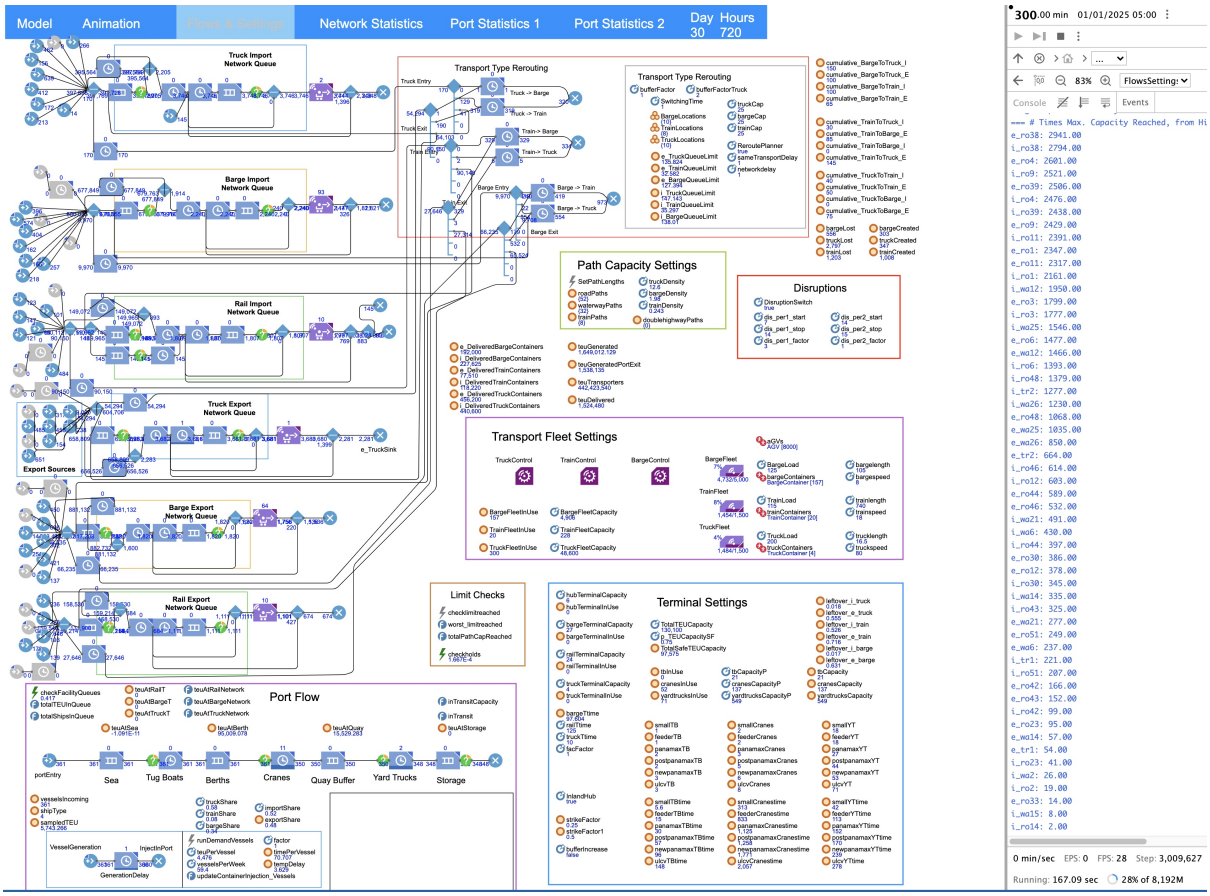

Figure B.53: Demand–Hub — settings and flow overview

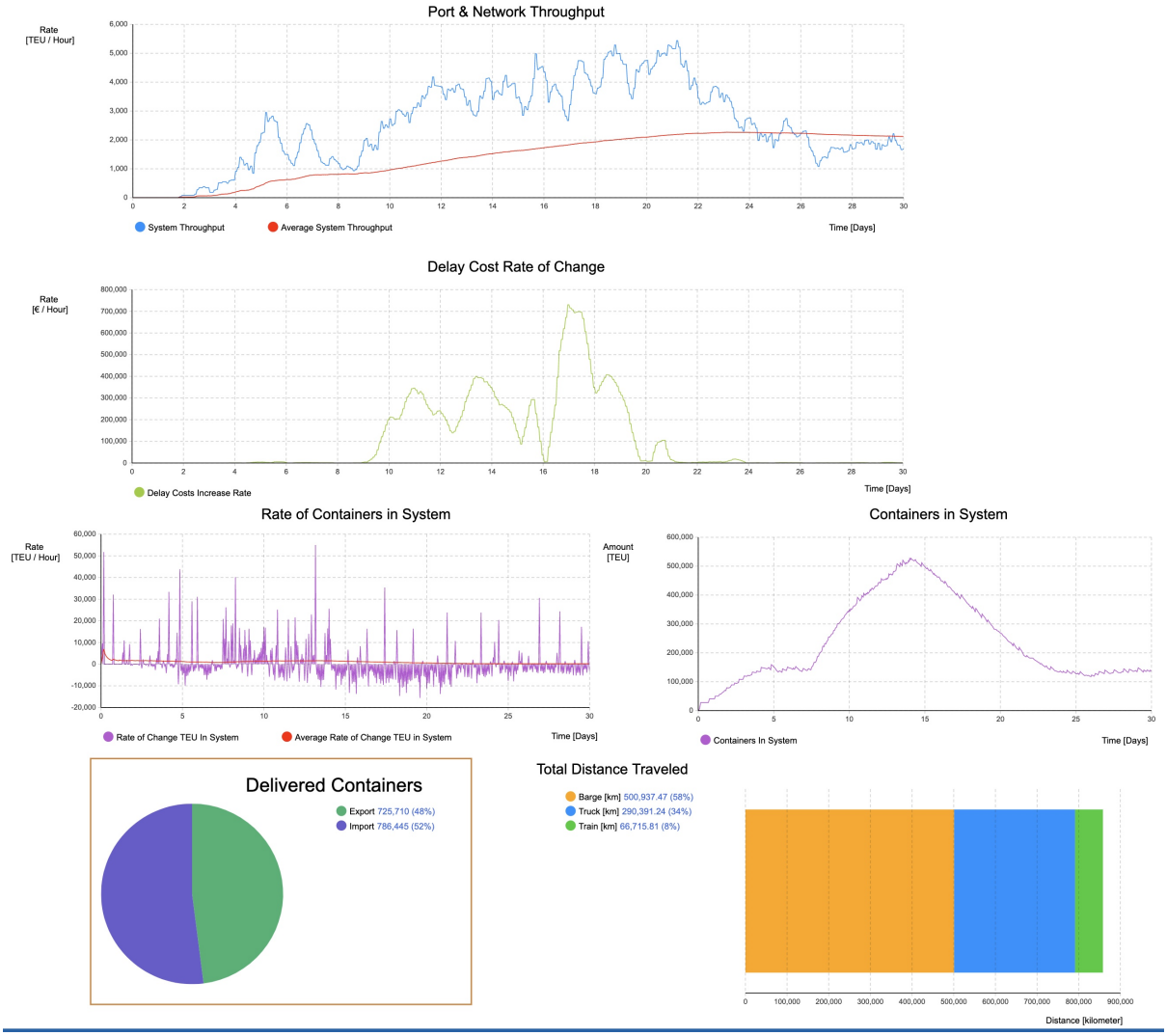

Figure B.54: Demand–Hub — network metrics and container throughput

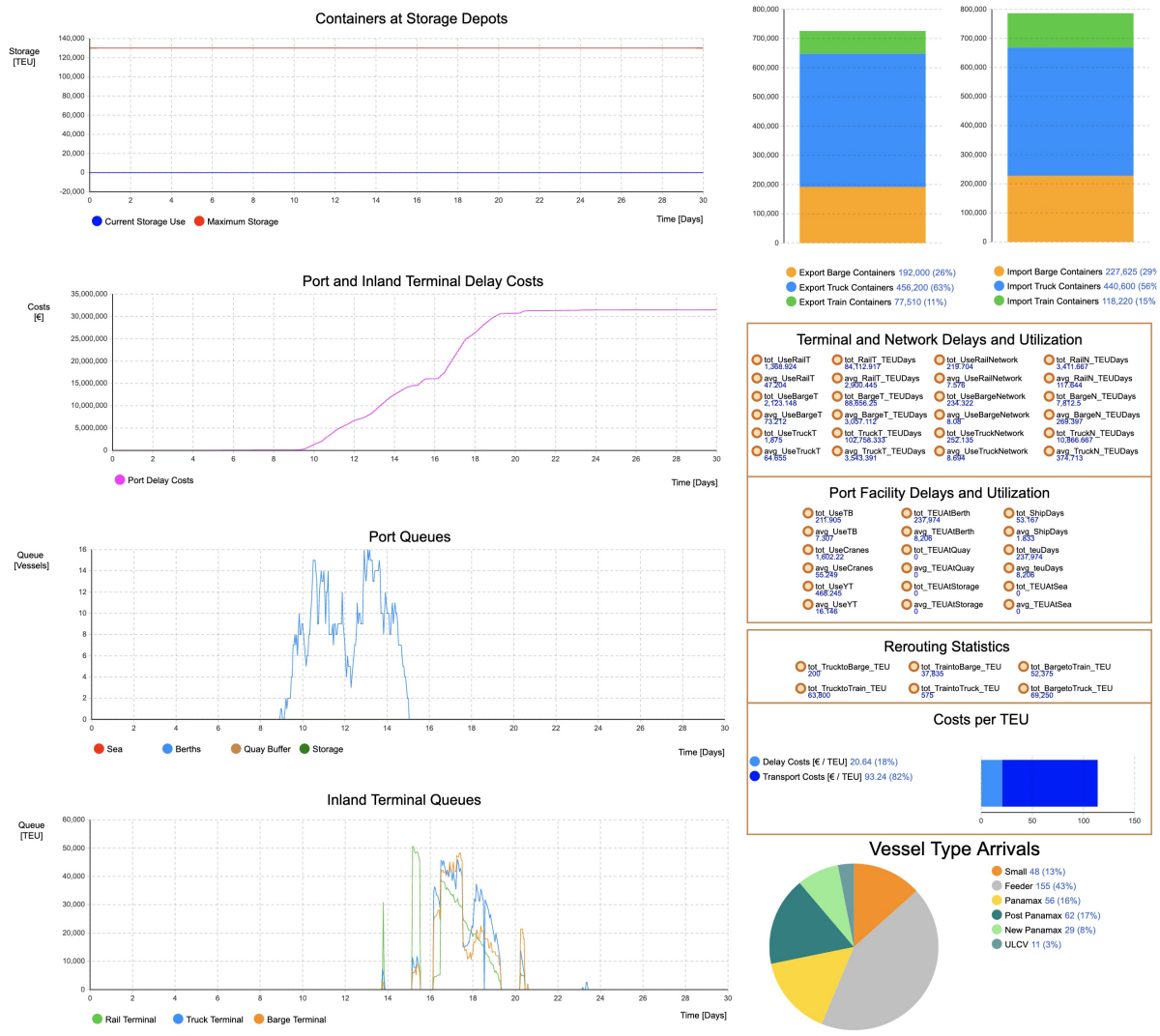

Figure B.55: Demand–Hub — delays in port system and general metrics

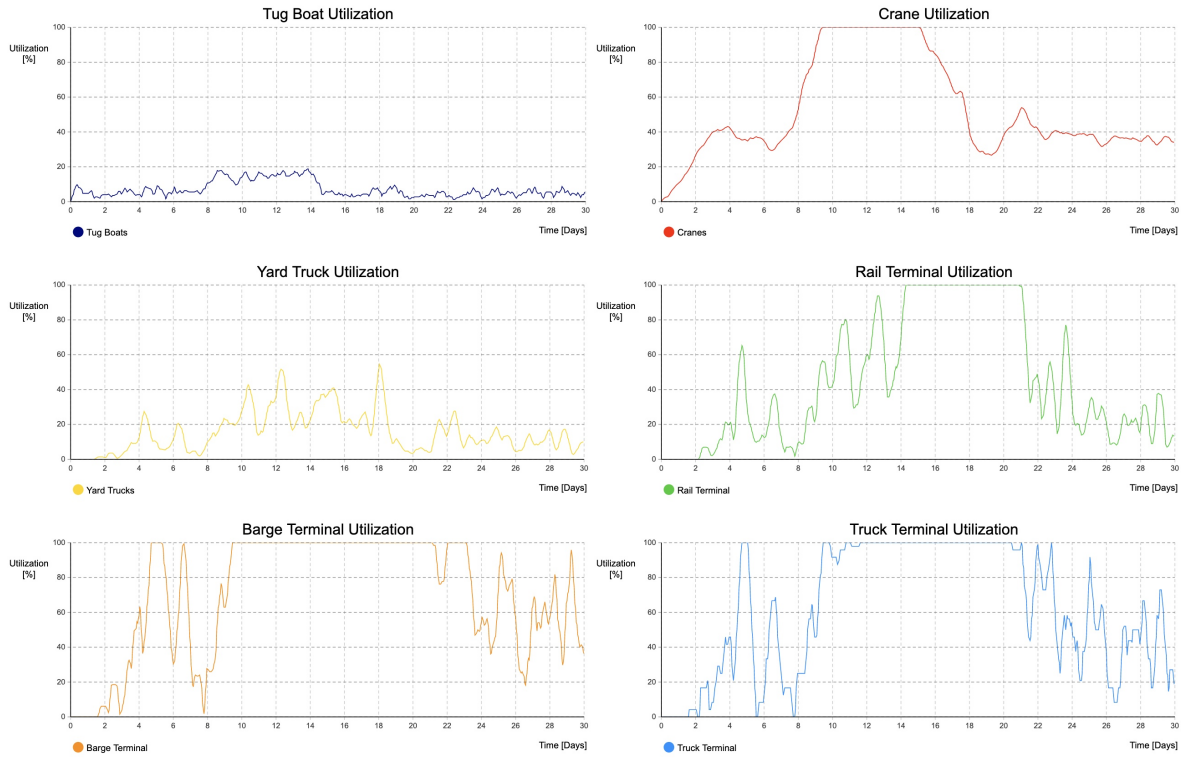

Figure B.56: Demand–Hub — utilization levels of facilities

B.2.14 Demand - Reroute

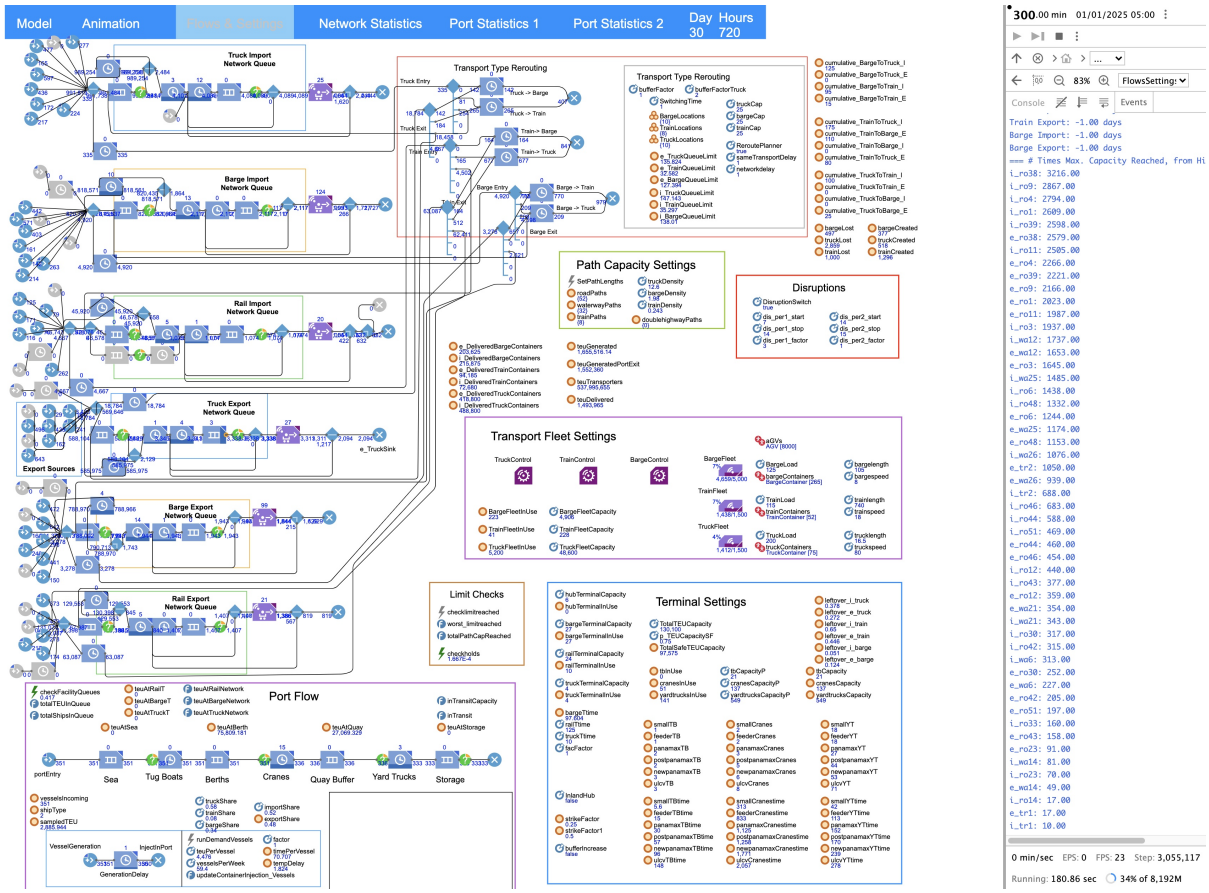

Figure B.57: Demand–Reroute — settings and flow overview

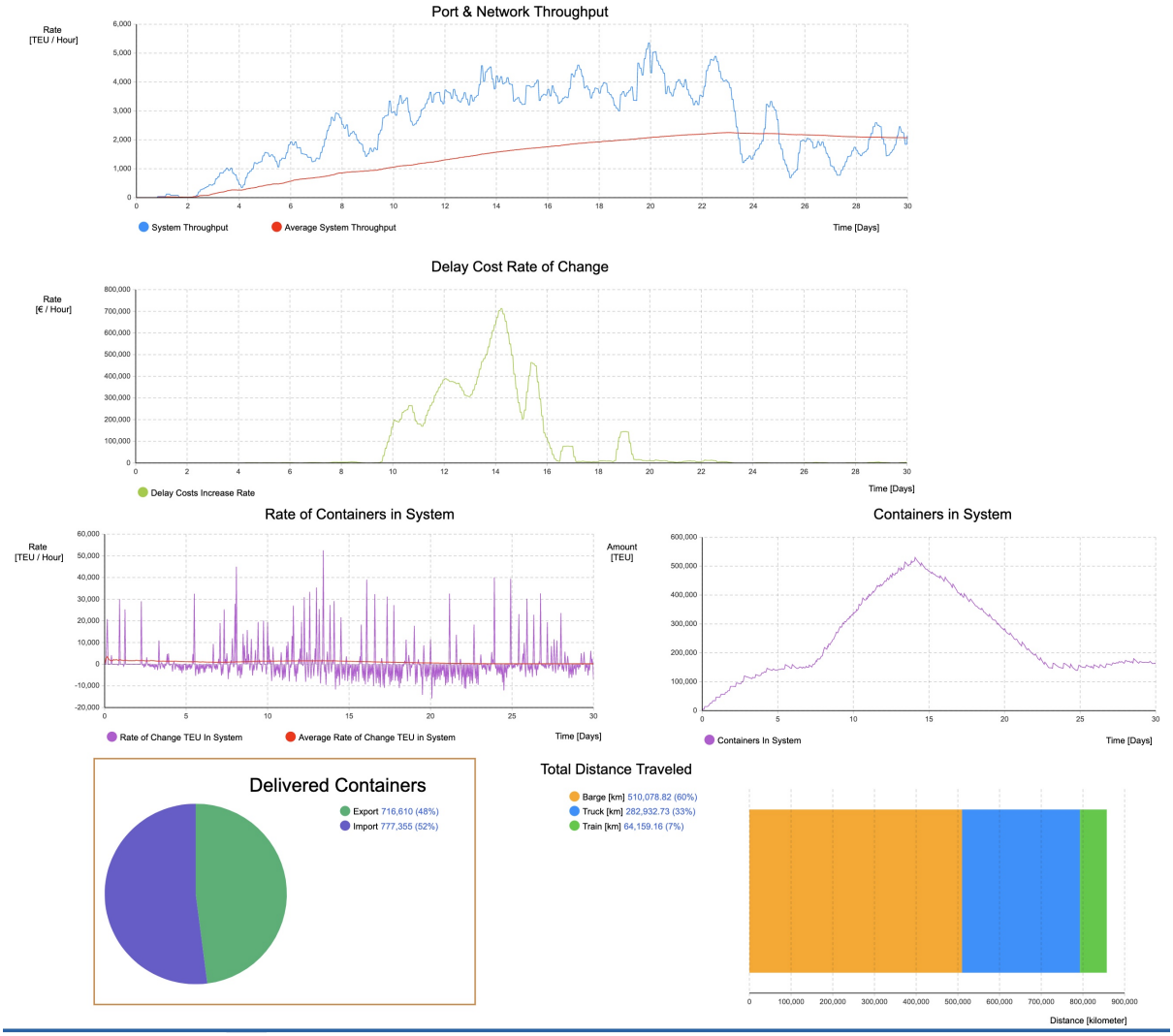

Figure B.58: Demand–Reroute — network metrics and container throughput

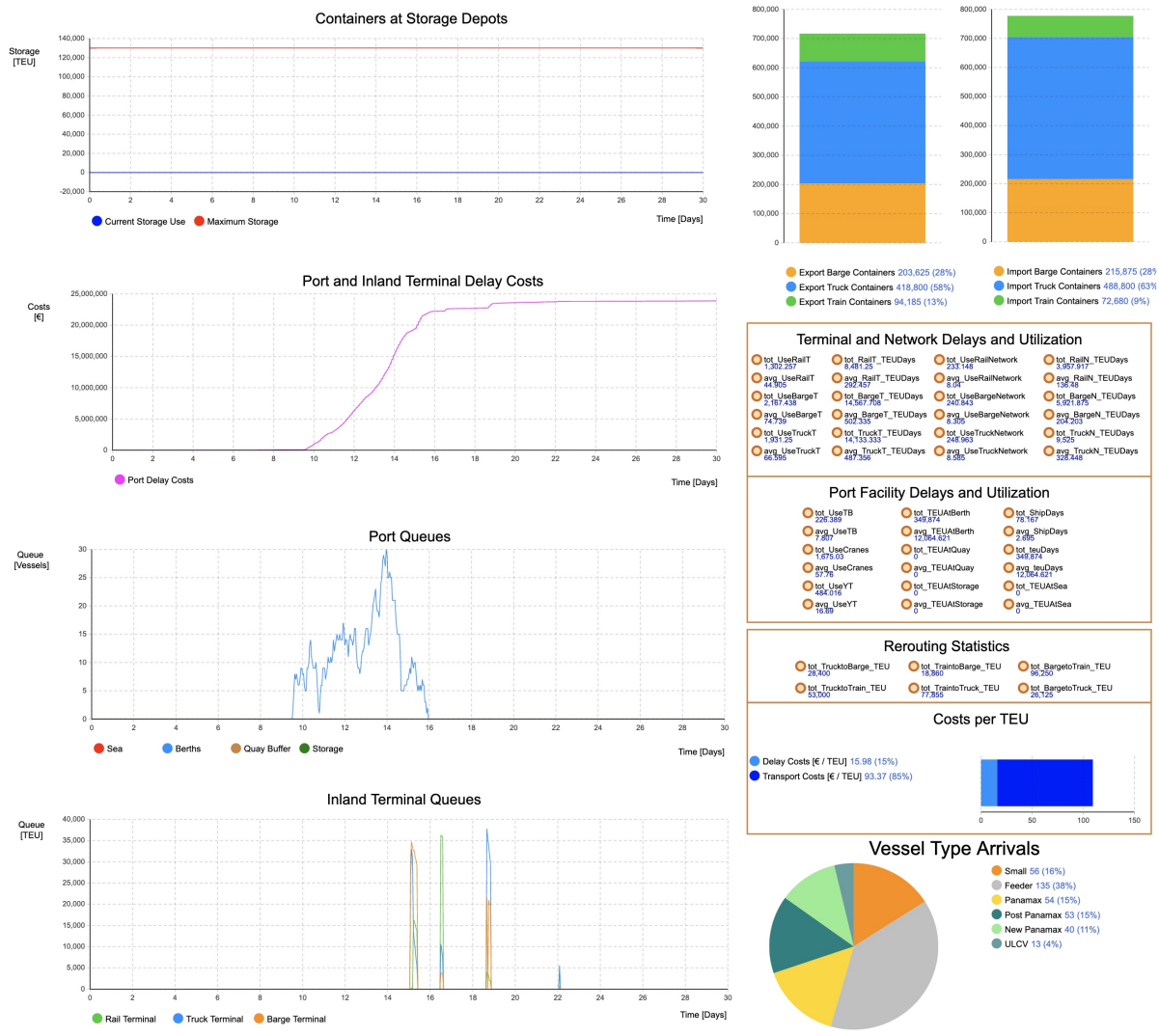

Figure B.59: Demand–Reroute — delays in port system and general metrics

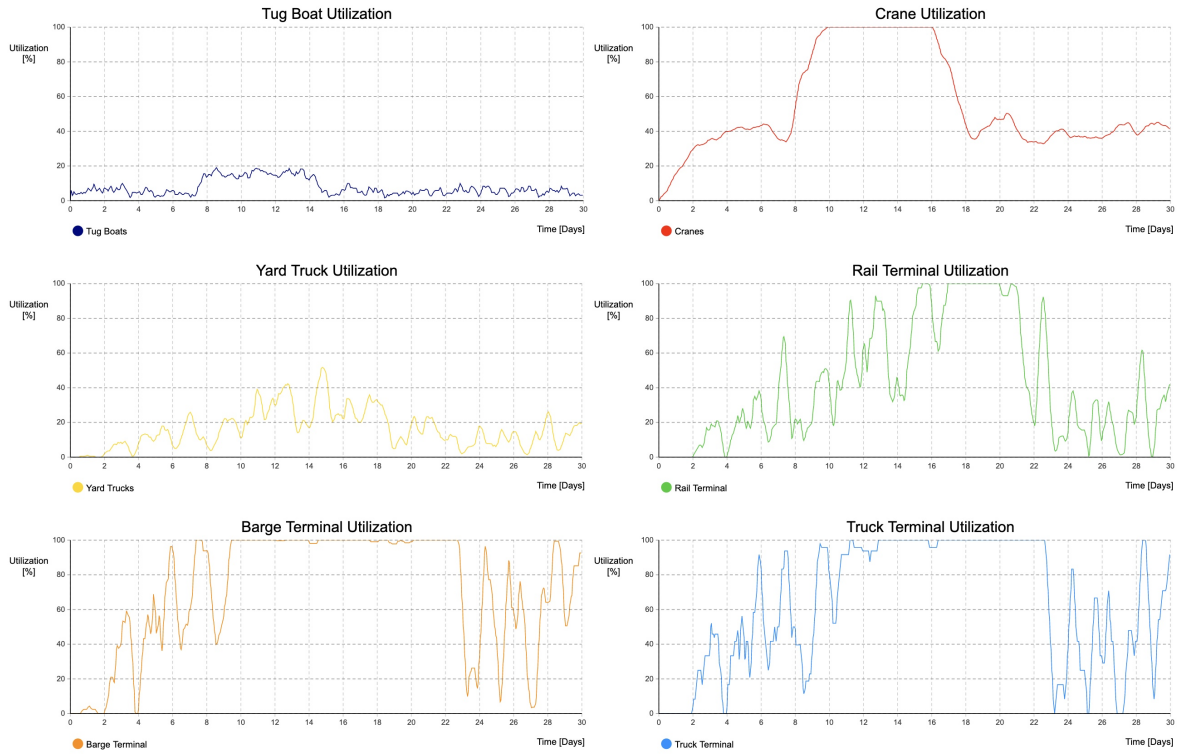

Figure B.60: Demand–Reroute — utilization levels of facilities

B.2.15 Demand - Storage

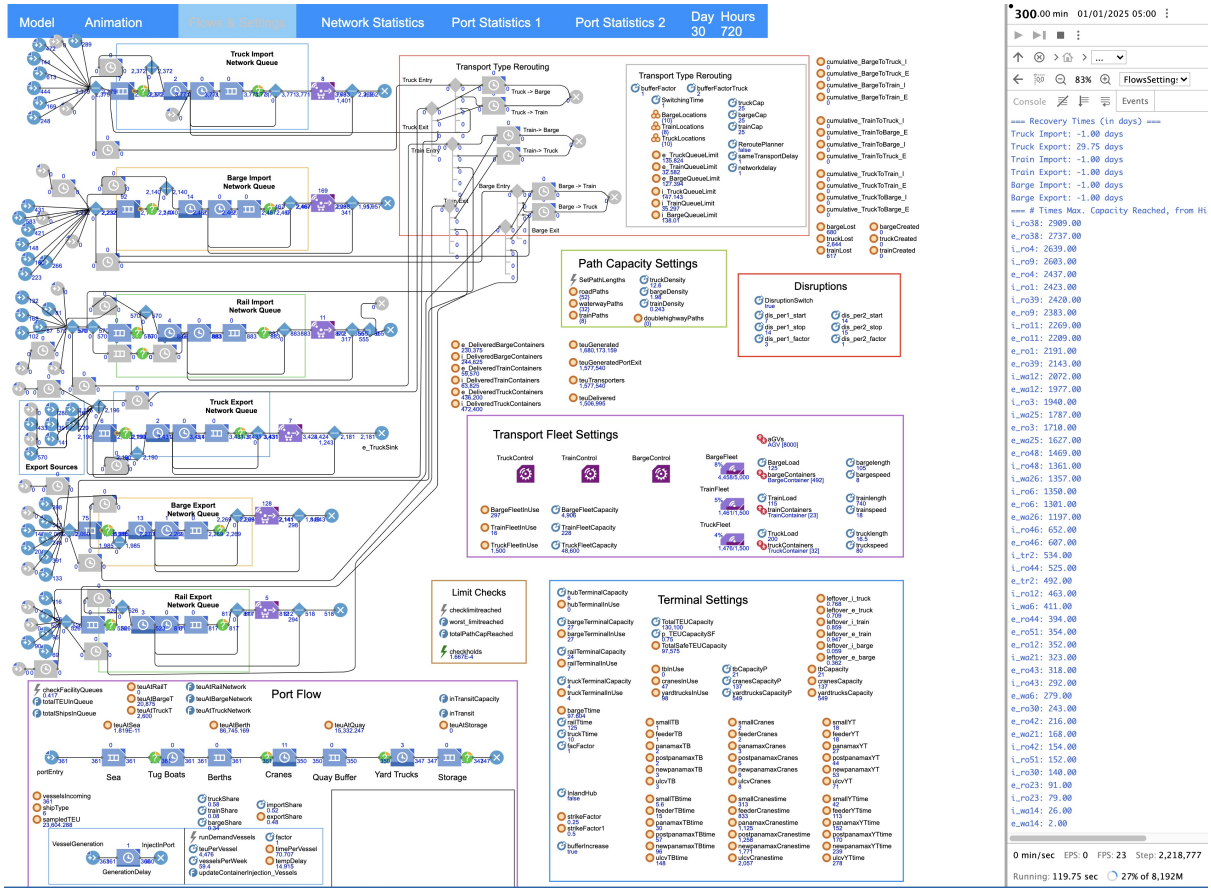

Figure B.61: Demand–Storage — settings and flow overview

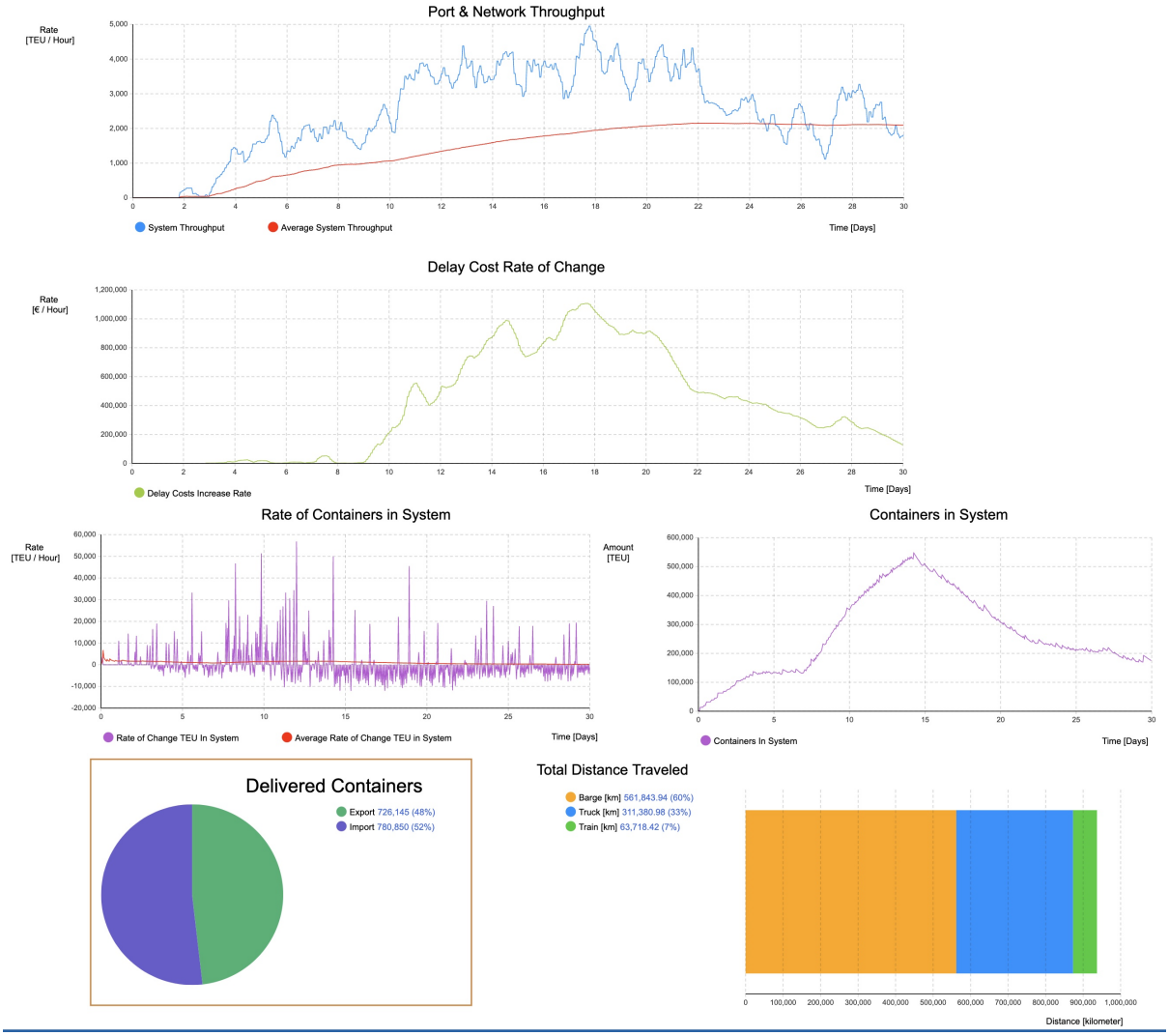

Figure B.62: Demand–Storage — network metrics and container throughput

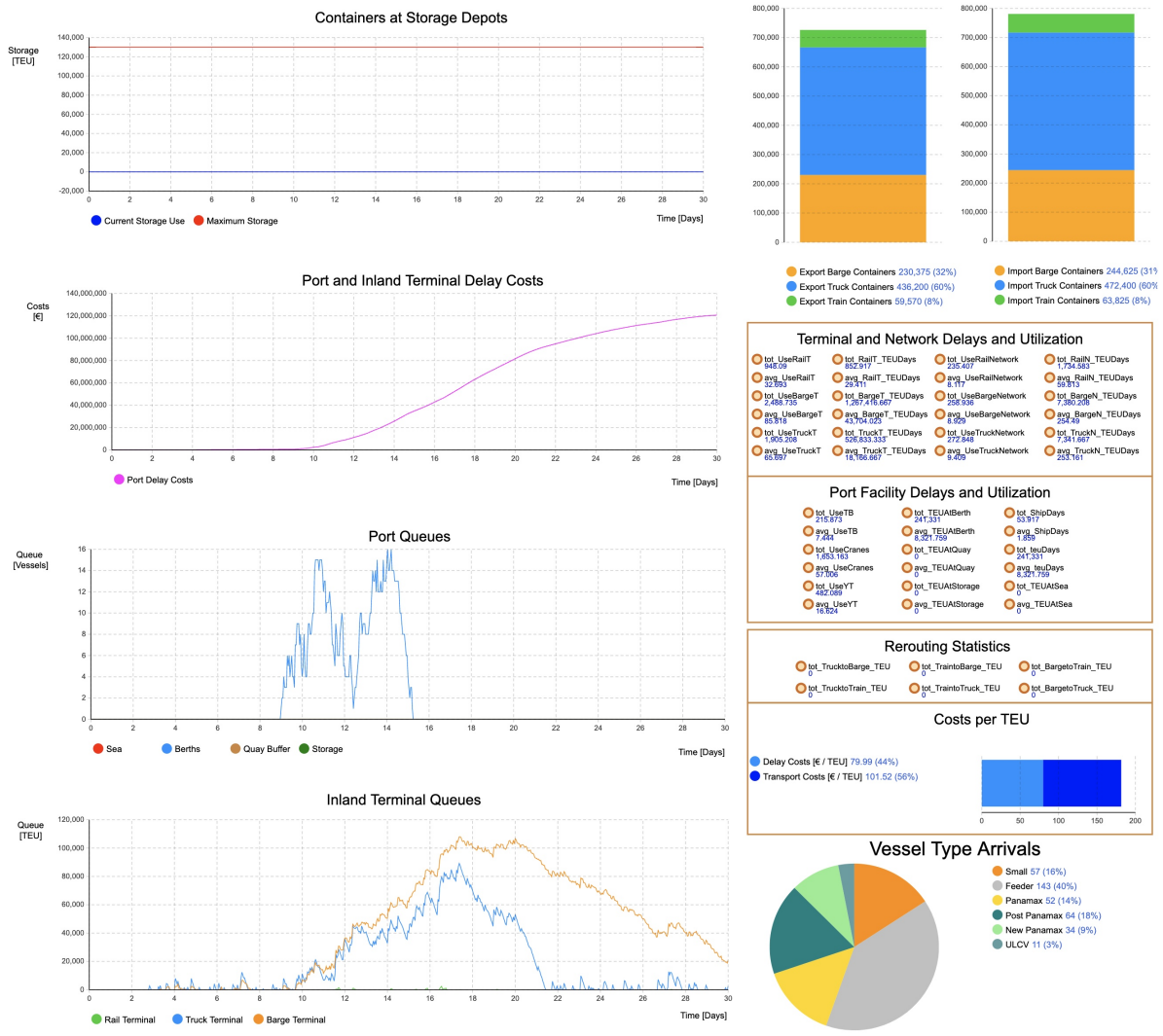

Figure B.63: Demand–Storage — delays in port system and general metrics

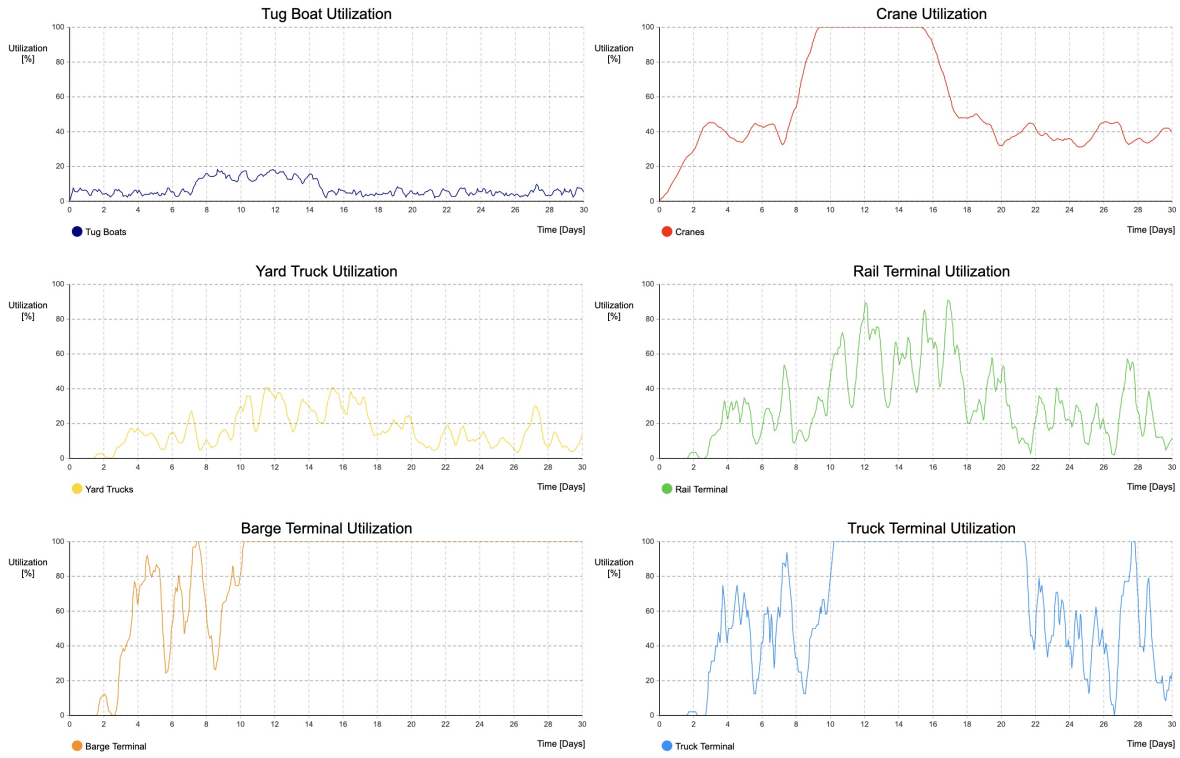

Figure B.64: Demand–Storage — utilization levels of facilities

B.2.16 Demand - Collaboration

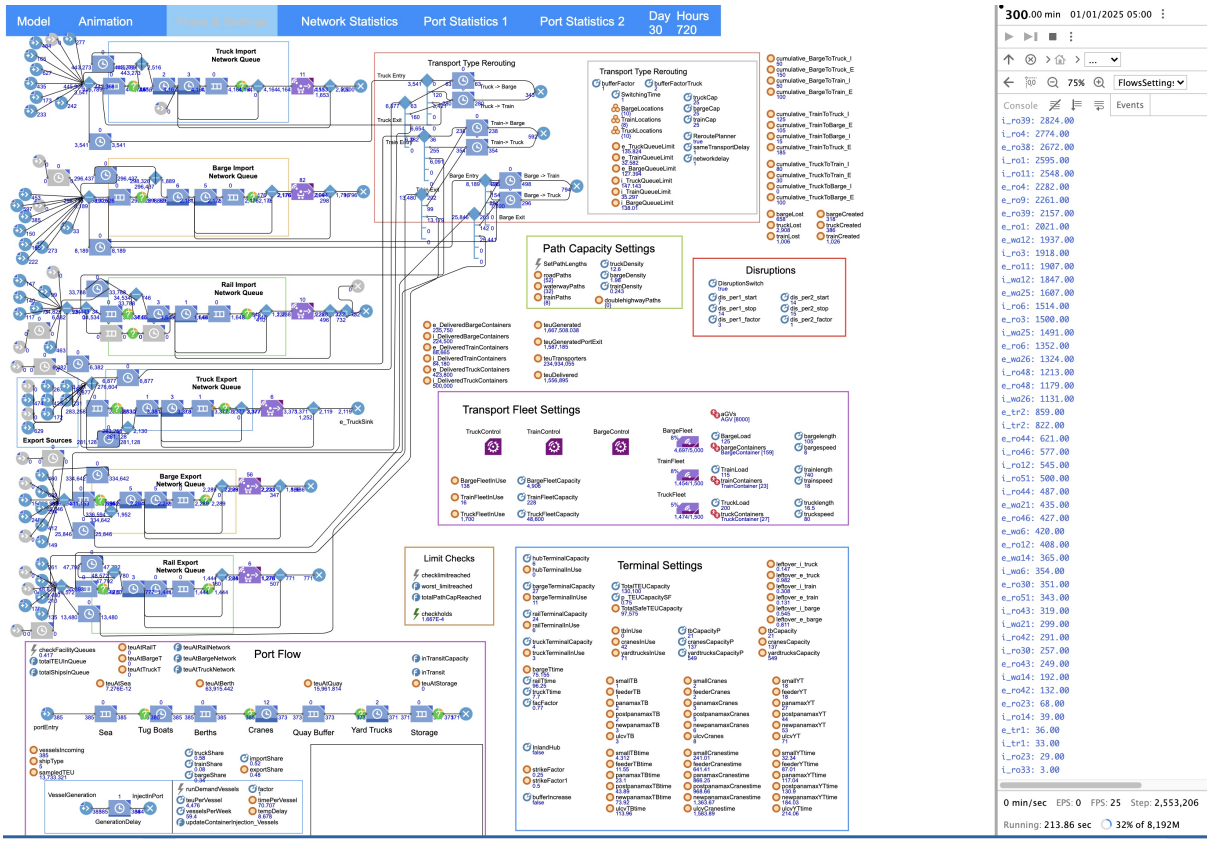

Figure B.65: Demand–Collaboration — settings and flow overview

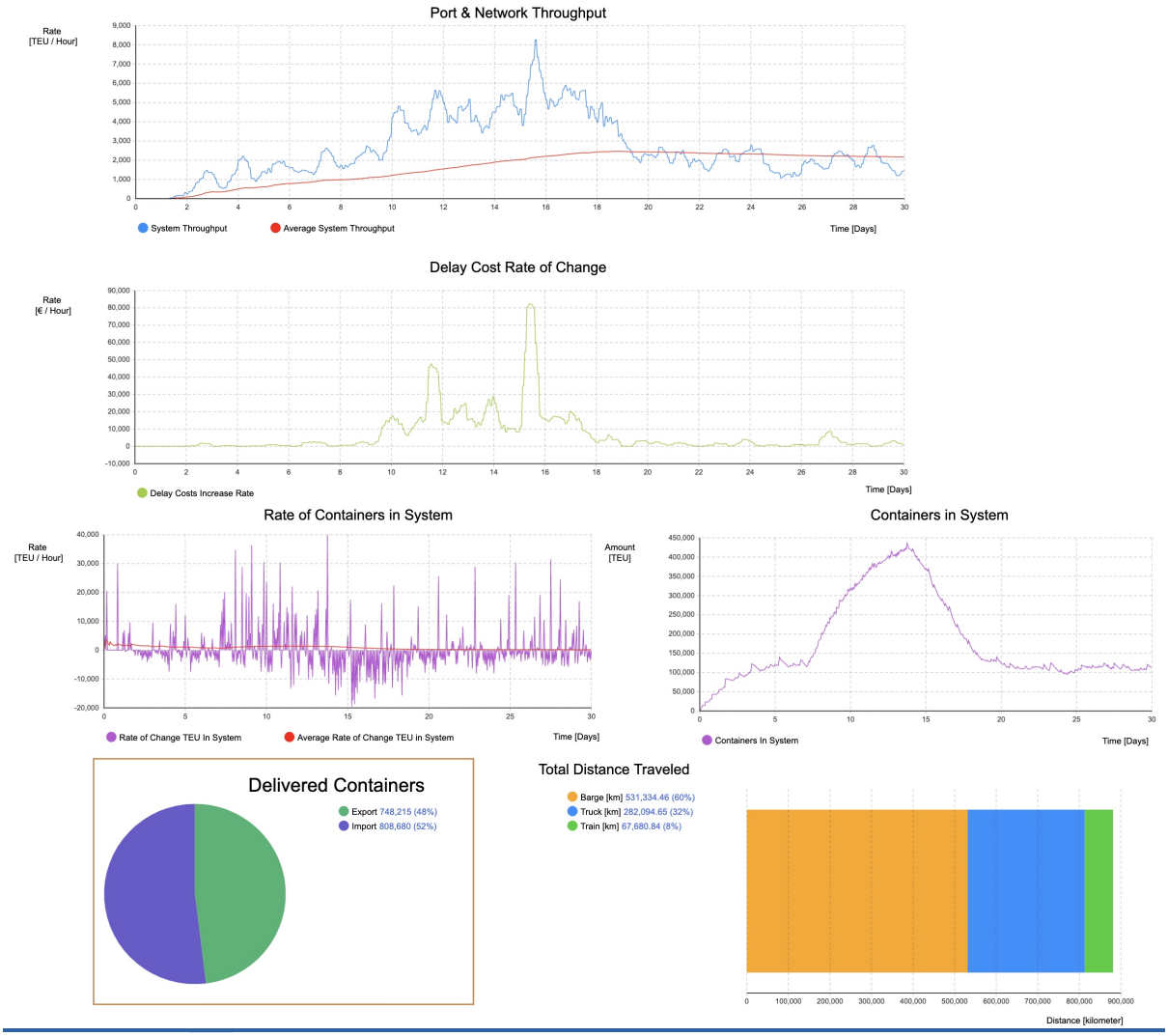

Figure B.66: Demand–Collaboration — network metrics and container throughput

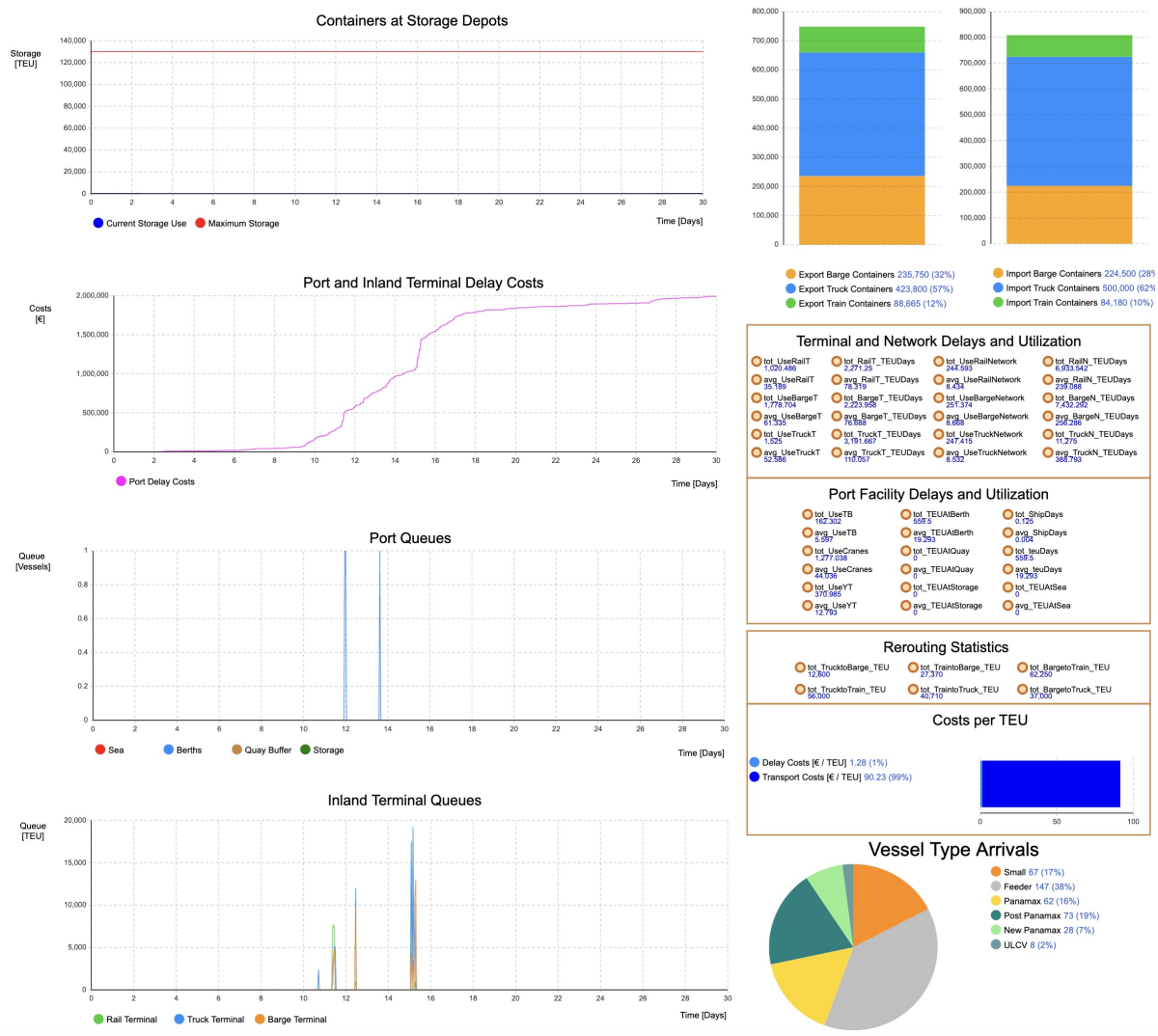

Figure B.67: Demand–Collaboration — delays in port system and general metrics

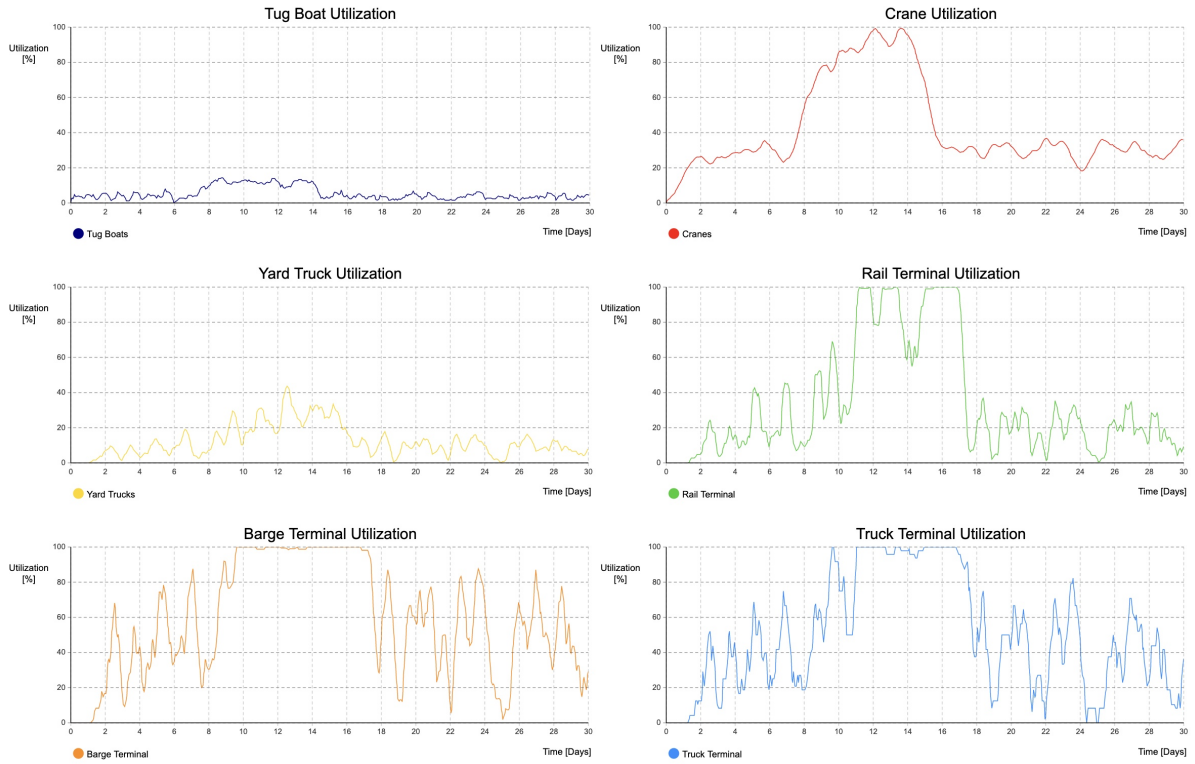

Figure B.68: Demand–Collaboration — utilization levels of facilities

Appendix C

Appendix C

C.1 Vessel Generation

Algorithm 1 Vessel Generation Process

1: Sample random number $r \in [0, 1]$
2: **if** $r < 0.175$ **then** Assign type = Small, TEU $\sim U(500, 999)$
3: **else if** $r < 0.557$ **then** Assign type = Feeder, TEU $\sim U(1000, 2999)$
4: **else if** $r < 0.715$ **then** Assign type = Panamax, TEU $\sim U(3000, 5100)$
5: **else if** $r < 0.876$ **then** Assign type = Post-Panamax, TEU $\sim U(5101, 10000)$
6: **else if** $r < 0.966$ **then** Assign type = New Panamax, TEU $\sim U(10001, 15500)$
7: **else**Assign type = ULCV, TEU $\sim U(15501, 24376)$
8: **end if**
9: Calculate base delay $= \frac{\text{week hours}}{\text{TEU per vessel} \times \text{vessels per week}} \times$ sampled TEU
10: Adjust delay using disruption scaling factor (if active)
11: Inject vessel into simulation at port entry

C.2 Hinterland Connection Block

The hinterland connection block logic specifies how containers are managed when leaving the port through truck, rail, or barge connections. It ensures that terminal and transit capacity constraints are respected and determines under which conditions containers are blocked from departure. When buffer expansion is enabled, blocking is bypassed to reflect additional resilience capacity. Otherwise, the logic distinguishes between scenarios with and without rerouting: without rerouting, blocking occurs if any single terminal reaches capacity, while with rerouting, blocking only takes place if all available modes and transit options are saturated. Algorithm 2 summarizes this stepwise logic.

Algorithm 2 Hinterland Gate Blocking Logic

```
1: if bufferIncrease = true then
2:     Allow container to move (no blocking)
3: else
4:     if not Rerouting active then
5:         if truckTerminalInUse ≥ truckTerminalCapacity OR railTerminalInUse ≥ railTerminalCapacity OR bargeTerminalInUse ≥ bargeTerminalCapacity OR inTransit ≥ inTransitCapacity then
6:             Block container
7:         end if
8:     else
9:         if truckTerminalInUse ≥ truckTerminalCapacity AND railTerminalInUse ≥ railTerminalCapacity AND bargeTerminalInUse ≥ bargeTerminalCapacity AND inTransit ≥ inTransitCapacity AND (if InlandHub active: hubTerminalInUse ≥ hubTerminalCapacity) then
10:            Block container
11:        end if
12:    end if
13: end if
```

C.3 Barge Import Flow Logic

The barge import flow logic governs how containers arriving at the inland barge terminal are processed within the simulation model. It determines whether containers remain in barge queues, are rerouted to alternative modes, or are temporarily blocked due to limited capacity. This decision-making process reflects the interplay between port infrastructure constraints, rerouting strategies, and inland accessibility. Algorithm 3 outlines the stepwise decision logic implemented in the model, which evaluates rerouting availability, capacity constraints, and route accessibility before final dispatch.

Algorithm 3 Barge Import Mode Flow

Step 1: Rerouting Decision
if ReroutePlanner = **true then**
    Stay in barge queue if:
- Barge queue has space, OR
- No alternative modes available:
  - Truck queues have space, OR
  - Train queues have space & destination reachable by train, OR
  - InlandHub active, has space, & destination reachable by train

else
    Always stay in barge queue
end if

Step 2: Capacity Blocking
if ReroutePlanner = **true then**
    Block container unless:
- Barge terminal has space, OR
- Truck queue has space, OR
- Train queue has space & destination reachable, OR
- InlandHub active, has space & destination reachable

else
    Block container unless barge terminal has space
end if

Step 3: Return to Initial Decision
if ReroutePlanner = **true then**
    Stay in flow if barge queue & terminal have space
else
    Always stay in flow
end if

Step 4: Route Availability Check
if Destination route blocked for barge **then**
    Block container
else
    Dispatch via barge
end if

C.4 Rerouting and Load-Based Batching Logic

Algorithm 4 outlines the rerouting logic applied when barge containers are redirected to trucks or trains. Unlike per-container dispatching, the model adopts a load-based batching mechanism: containers contribute incrementally to cumulative loads per mode until the respective capacity threshold is reached. Only then is a new transport agent (truck or train) instantiated and dispatched, ensuring that vehicle utilization reflects realistic operational constraints. This approach prevents excessive injection of underloaded vehicles and better captures the trade-off between transport availability, cost efficiency, and system resilience under disruption.

Algorithm 4 Rerouting with Load-Based Batching

Step 1: Container Arrival
if Container rerouted to **Truck** (Import) **then**
    Add container load to *cumulativeTruck_I*
    Reduce barge import total
    while cumulativeTruck_I $\geq$ TruckCapacity **do**
        Create new truck transport (capacity = TruckCapacity)
        Assign origin, destination, and link to original barge
        Decrease *cumulativeTruck_I* by TruckCapacity
        Update truck import total
    end while
else if Container rerouted to **Train** (Import) **then**
    Add container load to *cumulativeTrain_I*
    Reduce barge import total
    while cumulativeTrain_I $\geq$ TrainCapacity **do**
        Create new train transport (capacity = TrainCapacity)
        Assign origin, destination, and link to original barge
        Decrease *cumulativeTrain_I* by TrainCapacity
        Update train import total
    end while
end if

Step 2: Export Flow
if Container routed via **Barge** (Export) **then**
    Dispatch container to destination terminal
    Reduce barge export total
else if Container rerouted to **Train** (Export) **then**
    Add container load to *cumulativeTrain_E*
    Reduce barge export total
    while cumulativeTrain_E $\geq$ TrainCapacity **do**
        Create new train transport to destination
        Decrease *cumulativeTrain_E* by TrainCapacity
        Update train export total
    end while
else if Container rerouted to **Truck** (Export) **then**
    Add container load to *cumulativeTruck_E*
    Reduce barge export total
    while cumulativeTruck_E $\geq$ TruckCapacity **do**
        Create new truck transport to destination
        Decrease *cumulativeTruck_E* by TruckCapacity
        Update truck export total
    end while
end if